BERICHTE
aus dem Fachbereich Geowissenschaften
der Universität Bremen

No. 244

Inthorn, M.

LATERAL PARTICLE TRANSPORT IN NEPHELOID LAYERS - A KEY FACTOR FOR ORGANIC MATTER DISTRIBUTION AND QUALITY IN THE BENGUELA HIGH-PRODUCTIVITY AREA

Berichte, Fachbereich Geowissenschaften, Universität Bremen, No. 244, 124 pages, Bremen 2005

ISSN 0931-0800

The "Berichte aus dem Fachbereich Geowissenschaften" are produced at irregular intervals by the Department of Geosciences, Bremen University.
They serve for the publication of experimental works, Ph.D.-theses and scientific contributions made by members of the department.

Reports can be ordered from:

Monika Bachur

Forschungszentrum Ozeanränder, RCOM

Universität Bremen

Postfach 330 440

D 28334 BREMEN

Phone: (49) 421 218-65516

Fax: (49) 421 218-65515

e-mail: MBachur@uni-bremen.de

Online available titles: http://elib3.suub.uni-bremen.de/publications/diss/html

Citation:
Inthorn, M.
Lateral particle transport in nepheloid layers – a key factor for organic matter distribution and quality in the Benguela high-productivity area.
Berichte, Fachbereich Geowissenschaften, Universität Bremen, No. 244, 124 pages, Bremen, 2006.

ISSN 0931-0800

Lateral particle transport in nepheloid layers – a key factor for organic matter distribution and quality in the Benguela high-productivity area

Dissertation
zur Erlangung des Doktorgrades in den Naturwissenschaften
am Fachbereich Geowissenschaften der Universität Bremen

vorgelegt von
Maik Inthorn
(Diplom-Geologe)
Bremen, August 2005

Tag des Kolloquiums:
14.10.2005

Gutachter:

PD Dr. M.Zabel
Prof. Dr. G.Bohrmann

Prüfer:
Prof. Dr. T.v.Dobeneck
Prof. Dr. T. Wagner

Preface

This thesis was funded by the Deutsche Forschungsgemeinschaft as part of subproject B2 "Origin, reactivity, and transformation of particulate organic material in the benthic boundary layer in high productivity systems" of the Research Center "Ocean Margins" (RCOM) at the University of Bremen. This work is submitted as a dissertation and has been supervised by PD Dr. Matthias Zabel.

The first chapter of the thesis provides a general introduction into the subject and gives the scientific context of the manuscripts. The thesis comprises four manuscripts with me as first author that are submitted to international scientific journals (chapters 2-5). Additionally, a manuscript with me as second author, to which I contributed the sample material as well as most of the laboratory work, is attached, but is not yet ready for submission (chapter 6). A conclusion at the end of this thesis summarizes the main results and gives an outlook on potential future work. For the thesis as a whole, references to literature are given at the end of the text in chapter 8. Three appendices are attached to the thesis. Appendix 1 and 2 include the abstracts of two published papers that are not directly linked to the main subject of this thesis, but to which I contributed as a coauthor. To the manuscript presented in appendix 1 I provided bathymetric maps and interpretation of the tectonic structure of the Marmara Sea. To the manuscript presented in appendix 2 I supplied paleoceanographic information based on geochemical analyses on three sediment cores. Additionally, appendix 3 comprises data measured on particle samples from the water-column offshore Namibia in the course of my work, but not included in the manuscripts. All data presented in this thesis are available from the public database Pangaea (http://www.pangaea.de).

Content

Abstract

This thesis aims to identify and estimate the significance of lateral transport of particulate organic matter in the deep water-column of the Benguela upwelling system (BUS) offshore southwestern Africa. Although the BUS is regarded as the most productive of the four major eastern boundary systems of the ocean, and therefore of high importance for the global marine carbon cycle, little information is available on processes and fluxes involved in particulate matter transport in this area. To understand transport pathways in the water column, the distribution of particulate matter above the continental margin off Namibia was surveyed using optical sensor techniques. The sensor data are correlated with suspended particulate matter (SPM) and particulate organic carbon (POC) values from water sample filtration. Above the continental slope, water layers strongly enriched in particle content are identified in intermediate water depths and in the lowermost water column. These layers are termed intermediate and bottom nepheloid layers (INLs and BNLs, respectively). In such layers, the major part of the advective particle transport is supposed to take place. Although they are well known from other continental margin systems, this thesis presents the first systematic study on nepheloid layers in the BUS. A pronounced BNL covers the entire study area with maximum intensity above the outer shelf and at the shelf break. The detachment of this BNL at the shelf break feeds a major INL in 250 to 400 m water depth at 25.5°S, positioned at the lower boundary of the oxygen minimum zone. Together, these strong subsurface nepheloid layers are indicators of intensive lateral particle transport from the outer shelf towards a depocenter of organic matter (OM) on the upper continental slope.

To get a more detailed insight into particle transport in the BNL above the slope-depth depocenter, the radioactive particle tracer ^{234}Th was used at three stations, positioned within and outside the major organic carbon (OC) enrichment. Combined with the results of the sensor survey, ^{234}Th provides a powerful tool to identify and quantify particle transport processes, as well as fluxes in the BNL and towards the surface sediment. ^{234}Th depletion in the water samples from the BNL with respect to its parent ^{238}U, and surface sediment excess of ^{234}Th is interpreted to reflect intensive resuspension of surface sediment particles, and/or sedimentation of particles after long-distance transport in the BNL. Particle residence/ removal times in the BNL are comparably high (in the range of 9 to 12 weeks) at all three sampled stations. On the contrary, the particle inventory of the BNL, resuspension rates, and mass flux into the sediment at the depocenter location considerably exceed the measured values at the other stations. Mass flux into the sediment surpasses the predominantly vertical particle flux into sediment traps at intermediate water depth in the same area by up to an order of magnitude. This is evidence of the superior role of lateral particle transport processes at this continental slope.

The dominating significance of lateral particle transport at the continental slope of the BUS is confirmed by qualitative parameters determined on particles from the BNL and the underlying sediment. Close to the shelf-break and at the upper slope, lateral transport processes exceed vertical input of “fresh” particles from surface waters, resulting in high

sedimentary ^{14}C-ages, C/N-ratios, concentrations of POC, and sedimentation rates. At the lower slope, the influence of lateral transport progressively decreases to the benefit of the vertical component, as reflected by younger ^{14}C-ages, lower C/N-ratios, POC concentration and sediment accumulation. A comparably high relative fraction of labile OM in sediments from the shelf and the slope depocenter points to the shelf as the most probable source area for lateral OM transport to the slope. Earlier studies proposed that either the oxygen content of the bottom waters or vertical input of freshly produced OM from the surface waters would be the most significant factors concerning strong accumulation and preservation of OM in the depocenter sediments. However, our results reveal that high sedimentation rates driven through strong lateral transport are of highest importance in the BUS. The hydrocarbon content of the slope sediments from the BUS is comparable to results from other high-productive continental margins, proposing similar particle transport mechanisms, and relating these key areas of marine OM production and OC burial to each other.

Sampling of the particle content of the lowermost water column and monitoring of the physical conditions directly above the sea-floor was crucial to achieve many of the above mentioned results. This was carried out with a newly developed bottom water sampling system ("BeaWiS"), which is presented in this thesis. BeaWiS fills a gap in common ship-borne sampling techniques between sediment sampling gear, such as the multiple corer and the conventional rosette sampler that are inappropriate to sample the lowermost water column at discrete depth intervals relative to the sea-floor. Moreover, BeaWiS proved to be appropriate to obtain water samples that reflect the steep geochemical gradients in bottom waters, often occurring directly above the seafloor. Additionally, its stainless steel tripod works as a platform for a variety of sensors and optional additional equipment.

An important parameter to approach changes in primary production is the nitrogen isotope (^{14}N/^{15}N) composition of particulate organic matter, because it reflects the nutrient situation in the source environment. Using a large set of SPM and surface sediment samples as well as nutrient measurements, a direct linkage between enhanced δ^{15}N values in particulate organic matter to a deficit of fixed inorganic nitrogen is detected. The removal of fixed nitrogen, taking place in subsurface shelf waters off Namibia, is mainly attributable to activity of anammox-bacteria, oxidizing ammonium in the suboxic waters of a pronounced oxygen minimum zone. Upwelling of these deep waters that are depleted in nitrogen relative to phosphorous but nevertheless nutrient-rich takes place along the coast and induces intensive marine bioproduction. Our results contradict previous hypotheses, based on δ^{15}N-measurements on sediment core and sediment trap samples, that proposed increasing relative nitrate utilization with increasing distance to the coast as the major mechanism influencing the nitrogen isotope composition of the particles. These findings have major implications for the paleoceanographic interpretation of the sedimentary δ^{15}N record in the Benguela upwelling region.

The results on distribution, transport and quality of organic matter presented in this thesis confirm the major significance of lateral transport of pre-aged, but well-preserved

organic particles in the highly-productive Benguela upwelling area. Many indications suggest that the results from this study are also applicable to other continental margin settings. For example, high ^{14}C-ages of SPM and the deposition of OC-rich sediments with high hydrocarbon potential on the upper continental slope is also known from other high-productive areas of the modern ocean. Thus, the results may improve our understanding of the genesis of black shales and petroleum source rocks in the geological record, to which these depocenters may represent a modern analogue. Additionally, it is shown that advective processes have the potential to displace areas of enhanced OC burial effectively from maximum production cells along the coast towards the slope and possibly the deep-sea. These results limit the validity of often used, merely vertically oriented particle flux models. The findings from the BUS identify lateral transport as an important, yet hardly recognized, secondary mechanism, effectively transferring carbon from the atmosphere to long-term sequestration in the sediments. Therewith, the results contribute to the improvement of global models to predict the impact of environmental changes on the oceanic system.

Kurzfassung

Das Ziel dieser Doktorarbeit ist es, die Bedeutung des lateralen Transports organischer Partikel im Benguela Auftriebssystems (BUS) vor der Küste von Südwestafrika zu erfassen und abzuschätzen. Obwohl das BUS als das biologisch produktivste der vier wichtigsten Strömungsgebiete an den östlichen Ozeanrändern gilt und deshalb von großer Bedeutung für den globalen marinen Kohlenstoffkreislauf ist, gibt es bislang nur wenig Informationen über Prozesse und Raten des Partikeltransports in dieser Region. Um die Transportwege der Partikel in der Wassersäule zu verstehen, wurde ihre Verteilung über dem Kontinentalrand vor der Küste Namibias mittels optischer Sensoren untersucht. Die Sensordaten korrelieren mit den Gehalten an suspendiertem partikulärem Material (SPM) und partikulärem organischen Kohlenstoff (POC), welche anhand der Filtration von Wasserproben bestimmt wurden. Über dem Kontinentalhang wurden in mittleren Wassertiefen und im untersten Teil der Wassersäule Lagen mit stark erhöhten Partikelgehalten vorgefunden. Solche Trübungslagen werden als intermediäre bzw. Bodennepheloidlagen (INL bzw. BNL) bezeichnet. Es wird vermutet, dass der größte Anteil des advektiven Partikeltransports in diesen Trübungslagen stattfindet. Obwohl sie von anderen Kontinentalhängen wohlbekannt sind, stellt diese Doktorarbeit die erste systematische Studie zu Nepheloidlagen im BUS dar. Eine stark ausgeprägte BNL wurde im gesamten Arbeitsgebiet vorgefunden, wobei die Intensität dieser Lage über dem äußeren Schelf und an der Schelfkante am stärksten ausgeprägt war. Eine Ablösung dieser BNL vom Meeresboden an der Schelfkante führt zu einer starken INL in 250 bis 400 m Wassertiefe bei 25,5°S, am unteren Grenzbereich der Sauerstoffminimumzone. Zusammen stellen diese beiden Nepheloidlagen gute Indikatoren für intensiven lateralen Partikeltransport vom äußeren Schelf in Richtung eines Akkumulationszentrums für organisches Material (OM) auf dem oberen Kontinentalhang dar.

Um die Partikeltransportprozesse in der BNL über dem Akkumulationszentrum auf dem Kontinentalhang besser zu verstehen, wurde der radioaktive Partikeltracer ^{234}Th an drei Probenahmestationen verwendet. Eine Station befand sich innerhalb und zwei außerhalb dieses Bereichs starker Anreicherung von organischem Kohlenstoff (OC) im Sediment. Zusammen mit Ergebnissen der Sensorstudie ist die Verwendung von ^{234}Th sehr gut geeignet, um Partikeltransportprozesse, sowie Transportraten in der BNL und in das Sediment zu erfassen und zu quantifizieren. Abreicherung von ^{234}Th in Wasserproben aus der BNL sowie ein ^{234}Th-Überschuss im Oberflächensediment im Vergleich zum Gehalt des zugehörigen Ausgangs-Isotops ^{238}U werden als Hinweise auf intensive Resuspension von Oberflächensedimentpartikeln und/oder Sedimentation von Partikeln nach Langstrecken-transport in der BNL gedeutet. Die Partikelaufenthalts-/-abreicherungszeiten in der BNL sind an allen drei beprobten Stationen vergleichbar lang (9-12 Wochen). Hingegen übertreffen das Partikelinventar in der BNL, die Resuspensionsraten und der Gesamt-partikelfluss ins Sediment an der Station auf dem Akkumulationszentrum deutlich die an den anderen beiden Stationen gemessenen Werte. Der Gesamtpartikelfluss ins Sediment übertrifft den hauptsächlich vertikalen Partikelfluss in Sedimentfallen, die in mittleren

Wassertiefen verankert waren, um annähernd eine Größenordnung. Dies ist ein Beweis für die übergeordnete Rolle der lateralen Partikeltransportprozesse an diesem Kontinentalhang.

Die dominierende Bedeutung des lateralen Partikeltransports am Kontinentalhang im BUS wird durch qualitative Parameter bestätigt, die an Partikeln aus der BNL und an den selben Stationen beprobten Oberflächensedimenten gemessen wurden. Nahe der Schelfkante und am oberen Hang übertreffen die lateralen Transportprozesse den vertikalen Zufluss von „frischem" und erst kurz zuvor entstandenen Partikeln aus dem Oberflächenwasser deutlich, was zu hohen ^{14}C-Altern, C/N-Verhältnissen, POC-Konzentrationen und Sedimentationsraten führt. Am tieferen Hang nimmt der Einfluss des Lateraltransports im Vergleich zur vertikalen Komponente immer mehr ab, was sich im jüngeren ^{14}C-Alter, sowie niedrigeren C/N-Verhältnissen, POC-Konzentrationen und Sedimentationsraten widerspiegelt. Ein vergleichsweise großer, relativer Anteil von labilem OM in den Schelfsedimenten wie auch im Akkumulationszentrum auf dem Hang deutet darauf hin, dass der Schelf wahrscheinlich das Ursprungsgebiet für den Transport des labilen OM zum Hang darstellt. In früheren Arbeiten wurden der Sauerstoffgehalt des Bodenwassers, bzw. der vertikale Zufluss von frisch produziertem OM aus dem Oberflächenwasser als die wichtigsten Faktoren in Bezug auf die starke Anreicherung und gute Erhaltung von OM in Sedimentakkumulationszentren betrachtet. Unsere Ergebnisse zeigen hingegen, dass im BUS die durch den starken lateralen Eintrag erzeugten, hohen Sedimentationsraten den größten Einfluss haben. Der Kohlenwasserstoffgehalt der Hangsedimente des BUS ähnelt den Ergebnissen von anderen hochproduktiven Kontinentalrändern, was auf gleiche Partikeltransportmechanismen hindeutet und diese Schlüsselgebiete mariner OM Produktion miteinander verbindet.

Für viele Ergebnisse der oben genannten Studien waren die Beprobung des Partikelgehalts des untersten Bereichs der Wassersäule sowie die Bestimmung der physikalischen Rahmenbedingungen direkt über dem Meeresboden von äußerster Wichtigkeit. Dies wurde mit Hilfe eines neuentwickelten Bodenwasserbeprobungssystems („BeaWiS") erreicht, welches in dieser Doktorarbeit vorgestellt wird. BeaWiS schließt damit eine Lücke der auf den Forschungsschiffen gebräuchlichen Probenahmesysteme. Üblich sind der Multicorer sowie der normale Kranzwasserschöpfer, welche aber beide ungeeignet sind, um den untersten Meter der Wassersäule in definierbaren Abständen zum Meeresboden zu beproben. Darüber hinaus kann gezeigt werden, dass BeaWiS auch dazu geeignet ist, Wasserproben zu gewinnen, welche die steilen geochemischen Konzentrationsgradienten erfassen, die oft direkt über dem Meeresboden zu finden sind. Zusätzlich fungiert das dreibeinige Stahlgerüst des Geräts als Plattform zur Befestigung einer vielfältigen Auswahl von Sensoren und optionalen zusätzlichen Gerätschaften.

Da die Stickstoffisotopenzusammensetzung von partikulärem organischen Material die Nährstoffsituation im Quellgebiet widerspiegelt, stellt sie einen wichtigen Parameter dar, um Veränderungen in der Intensität der Primärproduktion nachzuvollziehen. Unter Verwendung einer großen Anzahl von SPM- und Oberflächensedimentproben konnte in

Kombination mit Nährstoffmessungen eine direkte Kopplung zwischen erhöhten $\delta^{15}N$-Werten in partikulärem organischem Material und dem Verlust fixierten, anorganischen Stickstoffs nachgewiesen werden. Dieser Verlust des fixierten Stickstoffs, welcher in tieferen Wasserbereichen der Schelfregion vor der Küste Namibias stattfindet, ist hauptsächlich auf die Aktivität von Anammox-Bakterien zurückzuführen, die im suboxischen Bereich einer starken Sauerstoffminimumzone Ammonium oxidieren. Der Auftrieb von Tiefenwasser, das im Verhältnis zu Phosphor an Stickstoff abgereichtert aber dennoch nährstoffreich ist, findet entlang der Küste statt, wo es eine intensive marine Bioproduktion antreibt. Unsere Ergebnisse widersprechen älteren Hypothesen, die, basierend auf $\delta^{15}N$-Messungen an Sedimentkern- und Sedimentfallenmaterial, die Verminderung der Nährstoffzugangsmöglichkeiten mit größer werdendem Abstand zur Küste als die Hauptursache für die Veränderung der Stickstoffisotopenzusammensetzung ansehen. Diese Ergebnisse haben große Auswirkungen auf die paläozeanographische Deutung sedimentärer $\delta^{15}N$-Datensätze aus der Benguela Auftriebsregion.

Die Resultate dieser Doktorarbeit bestätigen die große Bedeutung des lateralen Transports alter, aber dennoch guterhaltener, organischer Partikel in Bezug auf Verteilung, Transport und Qualität des organischen Materials im hochproduktiven Benguela Auftriebsgebiet. Viele Anhaltspunkte deuten darauf hin, dass die Ergebnisse dieser Studie auch auf andere Kontinentalränder übertragbar sind. So sind hohe ^{14}C-Alter des SPM sowie die Ablagerung OC-reicher Sedimente mit großem Kohlenwasserstoffpotential am oberen Hang auch von anderen Kontinentalrändern bekannt. Die Ergebnisse verbessern aber auch das Verständnis der Entwicklungsbedingungen von Schwarzschiefern und Erdölmuttergesteinen, zu denen die Akkumulationszentren auf den Kontinentalhängen ein rezentes Analogon darstellen können. Außerdem konnte gezeigt werden, dass advektive Prozesse das Potential besitzen, Gebiete erhöhter OC-Sedimentation effektiv von den Hauptproduktionszellen entlang der Küste zum Kontinentalhang und eventuell sogar bis in die Tiefsee zu verlagern. Dies schränkt die Verwendbarkeit der üblichen, rein vertikal ausgerichteten Partikelflussmodelle stark ein. Die Ergebnisse aus dem BUS identifizieren den Lateraltransport als einen wichtigen, jedoch wenig beachteten Sekundärmechanismus, welcher effektiv Kohlenstoff aus der Atmosphäre der langfristigen Speicherung in den Sedimenten zuführen kann. Somit tragen die erarbeiteten Resultate zur Verbesserung globaler Modelle zur Vorhersage des Klimawandels auf das System Ozean bei.

1. Introduction

1.1. Motivation and main objectives

Ocean margins are of great importance to the global biogeochemical cycles. Although they represent only about 20% of the surface area of the marine system, 50% of the global marine production takes place, and approximately 80% of the total organic carbon (OC) is buried in the margin sediments (Wollast, 1998). Hence, a proper understanding of the ocean margin system is important to get a complete picture of the ocean's potential to scavenge anthropogenic CO_2, a matter of great significance with respect to the greenhouse effect and global warming. Moreover, this understanding is necessary to consider potential feedback effects of global warming on oceanic systems. Most of the ocean models developed so far as part of global climate models are restricted to the open ocean, due to the highly complex and dynamic processes of the ocean margin system. Therefore, it is necessary to improve our knowledge on these systems to be able to extend the models. There is no doubt that on ocean-wide scales the accumulation and burial of organic matter (OM) in the sediments principally reflects (a) the distribution pattern of the primary production (PP) in the overlying euphotic surface waters and (b) the efficiency of OM degradation during particle settling through the water column. Especially at ocean margins, however, this approach of a simple vertical transport is not sufficient, since lateral transport processes in the deep water column can cause serious decoupling of surface water and benthic system.

Accordingly, the major aim of this thesis is to improve the understanding of lateral particle transport processes at a high-productive continental margin. Of particular interest is the organic matter fraction of the particulate material. Strategies had to be developed, to differentiate between the relative contribution of highly reactive organic material arriving from vertical fluxes versus the potentially more recalcitrant laterally transported material. Essentially, transport processes need to be quantified. For that purpose, an appropriate sampling strategy had to be designed to receive samples of suspended particles from the layers, in which lateral transport is taking place. Especially, the lowermost water column is bound to reveal the strongest gradients in concentrations of particulate matter. However, there is still a gap in common ship-board sampling techniques to achieve this goal. The particles are characterized through application of different sensor techniques, as well as geochemical, radioisotopic and pyrolytic analyses. Additionally, the suspended material is compared to samples from the underlying sediments. Therewith, this thesis provides important information about the influence of lateral transport on preservation/degradability of OM, which is fundamentally important for the interpretation of fossil organic carbon enrichments within the sedimentary record.

In this introduction, the importance of ocean margin systems for the marine carbon cycle is briefly summarized. Afterwards, an overview is given on different particulate organic matter sources, particulate matter distribution and possible transport mechanisms in the water column, as well as their influence on organic matter preservation. The study area is

the Benguela upwelling area. Therefore, the general geomorphologic and oceanographic setting of the continental margin offshore southwestern Africa is described, and the functionality of the upwelling process is briefly outlined.

1.2. Ocean Margins and the marine carbon cycle

Together, continental shelf, slope, and rise form the transitional zone between the oceans and the continents. There is a multitude of reasons for the large interest of modern geoscience to get a proper understanding of this part of the marine system. More than 60% of mankind live in the coastal regions of the continents. Human exploitation of resources at ocean margins is steadily increasing as both fisheries and hydrocarbon exploration are progressing from the outer shelves down the slopes, making it an area of immense commercial interest. However, margins are also a repository for anthropogenic wastes, transported by river discharges, currents, winds, and rain. On the other hand, people are susceptible to the potential hazard, the ocean may represent, as revealed by the large tsunami of Christmas 2004.

Coastal waters are generally rich in nutrients, originating from the continents, and from upwelling of nutrient-rich deep waters, inducing high productivity of the surface waters. Some of the resulting organic matter is deposited in shelf sediments, or exported to the slope and the deep-sea. Thus, CO_2 is transferred from the atmosphere to the ocean system (Bauer and Druffel, 1998). A tentative global marine carbon cycle was published by Wollast (1998; Fig. 1.1), but lateral particle fluxes between shelf, slope, and open ocean could only indicated as question marks. Up to now, most of the fluxes in concern are poorly quantified, with some limited regional exceptions, where large international projects considered the influence of lateral transport. These are, in particular, SEEP-I and SEEP-II on the outer margin of the Mid Atlantic Bight (Biscaye et al., 1994; Walsh et al., 1988), OMEX-I in the northern Bay of Biscay (van Weering et al., 1998) and Omex-II at the northwestern Iberian Margin (van Weering and McCave, 2002), ENAM on the European North Atlantic Margin (Mienert et al., 1998) and STRATAFORM on the margins off northern California and New Jersey (Nittrouer, 1999). The Benguela upwelling area off the south-west African continental margin. has not yet been area of study of such a large marine research project, although it is the most productive eastern oceanic upwelling region of the ocean (Carr, 2001), and therefore of major significance with respect to the marine carbon cycle. This thesis focuses on particulate (organic) matter distribution, transport, and quality in the Benguela, and is aiming to improve the understanding of the carbon cycle in this important area.

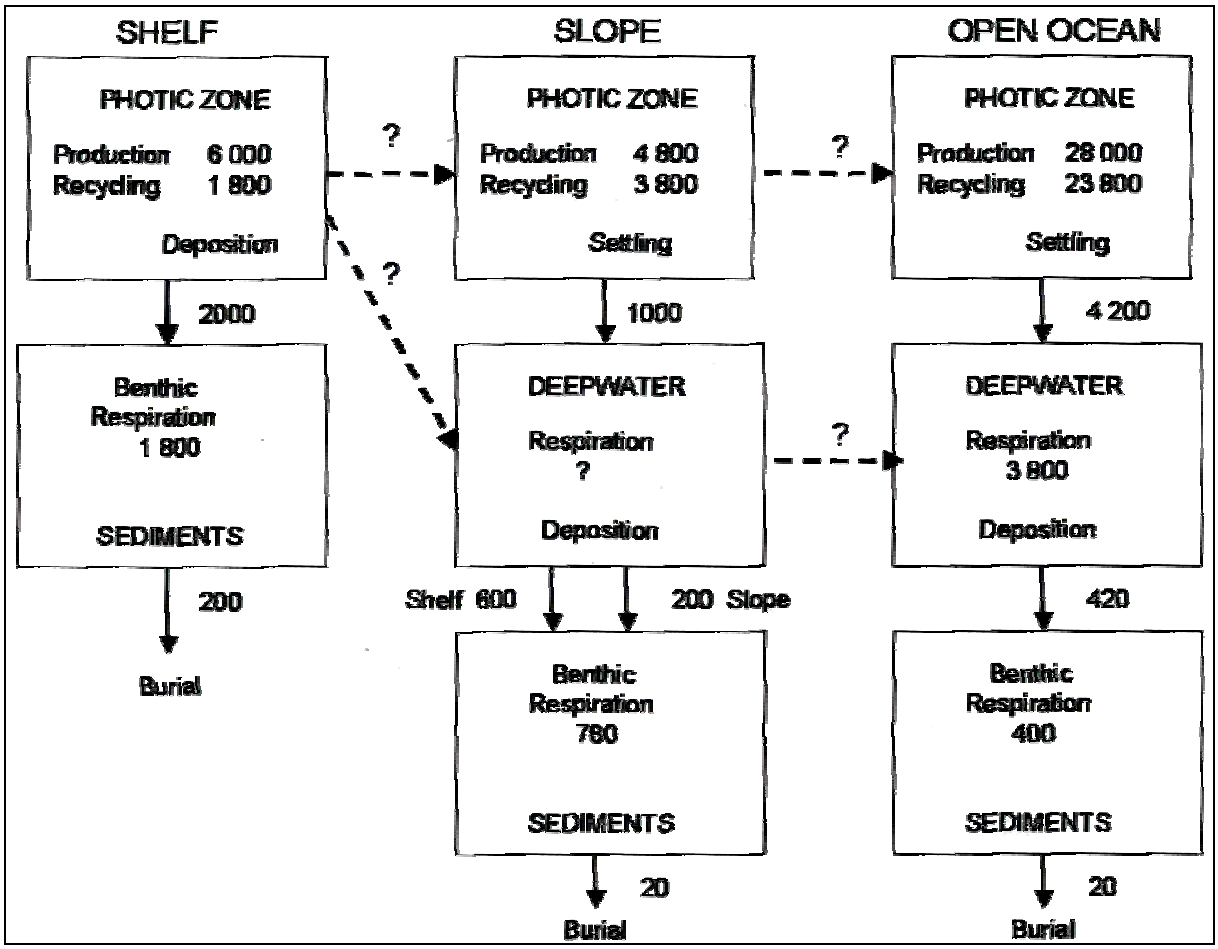

Fig. 1.1. Tentative global cycle of organic carbon in the oceanic system, expressed in MTC yr^{-1} (Wollast, 1998).

1.3. Particulate organic matter in the water column

In the previous chapter, it was established that turnover of organic matter is an important characteristic of ocean margin systems. In the following, an introduction to sources, transport, composition and degradation of particulate matter at ocean margins is given (Fig. 1.2). Thereby, the manuscripts presented in this thesis are put into each other's and a broader scientific context.

1.3.1. Sources

Autotrophic organisms are the backbone of the marine food chain, using sunlight and inorganic carbon to form organic matter. Coccolithophorids and diatoms constitute the majority of these marine algae, while a large variety of zooplankton, such as copepods, pteropods or foraminifera, feeds on the phytoplankton. Carcasses and excrements of these organisms are the most important source of marine particulate organic matter. Estimates of the potential global biomass production in the ocean, based on in situ data (i.e. ^{14}C uptake, sediment trap data) range between 20 and 50 Gt C yr^{-1} (Berger et al., 1989). Between 1978 and 1986 the CZCS-sensor (Coastal Zone Color Scanner) onboard the satellite Nimbus7 provided

worldwide long-term data of the chlorophyll-relevant colorspectrum of 400 to 700 nm. Algorithms based on empirical data were applied to calculate the overall amount of organic carbon in the euphotic zone from the sensor data, which resulted in estimates of the global PP ranging between 27 and 50 Gt C yr^{-1} (Fig. 1.3; Antoine et al., 1996; Behrenfeld and Falkowski, 1997). Since 1996, data of the SeaWiFS sensor (Sea-viewing Wide Field of View Sensor) are available, and have been used for several new estimates on potential production in selected regions of the ocean (e.g. Carr, 2001; McClain et al., 2004). However, PP is not evenly distributed across the ocean, but displays zones of higher activity mainly along the ocean margins, whereas the central ocean gyres are mostly characterized by low carbon fixation.

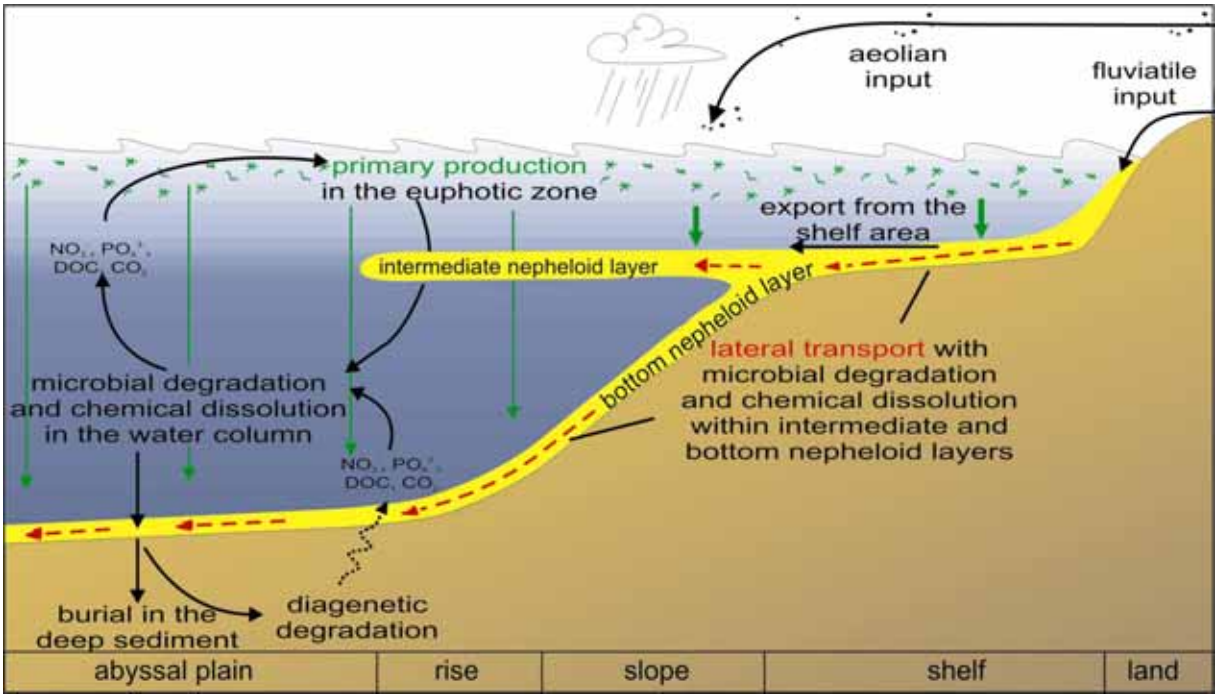

Fig. 1.2. Schematic representation of sources, transport, and degradation of organic matter in a continental margin system.

Input of land-derived organic matter is also of significance in the marine system. It is transported to the oceans by rivers (fluvial input), wind (aeolian input), as ice rafted debris, or originating from coastal erosion. The largest amount of terrestrial organic matter is supplied by rivers. However, significant amounts of this input, especially sand and gravel, are trapped in the coastal system and contribute to the growth of deltas and beaches. Two principal types of terrigenous OM have to be distinguished: 1) recently biosynthesized land plant material, and 2) OM derived from erosion/weathering of old soils or sedimentary rocks. Major importance has been attributed recently to the second type, which is sometimes very refractory and almost entirely depleted of radiocarbon ("graphitic black carbon"), but has a high potential to be preserved in the marine sediments (Dickens et al., 2004; Hwang et al., 2005).

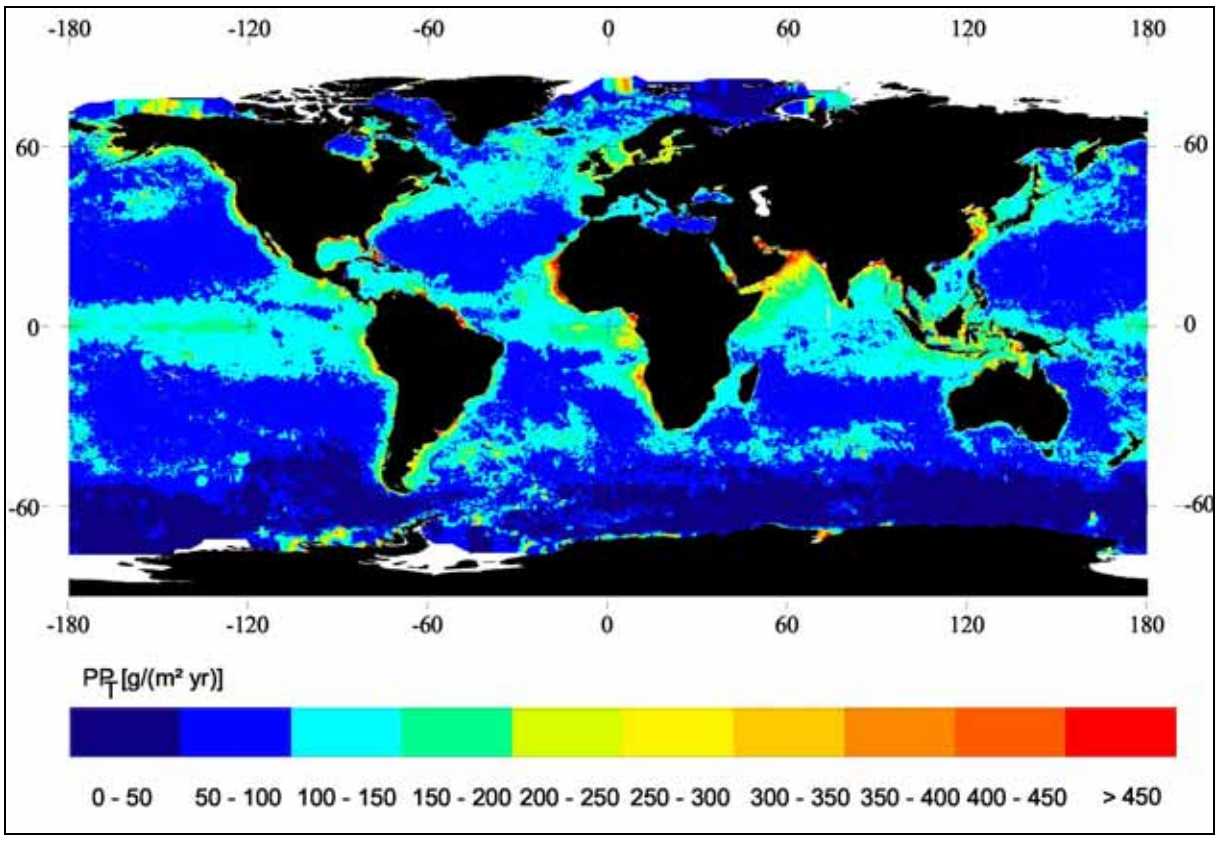

Fig. 1.3. Primary production calculated according to Antoine et al. (1996; from Seiter, 2004)

1.3.2. Distribution

Layers of enhanced particle content relative to the surrounding waters are termed nepheloid layers. Generally, three types of nepheloid layers are distinguished: 1) The biologically active, euphotic surface mixed layer is called surface nepheloid layer (SNL, e.g. Gardner et al., 1993; Gundersen et al., 1998; Oliveira et al., 2002), and generally contains the highest particulate matter concentrations of the water column. 2) Intermediate nepheloid layers (INL) result from the accumulation or advective transport of particles in intermediate waters in association with strong density gradients (e.g. Cacchione and Drake, 1986; Pak et al., 1980; Thorpe and White, 1988). 3) Bottom nepheloid layers (BNL) are found in the lowermost water column, and are maintained by turbulent mixing in the bottom boundary layer (BBL, e.g. Bacon and Rutgers van der Loeff, 1989; Graf and Rosenberg, 1997; McCave, 1986). The BBL, in turn, comprises the region above the seafloor, where current velocity is measurably slowed from a more vertically uniform mean velocity in overlying waters (Thomsen, 2003). Nepheloid layers extend may vary significantly with time and in dimension, from a few meters up to several hundred meters. The BNL is usually well pronounced along the shelf and slope areas, where near bottom currents are stronger compared to the open ocean. INLs often result from the detachment of a BNL at places of strong changes in slope gradient. This feature is well-known from the shelf-edge at different

ocean margins (McCave and Hall, 2002; McPhee-Shaw et al., 2004; Puig and Palanques, 1998).

The first manuscript of this thesis (M. Inthorn, V. Mohrholz, M. Zabel: *Nepheloid layer distribution in the Benguela upwelling area offshore Namibia*, chapter 2) provides the first systematic description of the particle distribution in the water column above the continental slope offshore Namibia. Different optical sensor techniques were used, and calibrated with particle samples from conventional bottle sampling. From the data, subsurface nepheloid layers are localized, and the significance of lateral particle transport in these layers is estimated in a conceptual particle transport model.

1.3.3. Transport

Sinking velocities of particles are controlled by their shape, density, porosity, composition, and size. Pure organic matter has a lower density than water, and would not sink at all. Marine organisms such as diatoms or coccolithophorids, and a large fraction of the aeolian dust would sink at negligible rates. However, Alldredge and Gotschalk (1988) and others estimated particle sinking velocities from sediment trap data in a range between 50 and 150 m d^{-1}. Extremely high sinking velocities of almost 3000 m d^{-1} are reported by Lampitt (1985) from the North Atlantic Ocean. It has been shown that calcite, opal, and lithogenic material may serve as ballast to achieve particle densities high enough to permit sinking of organic material through the entire water column (Armstrong et al., 2002; Klaas and Archer, 2002). Often, high-velocity sinking events occur in pulses and seasonal after strong algae blooms. They result from aggregation of faecal matter, microorganisms, and mineral particles, connected for example by sticky transparent exopolymer particles (TEP, e.g. Engel, 2004; Passow et al., 2001). High importance is attributed to "marine snow". It consists of marine aggregates with diameters greater than 5 mm, that largely escape degradation processes in the water column due to their high sinking velocity (Alldredge and Gotschalk, 1988; Ransom et al., 1998). Upon reaching the sediment surface, marine snow can trigger an awakening response of benthic organisms (Graf, 1989). Accordingly, a close coupling between the ocean surface and the deep-sea was proposed e.g. by Lampitt (1985). Therefore, remote sensing data on PP have been widely used to estimate organic carbon flux towards the sediment (e.g. Antia et al., 2001; Berger et al., 1989; Suess, 1980; Usbeck et al., 2003; Wenzhöfer and Glud, 2002). They are often combined with sediment trap data and assumptions concerning decomposition of organic matter as a function of water depth. Such vertically adjusted particle transport models aim to link the amount of fixation of organic carbon by marine phytoplankton in the euphotic zone with benthic recycling and burial rates at the underlying sediment. While potentially correct on a global scale, remarkable differences are observed, when rates of benthic remineralisation are used to calculate the organic carbon flux (Seiter et al., 2005; compare Figures 1.3 and 1.4). Additionally, numerous geochemical and oceanographic studies give evidence of a much more complex system (see Zabel and Hensen, 2003, for a review). Especially at continental margins, lateral particle

displacement in intermediate and bottom nepheloid layers is proposed as a potential reason for this discrepancy (e.g. Biscaye and Anderson, 1994; Jahnke et al., 1990). Along-slope boundary currents cause significant particle transport, particularly along western ocean margins (Alperin et al., 2002; Anderson et al., 1994; Fohrmann et al., 2001). Bottom currents may induce a "winnowing effect" that efficiently prevents or reduces the accumulation of smaller and lighter particles (like OM) in the sediments. When these currents subside, the particles previously held in suspension are deposited – a process called "focusing". Local bathymetry plays a significant role in this respect, trapping particles in morphologic depressions. Downslope transport can also be focused to canyon systems, or proceed in turbidity currents, sediment slides or slumps. Strong tidal currents perpendicular to the shelf-break are also often observed. However, due to the nature of tidal flow, there is little net transport attributed to these, unless asymmetry in the flow field causes local imbalances (van Weering et al., 2002). At pronounced density gradients within the water column, internal waves with large amplitudes can result from tidal energy and induce strong turbulent mixing processes, where the wave characteristic slope is close to the slope of the seabed (Cacchione and Wunsch, 1974; McPhee-Shaw et al., 2004). On longer timescales, sea level change induces major particle redistributions (McCave, 2003). At sea level low-stand, e.g. at the last glacial maximum with the sea level 120-130m below the present level, shelves were at least partially uncovered, and, thus, subject to erosion by rivers and wind. Additionally, the depth of significant wave attack was lowered, effectively transporting particles from the shelf towards the slopes and basins.

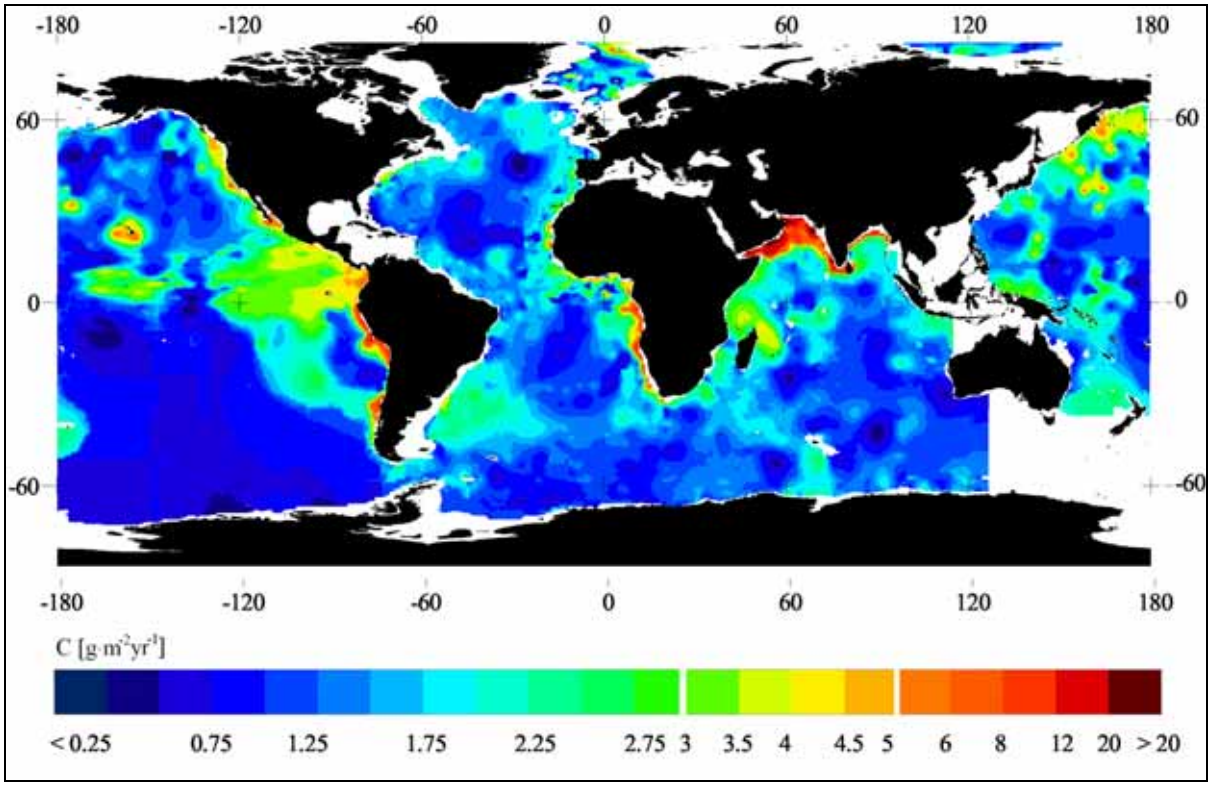

Fig. 1.4. Global distribution of calculated minimum flux of particulate organic carbon (POC) to the sea-floor at water depth greater than 1000m (Seiter et al., 2005).

The second manuscript (Maik Inthorn, Michiel Rutgers van der Loeff, Matthias Zabel: *Approaching particle exchange processes at the sediment water interface in the Benguela upwelling area based on $^{234}Th/^{238}U$ disequilibrium*, chapter 3) examines recent particle transport mechanisms, and the sedimentation regime at a slope-depth depocenter offshore Namibia with the particle reactive tracer ^{234}Th. Two different models concerning particle transport in the BNL are discussed, both of them explaining the observed ^{234}Th distribution. Based on the models, particle fluxes, residence times, and exchange with the sediment are quantified.

The third manuscript (Maik Inthorn, Thomas Wagner, Georg Scheeder, Matthias Zabel: *Lateral transport controls distribution, quality and burial of organic matter along continental slopes in high-productivity areas*, chapter 4) uses different geochemical parameters to discriminate the relative influence of vertical input of settling particles and lateral particle transport in the BNL and INLs at the south-west African continental slope. From radiocarbon age determinations and qualitative parameters of OM a conceptualized particle flux model is developed, approaching the relative influence of vertical and lateral particle input to shelf and slope offshore Namibia. The influence of lateral transport on quality and preservation of organic matter is estimated. By comparison to results from other continental margins, broader implications for the global biogeochemical cycles, limitations of common carbon flux models, and the interpretation of OC depocenters in the geological record are discussed.

1.3.4. Preservation

High particle sinking velocities through aggregational processes, and inorganic ballast minerals protect OM from degradation (e.g. Hedges et al., 2001). However, most of the organic matter produced in the euphotic zone is remineralized within the surface waters, thereby releasing dissolved organic carbon (DOC), CO_2, and nutrients into the water. The flux through the lower boundary of the photic zone is also termed "new production". In shelf areas, it makes up about 30% of the PP compared to only 15% in the open ocean. Remineralization continues throughout the water column so that only 4 - 17% of the PP reaches the sea-floor in ocean margin areas, and only about 1.5% in the deep-sea (Lampitt et al., 1995; Wenzhöfer and Glud, 2002; Wollast, 1998). Prior to final burial in the deep sediments, which is equivalent to sequestration of OC from the active global carbon cycle, diagenesis reduces this share to 0.5 - 3% along the ocean margins and to less than 0.01% in the deep-sea (Wollast, 1998). Accordingly, more than 90% of all organic carbon burial in the ocean occurs in continental margin sediments (Hartnett et al., 1998). The proportion of the organic matter being ultimately preserved in the sediments during burial is called the 'burial efficiency', and is primarily determined by the sedimentation rate (Armstrong et al., 2002; Müller and Suess, 1979). Most OM is deposited below the highly productive shelf seas. However, surface sediments on wide areas of the upper continental slope are also enriched in OC relative to their surroundings (Premuzic et al., 1982; Seiter et al., 2004). Such slope-depth "depocenters" of organic carbon are described for many continental margins all around the ocean, e.g. at the Mid Atlantic Bight (Anderson et al., 1994), offshore California

(Reimers et al., 1992), Peru (Arthur et al., 1998), Oman (Pedersen et al., 1992), Norway (Fohrmann et al., 2001; Rumohr et al., 2001), Argentina (Hensen et al., 2000) and Namibia (Bremner, 1981; Bremner and Willis, 1993).

It is still controversial, whether such depocenters develop due to enhanced preservation of OM in strongly oxygen-deficient bottom waters, and whether they represent modern analogues of black shales, sapropels, and petroleum source rocks in the geological record. Exposure to oxygen is commonly thought to be the master variable controlling the characteristics of organic matter reaching the sediment–water interface (e.g. Canfield, 1994; Dean and Gardner, 1998; Dean et al., 1994). However, several recent studies suggest that there may not be a difference in rate and extent of degradation of organic carbon OC in oxic vs. anoxic settings and that OC-content as well as OM preservation mostly do not reflect the boundaries of areas, in which oxygen-minimum zones impinge on the continental margins (Arthur et al., 1998; Calvert and Pedersen, 1992). Instead, enhanced PP of the surface waters is proposed as the key variable (Calvert et al., 1995; Ganeshram et al., 1999; Pedersen et al., 1992). The mediatory position attributes varying importance to the two parameters depending on the respective oceanographic settings. In this discussion, it is often neglected that lateral transport processes are also known to have significant impact on the quality of OM, and its preservation potential during diagenesis. Particles being laterally transported in suspension close to the seafloor are supposed to undergo repeated sedimentation and resuspension loops, combined with aggregation/disaggregation processes of the particles (Fig. 1.5; Thomsen and van Weering, 1998). This process increases the exposed area and exposure time of particles to oxic, bacterial degradation. Therefore, lateral transport has to be considered in paleoceanographic interpretations of sedimentary signals (Freudenthal et al., 2002; Hall and McCave, 1998; Mollenhauer et al., 2002), and in estimating the potential of the sediments to become petroleum source rocks (Ganeshram et al., 1999; Gelinas et al., 2001).

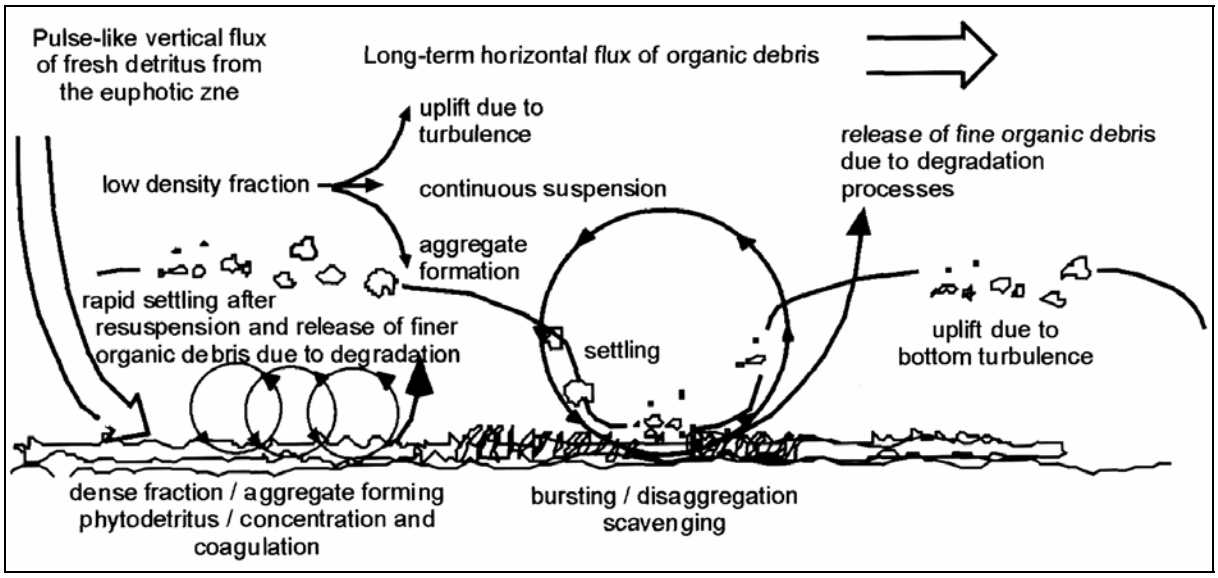

Fig. 1.5. Schematic model of a resuspension loop of aggregated particles (from Thomsen, 2003).

As Ransom et al. (1998) showed for samples from the California margin, the composition of typical BNL-aggregates differs considerably from pelagic marine snow. The benthic aggregates are assemblages of clay particles, clay flocs, and relatively dense clay-organic-rich microaggregates in an exocellular organic matrix. Predominantly, microbial exudates are responsible for the formation and strength of the aggregates transported within the resuspension loops. Up to 4% of the transported particulate organic carbon (POC) occurs in the form of bacterial organic carbon. 35 to 65% of these bacteria are attached to aggregates and thus perform the same resuspension loops (Ritzrau, 1996). Boetius et al. (2000a) point out that the laterally transported aggregates and DOC in the BNL are most likely the main source of energy for bacteria living in the BNL. However, macrobenthic animals also rely on advective particle transport as their most important food supply (Graf and Rosenberg, 1997). Bauer and Druffel (1998) used data on radiocarbon abundance to reveal that POC and DOC in the bottommost water layer above continental slopes in the western North Atlantic and the eastern North Pacific have a high ^{14}C-age of several thousand years. With respect to the composition of the adjacent deep-sea sediments, they derived that the input of this old OM is considerably higher, compared to vertical input of recently produced OM from the surface ocean.

With regard to the high significance of lateral particle transport, recent work has expanded a concept considering the influence of oxygen exposure time (OET) of OM with respect to its preservation. While Hartnett et al. (1998) and Gelinas et al. (2001) focused on the in-situ-OET ($_{is}$OET) of OM in the sediment prior to its burial to anoxic layers, Keil et al. (2004) considered the overall OET ($_{\Sigma}$OET) including $_{is}$OET as well as OET during transport ($_{t}$OET) from its place of production towards its final burial in the sediment. They estimated that $_{t}$OET would double the $_{\Sigma}$OET for OM transported across the Washington margin.

One reason for the comparatively low number of studies concerning processes in the BBL is the lack of suitable sampling techniques. A new sampling and monitoring system for the lowermost meter of the water column was developed in the course of this project. Its design and a review of results achieved with the bottom water sampler up to now are presented in the fourth manuscript (Maik Inthorn, Thomas Kumbier and Matthias Zabel: *BeaWiS - A new sampling and monitoring device for the benthic boundary layer*, chapter 5).

1.4. The Benguela upwelling system

The Benguela upwelling system (BUS) offshore southwestern Africa (Fig. 1.6) is one of the four major eastern boundary regions of the ocean together with California, Peru, and northwest Africa. Recent studies estimate the BUS to be even the most productive of these areas with an estimated PP of 0.37 Gt carbon per year (Carr, 2001). Due to the high bioproduction, the BUS is also one of the main fishing grounds of the ocean, and, therefore, of high economical interest.

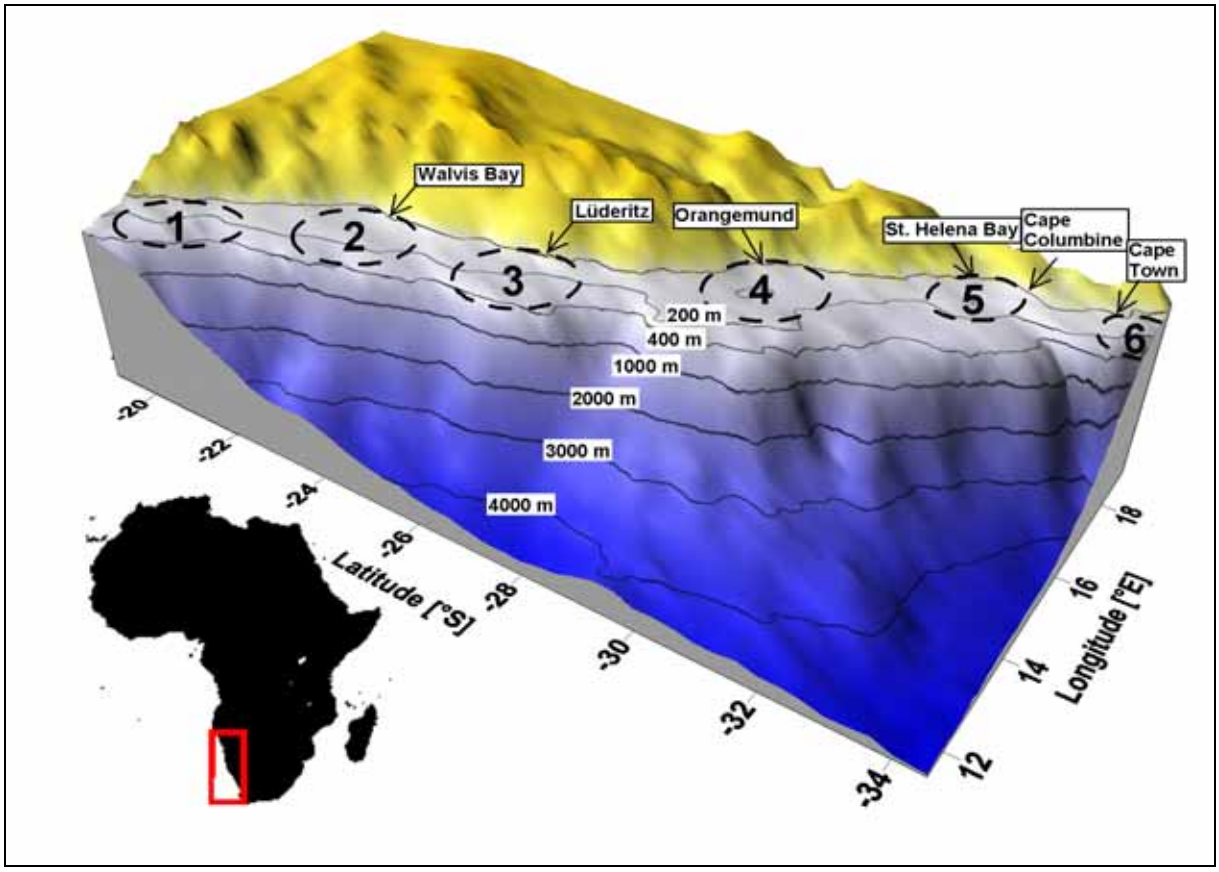

Fig. 1.6. Bathymetrical map of the continental margin offshore southwestern Africa. The major upwelling cells above the shelf are indicated by dashed lines (1: Namibia, 2: Walvis, 3: Lüderitz, 4: Namaqua, 5: Columbine, 6: Peninsula; the Kunene cell [17°S] is not shown here).

Consequently, scientific interest in the BUS was roused relatively early in the previous century. During the early METEOR expeditions in the 1920s a number of sediment samples were taken from the coast parallel belt of diatomaceous mud rich in OC, centered on the shelf off Walvis Bay. This was followed by the path leading work of Brongersma-Sanders (1948), who mentioned mass mortality events of fish along the beaches of Walvis Bay as well as the "very unpleasant odour reminiscent of H_2S and of the odour characteristic of putrefaction" of the "mudbelt" sediments for the first time in a scientific work. The research on the special geochemisty of the sediments was intensified since the 1970 (e.g. Calvert and Price, 1970; 1983). The composition of the shelf and upper slope sediments of the entire BUS was described in a major survey of the Geological Survey of South Africa and the University of Cape Town (Birch, 1975; Bremner, 1981; Rogers, 1977). In the course of that work, a secondary major OC enrichment at the continental slope offshore Namibia was detected (Bremner, 1981). An oxygen minimum zone (OMZ) extends above the shelf and upper slope in a water depth of 100 to 450 m (Bailey, 1991). Close to the coast, bottom waters and sedimentary porewaters are characterized by anoxic conditions, leading to the formation of sulfidic sediments (Berger and Wefer, 2002; Bremner, 1981; Brüchert et al., 2003), and temporary, large-scale emanations of hydrogen sulfide into the coastal waters, observable on satellite images (Weeks, 2001). In the sediments of the BUS, Thiomargarita namibiensis, the largest bacteria in the world, was detected for the first time (Schulz et al., 1999). They oxidize

sulfide and are connected to the formation of phosphorite deposits (Schulz and Schulz, 2005). These are only some of the most spectacular scientific results from the BUS. Accordingly, ecosystem, oceanography, surface water productivity, as well as composition and diagenetic processes in the underlying sediment have been subject to intensive scientific studies. However, it is noteworthy that up to now, only very little information on particle transport processes below the surface waters of the BUS have been published. Bishop et al. (1978) used a multiple-in-situ-pump at four stations north of Walvis Bay to gain information on chemistry, biology, and vertical flux of particulate matter. Giraudeau et al. (2000) provided flux data of biogenic particles from a single sediment trap deployed offshore Walvis Bay. They proposed for the first time that the bulk of biogenic particles deposited on the slope is resuspended material from the outer shelf. Conversely, the direct input from surface waters does not contribute to a high extent to the particle flux at depth (Giraudeau et al., 2000). Additionally, the relevance of advective processes in the BUS was proposed in studies on carbon turnover at the sediment interface (Seiter et al., 2005), studies of sedimentary processes (Mollenhauer et al., 2002; Summerhayes et al., 1995b), and onspecific sediment properties (Mollenhauer et al., 2003).

1.4.1. Geomorphology and oceanographic settings

The continental margin off southwestern Africa constitutes the eastern boundary of the 5000 m deep Cape basin, separated from the Angola basin in the north by the southwestward striking Walvis Ridge (Fig. 1.6). The Walvis Ridge, with water depths below 3000 m, provides a natural barrier for deepwater currents. Another southwestward striking ridge with water depths below 3000 m is the Agulhas Ridge, forming the southern boundary of the basin. The continental slope dips gently (with about 1°) to the west, and there are few reports on deep-water slumps at this passive margin (Rogers and Bremner, 1991). The shelf has wide (about 100 km) and rounded features with the main shelf break at 360 to 400 m water depth. Near Walvis Bay, a second, minor shelf break is distinguishable at about 160 m water depth.

The Orange river represents the only important freshwater discharge towards the southeastern Atlantic with a mean sediment load of 6×10^7 tons yr^{-1} (Rogers, 1979). Alongshore, south-eastern trade-winds dominate the wind-field so that the temporally occurring, strong E/NE-Bergwinds represent the most important aeolian particle source. Overall, there is little input of terrigenous material (Fischer et al., 1998; Shannon and Nelson, 1996).

The Benguela Current System (BCS) is part of the subtropical, anticyclonic gyre of the South-Atlantic (Fig. 1.7; Peterson and Stramma, 1991) and consists of two branches (Fig. 1.6): The Benguela Oceanic Current (BOC)is the equatorward drift of cool surface waters flowing along the Western coast of South Africa up to about 30°S, where its main branch diverges offshore from the Namibian coast. The Benguela Coastal current (BCC) is the smaller

component of the BCS that continues equatorward as far as 14°S above the Namibian shelf (Mohrholz et al., 2001). A significant poleward subsurface flow of nutrient-rich, but oxygen poor South-Atlantic Central Water (SACW) is known from the northern Benguela (Hart and Currie, 1960). There is little information on current directions and velocities in the deeper water column. A small-scale survey of Gordon et al. (1995) suggests predominant southeastward subsurface water flow.

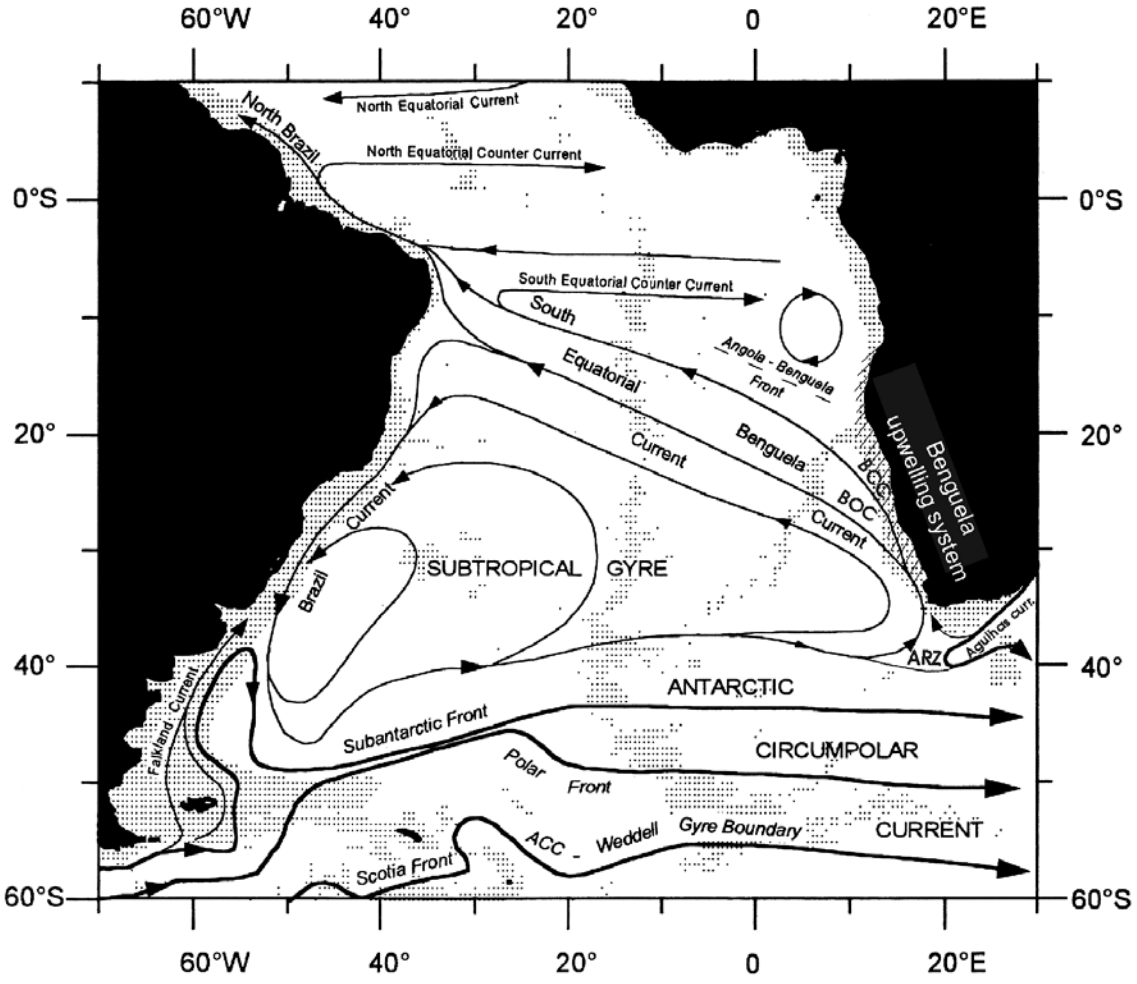

Fig. 1.7. Schematic representation of the large-scale surface currents and fronts in the South Atlantic (from Berger and Wefer, 2002). The Benguela upwelling system is shown hatched. BOC: Benguela oceanic current, BCC: Benguela coastal current, ARZ: Agulhas retroflection zone.

The northern boundary of the BCS is demarcated by the Angola-Benguela front, where it meets the warm Angola Current (Fig. 1.7; Mohrholz et al., 2001). This is the mixing site of warm, relatively nutrient rich, oxygen-poor surface waters from the north, and colder, relatively nutrient poor waters from the south. In the south, the Agulhas retroflection zone separates the Benguela from the warm Agulhas current originating in the Indic Ocean. Only occasionally, substantial intrusion of Agulhas water into the southern Benguela takes place (Shannon and Nelson, 1996). The hydrographic properties of the different water masses comprising the water column in the BUS are described in chapter 2.

South-easterly trade winds prevail most of the year. They cause offshore Ekmann transport of the surface waters along the southwest African coast and result finally in upwelling of cold subthermocline waters from water depth of 50 to 200 m (e.g. Shannon and Nelson, 1996; Fig. 1.8a). This water is additionally enriched in nutrients that stem from diagenetic processes in the lower water column and the surface sediments. Seven major centers of upwelling can be distinguished in the BUS (Fig. 1.6): Lüderitz (25°S), Namaqua (29°S), Columbine (32°S), Walvis (22°S), Namibia (19°S), Peninsula (34°S), Kunene (17°S). Remarkably, their positions often coincide with changes in orientation of the coastline. The most intensive and perennial upwelling centre is located north of Lüderitz. The Walvis cell is also strong but more susceptible to seasonal changes. Due to the coupling of PP to nutrient availability, it is mainly constrained to the inner shelf area, downstream of the turbulent upwelling cells (Fig. 1.8b; Campillo-Campbell and Gordoa, 2004; Carr, 2001). However, filaments of cold, low saline water were observed to extend up to a thousand kilometres further westward, and have a typical life-span of a few days to several weeks (Lutjeharms et al., 1991). The particular significance of these filaments lies in their surficial transport of microplancton perpendicular to the coast and across the shelf-break towards the slope area.

The cold upwelled water has the tendency of sinking back below the sea surface. This is one reason for the development of a frontal system. The boundary between the coastal upwelling and the oceanic basin regime often produces such a quasi-stationary front close to the position of the shelf-break. This is accompanied by a northward directed jet current, and distorted by eddies and filaments (Smith, 1995). Several studies (e.g. Barange and Pillar, 1992; Hart and Currie, 1960) suppose secondary upwelling to take place seaward of this shelf break front. The result would be a wide recirculation cell above the shelf. However, this process is still not fully understood, and the permanence of this feature has not been established. Dependence of the upwelling on seasonal changes in the wind field and the current system have to be considered. Upwelling might cease completely in the so called "Benguela Nino" events, which are accompanied by substantial intrusions of warm tropical surface waters into the Benguela (Mohrholz et al., 2001).

Hart and Currie (1960) suggested the poleward-flowing, nutrient-rich but oxygen-poor waters of the SACW as the major source of the upwelled waters. The upwelling induces strong PP. The resulting intensive decomposition of organic matter in the water column and the surface sediments leads to further consumption of oxygen of the subsurface waters. This was proposed to be the reason for the intensive oxygen minimum zone offshore Namibia (e.g. Bailey, 1991; compare chapter 2.1.). When oxygen is depleted, anaerobic bacteria use nitrate as an electron acceptor while oxidizing organic matter, which then becomes the dominant mineralization process in the water column. Globally, 30–50% of the total nitrogen loss occurs in OMZs, and is commonly attributed to denitrification (reduction of nitrate to N_2 by heterotrophic bacteria, e.g. Tyrrell and Lucas, 2002). Recently, however Kuypers et al. (2005) showed that instead the anammox process (the anaerobic oxidation of ammonium by nitrite to yield N_2) is mainly responsible for nitrogen loss in the OMZ waters of the Benguela upwelling system. Generally, carbon dioxide, ammonium, and phosphate are released in the

same ratio, the so-called Redfield ratio, when phytoplankton derived organic matter is remineralized (Redfield et al., 1963). However, a strong nitrogen deficit (i.e., a decrease in the ratio of fixed inorganic N to P) was detected in the bottom waters of the Benguela, and is attributed to the anammox process (Kuypers et al., 2005).

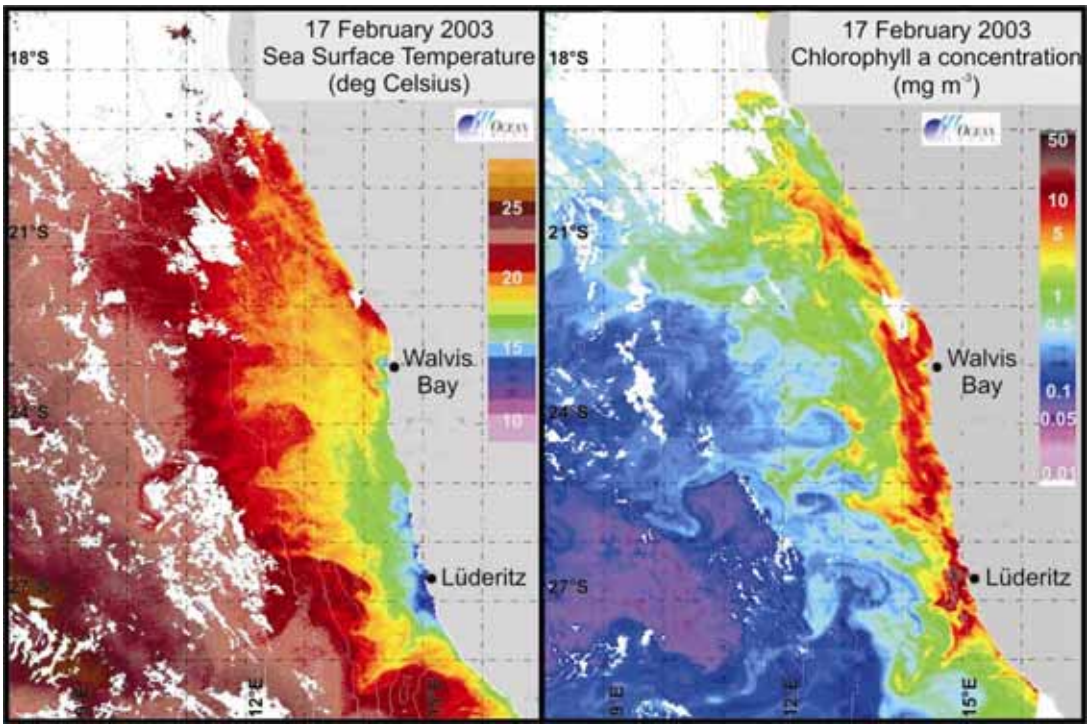

Fig. 1.8. a) Surface water temperature and b) chlorophyll α in the surface waters offshore Namibia, recorded with the SeaWiFS satellite on 17 February 2003, during cruise M57/2.

The fifth manuscript (Gaute Lavik and Maik Inthorn: *Upwelling of nitrogen depleted waters controls the nitrogen isotope composition of particulate matter on the Namibian shelf*, chapter 6) evaluates the effects of the nitrogen deficit in the upwelling water offshore Namibia on nitrogen isotope composition of suspended particles. This is compared to the influence of limited nitrate availability in the photic zone, which was previously preferred to explain high $\delta^{15}N$-values of particles that settle through the water column or are deposited in the sediments of the BUS. The distribution of $\delta^{15}N$ (together with POC and nutrients) in water column particles along several transects across the Namibian shelf and upper slope is compared to $\delta^{15}N$ of surface sediment samples.

2. Nepheloid layer distribution in the Benguela upwelling area offshore Namibia

Maik Inthorn[1], Volker Mohrholz[2], Matthias Zabel[1]

[1]*University of Bremen, FB5 – Geosciences, Klagenfurter Str., D-28359 Bremen, Germany*

[2]*Baltic Sea Research Institute, Seestraße 15, D-18119 Rostock Warnemünde, Germany*

2.1. Abstract

The distribution of nepheloid layers across the outer shelf and upper continental slope off Namibia was studied during a cruise with RV *Meteor* in late austral summer 2003. Optical measurements, carried out with a transmissometer and a backscattering fluorometer, are correlated with suspended particulate matter (SPM) and particulate organic carbon (POC) values from water sample filtration. Conductivity-temperature-depth and oxygen data are used to relate the nepheloid layers to hydrographic structures. The particle content of surface water at the continental slope is controlled primarily by the offshore extension of high-productive upwelling filaments. A pronounced bottom nepheloid layer (BNL) covers the entire area of study with maximum intensity above the outer shelf and at the shelf break – an area, where erosional forces dominate. The detachment of this BNL at the shelf break feeds a major intermediate nepheloid layer (INL) at 25.5°S. This INL is positioned at 250 to 400 m water depth, at the lower boundary of an oxygen minimum zone, and is likely connected to the poleward flow of South Atlantic Central Water (SACW) across the shelf break. Together, these strong subsurface nepheloid layers are indicators of intensive lateral particle transport from the outer shelf towards a depocenter of organic matter on the upper continental slope.

2.2. Introduction

Upwelling areas are of major importance regarding global ocean primary production and export of particulate organic matter from coastal areas towards the deep sea realm (Jahnke, 1996; Summerhayes et al., 1995a; Walsh, 1991). While surface water production can be studied in detail using satellite data (e.g. Behrenfeld and Falkowski, 1997; Campillo-Campbell and Gordoa, 2004; Carr, 2001), our knowledge of the fate of organic matter below the sea surface is comparatively limited. In this context, special importance has been ascribed to the lateral particle transport in nepheloid layers, defined by an enhanced particle content relative to the surrounding waters. Generally, three types of nepheloid layers have been described: 1) surface nepheloid layers (SNL) are generally associated with the biologically active surface mixed layer (e.g. Gardner et al., 1993; Gundersen et al., 1998; Oliveira et al., 2002), 2) bottom nepheloid layers (BNL) are found in the lowermost water column and are maintained by turbulent mixing in the bottom boundary layer (e.g. Bacon and Rutgers van der Loeff, 1989; Graf and Rosenberg, 1997; McCave, 1986), and 3) intermediate nepheloid layers (INL) result from the accumulation or transport of particles in intermediate waters in association with strong density gradients (e.g. Azetsu-Scott et al., 1995; Cacchione and Drake, 1986; McCave et al., 2001; Pak et al., 1980). These nepheloid layers vary significantly in intensity and dimension, from a few meters to hundreds of meters, and may be temporary features. BNLs and INLs are important phenomena concerning the lateral, long distance transport of particles from the shelf to slope and deep sea environments (Jahnke et al., 1990). Studies indicate that, together, lateral transport in shelf and slope-depth INLs contribute more significantly to the deposition of particulate organic matter on the lower slope than the direct vertical settling of particles from the surface layer (McPhee-Shaw et al., 2004).

A good option for tracing these deep lateral particle transport processes are optical sensors. Many studies used different sensor techniques to visualize the position and extent of nepheloid layers at continental margins all over the world, including the upwelling areas offshore California (Cacchione et al., 1999; McPhee-Shaw et al., 2004) and Peru (Pak et al., 1980), as well as the continental margin off eastern N-America (Richardson, 1987), NW-Europe (McCave et al., 2001; Thorpe and White, 1988), the Iberian peninsula (Hall et al., 2000; McCave and Hall, 2002; Oliveira et al., 2002; Puig and Palanques, 1998; van Weering et al., 2002) and Norway (Fohrmann et al., 2001). The major advantage of the sensor-techniques compared to water sampling at distinct depths and determination of the particle content by filtration is the higher spatial resolution of the data. Thus, optical measurements are well suited for studying the patchiness of particle distribution in the water column in detail that could be missed with conventional bottle sampling.

During cruise M57/2 of RV *Meteor* in February and March 2003, we conducted the first survey of that kind in the Benguela upwelling area. Nepheloid layer distribution across the continental slope offshore Namibia were determined through comparison of beam attenuation and light scattering with particle samples from conventional bottle sampling.

Salinity, temperature and oxygen were measured simultaneously to approach the general oceanographic settings as well as the position of the oxygen minimum zone (OMZ) that is known from this area (Bailey, 1991; Brüchert et al., 2003).

2.2.1. Study area

The Benguela upwelling area is one of four major eastern oceanic upwelling regions, where the supply of nutrient-rich deep waters to the euphotic zone maintains intense primary production. During M57/2, sampling was conducted along three transects normal to the coast. The transects follow the outer shelf down to the continental slope between 23° and 25.5°S off Namibia (Fig. 2.1), the area where most intense upwelling occurs in the Benguela. The main shelf break is at 360 to 400 m water depth. Close to Walvis Bay the shelf is broad, and a second, minor shelf break is distinguishable at about 180 m water depth. In the southern part of the area of study (24.5°S), the shelf break makes a significant inshore directed turn so that the complete shelf is generally narrower. The little terrigenous input to this area is dominated by eolian dust mostly from the adjacent Namib desert, and transported by temporally occurring, strong east/north-eastern bergwinds (Shannon and Nelson, 1996). At present, there is no perennial river in this region.

2.2.2. Oceanographic settings

The surface waters off Namibia are mainly influenced by the Benguela Current System, described previously (BCS, Fig. 1, Hart and Currie, 1960; Nelson and Hutchings, 1983; Shannon and Nelson, 1996). The BCS is part of the subtropical, anticyclonic gyre of the South-Atlantic (Peterson and Stramma, 1991) and consists of two branches: 1) The Benguela Oceanic Current (BOC) represents an equatorward drift of cool surface waters flowing along the western coast of South Africa up to about 30°S, where its main branch diverges offshore from the Namibian coast. 2) The Benguela Coastal Current (BCC), a smaller component of the BCS continues equatorward as far as 14°S above the Namibian shelf (Mohrholz et al., 2001).

South-easterly trade winds induce upwelling of subthermocline, nutrient-rich waters close to the coast, generally from water depth of 50 to 200 m (e.g. Shannon and Nelson, 1996). Within the investigated area, two separate centers of intense upwelling exist: 1) the southern, strong and perennial Lüderitz cell at about 26°S, and 2) the northern, seasonally active Walvis Bay cell at 23°S (Shannon and Nelson, 1996). The cold upwelled water tends to sink back below the sea surface, one reason for the development of a longshore frontal system (Summerhayes et al., 1995b). The boundary between the coastal upwelling and the oceanic basin regime often produces a quasi-stationary front. This front is accompanied by a northward jet current and distorted by eddies and filaments extending up to thousand kilometers from the adjacent coast (Campillo-Campbell and Gordoa, 2004; Lutjeharms et al., 1991; Smith, 1995).

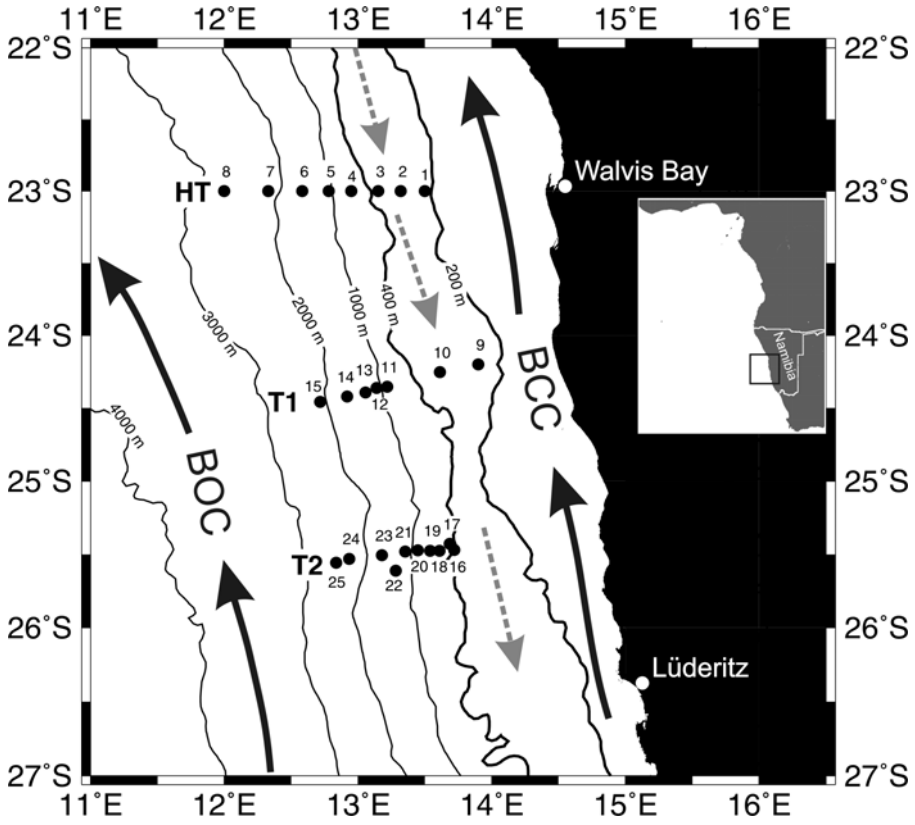

Fig. 2.1. Bathymetric map of the study area offshore Namibia showing station positions on the three major transects (HT, T1, T2). See Table 2.1 for date of sampling and the used devices. The main surface branches of the Benguela current system are indicated by black arrows: Benguela Oceanic Current (BOC) and Benguela Coastal Current (BCC). The poleward directed undercurrent over the outer shelf is indicated by grey arrows.

Much information has been collected regarding the surface and subsurface currents and water masses, as well as the upwelling process itself. However, little is known of the deeper water column. Shipboard ADCP measurements by Gordon et al. (1995) show that at 27°S only in a restricted area above the outer shelf the surface waters are actually moving northwest with the BCC. Further inshore, offshore, and everywhere below 100 m water depth, the overall water flow is southeastward.

2.3. Methods

During RV *Meteor* cruise M57/2 (11 February – 12 March 2003) a SEATECH transmissometer (path length r = 25 cm) connected to an SBE 19 CTD profiler was used to evaluate particle distribution during a total of 13 deployments (Fig. 2.1 and Table 2.1). The transmissometer was horizontally attached to the frame of a bottom water sampler (Inthorn et al., subm.-a; chapter 3). Because attenuation due to water is essentially constant for this instrument, the signal correlates linearly to the particle content of the water. Calibration of

the sensor-data using values for suspended particulate matter (SPM) or particulate organic carbon (POC) obtained from the filtration of appertaining seawater samples has been applied in a number of previous studies (Bishop, 1986; 1999; Gardner et al., 2003; Gardner et al., 1993; McCave et al., 2001; Mishonov et al., 2003). However, the linear correlation between these parameters holds only for particles with a small grain size range as well as comparable composition and surface characteristics (Richardson, 1987). Percent transmission is measured and then converted to beam attenuation (c) using the equation

$$Tr = e^{-cr}.$$

Raw data were sampled with two scans per second and binned to a standard 2 db pressure interval. Further processing and quality control of the data to receive beam attenuation values proceeded according to Gardner et al. (1993).

Table 2.1. Stations of M57/2 that were sampled using the bottom water sampler (BWS) and/or a standard rosette (ROS). For positions see Fig. 2.1.

site	station no.	device	depth [m]	date	water samples
1	8439	ROS	242	02-21-03	no
2	8440	ROS	355	02-21-03	yes
3	8441	ROS	318	02-21-03	yes
4	8442	ROS	596	02-21-03	yes
	84105	BWS	601	03-09-03	no
5	8443	ROS	951	02-22-03	yes
6	8444	ROS	1439	02-22-03	yes
	84104	BWS	1440	03-09-03	no
7	8445	ROS	2085	02-22-03	yes
8	8446	ROS	2724	02-22-03	yes
9	8431	ROS	257	02-21-03	no
10	8420	ROS	314	02-16-03	no
11	8419	ROS	834	02-15-03	yes
12	8418	ROS, BWS	998	02-15-03	yes
13	8421	ROS	1205	02-16-03	yes
	84101	BWS	1204	03-08-03	no
	84103	ROS	1231	03-08-03	no
14	8424	ROS, BWS	1518	02-17-03	yes
15	8422	ROS	1979	02-16-03	yes
16	8428	ROS	360	02-19-03	no
17	8457	ROS, BWS	390	02-24-03	yes
18	8458	ROS, BWS	500	02-25-03	yes
19	8456	ROS	630	02-24-03	yes
	8491	ROS, BWS	598	03-05-03	yes
20	8448	ROS	806	02-23-03	yes
	8459	BWS	801	02-25-03	no
21	8426	BWS	1049	02-19-03	no
	8490	ROS, BWS	1030	03-05-03	yes
22	8463	ROS, BWS	1328	02-27-03	no
23	8489	ROS, BWS	1510	03-05-03	yes
24	8462	ROS	2290	02-27-03	yes
25	8470	ROS	2472	03-02-03	no

In addition, light scattering (turbidity) was determined with a 2-channel DR. HAARDT BackScat II fluorometer connected to an SBE 911+ CTD with a SBE 43 oxygen sensor at a total of 27 stations (Fig. 2.1 and Table 2.1). Data were processed as mentioned above. The sensors were attached to a HYDROBIOS rosette sampler equipped with 12 five-liter free flow water sample bottles of HYDROBIOS. A bottom tracker was used to stop the rosette's descent 2-4 m above the sea floor.

From 19 of the rosette deployments, water was sampled for determination of the SPM and POC content spanning the whole profile of the water column. 1 to 5 liters of water (volumetrically determined) were filtered through 2.5 cm pre-combusted and pre-weighed glass fiber filters (SCHLEICHER & SCHUELL, GF52) with a pore size spectrum of 4 to 6 µm. All filters were rinsed with a few milliliters of distilled water to remove sea salt and stored deep frozen for transport to the home laboratory. SPM was determined by reweighing of the freeze-dried filters. Afterwards, sub-samples of the filters were exposed to smoking concentrated hydrochloric acid for at least 12 hours to remove inorganic carbon and combusted in a CARLO ERBA Element CNS Analyzer for photometric determination of the carbon content so that POC values could be calculated.

2.4. Results

2.4.1. Hydrographic structure

The northernmost "hydrographic" transect (HT) at 23°S was sampled four times during our cruise to gain information on the overall oceanographic situation. This transect intersects the Walvis Bay upwelling cell. Transect 2 (T2) is located at about 25.5°S, seaward of the Lüderitz upwelling cell, while transect 1 (T1) is positioned at about 24.3°S, an intermediate position between these two major cells of the Benguela upwelling area. Fig. 2.2 shows some characteristic properties of different water masses comprising the water column in the area of study. During M57/2, trade-winds and upwelling intensity were weak. The surface water layer was characterized by temperatures of 12 °C close to the coast, increasing offshore to 20 °C above the continental slope. Below the thermocline, two central water masses are identified. Salty, nutrient-rich, oxygen-poor South Atlantic Central Water (SACW) moves south as a poleward undercurrent (Fig. 2.1). The SACW is usually somewhat beneath the fresher and nutrient-poor Eastern South Atlantic Central Water (ESACW). Among these water layers, there is a significant oxygen deficit at most stations. Between 150 to 450 m depth, geochemical conditions are suboxic to anoxic. This oxygen minimum zone is more intense closer to the shelf, where the influence of the relatively salty, nutrient-rich, oxygen-poor, poleward flowing SACW is strongest. From figures 2.3, 2.4, and 2.5, the intensity of the oxygen minimum layer above the continental shelf decreases from the North to the South, consistent with a weakening of the SACW. Of note, the oxygen minimum layer extends further offshore at T2 than at T1. In this southerly area, the oxygen content of the

central water depth above the continental slope is more heterogeneous. The freshest water mass of the area is the Antarctic Intermediate Water (AAIW) with its core at 700-800 m water depth (Shannon and Nelson, 1996). The AAIW's main flow in the northern Benguela area is thought to be southward, accounting for increased salinity over its South Atlantic counterpart (Gordon et al., 1995). The lowermost water mass sampled is the salty and cold North Atlantic Deep Water (NADW) generally flowing southward (Shannon and Nelson, 1996).

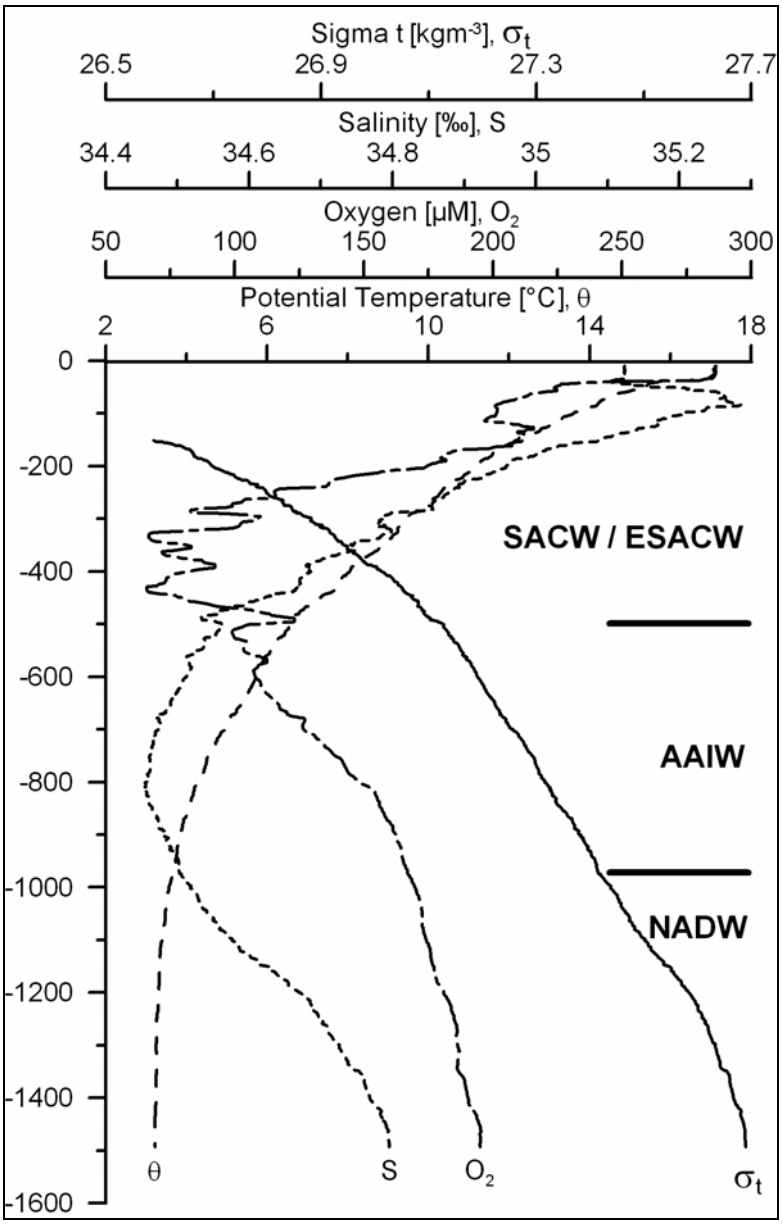

Fig. 2.2. Hydrographic parameters showing water mass distribution at the continental slope offshore Namibia at 25.5°S. SACW: South Atlantic Central Water, ESACW: Eastern South Atlantic Central Water, AAIW: Antarctic Intermediate Water, NADW: North Atlantic Deep Water.

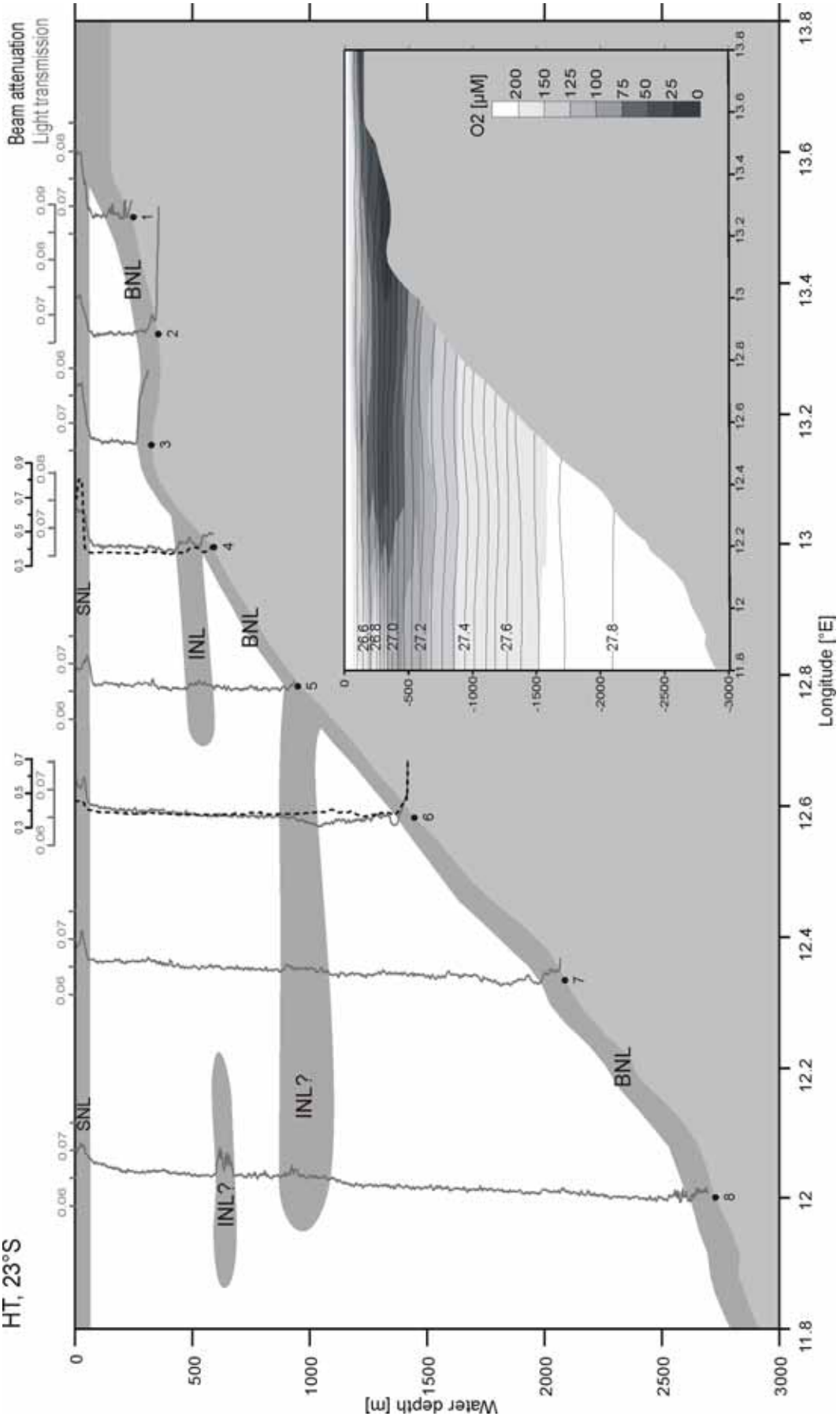

Fig. 2.3. Nepheloid layer distribution with depth, based on beam attenuation (scattered black lines) and light scattering (solid grey lines) profiles, across the continental margin off Namibia at HT at 23°S. For comparison, water density (sigma-t) as isolines and oxygen content of the same transect are shown on the inlay.

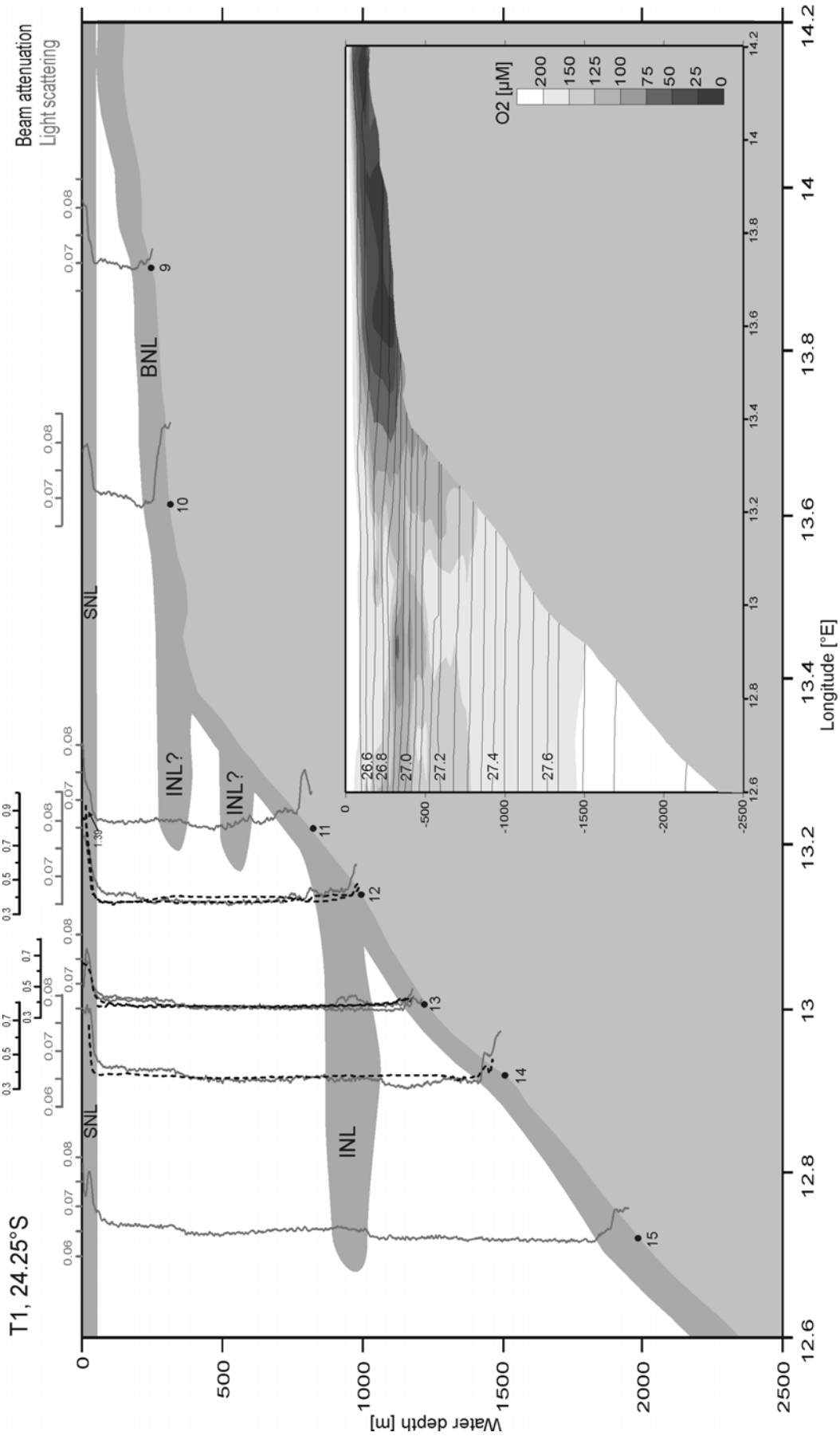

Fig. 2.4. Nepheloid layer distribution with depth, based on beam attenuation (scattered black lines) and light scattering (solid grey lines) across the continental margin off Namibia at T1 at 24.25°S. For comparison, water density (sigma-t) as isolines and oxygen content of the same transect are shown on the inlay.

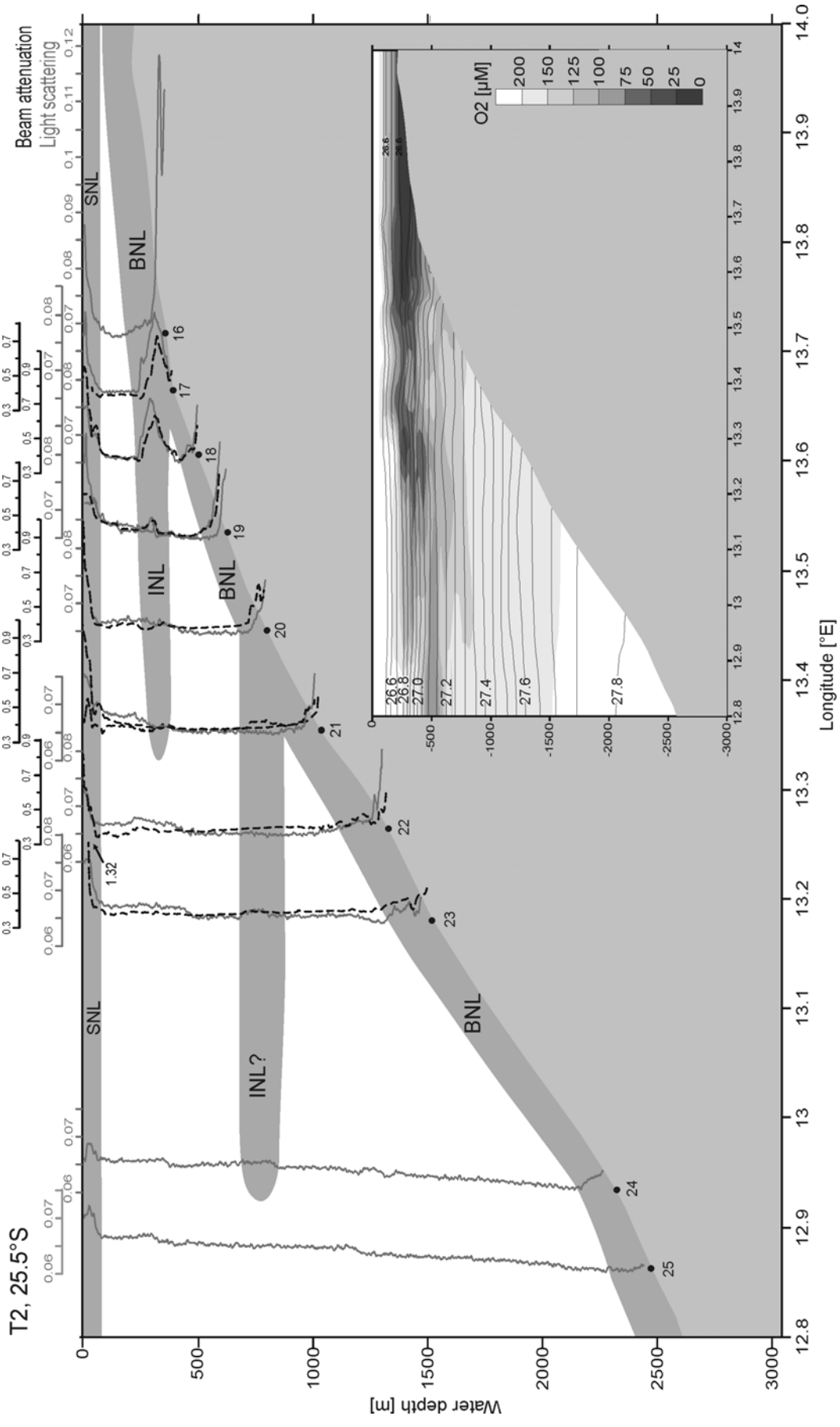

Fig. 2.5. Nepheloid layer distribution with depth, based on beam attenuation (scattered black lines) and light scattering (solid grey lines) across the continental margin off Namibia at T2 at 25.5°S. For comparison, water density (sigma-t) as isolines and oxygen content of the same transect are shown on the inlay.

2.4.2. Nepheloid layers in the water column

Surface nepheloid layer (SNL)

The SNL rather consistently covers the uppermost 50 to 75 m of the water column at all three transects (Figs. 2.3, 2.4, and 2.5). At most stations, highest attenuation and light scattering values are reached close to the sea surface. However, the overall thickness of the SNL seems to increase, the maximum shifting to the lower euphotic zone, with greater distance from the shore. Nutrient depletion of surface waters off the main upwelling centers on the inner shelf may account for this gradient.

SeaWIFS-satellite data of chlorophyll α indicate intensity of productivity in surface waters (Fig. 2.6). Highest productivity is located in shelf waters (Campillo-Campbell and Gordoa, 2004; Carr, 2001; Mollenhauer et al., 2002). Above the continental slope, productivity is restricted to filaments of nutrient-rich water. The position of these filaments is reflected in the particle content of surface waters, which varies significantly from station to station and between transects (Figs. 2.3, 2.4, and 2.5). A high-productivity filament had just passed the position of T1 during our sampling period. Another filament was active at T2. Accordingly, sensor signals are quite high in the SNL for these transects compared to HT, where no filaments are recorded. At HT, only stations proximate to the shelf break and on the shelf show high SNL-intensity. At all stations, there is a significant decrease in signal intensity below the thermocline.

Intermediate nepheloid layers (INL)

An intensive INL was detected at T2 in the lower part of the oxygen minimum zone at 250 to 400 m depth, with its maximum at 300 m (Fig. 2.5). This depth is also approximately the depth of the shelf break. Additionally, a sharp decrease in salinity and temperature is marked by tight iso-density lines at this depth (inlay in Fig. 2.5). Thus, 250-400 m demarcates the lower boundary of the SACW. At stations 17 and 18, the light scattering signal for the INL is as high as the respective SNL signal. Further offshore, the sensor signal of this INL diminishes drastically. There is no comparably prominent INL at any of the other transects. Light scattering and beam attenuation profiles from HT and T1 indicate only of a very weak rise in particle content at the same depth. Secondary INLs, much weaker than the shelf break INL at T2, are found in deeper waters at all three transects. At the lower boundaries of the central water mass at 500 to 600 m and the AAIW at 800 to 1000 m water depth, areas of enhanced particle content occur at least intermittently (Figs. 2.3, 2.4, and 2.5). Thus, these lower INLs are, at least during our sampling period, weak and impermanent features.

Bottom Nepheloid Layer (BNL)

Raised particle content close to the sea floor was detected at all stations (Figs. 2.3, 2.4, and 2.5). At most stations, SPM-values increase by about 100% with respect to clear water conditions, and reach up to 1 mg/l (Fig. 2.7a, b). The upper boundary of the BNL is generally 100 to 300 m above the sea floor, while a secondary sharp increase of the sensor signals is observable at the lowermost 20 to 50 meters, corresponding roughly to the height of the

bottom mixed layer as observable from density profiles. Nevertheless, thickness and strength of the BNL varies significantly. Along all transects, BNL-intensity is highest at the stations on the outer shelf near the shelf break (stations 2, 3, 10, 16), while the BNL is much weaker further inshore and offshore. Aside from the shelf break stations 2 and 3, BNL-activity and thickness is generally lesser at HT compared to the southern transects, except for station 6 at 1500 m water depth (Fig. 2.3). At T1, the BNL is strong on most of the slope stations (stations 11, 14, 15, Fig. 2.4). At T2, BNL-intensity remains continuously high down the slope to 1500 m water depth, and the BNL even shows a slight increase in thickness (Fig. 2.5). Below 1500 m depth, the BNL at T2 weakens significantly.

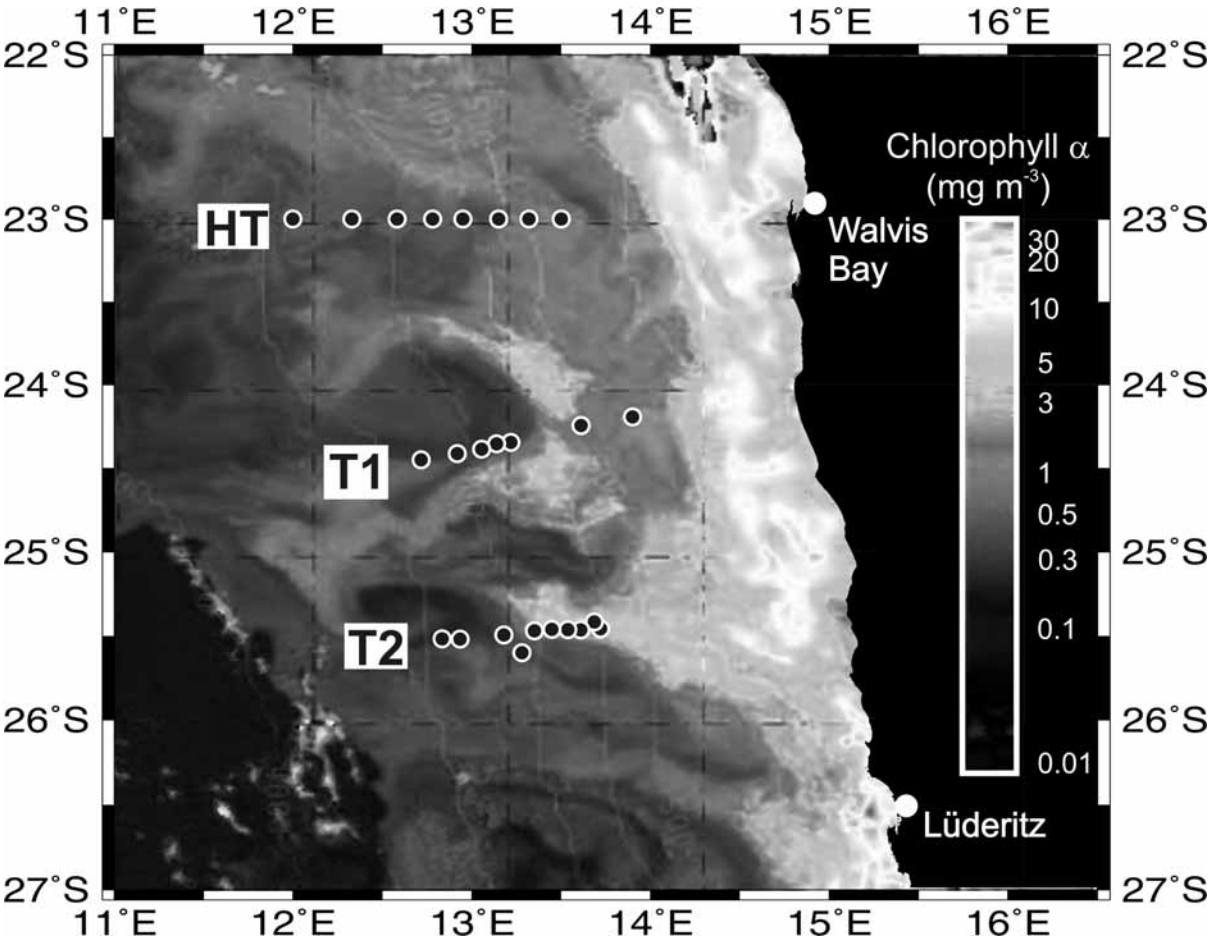

Fig. 2.6. SEAWIFS-picture of chlorophyll α concentration in the surface waters of the working area on 17th February 2003. Black and white circles are stations on the three transects of M57/2.

2.5. Discussion

2.5.1. Comparing beam attenuation and light scattering signal

Previous studies show that comparing data from different optical sensors and results of conventional bottle-sampling yields information concerning size and composition of the

suspended matter (Bishop, 1999; Gardner et al., 2003; Hall et al., 2000). In our data, beam attenuation usually exceeds the light scattering signal in the SNL (2.3, 2.4, and 2.5). Thus, our data show that transmissometers respond more intensively to the generally fresh, large, biogenic particles of the surface waters, as opposed to the BNL and the INLs, where light scattering exceeds beam attenuation. The fluorometer is more sensitive to these particles that are presumably finer and contain more refractory organic matter. However, there is good agreement between the two instruments for clear water conditions. Analogous results have been described for equivalent instruments by Hall et al. (2000). A calibration of transmissometer and fluorometer data with SPM and POC, determined from filtered samples, is complicated, due to the differences in optical properties of diverse types of suspended particles (Azetsu-Scott and Johnson, 1994; Richardson, 1987). Therefore, we didn't convert our sensor data to SPM or POC values, which was done in other papers (Hall et al., 2000; McCave and Hall, 2002; McCave et al., 2001).

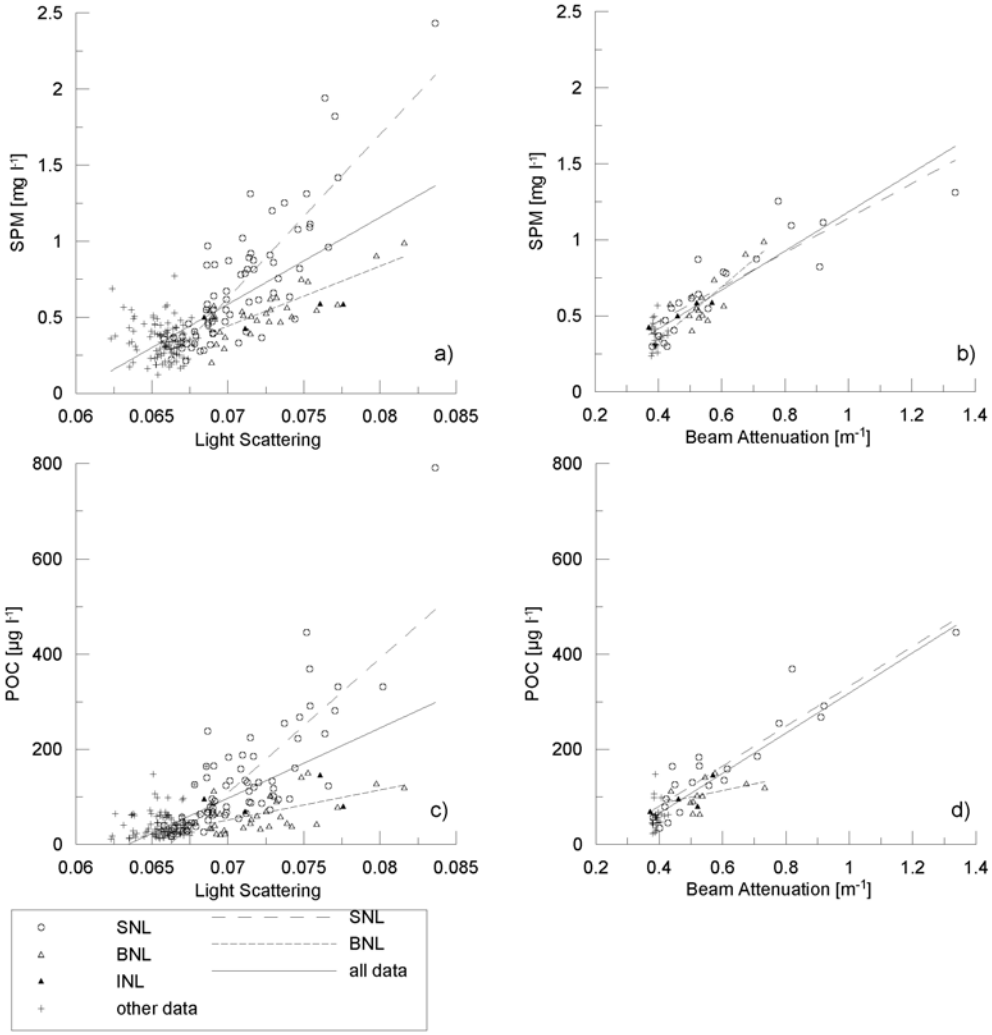

Fig. 2.7. Light scattering and beam attenuation calibration against SPM (a, b) and POC (c, d). For equations of the linear regression lines and their coefficient of determination see Table 2.2.

Table 2.2. Results of the calibration of light scattering and beam attenuation against SPM and POC visualized in Fig. 2.7.

x-axis	y-axis	sample locations	number of samples	equation	coefficient of determination (R^2)
light scattering	SPM	all data	203	Y = 57.1 * X - 3.41	0.49
		SNL	65	Y = 107.6 * X - 6.91	0.69
		BNL	29	Y = 39.4 * X - 2.31	0.63
	POC	all data	216	Y = 14800 * X - 936	0.45
		SNL	68	Y = 28300 * X - 1870	0.65
		BNL	30	Y = 6330 * X - 392	0.30
beam attenuation	SPM	all data	63	Y = 1.28 * X - 0.10	0.74
		SNL	20	Y = 1.13 * X - 0.01	0.75
		BNL	14	Y = 1.76 * X - 0.37	0.65
	POC	all data	63	Y = 422 * X - 103.7	0.81
		SNL	20	Y = 420 * X - 87.7	0.86
		BNL	11	Y = 140 * X + 29.3	0.17

Due to asynchronous deployments of the rosette and the BWS with intervals of more than one week at T1 and HT (see Table 2.1), beam attenuation can only be compared to SPM and POC determinations values from T2. Note that Fig. 2.7 and Table 2.2 illustrate the established difference in composition between particles from the SNL and from the deeper water column. We observed good correlation between beam attenuation and SPM and especially POC in the surface waters (Fig. 2.7, b and d), while correlation between light scattering and SPM and POC of SNL-samples is less but still significant (Fig. 2.7, a and c). Obviously, the high organic carbon content of these comparably fresh particles strongly influences the sensor-signal intensity. Below the SNL, there is much scatter in the data from all three transects (Fig. 2.7a and c). When data from a single transect (T2) are represented, a different pattern emerges, indicating general differences in particle composition at intermediate water depth between the three transects. One reason may be varying influence of high productivity filaments as well as terrigenous input. In subsurface waters, organic carbon plays an inferior role due to intense degradation processes. The light scattering signal is more sensitive to particles of the deep-water column than the beam attenuation, because though correlation of light scattering to SPM and POC remains strong for the BNL particles, it is lower for beam attenuation. Generally, data from the BNL and INLs show similar strong light scattering. But, as indicated by much shallower gradients of the regression lines for these data compared to the SNL-data, much smaller SPM and POC values occur (Table 2.2). Therefore, we assume that the suspension loads of BNL and INLs are dominated by fine, low-density particles depleted in organic matter compared to SNL particles. Nevertheless,

their organic carbon content, predominantly above 10%, is still considerably higher than in the underlying sediment.

2.5.2. Significance and source of subsurface nepheloid layers

The organic carbon content of surface sediments in our area of study shows a very heterogeneous distribution pattern. There is a prominent depocenter of organic carbon on the upper continental slope in water depth of 400 to 1500 m from 24.5° to 26°S (Fig. 8, Bremner, 1981; Mollenhauer et al., 2002; Inthorn et al., in press; chapter 4). Furthermore, suspiciously low organic carbon contents on the outer shelf and along the shelf edge support the hypothesis of locally prevailing erosion (Bremner and Willis, 1993; Inthorn et al., in press; chapter 4). Thus strong indication is given that intense lateral transport processes of suspended matter must take place in this region. Based on the absence of prominent canyons, submarine landslides or strong boundary currents, it is apparent that the main displacement of particles must occur within nepheloid layers. It is well known that particles can be transported laterally over large distances by cyclic sedimentation and resuspension within BNLs (Thomsen, 1999; Thomsen and van Weering, 1998). Due to aggregation, disaggregation, and microbial degradation processes, the organic fraction of SPM alters continuously (Thomsen and McCave, 2000). BNL-aggregates are known to be composed of clay flocs, and relatively dense, clay-organic-rich micro-aggregates in an exocellular organic matrix (Ransom et al., 1998). Our data from all three transects show highest BNL-intensities at stations 2, 3, 10, and 16, all positioned close to the shelf break (Figs. 2.3, 2.4, and 2.5). At these stations, light scattering in the BNL is so strong that it surpasses even sea surface values. Using the regression equation of SPM against light scattering in the BNL (Table 2.2), SPM-concentration in the BNL of station 16 would be as high as 2.1 mg/l. This supports the assumption that at least in this region the outer shelf is a non-depositional area.

INLs are also considered important factors in lateral transport of particles over long distances from the shelf to slope and deep sea environments (Jahnke et al., 1990; McCave et al., 2001). Frequently reported from the water depth adjacent to the shelf break (e.g. McCave and Hall, 2002; McPhee-Shaw et al., 2004; Puig and Palanques, 1998) INLs also occur at the continental margin off Namibia, according to our data (Fig. 2.5). Our results of the sensor calibration, showing similar characteristics of BNL and INL particles, support the common interpretation that this INL originates from the detachment of a shelf-BNL (Fig. 7). In comparison to the prominent INL expanding from the shelf break, the origin of enhanced particle loads in deeper zones is less clear. Initially, it is striking that these layers were observed in similar water depth at all three transects. Their position coincides with leaps in water density at the lower boundary of the central waters (500-600 m depth) and the AAIW (800-1000 m depth). However, two possible explanations for deep particle-enriched layers have to be considered: 1) momentary events, like sinking plankton blooms, or 2) stationary phenomena that also originate from the hydrographic structure of the water column. The first could be assumed, when looking on the depth positions of particle-rich zones and the

chronology of their measurements, for example along T1 (Table 2.1). Unfortunately, this must be left to speculation because particle samples from respective water depths do not exist. However, if this assumption were true, why should these particle enrichments occur at about the same water depth of all three transects? This would require a rare coincidence. On the other hand, studies at other continental margins have shown that such deep INLs often coincide with areas, where the topographic slope angle is critical for internal tide reflection (Cacchione and Wunsch, 1974; McPhee-Shaw and Kunze, 2002). Strong density gradients at water mass boundaries can cause the formation of internal waves with large amplitudes. Correspondingly, enhanced shear-stress and subsequent turbulent mixing processes in the BNL, where these internal waves hit the sea floor, have been mentioned as source areas for INL formation (e.g. Cacchione and Drake, 1986; Thorpe and White, 1988; Azetsu-Scott et al., 1995; McPhee-Shaw et al., 2004). As discussed before, the optical sensor data suggest transport of fine-grained, light particles of BNL-origin in the INL. This agrees with findings of McCave et al. (2001), who have described the typical INL signal as the "fine smoke after the shot has been fired". Nevertheless, although indications contradict a recording of temporal events, final answers to the origin of the deep INLs cannot be given.

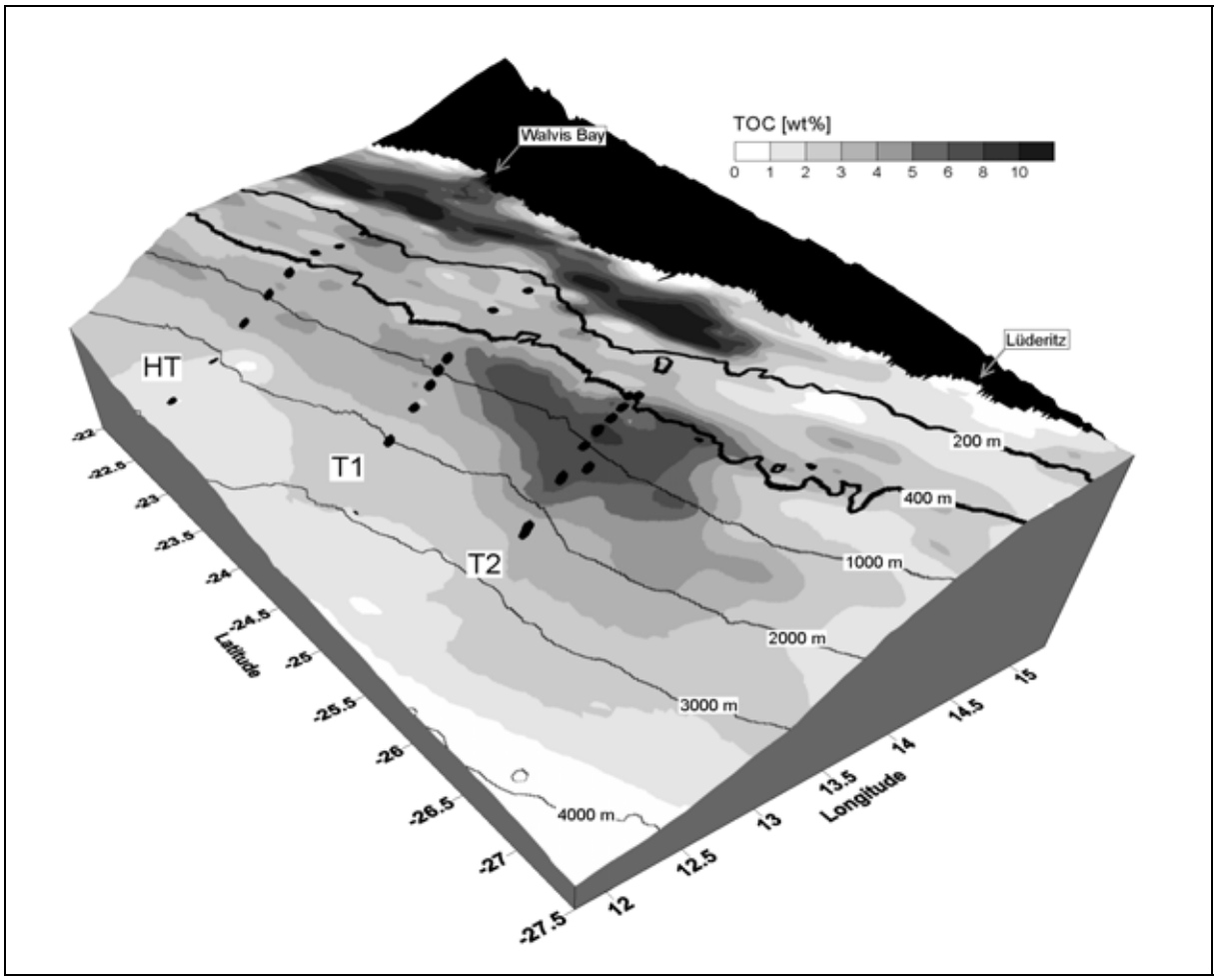

Fig. 2.8. Organic carbon distribution in the surface sediments on the continental margin offshore Namibia. The map is an extract from the map presented in Inthorn et al. (accepted; chapter 4). See Inthorn et al. (accepted; chapter 4) for information on data sources and preparation.

2.5.3. Particle transport

Strong offshore transport of particles at 25.5°S may be favored by a distinct inward turn of the outer shelf break between 24°S and 25°S (Fig. 2.1). This morphological feature should lead to an extension of the southward flowing central water undercurrent across the shelf break and an associated transport of particles towards the upper slope area. It is noteworthy that shelf break stations 1 and 2 on HT and 10 on T1 have an equally strong BNL of about 50 m thickness as station 16 at T2, while there is no indication of intense offshore transport at the two northern transects. Therefore we assume that the material suspended in the northern area represents an additional source for the intensive INL at T2. Another indication for the importance of the poleward undercurrent regarding particle transport is the strength of the oxygen minimum zone. The low oxygen content of the central waters at 150 to 400 m depth at T2 suggests, that the SACW may still be strong at this transect, although its influence should generally decrease to the south (Fig. 2.5). Intense microbial degradation processes on the high particle content at T2 and especially in the shelf break INL obviously intensify the oxygen minimum zone. The poleward undercurrent has not been described any further to the south, indicating that its particle load is deposited in this area, contributing to the slope depth depot center. This scenario is consistent with an equatorward directed friction between the undercurrent and the seabed, causing seaward Ekman transport of bottom waters over the outer shelf (Smith 1995). The assumed mass transport from the north to the south can also be derived from the distribution of the TOC-content in surficial sediments (Fig. 2.8), further supported by data of Inthorn et al. (subm.-a, in press; chapters 3 and 4) showing the highest massflux into the sediment and the highest sedimentation rates of the continental slope at the depocenter location.

2.6. Conclusions

Data and interpretations presented here fit well to a conceptual flow field model including the upwelling process and related subsurface currents suggested by Giraudeau et al. (2000) and based on former investigations by Barange and Pillar (1992). We adjusted that model to the general particle transport situation that we propose for the Namibian continental margin at 25.5°S (Fig. 2.9). While the general surficial water flow is offshore, driven by the equatorward wind stress and the resulting offshore directed Ekman transport, subsurface flow is more complicated. The upwelling process itself may be separated into at least two major cells. The main upwelling takes place at the coast and the inner shelf break at about 180 m water depth, where the BCC is inducing onshore transport of bottom waters, thereby additionally supplying nutrients from the degradation of organic matter at the sea floor. Resulting diatomea-dominated high productivity leads to the characteristic organic-rich, anoxic muds of the inner shelf area. This area is separated from the outer shelf by an upwelling front that produces a quasi-enclosed system. The major difference between the outer and inner shelf is the poleward directed subsurface current of the SACW in the deeper waters. Ekman forces at the sea floor result in a primarily offshore directed overall flow in the bottom layer. Thus, while there is considerable production of organic matter taking place

in the surface waters, the offshore transport in the very particle-rich BNL, visualized by our sensor data, prohibits particle deposition at the sea floor. These particles are transported in the form of comparatively fine-grained deep-water aggregates across the shelf break. Depleted in organic carbon in respect to SNL particles, nevertheless their carbon content is higher than in the underlying sediments. The strong BNL as well as the intensive shelf break depth INL induce effective transfer of these particles towards the major depocenter with organic carbon contents up to 8% on the upper to intermediate slope and towards the deep sea. The inward directed turn of the shelf break further to the north gives rise to additional particle import from the north, when the poleward SACW current and the associated BNL crosses the shelf break. This southern part of our working area is presumably an area where in the subsurface poleward directed currents from the north and equator ward directed currents from the south meet. An additional source of fresh organic material for the continental slope area is the high-productivity filaments, in which nutrient-rich water is transported across the slope in eddies originating at the shelf break. Secondary INLs may temporally occur at deeper water mass boundaries by internal tide reflection but are probably not as significant concerning particle redistribution.

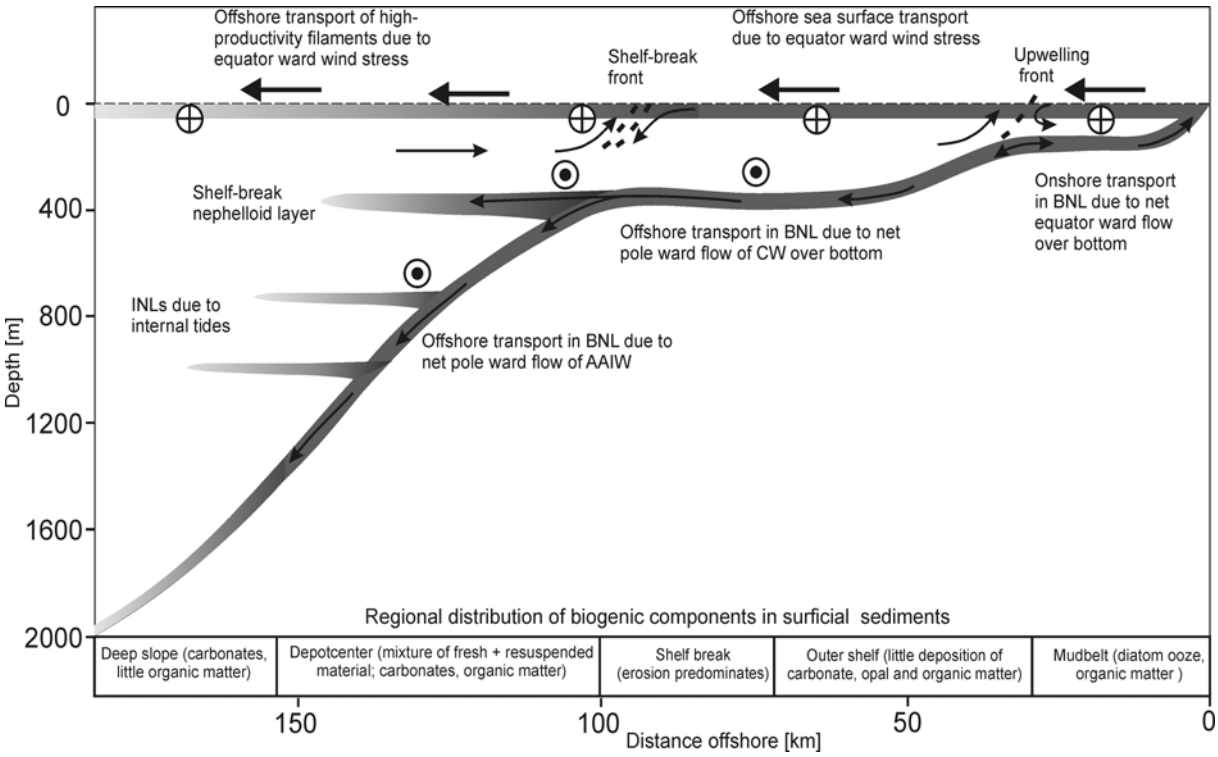

Fig. 2.9. Conceptual model of the flow field and the nepheloid layer distribution for the continental margin offshore Namibia at 25.5°S, and distribution of biogenic particles in the surficial sediments (based on Giraudeau et al., 2000). Encircled dots indicate poleward current, encircled crosses equatorward current.

Acknowledgments

We thank the captain and crew of RV Meteor for their strong support during the cruise M57/2. We highly appreciate the provision of sensors and technical help by M. Bergenthal. We thank T. Heene, B. Rajes, and U. Holzwarth for assistance onboard, and G. Klockgether, M. Bausch, and S. Pannike for assistance in the laboratory. This research was funded by the Deutsche Forschungsgemeinschaft as part of the Research Center "Ocean Margins" (RCOM) of the University of Bremen contribution no. XXXX.

3. Approaching particle exchange processes at the sediment water interface in the Benguela upwelling area based on $^{234}Th/^{238}U$ disequilibrium

Maik Inthorn[1], Michiel Rutgers van der Loeff[2], Matthias Zabel[1]

[1]*University of Bremen, FB5 – Geosciences, Klagenfurter Str., D-28359 Bremen, Germany*

[2]*Alfred-Wegener-Institute for Polar- and Marine Research, Am Handelshafen 12, D-27570 Bremerhaven, Germany*

3.1. Abstract

The natural isotope ^{234}Th is used in a small scale survey on particle transport and exchange processes at the sediment-water interface in the Benguela upwelling area. Results from water and suspended particulate matter (SPM) samples from the uppermost and lowermost water column as well as the underlying sediment of three stations in different sedimentological environments at 1200 to 1350 m water depth at the continental slope offshore Namibia are compared. Highly differing extension and particle content of the bottom nepheloid layer (BNL) are determined from transmissometer data. Depletion of the BNL and surface sediment excess with respect to ^{234}Th is interpreted to reflect intensive resuspension of surface sediment particles and/or sedimentation of particles after long-distance transport in the BNL. This is supported by high particle residence/removal times in the BNL in the range of 9 to 12 weeks at all three stations. Particle inventory of the BNL, resuspension rates, and mass flux into the sediment are highest at a depocenter of organic matter at 25.5°S, an area where strong deposition is presently taking place. Mass flux into the sediment exceeds the vertical particle flux into sediment traps at intermediate water depth in the same area by up to an order of magnitude, confirming the superior role of lateral particle transport processes at this continental margin. Comparison with carbon mineralization rates that are known from the area reveals that, notwithstanding the large fraction of advected particles, organic carbon flux into the surface sediment is remineralized to a large extent. The deployment of a bottom water sampler served as an in-situ resuspension experiment, and provided first data of ^{234}Th activity on in-situ resuspended particles. We found a mean specific activity of 86 dpm g^{-1} (39-339 dpm g^{-1}), intermediate between the high values for suspended particles (in-situ-pump: 580-760 dpm g^{-1}; CTD-rosette: 870-1560 dpm g^{-1}), and the low values measured at the sediment surface (26-37 dpm g^{-1}). This is essential information for the modeling of ^{234}Th exchange processes at the sediment-water interface.

3.2. Introduction

Increasing attention has been paid to lateral particle transport in subsurface nepheloid layers, e.g. concerning the evaluation of sediment trap data or organic matter flux models (Biscaye and Anderson, 1994; Jahnke et al., 1990; Seiter et al., 2005; Usbeck et al., 2003; Wefer and Fischer, 1993). Quantitatively important transport processes are assumed to occur in the bottom nepheloid layer (BNL), where concentrations of suspended particulate matter (SPM) are enhanced up to several hundreds of meters above the seafloor (Bacon and Rutgers van der Loeff, 1989; McCave, 1986). In the BNL, particles are transported laterally over large distances by cyclic sedimentation and resuspension (Thomsen and van Weering, 1998). Due to long oxygen exposure time, aggregation, disaggregation, and associated microbial degradation processes, the organic fraction of the SPM alters continuously (Boetius et al., 2000b; Thomsen and McCave, 2000). For the Benguela upwelling area, the most productive eastern boundary current system of the ocean (Carr, 2001), recent work provided strong indications for lateral particle transport (Giraudeau et al., 2000; Mollenhauer et al., 2003; Mollenhauer et al., 2002; Inthorn et al., in press; chapter 4). The transport takes place in intermediate and bottom nepheloid layers extending from the highly productive inner shelf towards a major depocenter of organic matter at the upper to central slope offshore Namibia (Inthorn et al., subm.-b; chapter 2).

Nevertheless, studies that quantify particle transport processes in the BNL are still few. One promising tool to assess and quantify particle transport in the BNL, and exchange with the surface sediment on a very short time scale is the radioactive isotope ^{234}Th (Aller and DeMaster, 1984; Bacon and Rutgers van der Loeff, 1989; DeMaster et al., 1991; Rutgers van der Loeff and Boudreau, 1997; Rutgers van der Loeff et al., 2002; Turnewitsch and Springer, 2001). It is produced from decay of ^{238}U in seawater, and has a half-life (λ) of 24.1 days. Compared to its parent, ^{234}Th is very particle reactive, and therefore a good tracer for particle dynamics in the water column on a time scale of weeks up to about 100 days. Where no removal processes proceed or particles have reached exchange equilibrium with the dissolved phase, total ^{234}Th (dissolved + particulate, $^{234}Th_t$) is in secular equilibrium with ^{238}U, which is the case in most of the deep water column below a depth of approx. 200 m. However, in waters with throughput of freshly produced or old, resuspended particles, scavenging causes depletion of $^{234}Th_t$ with respect to its parent ($^{234}Th_{depl} = {}^{238}U - {}^{234}Th_t$).

Here, we provide ^{234}Th data from the Benguela upwelling area using a set of water and sediment samples from three stations at about 1300 m water depth along the slope of the Namibian continental margin. One station is positioned directly over the depocenter of organic matter, while the two other stations are positioned north and south of it, where organic carbon (C_{org}) contents are significantly lower. The results of this small-scale study are the first data set to quantify lateral transport processes in the BNL of the Benguela upwelling area. They provide insight into the respective significance of vertical and lateral particle transport, as well as C_{org} remineralization at this continental slope environment. Additionally, specific ^{234}Th-activities of different particle types and from an in-situ

resuspension of sediment surface particles are determined, which will help to calibrate existing models for ^{234}Th exchange processes at the sediment-water interface.

3.3. Methods

3.3.1. Sampling

On the M57/2 expedition of RV *Meteor* from 27 February to 8 March 2003, three stations on the continental slope offshore Namibia (between 24°24' and 26°44'S, 1231 to 1353 m water depth, see Fig. 3.1 and Table 3.1) were sampled for ^{234}Th analysis. At every station, approx. 20 liters of surface water (SW) were obtained from the ships seawater supply. 20 liters of water from 10, 40, and 100 m above the seafloor were received, using a HYDROBIOS 12 bottle CTD-rosette sampler (CTD) equipped with five-liter free flow water sample bottles (HYDROBIOS), and by closing four bottles at a time. Additionally, a bottom water sampler (BWS) was used to retrieve 5 liters of water from 0.25, 0.4, 0.6, 0.9, and 1.1 m above the seafloor. The BWS consists of a three-footed steel-frame, aligning itself into the bottom current with a current-sail. In the respective depths intervals, five-liter free flow water sample bottles (HYDROBIOS) are horizontally attached to a central axis. These sampling bottles were closed about 30 minutes after the deployment of the device. At stations GeoB8463 and GeoB8467, SPM was additionally collected with an in-situ-pump (IP) attached to the BWS. The pumping was programmed to begin about 20 minutes after the deployment of the BWS. Unfortunately, the pump did not work properly at station GeoB84101. The BWS was equipped with a 0.25 m-pathlength SEATECH transmissometer measuring beam attenuation by suspended particles over the whole range of the water column. Surficial sediment was sampled with a multicorer system (MC) at stations GeoB8418, GeoB8451, GeoB8463 and GeoB84101. Samples from GeoB8418 and GeoB8451 were used for radiocarbon dating. These stations are located at about 1000 m water depth at 24.25°S and 25.5°S, less than 10km from stations GeoB84101 and GeoB8463 respectively (Fig. 3.1). Regrettably, surface sediments of station GeoB8467 were not sampled due to limited ship time.

3.3.2. Water samples

Water samples were treated according to the method of Rutgers van der Loeff and Moore (1999). Particles were removed for determination of particulate ^{234}Th ($^{234}Th_p$) by filtration through pre-weighed NUCLEPORE polycarbonate filters with a poresize of 0.4 µm using an air pressure pump and a pressure of 0.5 bar directly after sample retrieval. In the filtrate, dissolved ^{234}Th ($^{234}Th_d$) was precipitated quantitatively with MnO_2 and filtered as well. All filters were folded systematically, dried and kept in small plastic boxes for transportation.

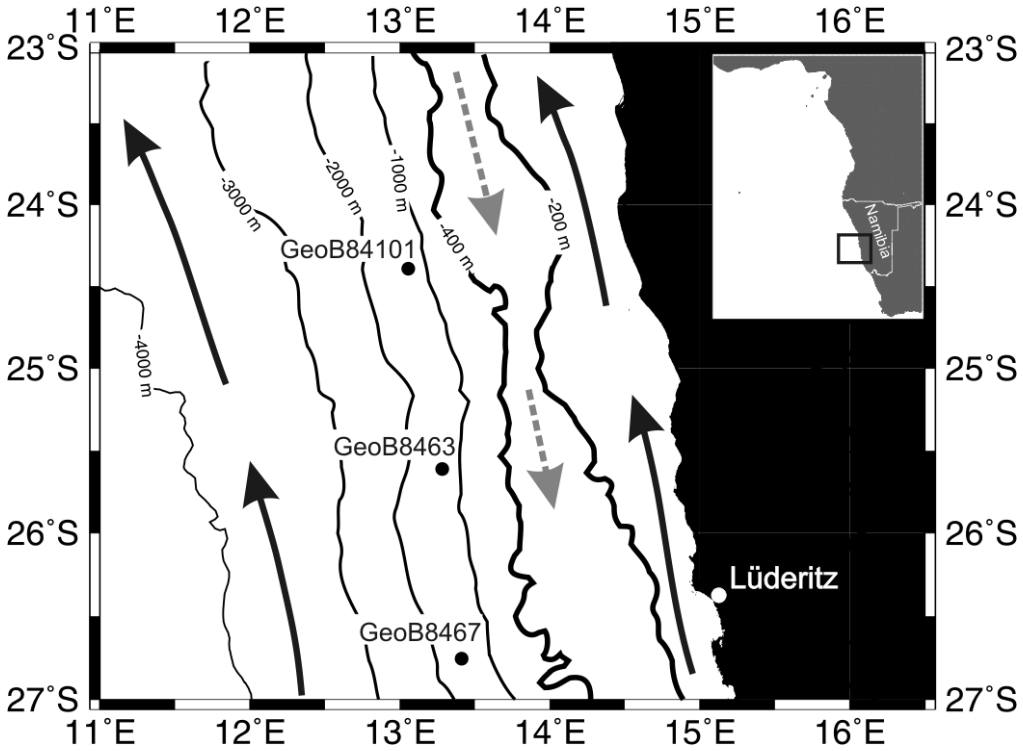

Fig. 3.1. Bathymetric map of the south-west African continental margin displaying the positions of the stations sampled for ^{234}Th. Main surface and subsurface currents are indicated by solid black and dashed gray arrows respectively.

Table 3.1.Position of the stations that were sampled for ^{234}Th analysis during M57/2 using the ships seawater supply (SW), a CTD-rosette (CTD), the bottom water sampler (BWS) with the in-situ-pump (IP) and a multiple corer system (MC).

station no.	latitude (°S)	longitude (°E)	devices	depth [m]
GeoB84101	24°24.0′	13°02.5′	SW, CTD, MC, BWS	1231
GeoB8463	24°35.7′	13°16.9′	SW, CTD, MC, BWS, IP	1335
GeoB8467	26°44.8′	13°25.3′	SW, CTD, BWS, IP	1353
GeoB8418	24°21.9′	13°08.2′	MC	1006
GeoB8451	25°28.9′	13°21.6′	MC	1028

Due to the comparatively small amount of water, sampled with the BWS bottles, only $^{234}Th_t$ was determined in these samples by adding MnO_2 directly to the unfiltered sample. By subsequent filtration, particulate and dissolved ^{234}Th was retrieved as $^{234}Th_t$ on one filter. Filters from the in-situ-pump were used to receive corresponding $^{234}Th_p$ from the lowermost water column, and dried and folded as described above.

All ^{234}Th-samples were measured with a gas-flow anti-coincidence beta counter with 10 cm lead shielding (Risø National Laboratory, Roskilde, Denmark) at the AWI Bremerhaven within 10 weeks after sampling. Determination of background count rates from other beta emitters was done nine month after the cruise according to Rutgers van der

Loeff and Moore (1999). Calibration was performed with spiked filters. $^{234}Th_t$ was calculated as the sum of corresponding $^{234}Th_p$ and $^{234}Th_d$ values. ^{238}U concentration in the seawater was calculated from salinity after Chen et al. (1986). The propagated measurement error (including sampling and 2σ counting error) was determined to be 5% for $^{234}Th_t$ in CTD/SW samples and 6% in BWS bottle-samples. For $^{234}Th_d$ in CTD/SW samples the error is 6%, and for $^{234}Th_p$ it is 4%.

Beam attenuation (c) profiles were used to derive SPM values for those depths, where ^{234}Th-samples were taken from the BNL and the surface nepheloid layer (SNL), comprising the particle-rich euphotic zone. This was done according to calibration algorithms, derived from a set of particle samples and the measurement of corresponding beam attenuation profiles on the Namibian continental margin during M57/2 (Inthorn et al., subm.-b; chapter 2), following procedures described by Gardner et al. (1993):

SNL: $SPM\ [mg\ l^{-1}] = 1.13 * c - 0.01$ ($R^2 = 0.74$, n = 20) (1),

BNL: $SPM\ [mg\ l^{-1}] = 1.77 * c - 0.37$ ($R^2 = 0.65$, n = 14) (2).

Due to high particle load on BWS-and IP-filters compared to CTD-samples, SPM could be determined by reweighing of the filters, and subtraction of the weight of the MnO_2-particles in case of the BWS bottle-samples.

3.3.3. Sediment samples

The sediment-cores were sampled in high resolution (one sample every 2 mm in the uppermost centimeter, every 5 mm down to 5 cm sediment depth) and treated generally according to Rutgers Van Der Loeff et al. (2002). Approximately 1 ml of sediment was resuspended in a few milliliters of distilled water. A subsample was filtered through preweighed Nuclepore filters and handled like the particle filters described above. After drying, filters were reweighed to determine sample weight, and measured for ^{234}Th as described above. Due to varying thickness of the filters, the results were corrected for self-absorption according to Rutgers van der Loeff and Moore (1999) by applying a calibration algorithm, derived from measuring strong beta sources below a subset of samples representative according to sample weight. When measuring the relatively weak activities of the beta-decay of ^{234}Th in the sediment, the influence of beta-signals from other beta-sources, such as ^{40}K, ^{226}Ra daughters and ^{210}Pb, has to be considered. Determination of background count rates from other beta emitters and supported ^{234}Th was done by recounting of all samples nine month after the cruise, the difference of the two measurements giving ^{234}Th excess ($^{234}Th_{xs}$) provided by recent deposition of particles to the sediment. The major advantage of this procedure is its simple and quick sample handling, because it doesn't involve any chemical preparation of the sediment. It is appropriate to get a good guess on $^{234}Th_{xs}$ in the surface sediment few centimeters of sediment, but with increasing sediment depth the uncertainties in the determination of background beta activity make the error in unsupported ^{234}Th large. We estimate the error in the $^{234}Th_{xs}$ inventories to be about 25%.

AMS radiocarbon analyses of bulk OC was performed at the Leibniz-Laboratory for Radiometric Dating and Isotope Research (University of Kiel, Germany), and at Woods Hole Oceanographic Institution on sediment from stations GeoB8418 and GeoB8451. Sedimentation rates were obtained by linear interpolation between the ^{14}C-age of the sediment surface sample and a deeper sample 10 to 20 cm below the seafloor.

3.4. Results

3.4.1. Nepheloid layer distribution in the water column

Surface and bottom nepheloid layers are well developed at the continental slope offshore Namibia, as visualized by the beam attenuation profiles (Fig. 3.2). At GeoB8463, beam attenuation is highest over almost the entire water column. A quite intensive SNL is distinguishable in the topmost 60 m of the water column, but also the BNL is most prominent and about 220 m thick. The northernmost station, GeoB84101, takes an intermediate position in beam attenuation. The SNL is 70 m thick, but less intensive, and the BNL extends with constant intensity 96 m above the seafloor. At the southernmost station GeoB8467, particle content is comparably low. A weak, double-humped SNL covers the topmost 70 m of the water column, and only at the lowermost 20 m a BNL is distinguishable. For a general description of the nepheloid layer distribution offshore Namibia see Inthorn et al. (subm.-b; chapter 2).

3.4.2. ^{234}Th in the water column

$^{234}Th_p$ values of the samples from the ships seawater supply are considerably lower at GeoB8463 compared to GeoB84101 and GeoB8467 (Fig. 3.2b and Table 3.2). But at this station, $^{234}Th_p$ values increase considerably towards the seafloor and reach up to 0.67 dpm l^{-1}. At station GeoB84101, $^{234}Th_p$ stays at a constant level of 0.4 dpm l^{-1} throughout the water column, slightly increasing towards the seafloor. At GeoB8467, $^{234}Th_p$ is higher in the surface waters than in the lower water column, with highest $^{234}Th_p$ of 0.31 dpm l^{-1}10 m above the seafloor.

$^{234}Th_d$ is generally depleted in the SNL and BNL compared to the intermediate water column (Fig. 3.2c and Table 3.2). Throughout the water column, $^{234}Th_d$ values are highest at station GeoB8467 and lowest at GeoB8463.

Fig. 3.2d illustrates the overall depletion of $^{234}Th_t$ with respect to the supply by its parent ^{238}U. At all stations, samples from the ships seawater supply are significantly depleted in $^{234}Th_t$, the depletion being more intense at GeoB8463 and GeoB84101 compared to GeoB8467. In the samples from the deep water column, $^{234}Th_t$ is generally higher. Nevertheless, there is significant depletion in ^{234}Th at all three stations. At GeoB8463, ^{234}Th is

depleted at all three sampling depth, while the depletion is quite small in the sample 100m above the seafloor at GeoB84101, and at the 100 and 40 m samples of GeoB8467.

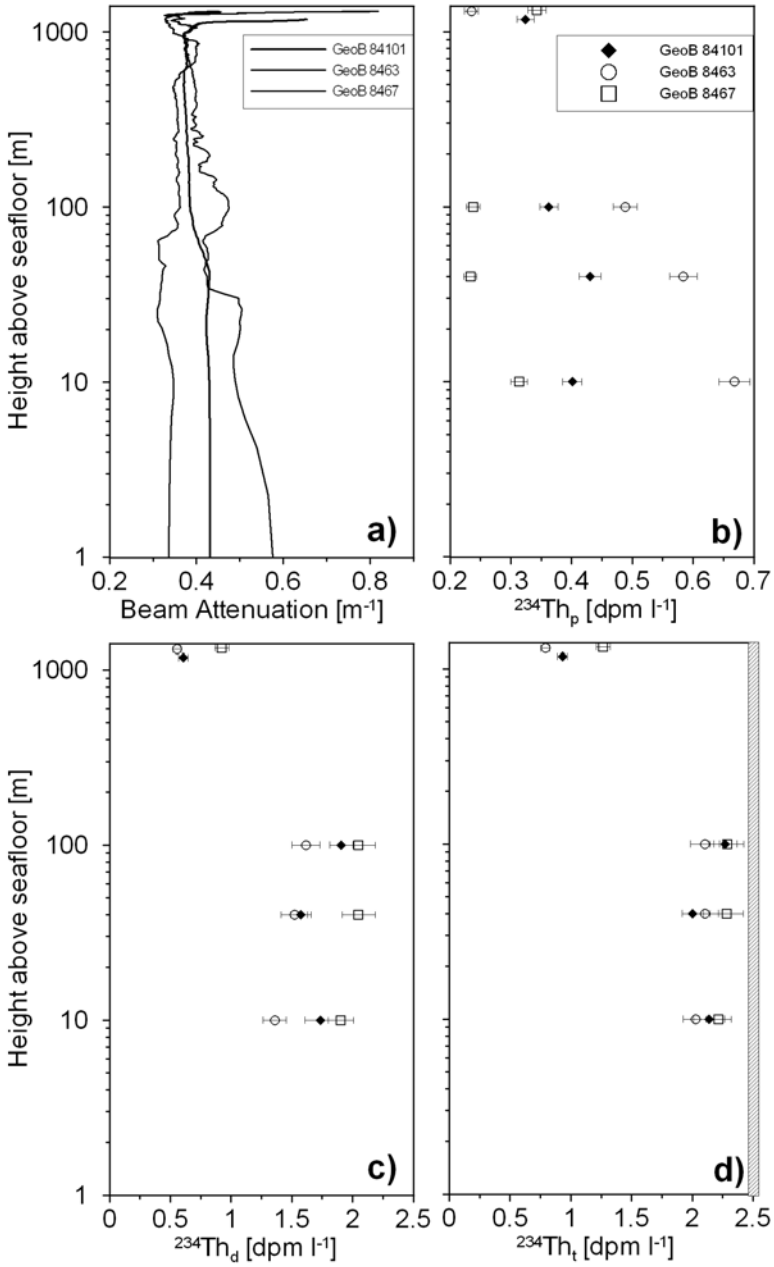

Fig. 3.2. Vertical profiles of a) beam attenuation, b) $^{234}Th_p$, c) $^{234}Th_d$, and d) $^{234}Th_t$ activity against sample height above the seafloor at stations GeoB84101, GeoB8463, and GeoB8467. Legend from graph b) is also valid for graphs c) and d). Topmost samples are from the ships seawater supply, samples from 10, 40 and 100 m above the seafloor are from the CTD-rosette. The hatched box in graph d) corresponds to the mean activity of ^{238}U in seawater. Horizontal error-bars indicate propagated errors and are sometimes smaller than symbol.

3.4.3. BWS-data

The BWS bottle-samples at GeoB8463 and GeoB8467 reveal a strong increase in SPM towards the seafloor (Fig. 3.3a and Table 3.2). The increase is exceptionally strong at station

GeoB8463, where SPM concentrations reach more than 100 mg l^{-1} at the two lowermost bottles. Only at GeoB84101, SPM values stay rather constant at a level of 6.24 to 9.89 mg l^{-1}. It is striking that SPM obtained with the in-situ-pump from the same deployments at stations GeoB8463 and GeoB8467 is considerably lower (0.41 and 0.29 mg l^{-1} respectively). SPM-data, calculated from beam attenuation 0.25 m above the ground, are in the range of the IP-results (0.68 to 0.22 mg l^{-1} at stations GeoB8463 and GeoB8467 respectively), but considerably below the bottle-data.

Table 3.2. ^{234}Th and SPM data of water column samples at the three stations. For explanation of sample type abbreviations see Table 3.1. $^{234}Th_p$ data of the BWS samples is calculated as the difference between the respective $^{234}Th_t$ value and $^{234}Th_d$ of the lowermost sample (10 m a.g.) at the respective station. h.a.g.: height above ground, n/d = no data.

station	type	h.a.g. [m]	SPM [mg l^{-1}]	$^{234}Th_p$ [dpm l^{-1}]	$^{234}Th_d$ [dpm l^{-1}]	$^{234}Th_t$ [dpm l^{-1}]	$^{234}Th_{depl}$ [dpm l^{-1}]	$^{234}Th_{spec}$ [dpm g^{-1}]
GeoB	SW	1224	0.73 ± 0.13	0.32 ± 0.01	0.61 ± 0.04	0.93 ± 0.04	1.48 ± 0.04	450 ± 80
84101	CTD	100	0.31 ± 0.04	0.36 ± 0.01	1.91 ± 0.10	2.27 ± 0.10	0.11 ± 0.10	1160 ± 160
	CTD	40	0.39 ± 0.05	0.43 ± 0.02	1.57 ± 0.09	2.00 ± 0.09	0.38 ± 0.09	1100 ± 150
	CTD	10	0.39 ± 0.05	0.40 ± 0.02	1.74 ± 0.13	2.14 ± 0.13	0.24 ± 0.13	1020 ± 140
	BWS	1.1	8.0 ± 1.0	0.57 ± 0.19	n/d	2.31 ± 0.14	0.07 ± 0.14	71± 25
	BWS	0.9	9.0 ± 1.0	1.23 ± 0.21	n/d	2.96 ± 0.16	-0.59 ± 0.16	137± 28
	BWS	0.6	6.2 ± 1.0	0.97 ± 0.20	n/d	2.71 ± 0.15	-0.33 ± 0.15	156± 41
	BWS	0.4	9.9 ± 1.0	1.06 ± 0.20	n/d	2.79 ± 0.16	-0.42 ± 0.16	107± 23
	BWS	0.25	7.7 ± 1.0	0.79 ± 0.19	n/d	2.53 ± 0.14	-0.15 ± 0.14	103± 29
GeoB	SW	1328	0.92 ± 0.17	0.23 ± 0.01	0.56 ± 0.04	0.79 ± 0.04	1.62 ± 0.04	250 ± 50
8463	CTD	100	0.46 ± 0.06	0.49 ± 0.02	1.62 ± 0.12	2.10 ± 0.12	0.27 ± 0.12	1050 ± 150
	CTD	40	0.38 ± 0.05	0.58 ± 0.02	1.52 ± 0.11	2.10 ± 0.11	0.27 ± 0.11	1560 ± 210
	CTD	10	0.49 ± 0.06	0.67 ± 0.03	1.36 ± 0.10	2.03 ± 0.10	0.35 ± 0.10	1360 ± 190
	BWS	1.1	3.1 ± 1.0	0.94 ± 0.19	n/d	2.30 ± 0.16	0.09 ± 0.16	304 ± 120
	BWS	0.9	3.3 ± 1.5	1.13 ± 0.19	n/d	2.49 ± 0.16	-0.10 ± 0.16	339± 117
	BWS	0.6	16.2 ± 1.0	2.12 ± 0.23	n/d	3.48 ± 0.21	-1.10 ± 0.21	131± 16
	BWS	0.4	122.6 ± 1.5	5.55 ± 0.68	n/d	6.91 ± 0.68	-4.53 ± 0.68	45± 6
	BWS	0.25	119.5 ± 1.0	16.1 ± 1.4	n/d	17.4 ± 1.4	-15.1 ± 1.4	134± 12
	IP	1.1	0.41 ± 0.01	0.39 ± 0.01	n/d	n/d	n/d	584 ± 39
GeoB	SW	1346	0.47 ± 0.08	0.34 ± 0.01	0.92 ± 0.06	1.27 ± 0.06	1.15 ± 0.06	730 ± 140
8467	CTD	100	0.27 ± 0.04	0.24 ± 0.01	2.05 ± 0.14	2.29 ± 0.14	0.09 ± 0.14	870 ± 120
	CTD	40	0.19 ± 0.03	0.23 ± 0.01	2.05 ± 0.14	2.28 ± 0.14	0.10 ± 0.14	1220 ± 170
	CTD	10	0.25 ± 0.03	0.31 ± 0.01	1.90 ± 0.10	2.22 ± 0.10	0.16 ± 0.10	1260 ± 180
	BWS	1.1	7.3 ± 1.0	0.60 ± 0.18	n/d	2.50 ± 0.15	-0.12 ± 0.15	82 ± 27
	BWS	0.9	10.8 ± 1.5	0.83 ± 0.21	n/d	2.73 ± 0.19	-0.35 ± 0.19	77 ± 23
	BWS	0.6	11.2 ± 1.0	0.44 ± 0.18	n/d	2.34 ± 0.15	0.04 ± 0.15	39 ± 16
	BWS	0.4	30.8 ± 1.5	3.14 ± 0.26	n/d	5.05 ± 0.14	-2.66 ± 0.14	102 ± 10
	BWS	0.25	20.6 ± 1.0	2.02 ± 0.23	n/d	3.93 ± 0.21	-1.54 ± 0.21	98 ± 12
	IP	0.3	0.29 ± 0.01	0.23 ± 0.01	n/d	n/d	n/d	764 ± 35

Fig. 3.3b shows $^{234}Th_t$ of the BWS bottle-samples. Corresponding to the SPM-data, $^{234}Th_t$ activity is strongly increasing towards the seafloor at GeoB8463 and GeoB8467. In the lowermost two bottles, $^{234}Th_t$ clearly exceeds the level of supported ^{234}Th activity from ^{238}U. Only at station GeoB84101, $^{234}Th_t$ activity stays around equilibrium at all five samples. Compared to $^{234}Th_t$ data of the lowermost CTD samples (Fig. 3.2d), $^{234}Th_t$ activities at all three stations are significantly higher. In contrast to this, $^{234}Th_p$ of the in-situ-pump filters (Fig. 3.3b) is in better agreement with the low values of the CTD particle samples.

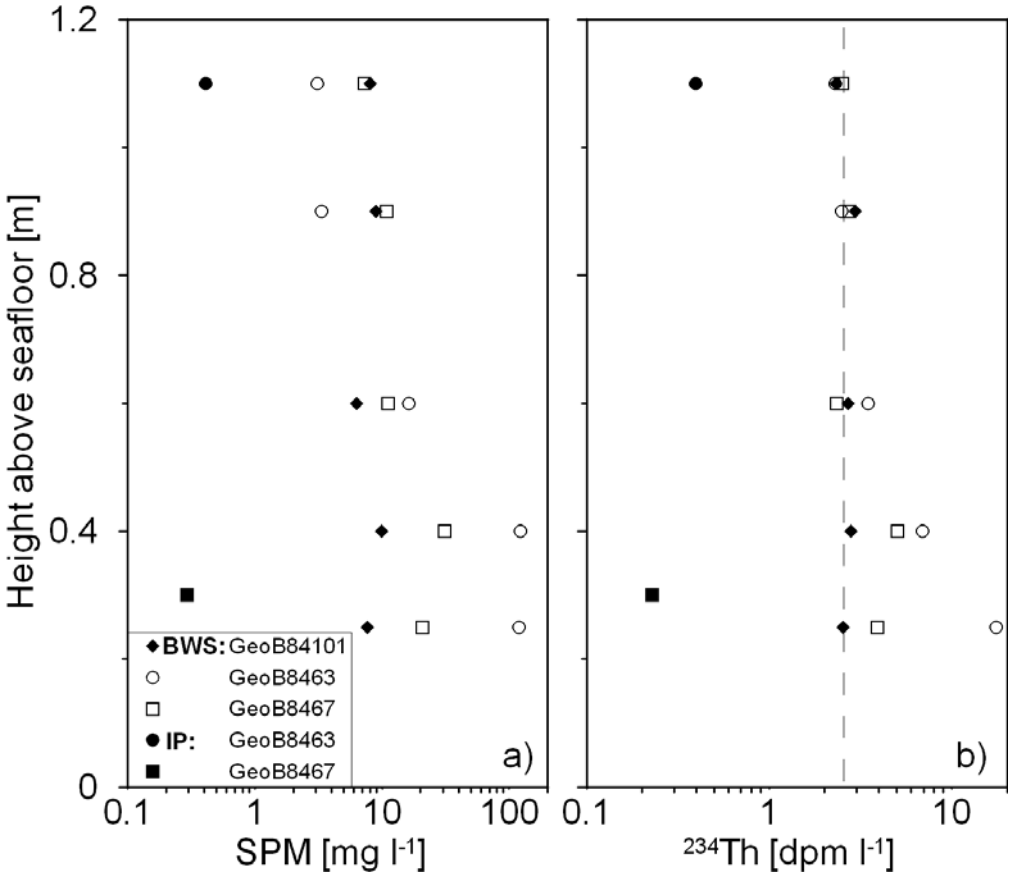

Fig. 3.3. a) SPM-values and b) $^{234}Th_t$ activities of BWS bottle-samples from stations GeoB84101, GeoB8463 and GeoB8467 against height above seafloor. In addition, SPM-values and $^{234}Th_p$ from the in-situ-pump attached to the BWS are given for stations GeoB8463 and GeoB8467. The dashed line corresponds to the mean activity of ^{238}U. Horizontal error-bars are smaller than symbols.

3.4.4. Sediment data

At GeoB8463, the maximum in $^{234}Th_{xs}$ is not at the sediment surface, but 0.6 to 0.8 cm below the sea floor, and no excess ^{234}Th was determined at 2.0 cm depth. There are two deeper maxima at 2.8 to 3.6 cm and 5.2 to 6.4 cm depth (Fig. 3.4). At station GeoB84101, the maximum is at 0.2 to 0.4 cm, and $^{234}Th_{xs}$ reaches zero activity at 0.6 cm depth. $^{234}Th_{xs}$ scatters around zero down to 3.0 cm, and shows unexpected negative values below this depth.

Calculated linear sedimentation rates are 14.6 cm ky^{-1} for station GeoB8418, and 39.2 cm ky^{-1} for GeoB8451.

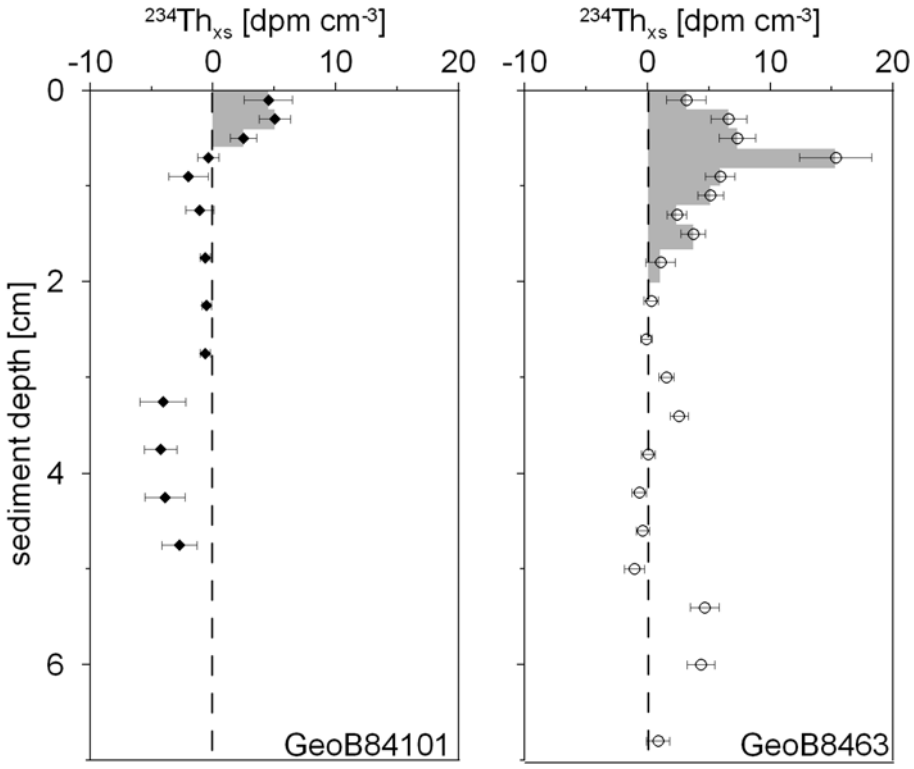

Fig. 3.4. $^{234}Th_{xs}$ in surficial sediments of stations GeoB84101 and GeoB8467. Gray areas are used for calculation of the inventory of $^{234}Th_{xs}$ in the sediments. Horizontal error-bars indicate propagated errors and are sometimes smaller than symbol.

3.5. Discussion

In the Benguela upwelling area, high C_{org} contents of up to 10% on the continental slope offshore Namibia are interpreted to indicate a depocenter of organic matter with its center in water depths of 400 to 1500 m at 25.5°S. This is reflected in high sedimentation, mass accumulation (Inthorn et al., in press; chapter 4; Mollenhauer et al., 2002) and carbon mineralisation rates (Aspetsberger et al., subm.-a; Ferdelman et al., 1999; Glud et al., 1994) in this area. Generally, vertical flux of fresh biogenic particles or lateral particle transport in subsurface nepheloid layers are possible organic matter sources. Here, the respective significance of the two sources is estimated, and $^{234}Th/^{238}U$ disequilibrium is used to quantify particle reworking, transport, and deposition processes. While station GeoB8463 is located directly over the depocenter (C_{org} content of the surface sediments is 8.06 %; Inthorn et al., in press; chapter 4), stations GeoB84101 and GeoB8467 are positioned north and south of it respectively, where C_{org} content of the surface sediments is lower (3.30 % and 4.08 % respectively; Inthorn et al., in press; chapter 4).

3.5.1. The in-situ resuspension experiment

It is improbable that the high SPM and $^{234}Th_t$ values of the BWS bottle-samples (Fig. 3.3 and Table 3.2) result solely from particles originally suspended in the bottom waters. Through the deposition of the BWS at the seafloor, varying amounts of particles from the surface sediment were resuspended and trapped in the open Niskin-bottles. Particles that entered the bottles, and were deposited on their bottom were apparently inhibited from flushing by the boundary-layer of the bottle itself. The SPM-values are much higher than the results from the in-situ-pump particle filters and the beam attenuation profiles, and considerably exceed known differences in the SPM-yield of the sampling methods alone (Bishop, 1999; Gardner et al., 2003; Liu et al., 2005; Moran et al., 1999). The bottle-sample SPM is also much higher than SPM-values derived from the beam attenuation profiles. Therefore, the most reasonable explanation for the high $^{234}Th_t$ values is the artificial resuspension of additional ^{234}Th on particles from the sediment surface. The difference of $^{234}Th_t$ of the BWS bottle-samples to $^{234}Th_d$ of the lowermost CTD-sample provides a low estimate of the particulate ^{234}Th in the BWS-samples, because previous studies (Rutgers van der Loeff et al., 2002; Turnewitsch and Springer, 2001) show that $^{234}Th_d$ generally decreases with decreasing distance to the sediment surface, where particle throughput and, as a result, scavenging is most intensive. The resulting $^{234}Th_p$ values are well correlated with the respective particle concentrations (Fig. 3.5):

$$^{234}Th_p\,[dpm\ l^{-1}] = 0.086 * SPM\,[mg\ l^{-1}] - 0.27 \qquad (R^2 = 0.73;\ n = 15) \qquad (3).$$

GeoB8463 and GeoB8467 are much more effected by this artificial resuspension compared to GeoB84101 (Fig. 3.3b). The difference may be due to varying grain size composition of the sediments, or the impact of the BWS during deposition. SPM values strongly decrease from the lowermost to the uppermost bottle in the results of the two first mentioned stations, while all five bottles show comparatively low values at GeoB84101. Although the sampling of bottom water with bottles of Niskin type horizontally fixed to a frame is comparatively easy to operate, and has proven to be useful regarding the sampling of fluids (Mau et al., subm.; Sauter et al., 2005), we show that such a deployment may not obtain representative samples of the naturally suspended particles. Nevertheless, this self-induced resuspension event of the BWS gives particularly interesting results, as described below.

3.5.2. Specific ^{234}Th activity of different particle sample types

Up to now, ^{234}Th models concerning particle exchange budgets between the seafloor and the BNL only use rough estimates concerning the specific ^{234}Th activities of resuspended particles ($^{234}Th_{spec}$, as ^{234}Th activity per gram of particles), based on ^{234}Th activity of sediment surface samples (e.g. Aller and DeMaster, 1984; Bacon and Rutgers van der Loeff, 1989; Rutgers van der Loeff et al., 2002). Therefore, the results of the in-situ resuspension experiment, as sampled with the BWS, will help to calibrate existing models (Rutgers van der Loeff and Boudreau, 1997). $^{234}Th_{spec}$ was calculated from $^{234}Th_p$ and SPM data for the different sample types from the deep water column. For the sediment surface samples $^{234}Th_{spec}$ was

determined from sample weight and $^{234}Th_{xs,}$ because in the sediments, contribution of supported Th has to be considered (Fig. 3.6 and Table 3.2). The linear trend (equation 3) of the BWS-samples corresponds with an average $^{234}Th_{spec}$ of the resuspended particles of 86 dpm g^{-1}. Nevertheless, the samples cover a wide range of $^{234}Th_{spec}$ values (39-339 dpm g^{-1}). The two BWS-samples with high activities of about 300 dpm g^{-1} at GeoB8463 are from the uppermost bottles, and thought to contain very little self-resuspended material, but a higher fraction of long-time suspended material. All other BWS-samples show values below 160 dpm g^{-1}. $^{234}Th_{spec}$ of the BWS bottle-samples is intermediate between the high values from the in-situ-pump (580-760 dpm g^{-1}) and the CTD-rosette (870-1560 dpm g^{-1}), and the low values measured at the sediment surface (26-37 dpm g^{-1}). The low $^{234}Th_{spec}$-data of the surface sediments result from intensive dilution through bioturbative mixing, and are in the same range as sediment data from the Middle Atlantic bight (10 to 40 dpm g^{-1}, Santschi et al., 1999), and somewhat lower than at the Fram Strait (40 to 80 dpm g^{-1}, Rutgers van der Loeff et al., 2002). According to our data, an intensive resuspension event as it can be induced by storm events or internal wave action is thought to preferentially resuspend particles with higher $^{234}Th_{spec}$ compared to bulk sediment surface samples. Sediment surface samples represent the uppermost 0.2 mm of the sediment, and therewith exceed the very thin layer of easily resuspended particles. This is the advantage of our resuspension experiment. On the other hand, $^{234}Th_{spec}$ of the BWS bottle-samples is low compared to particles suspended in the BNL otherwise. The high $^{234}Th_{spec}$ of the in-situ-pump and CTD-samples, representing the "background" situation, indicate fine particles that stay in suspension or directly at the sediment-water interface during longer time intervals, and hence are strongly enriched in ^{234}Th.

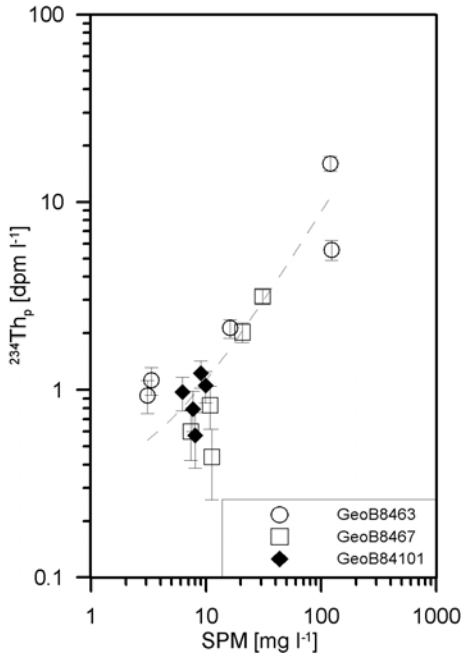

Fig. 3.5. $^{234}Th_p$ activities of BWS bottle-samples, as difference of $^{234}Th_t$ of the BWS bottle-samples to $^{234}Th_d$ of the lowermost CTD-sample, from stations GeoB84101, GeoB8463 and GeoB8467 against SPM values. Dashed line is from linear regression of all data. Vertical error-bars indicate propagated errors and are sometimes smaller than symbol.

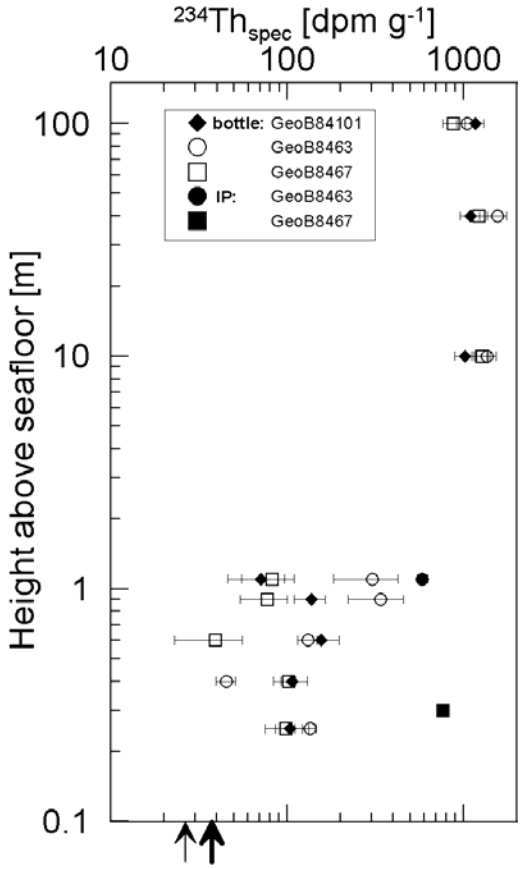

Fig. 3.6. $^{234}Th_{spec}$ of suspended particles of different sample types from the deep water column at stations GeoB84101, GeoB8463 and GeoB8467 against water depth. Samples from lowermost 1.1 m above the seafloor are from the BWS, other samples are taken with the CTD-rosette. The arrows at the lower abscissa indicate $^{234}Th_{spec}$ values of sediment surface samples at stations GeoB84101 (thick arrow), GeoB8463 (thin arrow). Horizontal error-bars indicate propagated errors and are sometimes smaller than symbol.

3.5.3. ^{234}Th in the surface waters

^{234}Th data of the samples from the ships seawater supply provide a first insight into the intensity of particle export from the surface waters during our survey (Coale and Bruland, 1985). To determine the export flux accurately, a depth profile of ^{234}Th would be necessary, which was not done during this study. The three stations show $^{234}Th_{depl}$ of 1.15 to 1.62 dpm l^{-1} (Fig. 3.2d and Table 3.2). Although beam attenuation profiles reveal the most intensive SNL at station GeoB8463 (Fig. 3.2a), there is comparatively little ^{234}Th attached to the particles at this station, while the overall depletion in $^{234}Th_t$ is most pronounced, and $^{234}Th_{spec}$ is low (Fig. 3.2 b, d and Table 3.2). We interpret this to result from stronger efflux of freshly produced biogenic particles from the SNL at GeoB8463. At GeoB8467 on the other hand, the SNL is weak, while $^{234}Th_p$ is highest and $^{234}Th_{depl}$ lowest, indicating lower

productivity and higher residence time of the particles in the SNL at this position. Station GeoB84101 is intermediate in all of these aspects.

3.5.4. Particle dynamics at the sediment-water interface

Up to now, only few examples of simultaneous determination of ^{234}Th inventories of the BNL and the corresponding surface sediment exist (DeMaster et al., 1991; Rutgers van der Loeff et al., 2002; Turnewitsch and Springer, 2001), and this study provides the first ^{234}Th data reported from the Benguela upwelling area. At all stations, the water samples taken with the CTD at near bottom depths are depleted in $^{234}Th_t$ (Fig. 3.2d and Table 3.2), while there is excess ^{234}Th in the sediments. This ^{234}Th depletion in the BNL is explainable with two different models. The first is based solely on local resuspension, while the second approaches sedimentation of particles that have been transported in the BNL over long distances. In the following, both models will be discussed and compared to each other.

Model 1: local resuspension

This model assumes that local cyclic resuspension of sediment surface particles to the BNL by bottom currents and later resedimentation on a time scale of weeks is the source of ^{234}Th depletion in the BNL, resulting from scavenging of $^{234}Th_{diss}$ to the suspended particles (Bacon and Rutgers van der Loeff, 1989). Accordingly, the depletion in the BNL must be balanced by ^{234}Th excess in the surface sediments. Subsurface $^{234}Th_{xs}$ is explained solely by bioturbative mixing without any net sediment accumulation.

Good correlation of SPM-values derived from beam attenuation profiles, to $^{234}Th_{depl}$ and $^{234}Th_p$ (Fig. 3.7) in the BNL from samples obtained with the CTD-rosette is observed, according to the relations

$$^{234}Th_{depl}\ [dpm\ l^{-1}] = 0.92 * SPM\ [mg\ l^{-1}] - 0.10 \qquad (R^2 = 0.70,\ n = 9) \qquad (4),$$

$$^{234}Th_{p}\ [dpm\ l^{-1}] = 1.29 * SPM\ [mg\ l^{-1}] - 0.04 \qquad (R^2 = 0.75,\ n = 9) \qquad (5).$$

The observation of higher $^{234}Th_{depl}$ with higher SPM concentrations supports the model, indicating constant settling rates/residence times of the particles during relatively long resuspension cycles in the BNL. Interestingly, such a relationship between SPM and $^{234}Th_{depl}$ is also reported by Rutgers van der Loeff et al. (2002) for the Fram Strait, but for a much higher amount of samples, indicating principally comparable particle exchange processes in the two areas.

The 40 m sample at station GeoB8463 is taken from an intermediate position between two sublayers of the BNL with higher particle content (Fig. 3.2a). Due to the fact that nepheloid layers are subject to varying current conditions, e.g. tidal influences, this sublayer situation is probably no permanent feature. This explains the relatively low SPM value compared to relatively high $^{234}Th_{depl}$, integrating over several days. At GeoB84101, the 100 m sample is positioned above the upper boundary of the BNL. Therefore, it shows a lower SPM concentration and less $^{234}Th_{depl}$ compared to the samples from 10 and 40 m above the

seafloor. The weak and shallow BNL at station GeoB8467 is reflected in low SPM and $^{234}Th_{depl}$ values. The regression in Fig. 3.7 gives a background SPM-level of about 0.1 mg l^{-1} for zero $^{234}Th_{depl}$, a reasonable number for a "standing stock" of particles, not involved in particle exchange processes with the sediment.

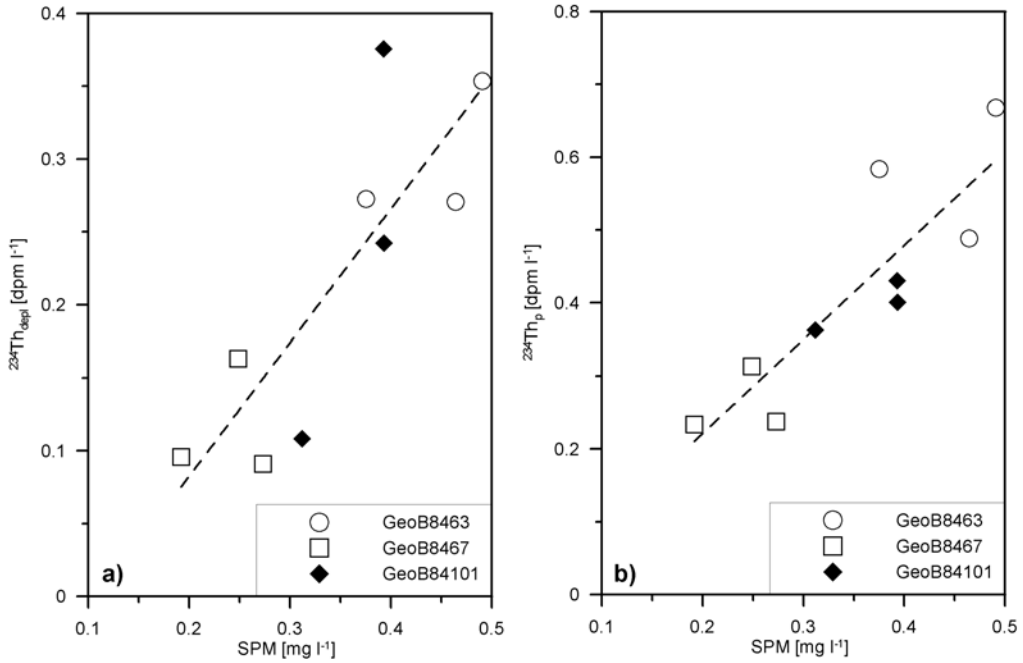

Fig. 3.7. a) $^{234}Th_{depl}$ and b) $^{234}Th_p$ of the CTD-rosette samples of GeoB84101, GeoB8463 and GeoB8467 against SPM as calculated from beam attenuation. Dashed lines are from linear regression of all data.

The inventories of $^{234}Th_{depl}$ (I_{depl}) and $^{234}Th_p$ (I_p) in the BNL at the three stations are calculated by applying equation (2) to derive SPM-distribution for the overall height of the BNL from beam attenuation, and equations (4) and (5) respectively to determine $^{234}Th_{depl}$ and $^{234}Th_p$ (Table 3.3). Based on the model of Rutgers Van Der Loeff and Boudreau (1997), the average residence time of particles in the BNL is determined by comparison of the overall inventory of $^{234}Th_p$ in the BNL (I_p) with the fluxes of $^{234}Th_p$ into this reservoir (D: ingrowth from depletion; R: resuspension flux; S: settling flux) according to the equation

$$\tau = \frac{I_p}{D + R + S} \qquad (6).$$

Equation (6) is, strictly taken, only valid for a single class of particles in a well-mixed BNL at steady-state conditions.

Inthorn et al. (accepted; chapter 4) give predominant significance to lateral particle transport in the sampling area based on ^{14}C-ages of 1800 to 3500 years and qualitative properties of Namibian slope surface sediments and suspended particles from the BNL, supporting previous studies by Giraudeau et al. (2000) and Mollenhauer et al.(2003). Accordingly, minor significance of vertical input to the BNL at the three sampled stations during M57/2 is assumed, and the vertical flux (S) in equation (6) is neglected. $^{234}Th_{spec}$ of

suspended particles in the BNL exceeds $^{234}Th_{spec}$ of resuspended particles as sampled with the BWS considerably, so that we neglect the resuspended activity R as well. Therefore, equation (6) is reduced to

$$\tau = \frac{I_P}{I_{depl}\lambda} \quad (7).$$

According to equation (7), the average residence time of particles in the BNL at the three stations is in the range of 9 to 12 weeks (Table 3.3). These values are relatively high compared to 6 weeks at the Fram Strait (Rutgers van der Loeff et al., 2002) and 1 to 3 weeks at the Middle Atlantic Bight (Santschi et al., 1999).

Table 3.3. Height, as well as inventories of $^{234}Th_{depl}$, $^{234}Th_p$, and SPM of the BNL, $^{234}Th_{xs}$ inventory of the sediments, ingrowth from depletion, particle residence/removal time, particle resuspension flux, and ^{234}Th resuspension flux from the sediment to the BNL, as calculated according to model 1, massflux and C_{org} flux into the sediment according to model 2. Surface sediments at station GeoB8467 were not sampled for $^{234}Th_{xs}$.

	GeoB84101	GeoB8463	GeoB8467
BNL height [m]	*96*	*220*	*20*
$^{234}Th_{depl}$ inventory BNL I_{depl} [dpm cm^{-2}]	2.2	6.1	*0.2*
$^{234}Th_p$ inventory BNL I_p[dpm cm^{-2}]	*4.2*	*11.0*	*0.5*
SPM inventory BNL I_{SPM}[mg cm^{-2}]	*3.5*	*9.1*	*0.5*
$^{234}Th_{xs}$ inventory sediment I_{sed} [dpm cm^{-2}]	2.4	10.5	n/d
model 1			
ingrowth from depletion D [dpm cm^{-2} d^{-1}]	0.063	0.175	0.006
particle residence/removal time τ [days]	*66*	*63*	*83*
particle resuspension flux F_{res} [mg m^{-2}d^{-1}]	*605*	*1330*	*56*
^{234}Th resuspension flux R [dpm cm^{-2} d^{-1}]	0.005	0.011	0.0005
model 2			
mass flux into sediment F_{sed} [mg m^{-2} d^{-1}]	630	2750	n/d
C_{org} flux into sediment F_{Corg} [mg m^{-2}d^{-1}]	76	329	n/d

Based on the residence time and the overall inventories of SPM ($I_{SPM,}$ Table 3.3) as calculated from beam attenuation according to equation (2), values for the particle resuspension flux F_{res} are derived using the equation

$$F_{res} = \frac{I_{SPM}}{\tau} \quad (8).$$

Resuspension fluxes are significantly higher at GeoB8463 and GeoB84101 compared to GeoB8467 (Table 3.3), where there is only little particle exchange at the seafloor. The actual resuspended ^{234}Th activity R can now be calculated by applying the average $^{234}Th_{spec}$ of

resuspended particles as derived from the BWS samples, giving 0.5-11.4*10^{-3} dpm $cm^{-2}d^{-1}$, supporting the assumption, that R is negligible with respect to D.

According to the model, I_{depl} must be balanced by an equivalent sedimentary $^{234}Th_{xs}$-inventory (I_{sed}). $^{234}Th_{xs}$-profiles at GeoB84101 and GeoB8463 reach zero activity at 0.6 and 2.0 cm sediment depth respectively, but reveal considerable variation and even unexpected negative values below this depths (Fig. 3.4). This is attributable to errors related to increasing influence of other beta-sources with lower ^{234}Th content of the sediment. Some nuclides may not have been in equilibrium or escaped as a gas-phase prior to the first count after sampling. For calculation of I_{sed}, only the uppermost samples down to the depth where zero activity is reached for the first time, have been considered (Table 3.3). At GeoB84101, I_{depl} is equivalent to I_{sed} (2.2 and 2.4 dpm cm^{-2} respectively). I_{sed} is considerably higher at GeoB8463 (10.5 dpm cm^{-2}), and surpasses the according I_{depl} (6.1 dpm cm^{-2}).

Model 2: sedimentation after long-range lateral transport in the BNL

The second model explains ^{234}Th depletion in the BNL with sedimentation of particles that have stayed in suspension during long-range transport. There are some indications supporting the significance of the processes involved in this model:

- The excess of I_{sed} relative to I_{depl} at GeoB8463 indicates lateral particles transport to this location, positioned directly over the depocenter.
- Even if we use the results of model 1, the calculated long residence times corroborate the high significance of long range advective transport.
- 14C-based sediment accumulation rates for the stations at 1000m water depth at 24.25°S and 25.5°S indicate high present-day deposition of particles (14.6 and 39.2 cm ky-1 respectively), supporting the role of parts of the Namibian slope as a particle depocenter.
- Mollenhauer et al. (2003) present long-term current measurements from slope depth bottom waters offshore Namibia, revealing tidally driven changes in current direction, but offshore directed mean flow, and velocities up to 25 cm s-1,high enough to keep particles in suspension for a long period of time.

According to this model, the particle residence time calculated from the ^{234}Th depletion in the BNL rather represents the removal time of particles from the BNL.

Concerning sedimentation, ^{234}Th is suitable for tracing mass flux of particles to the sediment (F_{sed}) on a short time-scale. Due to the short half-life of ^{234}Th, the sediments are supposed to reflect steady-state conditions. Thus, F_{sed} can be calculated from I_{sed} according to Biscaye and Anderson (1994):

$$F_{sed} = \frac{I_{sed} * \lambda}{^{234}Th_{spec}} \quad (9).$$

An average value of all in-situ-pump and CTD $^{234}Th_{spec}$ data from the BNL of 975 ± 244 dpm g^{-1} has been used as a best estimate of the specific activity of the particles settling to the

seafloor. F_{sed} is significantly higher at station GeoB8463 (2750 mg m^{-2} d^{-1}) compared to GeoB84101 (630 mg m^{-2} d^{-1}), reflecting the role of this part of the Namibian slope as an area of intensive particle deposition.

In 2000, particle settling fluxes were determined in the mid water column (960 m) somewhat further down the slope (1800 m water depth) offshore Walvis Bay (206 mg $m^{-2}d^{-1}$) and Lüderitz (316 mg $m^{-2}d^{-1}$) using sediment traps (G. Fischer, pers. comm.). The mass-fluxes calculated from ^{234}Th exceed the trap-data by factor 2 to 13, reflecting the dominant role of lateral particle transport at the continental slope offshore Namibia. One reason for the high relative importance of lateral supply may be effective remineralization of the vertical flux in the water column, as indicated by an intensive oxygen minimum zone in 200-400m water depth (Bailey, 1991; Inthorn et al., subm.-b; chapter 2). It is likely that part of the ^{234}Th exported from the euphotic zone is released in this zone of mineralization, as was shown previously by Usbeck et al. (2002) and Savoye et al. (2004). This zone was not sampled for ^{234}Th in this study.

Applying C_{org} values of BNL-particles of 12% as determined by Inthorn et al. (subm.-b; chapter 2), the flux of C_{org} into the sediment ($F_{Corg)}$ amounts to 76 mg C_{org} $m^{-2}d^{-1}$ at station GeoB84101, and 329 mg C_{org} $m^{-2}d^{-1}$ at station GeoB8463 (Table 3.3). These values are of the same magnitude as carbon mineralization rates of 117 mg C_{org} $m^{-2}d^{-1}$ at a station at 1000 m depth and about 15 km onshore of station GeoB84101 and 72 mg C_{org} $m^{-2}d^{-1}$ at station GeoB8463 (Aspetsberger et al., subm.-a), indicating that, notwithstanding the large fraction of advected particles, C_{org} is remineralized to a large extent in the surface sediment.

Model comparision

The local resuspension model as well as the sedimentation model represent extreme cases in describing particle transport and exchange processes at the sediment water interface. Both models can explain ^{234}Th depletion in the BNL and ^{234}Th excess in the surface sediments.

Good correlation of SPM and $^{234}Th_{depl}$ supports model 1, addressing ^{234}Th-scavenging in the BNL, resettling of the particles, bioturbation in the surface sediments and resuspension of low activity particles. The assumption of negligible vertical ^{234}Th flux to the BNL, necessary to calculate particle residence times, induces some error in the results. Even if complete profiles of ^{234}Th distribution in the water column had been available, the uncertainty in S would be large (Rutgers van der Loeff et al., 2002). Additionally, the comparison of mass fluxes from the sediment traps with the results of model 2 reconfirms the suitability of the assumption. It has to be kept in mind though that model 1 is incompatible with net sedimentation. Radiocarbon data clearly show net sedimentation, but ^{14}C integrates over much longer time intervals than ^{234}Th, and may be influenced by seasonality so that it does not necessarily reflect the sampling situation. Model 2, focusing on sedimentation of particles after long-range transport in the BNL, better reflects the role of the

Namibian continental slope as a particle depocenter. Additionally, the calculated massfluxes are consistent with carbon mineralization rates in this area. On the other hand, model 2 does not give an explanation for the correlation of SPM and $^{234}Th_{depl}$, leading to the conclusion that reality is presumably best described by a combination of both model approaches.

3.6. Conclusions

In spite of the limited extent of our study, particle exchange and transport processes at the sediment-water interface and in the BNL are successfully addressed with the natural radiotracer ^{234}Th. Other studies point to high importance of deep lateral particles transport on the continental slope offshore Namibia (Giraudeau et al., 2000; Mollenhauer et al., 2003; Inthorn et al., subm.-b, in press, chapters 2 and 4), but here, first quantitative measures of involved processes are given. With respect to the observed ^{234}Th distribution, two models could explain depletion in the BNL and excess in the surface sediments, both emphasizing strong significance of processes at the sediment-water interface. High mass flux into the sediment at a slope depth depocenter, compared to order-of-magnitude lower vertical particle fluxes towards nearby positioned sediment traps, strongly support the findings of the other studies. Comparable residence/removal times of the particles in the BNL at all three stations indicate generally identical transport/removal processes along the slope, while the extent and particle concentration of the BNL as well as the sediment accumulation rate vary significantly. Nevertheless, a higher number of stations, and a better vertical resolution of samples would be necessary to differentiate between resuspension and sedimentation processes, to verify the quantities, to get an overview over larger scale particle export, and to localize sources and sinks.

^{234}Th and SPM samples from the bottom water sampler represent an in-situ resuspension of particles from the sediment surface. The obtained results represent the first specific ^{234}Th activity data of the easily resuspendable fraction of the surface sediment. This will prove useful for future modeling of ^{234}Th exchange processes at the sediment-water interface.

Acknowledgments

We would like to thank the captain and crew of RV *Meteor* for their strong support during the cruise M57/2. We are very grateful for the introduction to the ^{234}Th-sampling procedure, and the measurements provided in a very friendly way by I. Voege. We highly appreciate the provision of sensors and technical help by M. Bergenthal, and the in-situ-pump by W. Balzer. We thank Ulrike Holzwarth for assistance onboard. G. Fischer kindly provided unpublished sediment trap data. T. Ferdelman contributed helpful comments on the manuscript. This research was funded by the Deutsche Forschungsgemeinschaft as part of the Research Center "Ocean Margins" (RCOM) of the University of Bremen contribution no. XXXX.

4. Lateral transport controls distribution, quality and burial of organic matter along continental slopes in high-productivity areas

Maik Inthorn[1], Thomas Wagner[2], Georg Scheeder[3], Matthias Zabel[1]

[1]*University of Bremen, FB5 – Geosciences, Klagenfurter Str., D-28359 Bremen, Germany*

[2]*School of Civil Engineering & Geosciences, University of Newcastle, Newcastle upon Tyne, NE1 7RU, UK*

[3]*Bundesanstalt für Geowissenschaften und Rohstoffe (BGR), Stilleweg 2, D-30655 Hannover, Germany*

4.1. Abstract

In this study, we demonstrate the relevance of lateral particle transport in bottom nepheloid layers (BNL) for organic carbon (OC) accumulation and burial across high-productive continental margins. We present geochemical data from surface sediments and suspended particles in the BNL from the most productive coastal upwelling area of the modern ocean, the Benguela upwelling system (BUS) offshore SW-Africa. Interpretation of depositional patterns, and comparison of downslope trends in OC content, organic matter (OM) composition, lability, and ^{14}C age between suspended particles and surface sediments indicate lateral particle transport as the primary mechanism controlling supply and burial of OC. We propose that effective, seaward particle transport along BNLs is a key process that promotes and maintains local high sedimentation rates, ultimately causing the extraordinary high preservation of OC in a depocenter on the upper slope offshore Namibia. As lateral transport efficiently displaces areas of enhanced OC burial from maximum production at high-productive continental margins, vertical particle flux models do not sufficiently explain the relationship between primary production and shallow marine OC burial. On geological time scales, widest distribution and strongest intensity of lateral particle transport is expected during periods of rapid sea level change. At times in the geological past, widespread downslope lateral transport of OC thus may have been a primary driver of enhanced OC burial at deeper continental slopes and abyssal basins.

4.2. Introduction

The Benguela Upwelling System (BUS) offshore south-western Africa is the most productive coastal upwelling region of the ocean. With an estimated primary production of 0.37 Gt carbon per year (Carr, 2001), extraordinary high organic carbon (OC) concentrations up to 15% in surface sediments, and a widespread oxygen minimum zone (OMZ) expanding from the shelf far across the upper continental margin, the BUS constitutes a major carbon sink for atmospheric CO_2 (e.g. Mollenhauer et al., 2002). Due to these features, the BUS and other high-productive upwelling systems are considered modern analogues of Mesozoic marine black shales (Calvert and Pedersen, 1992).

Principal relationships between marine production, OM flux, and burial in the sediments are well documented from sediment trap and core top data (e.g. Antia et al., 2001). Recent studies, however, emphasize the importance of lateral transport with respect to OM preservation (e.g. Arthur et al., 1998; Ganeshram et al., 1999) quality, and age along continental margins (e.g. Bauer and Druffel, 1998; Hwang et al., 2005). Lateral processes have been proposed to be capable to offset areas of highest production on the shelf from depositional centers of primary OC burial at greater water depths with strong influence on marine organic carbon cycling (e.g. Jahnke et al., 1990; Seiter et al., 2005). Due to the exceptional role as a carbon sink for atmospheric CO_2, high productive continental margins need specific attention and optimized research strategies to assess the importance of lateral processes.

The samples used for this study were collected during cruises M57/1 and M57/2 of RV *Meteor* in February and March 2003 and AHAB1 of RV *Alexander von Humboldt* in January 2004 (Fig. 4.1). Sediment samples were retrieved at 95 stations using a multiple corer system (Fig. 4.1). Suspended particulate matter (SPM) from the lowermost part of the bottom nepheloid layer (BNL) with a MCLANE in-situ-pump attached to a bottom water sampler at 13 stations across the continental slope offshore Namibia (Fig. 4.1). We present data on OC content, C/N-ratio, ^{14}C-age, hydrogen richness and preservation of the particles that allow discrimination of vertical from lateral OM input and subsequent burial. The results document the relevance of lateral processes in the study area, and provide broader implications for conceptual models addressing the relationship between marine production, OM burial and periods of sea level regression in the geological past.

4.3. Study area

Below the BUS, the southwest African continental margin slopes westward to the abyssal plain of the Cape Basin with the Walvis and Agulhas Ridges forming its northern and southern boundaries (Fig. 4.1). No major slides or turbidites are reported, while double shelf breaks are common, with inner and outer breaks at water depths (wd) of 140 to 180 m and 360 to 400 m, respectively (Shannon and Nelson, 1996). Terrigenous matter input to the SW-African shelf is low due to the absence of perennial rivers except for the Orange in the

south (Shannon and Nelson, 1996). Upwelling takes place along the entire coast, but is most prominent in several upwelling cells, with the Lüderitz cell at about 27°S being the strongest and perennial (Shannon and Nelson, 1996). Accordingly, primary production is mainly constrained to the inner shelf (Carr, 2001). Mesoscale filaments and plumes temporarily transport nutrient-rich and highly productive filaments seaward across the continental slope (Lutjeharms et al., 1991).

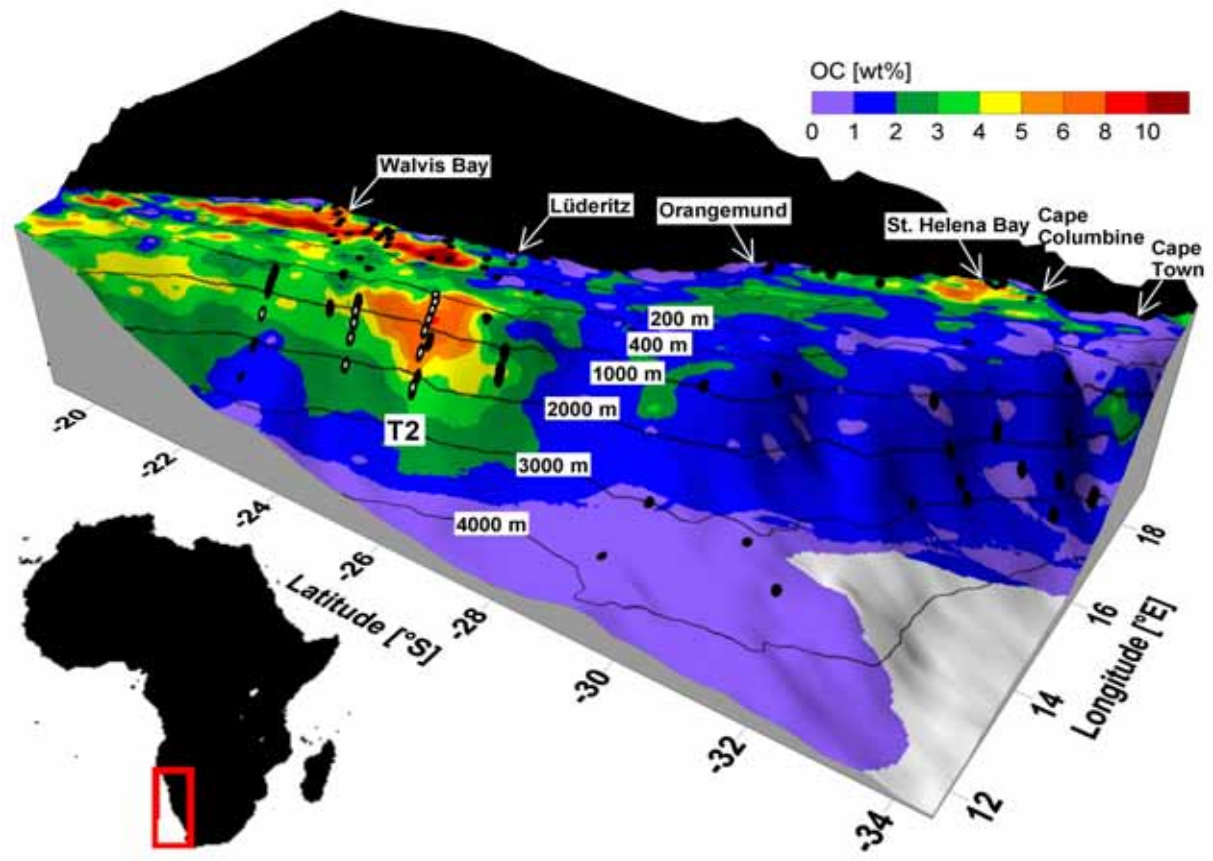

Fig. 4.1.Organic carbon distribution in the surface sediments on the continental margin offshore south-western Africa. The dataset comprises 1560 data points (Birch, 1975; Bremner, 1981; Calvert and Price, 1970; Levitan et al., 1990; Lisitzin et al., 1975; Mollenhauer et al., 2002; Rogers, 1977; Romankevich, 1994; Schmiedl et al., 1997). Stations sampled for Rock Eval pyrolysis and determination of the C/N-ratio are indicated by black (sediment samples) and white (SPM) circles.

4.4. Sampling and methods

The samples used for this study were collected during cruises M57/1 and M57/2 of RV Meteor in February and March 2003 and AHAB1 of RV Alexander von Humboldt in January 2004 (Fig. 4.1). Sediment samples were retrieved at 95 stations using a multiple corer system (Fig. 4.1), sampled in one to several centimeters depth increments, and stored deep-frozen until they were freeze-dried and powdered in a mortar in the home laboratory.

During cruise M57/2, suspended particulate matter (SPM) from the lowermost water column was sampled at 13 stations across the continental slope offshore Namibia (Fig. 4.1). Samples were retrieved from approximately 30 cm above the seafloor with a MCLANE in-situ-pump attached to a bottom water sampler, and equipped with 143 mm pre-combusted and pre-weighed glass fiber filters (SCHLEICHER & SCHUELL, GF52). On average, 230 liters of bottom water were filtered in 60 minutes time. All filters were rinsed with distilled water to remove sea salt, and stored deep frozen for transport to the home laboratory. For determination of the total carbon (TC) and nitrogen (TN) content, sub-samples of the sediments and filters were combusted in a CARLO ERBA Element CNS Analyzer (precision: ±3%). Inorganic carbon (IC) was determined with a UIC INC. COULOMETRICS CM5012 coulometer after CO2 liberation with 2N phosphoric acid (precision: ±1%). OC was calculated as the difference between TC and IC. C/N ratios are based on OC and TN. Reweighing of the filters, and determination of the OC content gave the concentration of particulate organic carbon (POC), suspended in the bottom water.

OC data from our samples were merged with records from the literature (Birch, 1975; Bremner, 1981; Calvert and Price, 1970; Levitan et al., 1990; Lisitzin et al., 1975; Mollenhauer et al., 2002; Rogers, 1977; Romankevich, 1994; Schmiedl et al., 1997) to generate a contour map of OC distribution offshore southwest Africa (using the kriging and gridding method of "Surfer 8.0", Golden Software Inc.). Of all 1560 data points, 86% are from locations less than 1000 m wd, resulting in a data density of about one sample per 200 km2 for the shelf and upper slope (Fig. 4.1). A complete list of all data is provided in the data archive PANGAEA (http://www.pangaea.de).

AMS radiocarbon analyses of bulk OC was performed at the Leibniz-Laboratory for Radiometric Dating and Isotope Research (University of Kiel, Germany), and at National Ocean Science AMS (NOSAMS) facility (Woods Hole, USA) on seven filter samples, and sediment from three stations (precision: 1%). Sedimentation rates were obtained by linear interpolation between the ^{14}C-age of the sediment surface sample and a deeper sample 10 to 20 cm below the seafloor. All stations are positioned along one transect at approximately 25.5°S offshore Namibia (T2, Fig. 4.1).

Rock-Eval pyrolysis is a well established geochemical tool to determine the hydrogen-richness (a measure for composition), and to characterize the preservation (a measure for reactivity/maturity) of bulk OM in unconsolidated marine deposits (see e.g. Tyson, 1995; Wagner and Dupont, 1999 for reviews). This study provides the first parallel application of Rock-Eval to modern surficial sediments and suspended particles from the BNL at the same positions. Rock-Eval pyrolysis was performed with a Rock-Eval VI on 13 filters and 95 sediment samples, according to Espitalié et al. (1977). Hydrocarbons (HC), released during the pyrolysis cycle below 300°C and between 300 and 550°C, are presented as S1 and S2 yields, respectively. Precision of the HC determination was better than 6%.

4.5. Results

Concentrations of OC in surface sediments reveal a very heterogeneous distribution across the continental margin off SW Africa (Fig 1). OC is generally above 2% north of 27°S, while it is generally below 2% to the south. In the deep Cape Basin and around Cape Town in the far south, OC is below 1%. Highest OC values up to 15% are recorded in a "mudbelt" of about 25,000 km² on the inner shelf between 20.6 and 25.5°S below the Walvis Bay and Lüderitz upwelling cells. Slope depths do not show OC enrichment, except for one distinct depocenter of about 5000 km² between 24° to 26.5°S, and about 400 and 1500 m wd with up to 9% OC.

Across this depocenter (T2, Fig. 4.1), sedimentary ^{14}C-ages and corresponding sedimentation rates, calculated from the ^{14}C data, are highest on the uppermost slope (3110 years, 112 cm ky^{-1} at 646 m) and decrease downslope to 1870 ^{14}C years and 22 cm ky^{-1} at 2289 m (Fig. 4.2a and Table 4.1). ^{14}C ages of SPM increase from 2105 ^{14}C years close to the shelf edge (390 m wd) to the upper slope (Table 4.2), where they are slightly younger than the sediments (2795 ^{14}C years 598 m wd). Further down the slope, the age of the SPM remains at the same level, reaching 2590 ^{14}C years at 2280 m wd. The data evidence that SPM is older than the underlying sediments at the upper slope, but more than 700 ^{14}C years younger on the deep slope, accompanied by a strong decrease in POC concentrations (Fig. 4.2a and Table 4.2). Sedimentary C/N data reveal values below 10 on the inner shelf down to 200m wd, increasing at greater water depth to values between 10 and 14 (Fig. 4.2b).

Table 4.1. Conventional radiocarbon ages of particles at the sediment surface, and calculated sedimentation rates.

station	latitude [°N]	longitude [°E]	water depth [m]	age [^{14}C years]	sedimentation rate [cm ky^{-1}]
RCOM2506	-25.47	13.53	646	3110±40	112
GeoB 8451	-25.48	13.35	1028	2520±35	39
GeoB 8462	-25.53	12.94	2289	1870±35	22

The slope of the regression line on a plot of the S2 yields from Rock Eval pyrolysis vs. OC content multiplied by 100 provides the mean hydrogen index (HI in mgHCg^{-1}OC) of the sample suite (Langford and Blanc-Valleron, 1990). Three sample subsets with different slopes of the regression line were identified (Fig. 4.3a): 1) Surface sediments north of 27°S, and from the southern upwelling cells show a mean HI of 343. 2) Corresponding SPM samples from the Namibian continental slope exhibit a shallower slope than the surface sediments, representing about 30% lower S2 yields at comparable OC. 3) Lowest hydrocarbon equivalent yields (HC) with a low mean HI of 173 are recorded for OC poor sediment samples south of 27°S.

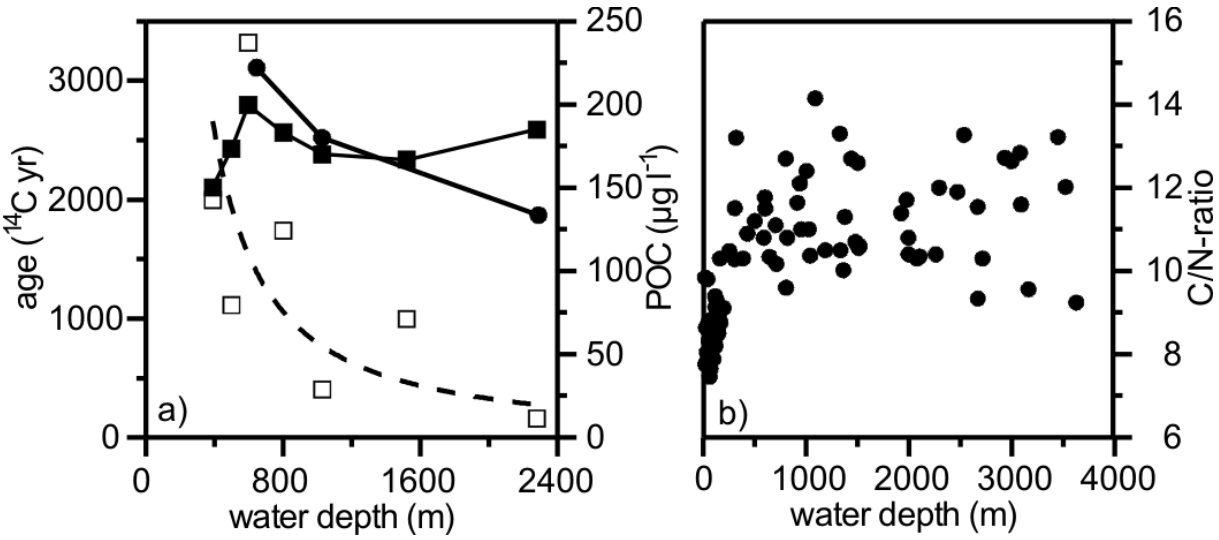

Fig. 4.2. a) Conventional radiocarbon ages of sedimentary (filled circles) and suspended OM (filled squares), as well as POC (open squares) of samples on transect T2 vs. water depth (Fig. 4.1, Tables 4.1 and 4.2). b) C/N-ratio of surficial sediments offshore SW Africa vs. water depth.

Table 4.2. OC-content, C/N-ratio, conventional radiocarbon ages, S2-yield and fraction of labile OM over total hydrocarbons of particles suspended in the lowermost BNL.

Station	location		depth	OC	POC	C/N-	age	S2	labile HC
	[°S]	[°E]	[m]	[%]	[µg l^{-1}]	ratio	[^{14}C years]	[mg HC g^{-1}]	/total HC [%]
GeoB 84104	23.00	12.58	1439	1.3	11.5	6.4	n/d	3.73	28.9
GeoB 8495	24.36	13.14	1008	2.9	21.1	8.6	n/d	8.70	32.1
GeoB 8418	24.36	13.14	1006	2.4	21.4	7.3	n/d	6.41	32.3
GeoB 8496	24.39	13.06	1187	1.9	11.5	7.1	n/d	4.23	36.9
GeoB 8497	24.42	12.92	1519	3.6	20.0	9.8	n/d	8.14	29.1
GeoB 8425	24.46	12.72	1998	2.1	9.7	11.3	n/d	4.57	32.1
GeoB 8457	25.43	13.69	390	8.5	142.5	9.4	2105±30	18.76	30.9
GeoB 8458	25.48	13.61	500	8.4	79.4	10.8	2430±45	18.10	30.0
GeoB 8491	25.48	13.54	598	9.3	237.1	9.2	2795±35	21.52	31.7
GeoB 8459	25.47	13.45	801	8.0	124.2	9.8	2565±30	23.61	31.5
GeoB 8490	25.48	13.35	1030	4.1	28.8	9.7	2380±35	11.59	27.6
GeoB 8489	25.51	13.18	1522	7.0	71.3	11.4	2335±35	13.95	27.4
GeoB 8462	25.53	12.94	2280	2.2	11.4	6.2	2590±100	5.56	35.3

Sediment and SPM samples from the mudbelt and depocenter area offshore Namibia reveal a distinct bi-modal S2-peak during pyrolysis, a feature that was not observed in any of the other samples. Comparable observations have been reported from surface and late Quaternary sediments from the equatorial west African continental margin (Holtvoeth et al., 2001; Wagner et al., 2004). In agreement with these studies, we assume two types of OM that release HC within the S2 window, according to their thermal stability/reactivity. Integration of the two sub-peaks of the S2 thus enables quantification of the relative proportion of HC generated by labile (summarized S1 and S2 peak area up to 375°C) and more stable OM (S2 yield above 375°C). The HC fraction from labile OM is not correlated to OC (R^2=0.19, n=108), supporting the conclusion that this proxy is a qualitative measure of the bulk OM, rather

than dependent on OM quantity. The projection of the HC fraction from labile OM relative to the total HC fraction (S1 and S2) against wd (Fig. 4.3b) shows a contribution of 25% to 47% of the total HC yield in sediments and SPM samples from the mudbelt and slope depocenter. Outside these areas, the contribution of labile OM is typically lower than 25% and shows minima below 20% at about 2000 m wd. The HC contribution of the labile fraction rises above 25% in sediments from the deep slope below 2600 m wd, but in these low OC-samples the S2 shows up as a broad peak without a pronounced maximum in the range of the labile fraction.

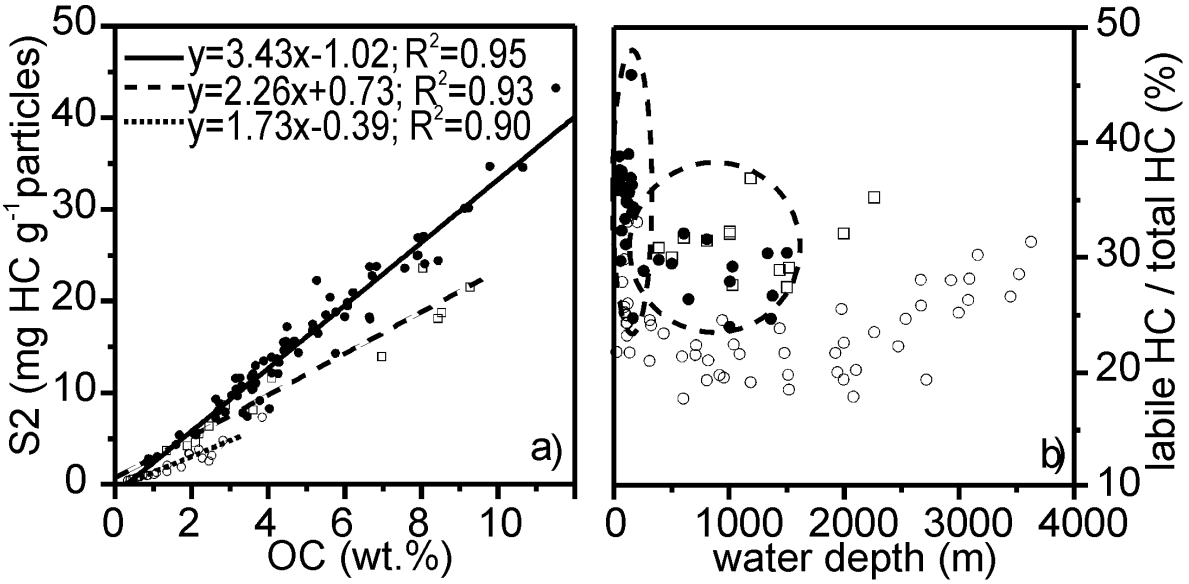

Fig. 4.3. a) Scatter plots of wt%-OC versus S2 yield for surficial sediments, sampled north of 27°S and in the vicinity of southern upwelling cells (solid circles, solid line), all other sediment samples south of 27°S (open circles, dotted line), and SPM samples from the BNL (squares, dashed line). b) Fraction of hydrocarbon equivalent (HC) yield of labile over total OM against water depth in mudbelt and depocenter sediments offshore Namibia (solid circles), all other sediment samples (open circles), and in the SPM samples from the BNL (open squares).

4.6. Discussion

Based on the observations from the SW-African continental slope, we propose a conceptional particle flux model, likely also representing other high-productive continental upwelling areas of the modern ocean (Fig. 4.4). The particle flux model suggests strongest primary production and preservation above the inner shelf, reflected in bottom water oxygen depletion (Bailey, 1991), low C/N-ratio as well as a better preservation of labile OM, while resuspension induces effective offshore directed OM export. Below the shelf-break, at the upper slope, particle input from lateral transport in INLs and BNLs exceeds vertical input of "fresh" material from surface waters, resulting in high sedimentary ^{14}C-age (although a reservoir age of up to 1000 years has to be considered according to Mollenhauer et al., 2003), C/N-ratio, POC concentration, and sedimentation rate at the sea floor. At the lower slope,

the influence of lateral transport progressively decreases to the benefit of the vertical component, as reflected by younger ^{14}C-ages, and lower C/N-ratio, POC and sedimentation rate. Due to its rather homogenous high ^{14}C-age and low mean-HI, SPM from the BNL likely represents the lateral endmember of this particle transport model.

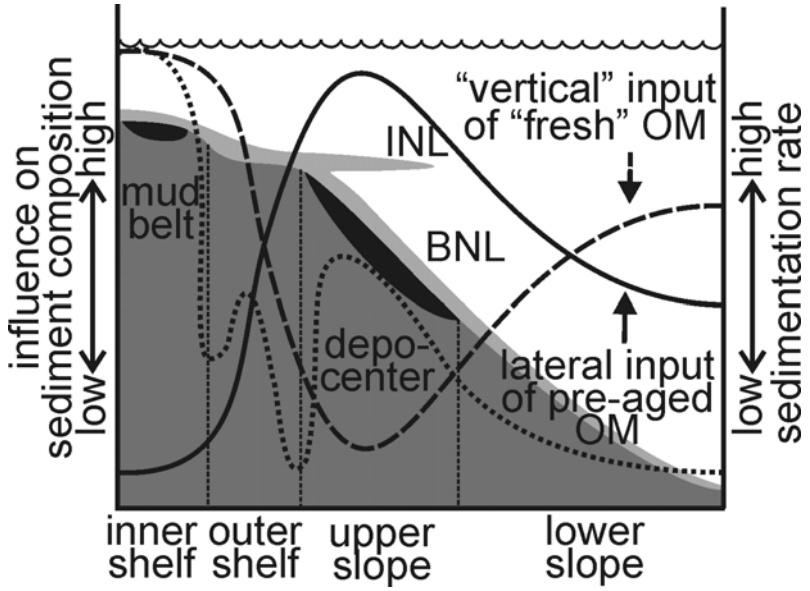

Fig. 4.4. Particle transport model, discriminating between the relative importance of "vertical" (dashed line) and lateral (solid line) organic matter input to the sediments of the Namibian continental margin at about 25.5°S. Sedimentation rate (dotted line), shelf and slope depth enrichments of OC (mudbelt and depocenter, resp., black areas), and bottom and intermediated nepheloid layers (BNL and INL resp., bright grey) are displayed.

The lowermost 20 cm above the seafloor of the Namibian slope is well oxygenated (199-238 µM O_2; Aspetsberger et al., subm.-b). Accordingly,, the enhanced preservation of OM in the slope depocenter is mainly attributable to particle aggregation in the BNL (Ransom et al., 1998), and the high sedimentation rate (Armstrong et al., 2002) induced by intensive lateral particle transport. The advective processes effectively displace areas of enhanced OC burial from maximum production cells along the inner shelf towards the slope and possibly the deep-sea. Mean HI-values from the BUS and other continental margins propose similar mechanisms (Fig. 4.5), relating these key areas of marine OM production and OC burial to each other. We therefore assume that the applicability of vertical particle flux models is also limited for comparable depositional systems.

On a short time scale, seasonality, local topography, the wind field, and the ocean current system control the position of high productive cells in surface waters, and OC depocenters at the sea floor. On geological time scales, however, changes in atmospheric and oceanic circulation, and, probably even more important, sea level has a much more profound impact on lateral transport. Lowering of the sea level at the end of warm periods, for example, stimulated the offshore displacement of active upwelling systems, and relocated large OM reservoirs from the previously wide, productive shelf-seas to the deeper ocean

(McCave, 2003). During glacials, lowering of sea level extended the area subject to storm-wave activity and associated resuspending forces towards the outer shelf break exposing the inner shelf to erosional forces of wind and rivers. A link between our results on present-day OM quality at the sediment-water interface and past oceanographic situations is provided by Pichevin et al. (2004). They report organic-rich sediments with high HI-values for the glacial isotope stages 2 and 4 on the Namibian continental slope, indicating enhanced organic matter input and/or preservation. For the same area and time periods, Summerhayes et al. (1995b) report high ^{14}C-data and fractions of terrigenous material. They conclude that lateral input from erosion on the shelf accounts for up to 43% of the total OC, emphasizing the importance of reworked OM in that area. Mollenhauer et al (2002) estimated that TOC accumulation on the Namibian continental slope was approximately 84 % higher during the last glacial maximum compared to the Holocene, also stressing the significance of lateral transport. Depocenters for OC on the shelf rarely persist for long time periods, and thus do not serve as carbon sinks over geological times. Different from that, enrichment of OM in deep marine sediments has a much better chance to enter the geological record, and thus has a sustainable effect on sequestration of carbon from the atmosphere.

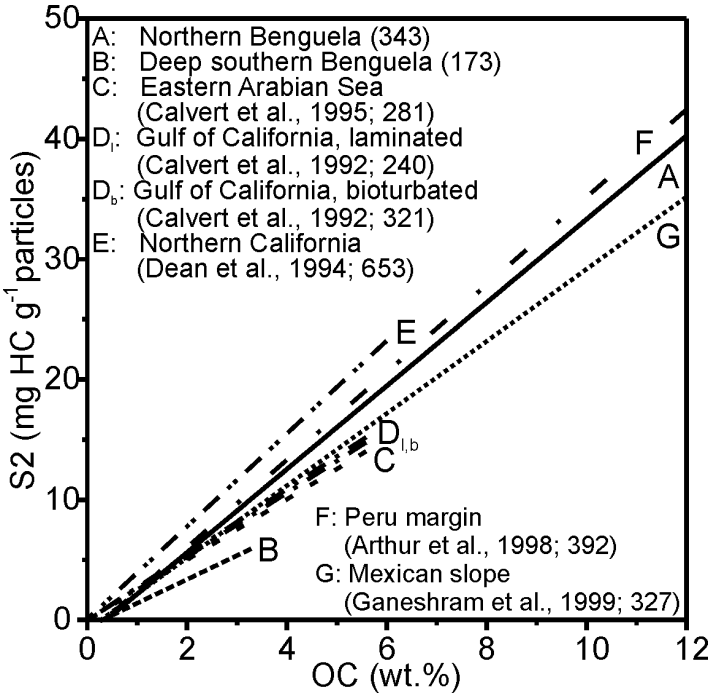

Fig. 4.5. Relationship between S2 and total organic carbon (OC) in sediments offshore Namibia in comparison with other continental margin sediments. Numbers in parentheses indicate the mean HI value for the respective data set.

4.7. Conclusion

Geochemical data from surface sediments and suspended particles in bottom nepheloid layers (BNL) from the most productive upwelling area of the modern ocean, the Benguela upwelling system (BUS), confirm the importance of lateral transport in this key

area of modern carbon production and marine sequestration. Depositional patterns and downslope trends in OC, OM composition, lability, and ^{14}C age reveal lateral particle transport as the primary mechanism controlling supply and burial of OC. Intense lateral transport of aggregated, labile OM in BNLs, originating from the shelf break, supports high sedimentation rates, and ultimately promotes the exceptionally high preservation of OM in slope depocenters off Namibia. A conceptional particle flux model, distinguishing the relative significance of vertical and lateral input across the Namibian margin, is proposed that explains the distribution of geochemical proxies, and is likely transferable to other high-productive continental margins of the modern ocean. Strong remobilization and lateral export of OM from shelf areas towards the slope and the deep-sea during periods of rapid sea level change is suggested as a major factor inducing deep-water OM depocenters in the geological record. The results from the BUS identify lateral transport as an important, yet hardly recognized secondary mechanism, effectively transferring carbon from the atmosphere to long-term sequestration in the deep sea, and supporting the deposition of OC-rich sediments with high hydrocarbon potential.

Acknowledgments

We thank the captains and crews of RV *Meteor* and RV *Alexander von Humboldt* for their support during the cruises M57/2 and AHAB1. S. Calvert and the Council for Geoscience, Marine Geoscience Unit, South Africa, kindly provided literature data. K. Seiter helped considerably in preparing the OC distribution map. We thank F. Aspetsberger, T. Leipe and G. Mollenhauer for provision of oxygen data, sediment samples and unpublished ^{14}C-data. This research was funded by the Deutsche Forschungsgemeinschaft as part of the Research Center "Ocean Margins" (RCOM) of the University of Bremen contribution no. 0351.

5. BeaWiS - A new sampling and monitoring device for the benthic boundary layer

Maik Inthorn[1], Thomas Kumbier[2], Matthias Zabel[1]

[1]*University of Bremen, FB5 – Geosciences, Klagenfurther Str., D-28359 Bremen, Germany*

[2]*K.U.M. Umwelt- und Meerestechnik Kiel GmbH, Wischhofstraße 1-3, D-24148 Kiel, Germany*

5.1. Abstract

The benthic boundary layer (BBL) of continental margin and deep-sea environments represents a gap in common ship-borne sampling techniques, in spite of its high scientific significance. The new bottom water sampler BeaWiS is suitable for snapshot studies of particle and fluid distribution in combination with the prevailing physical parameters in the benthic boundary layer, which represents an environment of strong vertical gradients in these properties. It provides a combination of a reliable and easy to use water sampling technique for the lowermost meter of the water column with a stainless steel tripod. The tripod works as a platform for a variety of sensors and additional equipment. The sampling unit aligns itself to the prevailing current directions, and permits undisturbed sampling of five times five liters of bottom water. Instrumentation includes a CTD profiler with oxygen sensor and transmissometer attached to it, a profiling current meter, an in-situ-pump and a deep sea camera. This paper presents the principal construction of BeaWiS together with first results from deployments offshore Central America and Namibia, focusing on fluid venting, particle transport and organic matter quality in the bottom nepheloid layer (BNL) respectively.

5.2. Introduction

In recent years, high scientific interest has been attributed to the benthic boundary layer (BBL), representing the lowermost part of the open water column, that is influenced by a decrease in fluid motion towards the surface sediment, accompanied by strong vertical gradients in physical as well as chemical properties of fluids and solids. At the sediment-water interface, fluids are emanating, particles are resuspended by physical and/or biological forcing, and pollutants are laterally transported by bottom currents. A major problem of studies, addressing processes in the lowermost water column, is the insufficient availability of water samples with exactly determinable height intervals above the seafloor, because it represents a gap in common ship-borne sampling techniques. While the sediment surface is usually sampled with multiple corer systems (Barnett et al., 1984), the water column is sampled by CTD-rosette samplers. But due to ship movement it is impossible to obtain accurate sampling depth relative to sea floor with these CTD-rosettes. Up to now, a couple of techniques for sampling the benthic boundary layer (BBL) have been developed (e.g. Chapalain and Thais, 2004; Milligan et al., 1998; Reed et al., 1997; Sauter et al., 2005; Schink et al., 1966; Sternberg et al., 1986; Thomsen et al., 1994). But these techniques are either restricted to low water depth, very sophisticated, and therefore expensive, often uneasy to handle or even unreliable, do not give undisturbed samples, and/or are not adequate to carry an extensive set of additional sensors. Therefore, up to now only a limited set of surveys regarding BBL processes in the deeper marine environment have been carried out.

In this paper, we present the design of a tethered device, capable of fast and reliably providing water samples from the lowermost 1.2 meters of the water column. Due to its design as a steel-frame tripod, it can be additionally equipped with an extensive set of monitoring tools, matching the scientific requirements. A compilation of selected results is presented, proving its suitability concerning fluid sampling in a survey on methane emanations at an active mud extrusion offshore Nicaragua. A second study focuses on transport and quality of suspended particulate matter (SPM) in the bottom nepheloid layer (BNL) on the continental margin offshore Namibia.

5.3. Materials and Methods

The bottom water sampling (BWS, called "BeaWiS") and monitoring system consists of a stainless steel tripod with a sampling unit along a central axis, and a set of independent monitoring equipment (Fig. 5.1). The whole device is tethered to the ships line via a revolving connector, and both the frame and the inner central axis have current-sails for a best possible alignment into the current direction. The side of the tripod opposite to the current sail has no cross struttings to minimize flow interruption during sampling.

Bottom water sampling – A simple arrangement of five 5-liter HYDROBIOS free-flushing sampling bottles is used. They do not taper off towards their ends, as common Niskin-bottles do, which would significantly influence the water flow. The bottles are horizontally attached to the central axis of the frame. Their diameter is 15 cm, while the efficient sampling diameter might be smaller due to boundary layer development on the insight of the bottles. Nevertheless, we consider flow perturbation due to these boundary layers to be tolerable for most applications. The bottle-caps are opened against drag of an elastic silicon band, running through the bottle interior, and are fixed to a revolving mandrel at the central axis. The position of the bottles can be shifted along the central axis between 10 and 120 cm above ground. With its current-sail, the central axis adjusts its position relative to the outer frame in an angle of about 100 degrees along the sampling side of the tripod. This ensures alignment of the bottles directly into the current and, therewith, proper flushing. However, the position of the axis is fixed by spikes that stick into the sediment as soon as it hits the seafloor. The central axis can move upwards by up to 10 cm relative to the outer frame, balancing uneven bottom conditions and guarantees exact sampling heights above the seafloor, even when the heavier outer frame should sink into the sediment due to soft sea floor conditions. Additionally, this movement closes a magnetic contact, thereby activating a timer that is programmed prior to deployment. The timer is connected to a burnwire-system that releases the mandrel, and thereby closes the sampling-bottles after a specified time-interval. This delay ensures that all turbulence and all resuspended particles, originating from the deployment of the device, are transported away by the bottom currents, and that the bottles are properly flushed by bottom water before sampling.

Sensor technology – A SEABIRD SBE 19 CTD (conductivity-temperature-depth) profiler is positioned about 50 cm above the seafloor. An oxygen-sensor and a 0.25 m-pathlength SEATECH transmissometer are connected to the CTD. These sensors collect data over the whole water column from the beginning till the end of the deployment of BeaWiS. The transmissometer is attached to the frame about 25 cm above the seafloor. Beam attenuation data were processed according to Gardner et al. (1993) and Inthorn et al. (subm.-b; chapter 2). A NORTEK AQUADOPP current-profiler is attached very close to the bottom of the outer frame, looking upwards into the water column. It measures direction and speed of the bottom water current in distinct cells of 10 cm thickness. Data from the internal compass and tilt-sensor are used to control the proper alignment of BeaWiS relative to the direction of the current.

Additional equipment – A PHOTOSEA 1000 deep-sea camera system is used to survey sediment surface characteristics. With the MCLANE in-situ-pump, equipped with 143 mm pre-weighed polycarbonate filters, large amounts of water are filtered to achieve high particle quantities for further analysis in the laboratory. The pumping rate was fixed to 250 liters per hour – an adaptation to the prevailing current conditions at the sea floor can not be performed with this instrument.

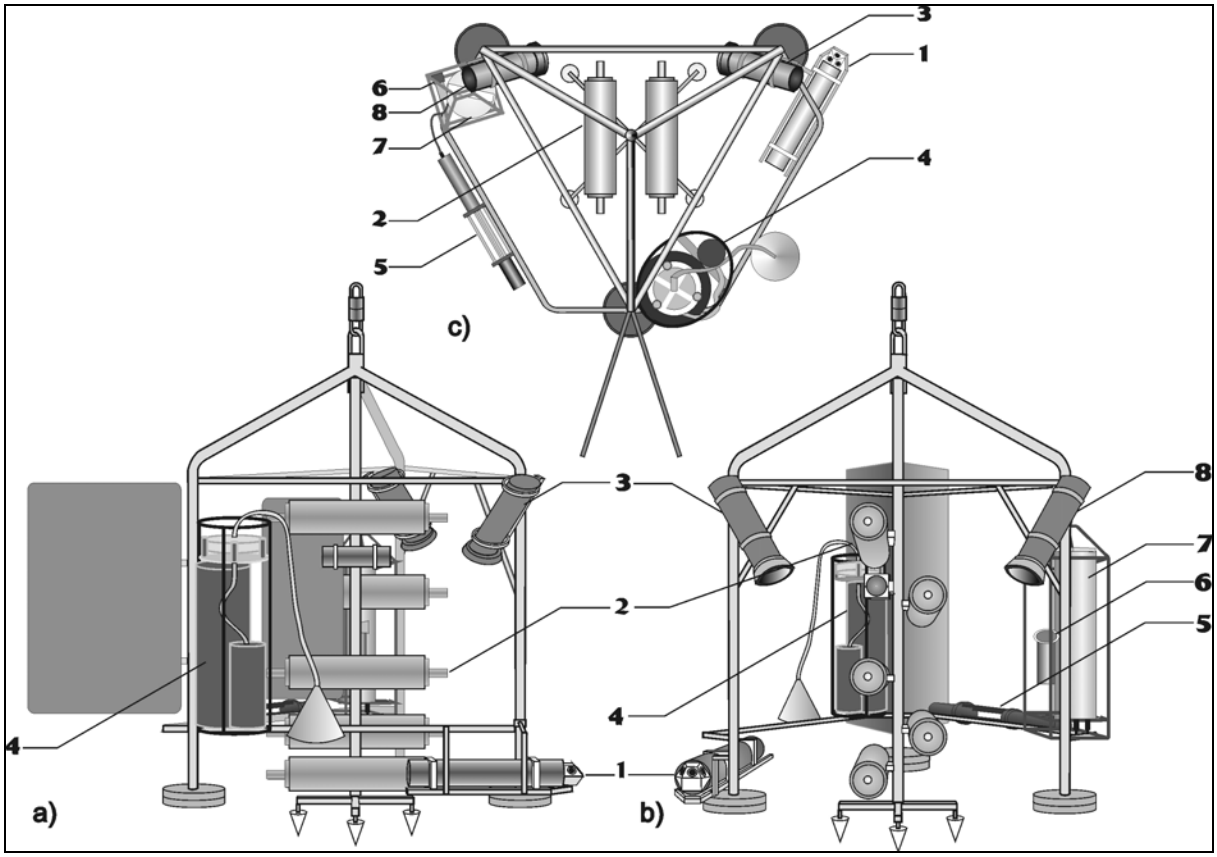

Fig. 5.1: Schematic drawing of the bottom water sampler (BWS) in side (a), front (b), and top (c) view. The stainless-steel tripod is equipped with a current profiler (1), five free-flushing HYDROBIOS sampling-bottles (2), deep-sea camera (3), in-situ-pump (4), transmissometer (5), oxygen-sensor (6), CTD (7) and deep sea flash (8).

The sensors as well as the camera system, the in-situ-pump, and the timer of the sampling unit are programmed prior to deployment, and are therefore independent of a data connection to the ship. The bottom-tracking signal of a pinger, attached to the line, permits to stop the device for a couple of minutes 5 to 10 m above the seafloor (depending on the wave and wind conditions) to give it some time to align with the bottom current.

Sample treatment – For SPM determination, 1 to 5 liters of the water samples (volumetrically determined) were filtered through 2.5 cm pre-combusted and pre-weighed glass fiber filters (SCHLEICHER & SCHUELL, GF52) with a pore size spectrum of 4 to 6 µm. All filters were rinsed with a few milliliters of distilled water to remove sea salt and stored deep frozen for transport to the home laboratory. SPM was determined by reweighing of the freeze-dried filters.

The method for gas-chromatographic determination of methane in the water sampled with the BeaWiS-bottles is described by Mau et al. (subm.).

5.4. Results

5.4.1. Sampling of fluids in the benthic water column

During cruises M54/3 and SO173 with the German research vessels RV *Meteor* and RV *Sonne* to the continental margin off the Pacific coast of Nicaragua and Costa Rica, BeaWiS was used at several stations in combination with a common rosette sampler to determine methane concentrations in the water column above mud extrusions (Mau et al., subm.). Fig. 5.2 shows CH_4 concentration in the water column above Mound Carablanca that are generally increasing towards the seafloor. 3-4 nmol l^{-1} CH_4 are detected about 9 m above the ground in the lowermost samples taken by the CTD/rosette. CH_4 concentrations are distinctly higher in the water samples collected by BeaWiS, i.e. 24 – 112 cm above the seafloor (8.5-24.2 nmol l^{-1}). CH_4 concentration strongly increases towards the seafloor in this last meter above ground. The water, collected by BeaWiS, is enriched in methane by one order of magnitude above the regional background of 0.5 – 2 nmol l^{-1}.

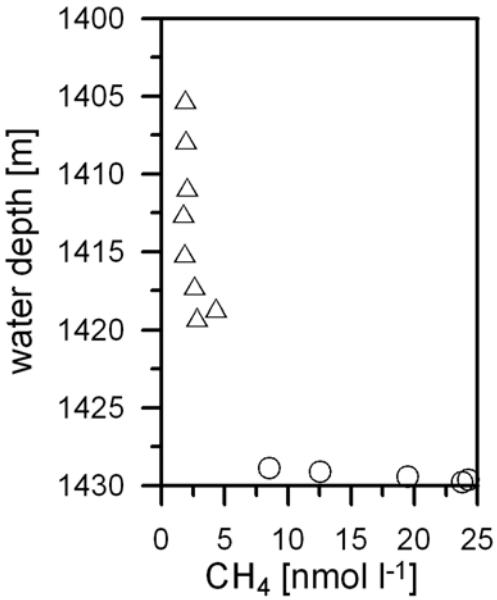

Fig. 5.2: Methane concentration in the water column above the mud extrusion Mound Carablanca at the continental margin off the Pacific coast of Nicaragua as sampled with a CTD-rosette (open triangles), and BeaWiS (open circles).

5.4.2. Suspended particulate matter in the BNL

The main focus of cruise M57/2 with RV *Meteor* to the continental margin offshore Namibia was on lateral particle transport and organic matter quality in the BNL. Beam attenuation profiles, measured with the transmissometer attached to BeaWiS, give an overview over the extent of nepheloid layers in the whole water column. Beam attenuation can be compared and calibrated with the gravimetrically determined SPM from filtered

seawater samples, taken with the in-situ-pump attached to BeaWiS and a CTD-rosette (Fig. 5.3). Along the transect of stations across the continental margin offshore Namibia, beam attenuation and SPM concentrations are generally highest in the euphotic zone, with pronounced decrease at 50 to 80 m water depth. Intermediate waters are low in particulate matter aside of two layers of enhanced particle content at the approximate depth of the shelf break at 200 to 400 m depth, and at 700 to 850 m water depth. The BNL in the lowermost 20 to 100 m of the water column is significantly enriched in SPM, with a distinct increase at the lowermost meter, as sampled with the in-situ-pump. While SPM content determined from the lowermost CTD-rosette sample and the in-situ-pump are comparable to each other in a range of 0.6 to 1.5 mg l^{-1}, SPM, determined from filtration of the BWS-bottle samples, is significantly higher in most of the samples (0.7 to 60 mg l^{-1}), and increases generally towards the sea-floor (Fig. 5.4).

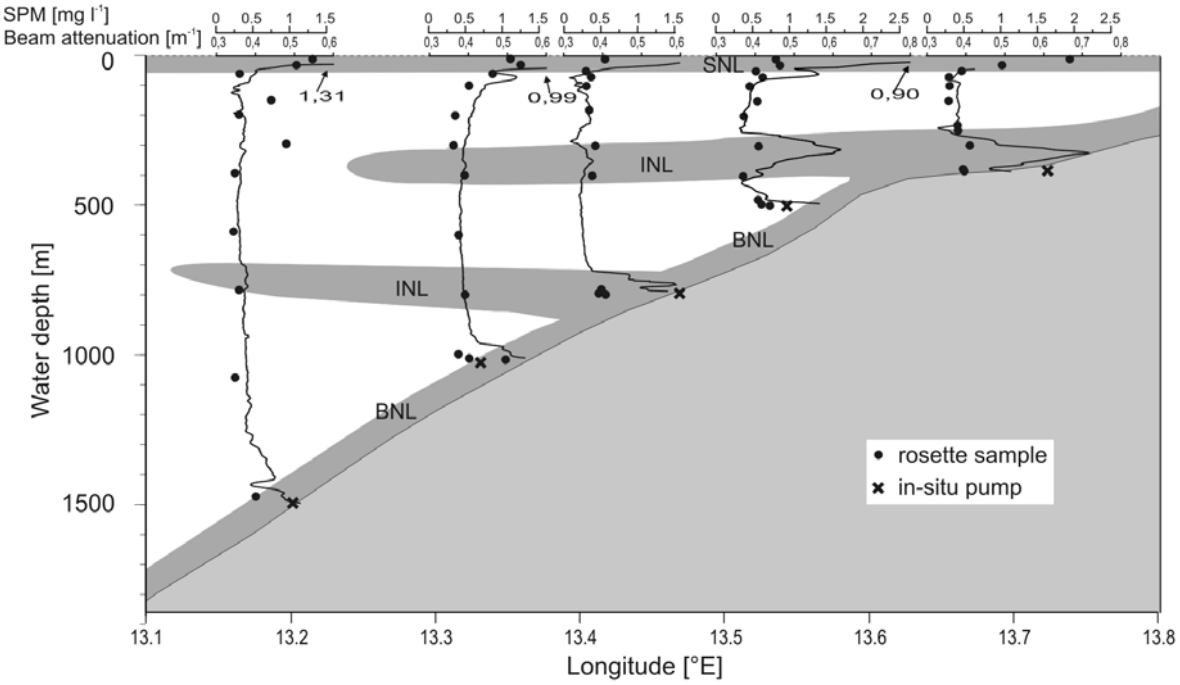

Fig. 5.3: Beam attenuation profiles (black lines) and suspended particulate matter concentrations, received from rosette water samples (filled circles) and the in-situ-pump (black crosses), attached to BeaWiS 25 cm above the seafloor, on a transect at 25.5°S across the Namibian continental margin. Position and extent of nepheloid layers are indicated by dark-gray shaded areas according to Inthorn et al. (subm.-b; chapter 2). SNL: surface nepheloid layer, INL: intermediate nepheloid layer, BNL: bottom nepheloid layer.

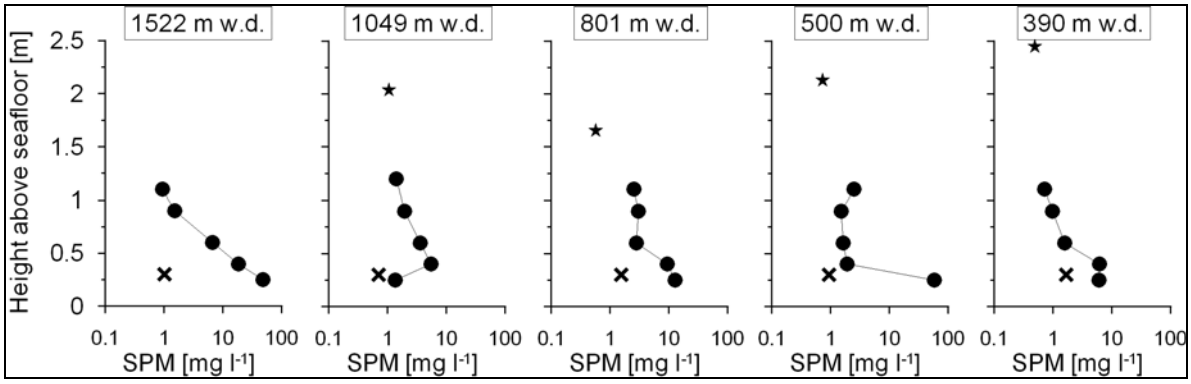

Fig. 5.4: Suspended particulate matter, visualized in log-scale, of the lowermost sample from the CTD-rosette (asterisks), the in-situ-pump (crosses), and the BeaWiS bottle-samples (filled circles) against height above sea-floor at 5 stations on a transect across the Namibian continental slope.

The current meter attached to BeaWiS gives information on predominant current directions during the 2-hour deployments in the bottom waters of the Namibian continental slope (Fig. 5.5). Variation in current direction is mainly attributable to tidal influence at different sampling times, but it is evident, that the main direction of the low-velocity (mean of 5 to 10 cm s^{-1}, 60 cm above the ground) bottom current is offshore.

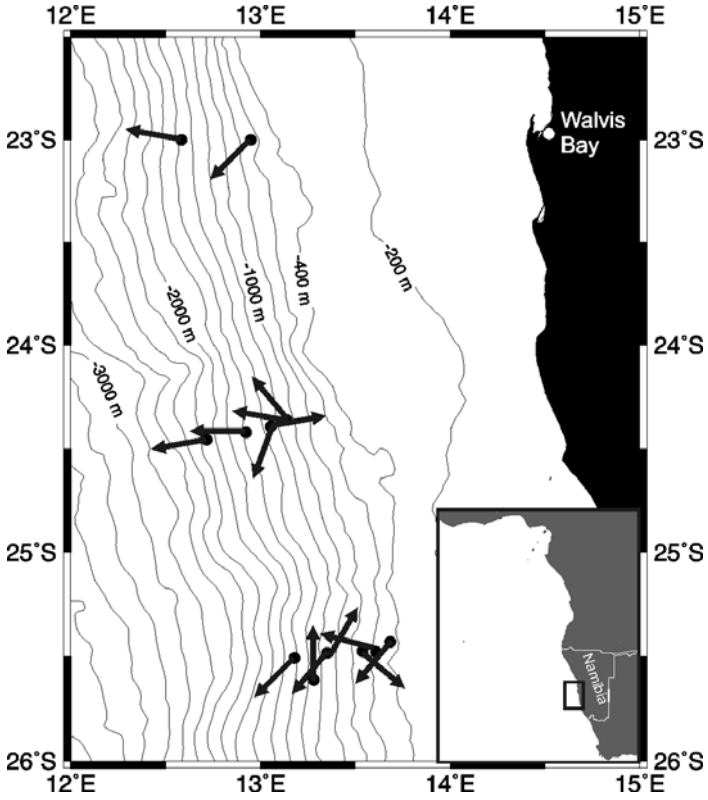

Fig. 5.5: Average current directions during the 2-hour-deployment of BeaWiS in the bottom waters of the Namibian continental slope.

5.5. Discussion

Fluid emanations from the seafloor, lateral particle and pollutant transport processes, intensive diagenetic degradation of the particles, food supply for deep marine biota – these topics make the lowermost part of the water column an environment of high interest to present-day marine science. Nevertheless, it still represents a gap in common ship-borne sampling techniques.

The example regarding fluid sampling at the continental margin off Nicaragua (Fig. 5.2) visualizes that BeaWiS actually filled the gap between the lowermost CTD-rosette samples, taken about 10 m above the sea-floor and the sediment surface. The constant increase of CH_4 concentrations towards the seafloor without spikes in the profile points to venting of methane dissolved in the fluid. It also illustrates that Mound Carablanca is an active seepage site.

At the continental margin offshore Namibia, sample material and sensor data from BeaWiS gave important, and in some respect unique information on the significance of lateral particle transport processes and the quality of organic matter in the BNL, contributing considerably to the integrated study. Through comparison and calibration, beam attenuation profiles extended the data-set on suspended particulate matter and organic carbon content in the water column, and allowed identification of nepheloid layers by Inthorn et al. (subm.-b; chapter 2, Fig. 5.3). They proposed offshore directed, lateral transport of particles in the BNL and a strong intermediate nepheloid layer at shelf-break depth. Current directions, determined with the current meter attached to BeaWiS (Fig. 5.5), support this proposition, indicating predominant offshore flow of the bottom waters in a low-energy environment that is influenced by tidal currents. For the first time, Inthorn et al. (subm.-c; chapter 4) determined a set of important parameters approaching organic matter quality (radiocarbon-age, C/N-ratio, RockEval pyrolisis) on particles, suspended in the BNL, using in-situ-pump particle samples obtained with the BWS. At three stations along the slope at 1200 to 1300 m water depth, Inthorn et al. (subm.-a; chapter 3) traced particle exchange processes between the BNL and the surface sediment in high resolution with the radionuclide ^{234}Th. In combination with samples from the CTD-rosette and the multiple-corer, they applied BeaWiS to determine the extent and intensity of the BNL, and to sample the particulate phase of the lowermost water column with the in-situ-pump. In addition, the 5-liter, Niskin-type sampling bottles, were used to gain the first specific ^{234}Th activity data of the easily resuspendable fraction of the surface sediment. These data will prove useful for future modeling of ^{234}Th exchange processes at the sediment-water interface. Total ^{234}Th activity and SPM content of the bottle samples was significantly higher compared to the in-situ-pump samples and the beam attenuation signal, although methodological differences in sampling techniques have to be taken into account (Moran et al., 1999). This situation is reflected in SPM data from other BeaWiS-deployments as presented here (Fig. 5.4), revealing strong increase in particle content from the upper towards the lowermost bottle. Obviously, the deposition of the BWS on muddy seafloor causes resuspension of particles from the surface sediment that are then trapped in the open Niskin-bottles. Particles that enter the

bottles, and settle on their bottom, are apparently inhibited from flushing by the boundary-layer of the bottle itself. On the other hand, the in-situ-pump samples are not effected by this resuspension, for pumping started only about 20 minutes after the deployment, when the resuspended particles had drifted away with the bottom current. If representative samples of the particle distribution in the lowermost meter of the water column without self-induced resuspension, or sampling of particle-reactive fluids are the focus of a study, a necessary improvement of the BeaWiS sampling technique would be to keep the bottles closed until the original state of the bottom waters has been restored. Additionally, bottles should be closed slowly to avoid disruption of particle aggregates.

Chapalain and Thais (2004), who presented a shallow-water sampling technique (ECMUL) comparable to BeaWiS, report avoidance of this resuspension effect by a stop of the lowering of the device just above the sea-floor to allow flushing of the bottles, as well as very slow landing velocities at the seafloor and immediate closure of the bottles. A comparable system was previously developed by Reed et al.(1997). However, these sampling techniques are ineffective at higher water depths and strong ship movement, where landing of the device cannot be as thoroughly timed. Additionally, we doubt proper flushing, if no alignment of the bottles directly into the current is ensured, and due to the instantaneous closure. ECMUL was deployed in a coastal regime with very high SPM-concentrations (10-40 mg l^{-1}) so that the results are hardly comparable to our results. Sauter et al. (2005) recently presented the BoWaSnapper using a sampling system and even a deployment procedure rather similar to the BeaWiS system. They achieved convincing fluid samples from an active vent site, but presented no explicit data on particle samples. Other bottom water samplers use pumps to suck water through small intake nozzles and a tube system. The online adjustment of the suction power and the orientation of the nozzles according to sensor-data (Thomsen, 1999) depends on considerable technical efforts and is susceptible to failures. If suction power cannot be adjusted, this induces a general uncertainty into the sampling-results (Sternberg et al., 1986). Other systems use syringes with very limited sample amounts (Milligan et al., 1998). In addition, lowered pressure and turbulent flow develops due to the suction through nozzles and tubes, which induces outgasing of dissolved fluids and destruction of particles.

5.6. Conclusion

Well aware of the limitation of the current BeaWiS system concerning particle sampling with the bottles, the multi-sampling and multi-sensor system provides a snapshot-view of the prevailing conditions in the bottom water. The major advantages of this system are:

- a vertical profile of five 5-liter water samples, variable in their position, from the lowermost 1.2 meter of the water column,
- proper alignment into the preceding bottom current,

- a set of sensor data (CTD, oxygen, beam attenuation, current velocity) and additional equipment (in-situ-pump, deep-sea camera), that offers many possibilities for integrated studies,
- the optional attachment of additional instruments to the steel tripod,
- easy handling onboard due to its comparatively low weight and size,
- little requirements in respect of ship capabilities, as no data-conducting wires are necessary,
- short deployment time of 10 to 15 min (if no in-situ-pump is applied).

Acknowledgments

We would like to thank the captains and crews of RV Meteor and RV Sonne for their support during the cruises M54/3, M57/2 and SO173. Erik Labahn and the other employees of KUM we thank for the construction of the BWS tripod. For technical assistance we are indebted to K. Dehning, F. Janßen, J. Langreder, A. Nordhausen, R. Schäfer, O. Wilhelm and N. Zatloukal.. We highly appreciate the provision of sensors and technical help by M. Bergenthal, the deep-sea camera by U. Witte and the in-situ-pump by W. Balzer. Our special appreciation goes to S. Forster, H. Pielenz, V. Ratmeyer, and C.Waldmann for technical and scientific advice. G. Rehder and S. Mau kindly provided unpublished methane-data. Furthermore we would like to thank the B2-project group as well as the geochemistry working group for helpful discussions. This research was funded by the Deutsche Forschungsgemeinschaft as part of the Research Center "Ocean Margins" (RCOM) of the University of Bremen contribution no. XXXX.

6. Upwelling of nitrogen depleted waters controls the nitrogen isotope composition of particulate matter on the Namibian shelf

Gaute Lavik[1], Maik Inthorn[2]

[1]*Max Planck Institute for Marine Microbiology, Celciusstrasse 1, D-28359 Bremen, Germany*

[2] *University of Bremen, FB5 – Geosciences, Klagenfurter Str., D-28359 Bremen, Germany*

6.1. Abstract

This study provides first evidence for a direct linkage between enhanced $\delta^{15}N$ values in particulate organic matter (POM), water column and sediments, and the removal of fixed inorganic nitrogen from the Namibian shelf waters. Although the source waters in the Benguela upwelling system are oxic, the water column becomes suboxic above the Namibian shelf due to bacterial respiration. Associated with this suboxic zone a major deficit in fixed nitrogen, mainly attributed to anammox activity, develops above the shelf. For POM from the water column above the inner Namibian shelf (<170m water depth), sampled during cruise AHAB1 with RV *A. v. Humboldt* in January 2004, $\delta^{15}N$ values strongly correlate with fixed nitrate deficit (N*). Over the shelf, a corresponding trend in $\delta^{15}N$ of the surface sediments indicates that these conditions have been prevailing during the last decades and are preserved in the paleorecord. Contrary to previous hypotheses, we find no correlation between dissolved nitrate in the photic zone and the $\delta^{15}N$ of the particles or other evidence of an influence of increasing relative nitrate utilization with increasing distance to the coast in the $\delta^{15}N$ record. Diagenetic effects during sedimentation can explain the observed increasing sedimentary $\delta^{15}N$ values with increasing water depths and distance to the coast. These findings have major implications for the paleoceanographic interpretation of the sedimentary $\delta^{15}N$ record in the Benguela upwelling region.

6.2. Introduction

In the Benguela current system, upwelling of nutrient-rich South Atlantic central waters along the southwest African continental margin (Fig. 6.1) sustains some of the highest primary production rates in the ocean (Carr, 2001; Chapman and Shannon, 1985). The high primary production makes this region interesting for studies of both present day conditions and processes as well as paleo-reconstructions. A large number of studies have used the nitrogen isotope ($^{14}N/^{15}N$) composition of sedimentary organic matter to reconstruct past nutrient conditions and primary production in regions with high productivity (see below). Changes in the nitrogen isotope ratio have been interpreted to reflect either varying loss of fixed inorganic nitrogen (nitrate, nitrite and ammonium) due to denitrification (heterotrophic) in the suboxic water column (e.g. Altabet et al., 1995; Altabet et al., 1999a; Ganeshram et al., 1995; Pride et al., 1999), or changes in the relative nitrate utilisation (e.g. Altabet and Francois, 1994; Farrell et al., 1995; Francois et al., 1992; Holmes et al., 2003; Holmes et al., 1997). These two scenarios would potentially result in opposite relationships between upwelling intensity and sedimentary $\delta^{15}N$ values.

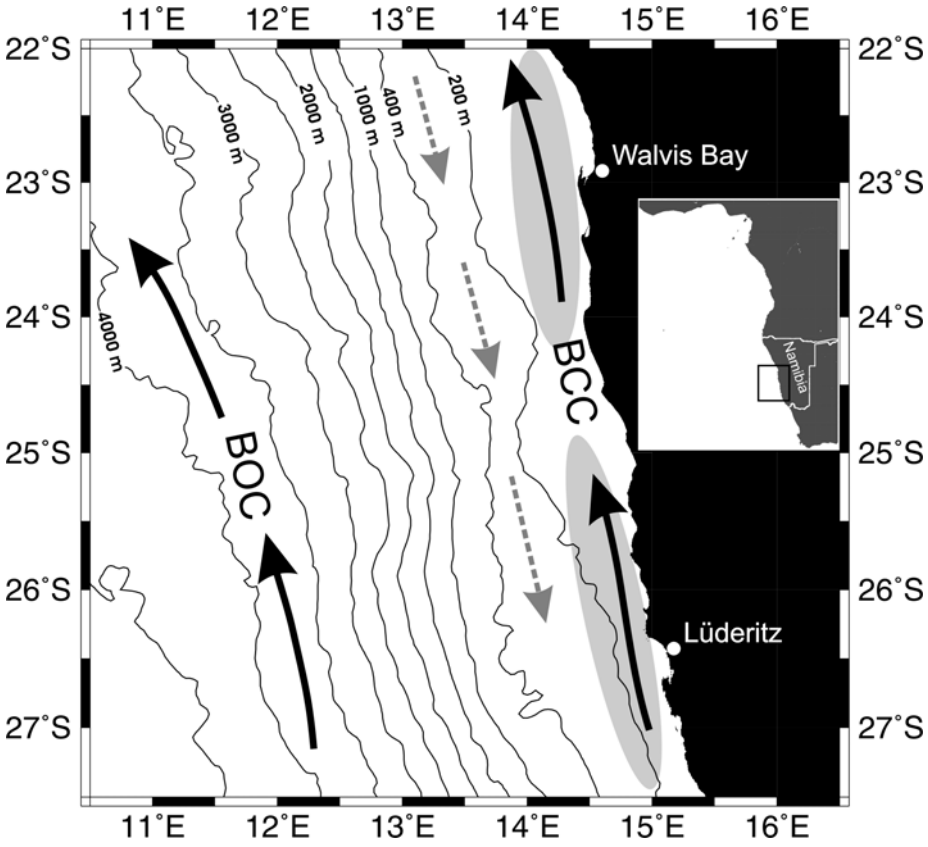

Fig. 6.1. Bathymetric map of the study area offshore Namibia. The main surface branches of the Benguela current system are indicated by black arrows: Benguela Oceanic Current (BOC) and Benguela Coastal Current (BCC). The poleward undercurrent over the outer shelf is indicated by grey arrows. The positions of the upwelling cells offshore Walvis Bay and Lüderitz are indicated by grey areas.

The nitrogen isotopic composition of organic matter produced in the photic zone depends on the isotopic composition of the nutrients in the surrounding waters (Montoya, 1994; Wada and Hattori, 1978). The preferential uptake of ^{14}N-nitrate by phytoplankton leads to ^{15}N depletion of the organic matter compared to the nitrate source (Montoya, 1994; Wada and Hattori, 1978), leaving the nitrate source relatively enriched in ^{15}N. Thus the $^{14}N/^{15}N$-ratio of the organic matter is increasing with enhanced utilisation of the nitrogen pool (Altabet et al., 1991; Voss et al., 1996; Wada, 1980). Holmes et al. (2002) identified a close relationship between upwelling intensity and $\delta^{15}N$ in sinking particles. They propose that intensified upwelling leads to a decrease in $\delta^{15}N$-values, and attribute this to reduced relative nitrate utilisation. Rising sedimentary $\delta^{15}N$ values with increasing distance to the nutrient source on the Namibian shelf have been interpreted to represent increasing relative nutrient utilization away from the coast (Holmes et al., 1999; Holmes et al., 2003).

Nutrient measurements indicate that 30-50% of the total nitrogen loss in the ocean occur in the oxygen deficient waters of oxygen minimum zones (OMZ; Codispoti et al., 2001; Gruber and Sarmiento, 1997). Although the South Atlantic Central Water (SACW) that represents the main source of the upwelling water entering the Namibian shelf is generally well oxygenated (>200 µM O_2, Fig. 6.2a; Chapman and Shannon, 1985), bottom waters become severely oxygen depleted (< 10 µM O_2; Fig. 6.2a) over large areas of the southwest African shelf resulting from oxygen consumption associated with the decomposition of settling algal biomass (Bailey, 1991; Chapman and Shannon, 1985). Extensive deficit in fixed inorganic nitrogen (N*), determined from the nitrate to phosphorous concentrations (relative to the Redfield ratio P/N = 1/16), along the Namibian coast (Fig. 6.2b) have been reported in earlier studies and attributed to heterotrophic denitrification (Chapman and Shannon, 1985; Tyrrell and Lucas, 2002). The loss of fixed nitrogen from the water column is commonly associated with high export production (high particle flux), where the oxic degradation of organic matter exceeds the oxygen supply in the sub surface waters and nitrate is expected to be used as an alternative electron acceptor by heterotrophic denitrifying bacteria. Hence, increasing upwelling/production would relate to increasing $\delta^{15}N$ values due to increasing denitrification (e.g. Altabet et al., 1995; Altabet et al., 1999a; Ganeshram et al., 1995; Pride et al., 1999). Recently, evidence was provided for extensive anammox activity in the OMZ waters of the Benguela upwelling system (Kuypers et al., 2005). Based on *in situ* ^{15}N-labeling experiments, these authors find that nitrate is not directly converted to N_2 by heterotrophic denitrification in the suboxic zone. Instead, nutrient profiles, labeling experiments, abundances of anammox cells, and specific biomarker lipids indicate fixed nitrogen loss through anammox activity. Anammox have also been shown to dominate the fixed nitrogen loss from the water column in other ocean regions (Kuypers et al., in Press; Kuypers et al., 2003).

Due to the preferential use of $^{14}NO_3^-$ by bacterial respiration, denitrification is accompanied by a large isotopic fractionation (20-40‰, Barford et al., 1999; Cline and Kaplan, 1975). No published data exist on the isotope fractionation by annamox bacteria, but based on Rayleigh kinetics a similar isotope fractionation by anammox bacteria compared to

heterotrophic denitrifiers would be expected. This is supported by unpublished experimental data (G. Lavik, M. Kuypers, B. Kartal, M. Strous).

6.3. Study area

The Benguela current system is part of the subtropical, anticyclonic gyre of the South-Atlantic (Peterson and Stramma, 1991) and consists of two branches (Fig. 6.1): 1) The Benguela Oceanic Current (BOC) represents an equatorward drift of cool surface waters flowing along the western coast of South Africa up to about 30°S, where its main branch diverges offshore from the Namibian coast. 2) The Benguela Coastal Current (BCC) is the smaller component of the BCS, which continues equatorward as far as 14°S above the Namibian shelf (Mohrholz et al., 2001).

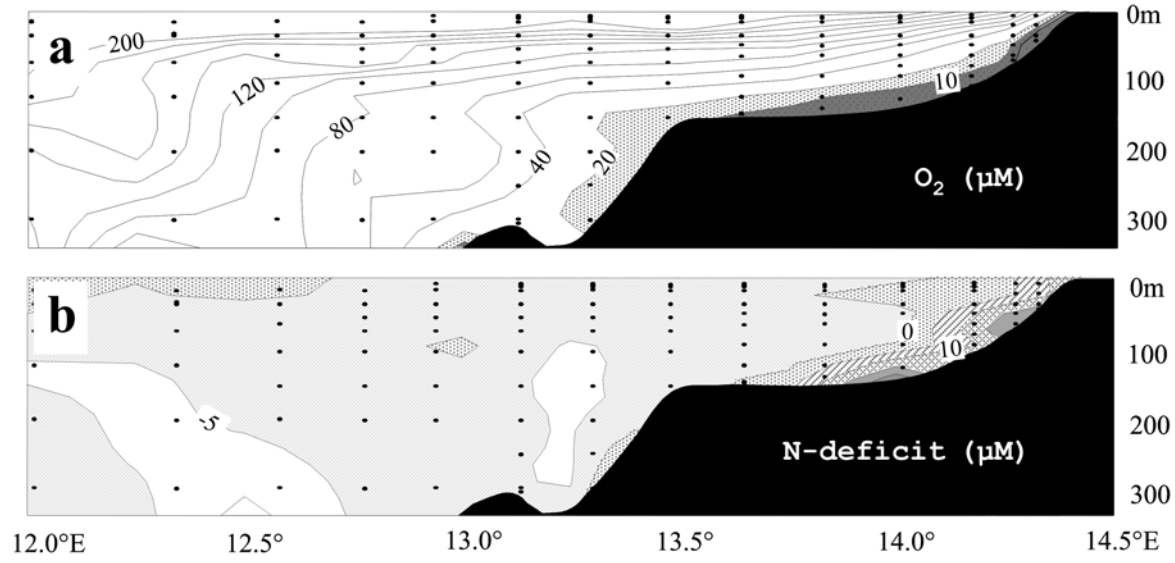

Fig. 6.2. Vertical transect showing the lateral extension of a) the oxygen minimum zone and b) the fixed inorganic nitrogen deficit (N*) off Namibia at 23° south (Kuypers et al., 2005).

Upwelling of cold, nutrient rich waters is driven by alongshore tradewinds, and takes place in several upwelling cells along the southwest African coast (Shannon and Nelson, 1996). It is strongest and perennial at the Lüderitz cell (Fig. 6.1). The Walvis cell is also strong but more susceptible to seasonal changes. The upwelling drives high primary production in the surface waters, estimated to be as high as 0.37 Gt carbon per year (Carr, 2001). Primary production is most intensive above the shelf, and Mollenhauer et al. (2002) calculated, that 85 % of the total mass accumulation of organic carbon on this continental margin takes place in the shelf sediments. Only temporary occurring, mesoscale filaments and plumes transport nutrient-rich and highly productive filaments seaward across the continental slope (Lutjeharms et al., 1991).

The continental margin off southwestern Africa is dipping towards the abyssal plain of the Cape Basin with the Walvis and Agulhas Ridges forming its northern and southern boundaries. Double shelf breaks are common with inner and outer breaks at depths of 140 to 180 m and 360 to 400 m respectively.

6.4. Material and methods

The fieldwork for this investigation focused on shelf and slope in the northern Benguela off Namibia, where cruise AHAB1 of RV *Alexander von Humboldt* in January 2004 took place. To increase the areal coverage of stations, surface sediment samples from *Meteor* cruise M57/2 (February/March 2003, ref) from the same area were analyzed, and literature data (Holmes et al., 2003) from the overall Benguela area were integrated to the data set. Altogether, 39 sediment samples and 10 literature data were used (Fig. 6.3a, Table 6.1). Sediment cores were recovered with a multiple corer, and the uppermost centimeter was sampled, freeze-dried and powdered in a mortar.

Suspended particle samples were retrieved from several transects from 27°S to 23°S covering the shelf from the coast to 100 sea miles offshore (Fig. 6.3b, Table 6.2). In total, 68 water samples from different water depths, but mostly from the euphotic surface waters were retrieved with Go-flo bottles attached to a Seabird Rosette CTD system, and 3-5 liters were filtered through pre-combusted and pre-weighed glass fiber filters (SCHLEICHER & SCHUELL, GF52). The amount of particulate organic carbon (POC) on the filters was determined by reweighing and determination of the organic carbon content of the particles with a CARLO ERBA Element CNS Analyzer according to Inthorn et al. (subm.-b; chapter 2).

420 nutrient samples were taken from the same rosette system or directly from the IOW/MPI pump-CTD system (see Kuypers et al., 2003). Nitrate, nitrite, ammonium and phosphate concentrations (detection limits: 0.1, 0.03, 0.3 and 0.1 µM, respectively) were determined on board with an autoanalyzer, immediately after sampling. The fixed inorganic nitrogen (N*) deficit, was calculated from nutrient concentrations using the following equation: N* = 16 * [phosphate] - ([nitrate] + [nitrite] + [ammonium]). In which 16 is the standard fixed inorganic nitrogen to phosphate ratio according to Redfield (cf. Tyrrell and Lucas, 2002). The chlorophyll α content of the water was approached with a 2-channel DR. HAARDT BackScat II fluorometer connected to an SBE 911+ CTD.

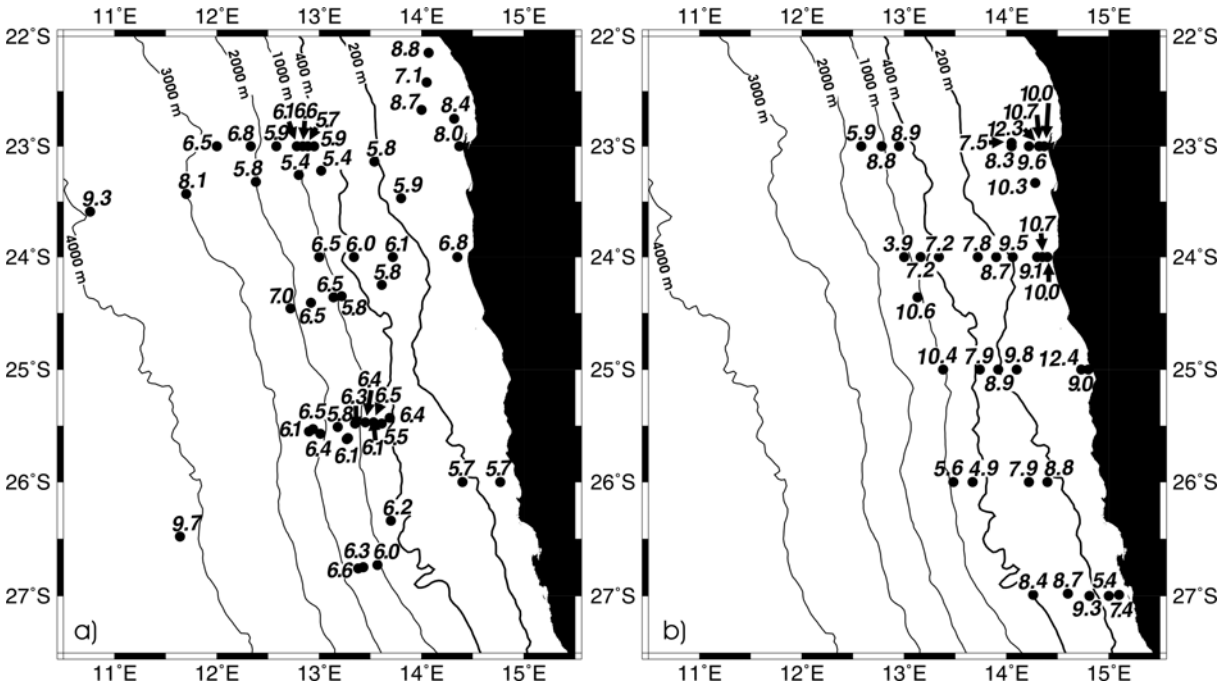

Fig. 6.3. (a) $\delta^{15}N$-values of the samples of surficial sediments (cf. Table 6.1), and (b) average isotope signal of the particulate matter samples (cf. Table 6.2) in the study area.

The $\delta^{15}N$ measurements were performed on a Finnigan Delta Plus attached to a Carlo/Erba NC2500 automatic elemental analyzer as preparation line. The stable isotope determination was made from N_2 gas released by flash combustion in excess oxygen at 1050°C. Sediment and filter samples were measured against 99.996% pure N_2 tank gas. One internal standard (WST2 6.66‰) was measured after every fifth sample. The N_2 tank gas and the WST2 house standard were calibrated against the IAEA standards N-1 and N-2. Standard deviation on replica measurements was less than 0.3‰.

6.5. Approach

This study aims to approach the relationship between availability of nitrate, N* of the seawater and $\delta^{15}N$ of the particulate organic matter (POM or PON) from the same samples. Although fixed nitrogen assimilation by autotrophically growing bacteria (i.e. nitrifiers, anammox) occurs, we assume that phototrophic production is the dominant pathway of nitrogen from the nutrient pool to the PON pool. Accordingly, only the nutrients available for phototrophic production in the surface waters determine the isotopic composition of the PON and are considered here. The lower boundary of the photic zone was defined for each station as the depth, where the chlorophyll data was less than 5% of the profile's maximum value. The nutrient data from the samples above this depth were integrated, with each sample being integrated to the water column above and below the sampling depth, depending on the sampling resolution (i.e. in case of 10 m vertical sampling resolution the nutrient conditions for one sample were extrapolated to the water column 5 m below and above it). Based on these values, the total available fixed nitrogen as well as N* for the photic

zone (per surface area [mol m^{-2}]) was calculated, giving numbers that are independent of the depth of the photic zone. This was important, because sometimes the main chlorophyll peak was several meters below the surface due to nutrient limitation of the surface waters, and the overall depth of the (nevertheless quite productive) photic zone was increased. Consequently, the total amount of available nutrients and total N* in the photic zone and not the average concentration are important for the comparison to particulate matter. The average isotope signal of the particulate matter was determined by weighting against the amount of organic nitrogen (mg N l^{-1}) in each particle sample. Particle samples from the whole water column were used to gain the average particulate $\delta^{15}N$ value that was afterwards compared to the underlying sediment. Due to the dominant particle load in the photic zone, no relevant differences were noticeable in comparison with average $\delta^{15}N$ values for particle samples from the photic zone alone.

6.6. Results

$\delta^{15}N$ of the suspended particulate organic matter ranges between 3.9‰ and 12.4‰ (Table 6.2). The measured nitrate concentrations varied from detection limit (<0.1µM) in some surface water samples to 42.3 µM. The lowest measured phosphate concentration was 0.1µM in some surface water samples, but was generally between 0.35 to 1.2µM in the surface waters and between 2.3 and 3µM in the deeper water column. Close to the coast, phosphate concentrations as high as 5.3µM were detected. Ammonium concentrations up to 8.3µM were measured in bottom waters, but were generally close to detection limit in the photic zone. In suboxic waters, nitrite values up to 3.4µM were detected, but were rarely above 0.5µM in the photic zone.

Our results show no correlation between the amount of nitrate, the dominating fixed nitrogen source in the photic zone, and the $\delta^{15}N$ values of the PON (r^2=0.00; Fig. 6.4a). Likewise, other ways of calculating the concentrations or amount of fixed nitrogen available for photic production gave no relevant correlations to the $\delta^{15}N$ values of the PON, i.e nitrate in the upper 20m (r^2=0.00; Fig. 6.4b).

Our results give a relevant positive correlation between N* in the photic zone and the $\delta^{15}N$ values of the PON (r^2=0.5, Fig. 6.5a). We got the best correlation for samples from the inner shelf for water depths less than 170m (r^2=0.75; Fig 4a). There is also a general trend of increasing $\delta^{15}N$ values with increasing particle load (r^2=0.14; Fig. 6.5b).

The $\delta^{15}N$ values measured in surface sediments from the shelf increase with increasing organic carbon content (TOC; Fig. 6.3a, Table 6.1). From the outer shelf towards the open ocean the $\delta^{15}N$ values in the surface sediments increase again but accompanied by decreasing TOC. On the inner shelf the $\delta^{15}N$ values seem to be heavier in the northern part of the study area (22-24°S) compared to the south (26-27°S), both for the surface sediments and in the water column (Fig. 6.3a and b).

Table 6.1. Location, water depth, organic carbon content and $\delta^{15}N$ of surface sediment samples. Stations marked with an asterisk (*) are from Holmes et al. (2003).

station	latitude [°S]	longitude [°E]	depth [m]	TOC [%]	$\delta^{15}N$ [‰]
226720*	22,15	14,07	69	6,2	8,8
GeoB4501*	22,42	14,05	98	3,3	7,1
Nam1*	22,67	14,00	125	6,7	8,7
226620*	22,75	14,32	84	5,1	8,4
GeoB8404	23,00	14,37	44	4,4	8,0
GeoB8402	23,47	13,80	164	4,5	5,9
GeoB8481	23,00	12,95	590	3,6	5,9
GeoB8482	23,00	12,89	706	3,9	5,7
GeoB8483	23,00	12,84	805	4,2	6,6
GeoB8484	23,00	12,78	953	3,5	6,1
GeoB8498	23,00	12,58	1439	3,7	5,9
GeoB8499	23,00	12,33	2080	1,7	6,8
GeoB84100	23,00	12,00	2715	0,8	6,5
GeoB1714-1*	23,14	13,54	200	5,69	5,88
GeoB1713-6*	23,22	13,02	597	3,60	5,45
GeoB1712*	23,26	12,80	1007	3,71	5,43
GeoB1711*	23,32	12,38	1964	1,74	5,81
GeoB1710*	23,43	11,70	2983	0,49	8,13
GeoB1709*	23,59	10,76	3837	0,24	9,35
WW24005	24,00	14,35	85	5,2	6,8
WW24040	24,00	13,72	256	4,5	6,1
WW24060	24,00	13,34	309	2,7	6,0
WW24080	24,00	13,00	1040	4,3	6,5
GeoB8403	24,25	13,61	320	2,7	5,8
GeoB8419	24,35	13,22	817	4,2	5,8
GeoB8418	24,36	13,14	1006	4,8	6,5
GeoB2402*	24,41	12,92	1512	3,6	6,5
GeoB8422	24,46	12,72	1997	2,1	7,0
GeoB8493	25,43	13,69	387	4,5	6,4
GeoB8492	25,48	13,61	501	4,7	5,5
GeoB8449	25,48	13,54	605	6,8	6,1
GeoB2506*	25,47	13,53	646	7,9	6,5
GeoB8448	25,47	13,45	806	9,1	6,4
GeoB8451	25,48	13,35	1028	7,9	6,3
GeoB8447	25,61	13,28	1334	8,1	6,1
GeoB2503*	25,62	13,27	1363	7,6	6,1
GeoB8455	25,51	13,18	1503	8,4	5,8
GeoB2507*	25,57	13,01	2103	4,1	6,4
GeoB8462	25,53	12,94	2261	3,1	6,5
GeoB8462	25,53	12,94	2293	3,5	6,5
GeoB8470	25,55	12,90	2470	3,2	6,1
WW26010	26,00	14,77	118	3,0	5,7
WW26030	26,00	14,40	199	1,1	5,7
GeoB8464	26,34	13,70	430	3,5	6,2
GeoB8466	26,73	13,57	940	2,9	6,0
GeoB8465	26,75	13,43	1329	4,9	6,3
GeoB8465	26,75	13,43	1377	4,1	6,3
GeoB8469	26,76	13,38	1480	4,2	6,6
GeoB1715*	26,48	11,64	4097	0,34	9,79

Table 6.2. Location, water depth, depth of the photic zone (p.z.), results of nutrient measurements together with the respective integrated POC and averaged $\delta^{15}N$-values of the particulate matter samples.

Station	latitude [°S]	longitude [°E]	depth [m]	depth p.z. [m]	$N0^{3-}$ [mmol m^{-2}]	$N0^{3-}$, 0-20m [µM]	N* [mmol m^{-2}]	POC [g m^{-2}]	$\delta^{15}N$ [‰]
Nam2004	22,97	14,05	128	30	120	1,46	14	11,5	7,5
WW23002	23,00	14,37	41	41	335	13,04	1230	15,8	12,3
WW23005-1	23,00	14,32	70	29	668	23,25	302	9,6	10,7
WW23005-2	23,00	14,32	72	50	823	17,82	634	16,1	10,0
WW23010	23,00	14,22	106	30	209	12,48	340	13,9	9,6
WW23020	23,00	14,05	126	19	296	18,96	489	13,4	8,3
WW23080	23,00	12,95	579	30	362	12,39	-79	4,6	8,9
WW23090	23,00	12,78	912	49	522	6,28	-29	5,6	8,8
WW23100	23,00	12,58	1377	49	468	7,82	-55	6,1	5,9
AH_0008	23,33	14,28	95	40	715	7,20	513	15,9	10,3
WW24002	24,00	14,40	61	40	189	2,38	1270	19,0	10,7
WW24005	24,00	14,35	83	30	129	8,78	614	20,4	10,0
WW24010	24,00	14,30	101	20	54	11,06	267	16,5	9,1
WW24020	24,00	14,06	176	20	261	17,37	-20	10,3	9,5
WW24030	24,00	13,90	223	28	162	9,03	220	5,4	8,7
WW24040	24,00	13,72	247	19	207	12,14	221	4,1	7,8
WW24060	24,00	13,34	297	20	278	15,97	112	1,6	7,2
WW24070	24,00	13,16	578	50	487	15,37	92	8,9	7,2
WW24080	24,00	13,00	1005	30	301	16,47	-19	9,1	3,9
RCOM2403	24,36	13,13	973	20	153	21,99	-232	2,6	10,6
WW25002	25,00	14,80	28	28	100	6,15	1365	10,7	12,4
WW25005	25,00	14,73	53	20	116	7,62	628	24,2	9,0
WW25040	25,00	14,10	168	60	200	4,05	560	22,8	9,8
WW25050	25,00	13,92	178	50	713	11,48	-246	12,3	8,9
WW25060	25,00	13,74	297	50	313	9,43	-243	6,3	7,9
WW25080	25,00	13,38	938	49	964	13,03	-474	7,6	10,4
WW26030	26,00	14,40	192	40	321	17,72	32	17,3	8,8
WW26040	26,00	14,22	250	50	254	13,89	-73	12,9	7,9
WW26070	26,00	13,67	490	49	266	9,86	-58	6,5	4,9
WW26080	26,00	13,48	823	30	145	8,36	-7	5,2	5,6
WW27005	26,99	15,10	117	50	797	16,32	-177	7,7	7,4
WW27010	27,00	15,00	141	40	324	10,75	-192	5,6	5,4
WW27020	27,00	14,81	201	20	95	6,63	-56	4,3	9,3
WW27030	26,98	14,60	273	19	6	0,36	26	4,0	8,7
WW27050	26,99	14,26	367	50	135	1,05	-24	3,3	8,4

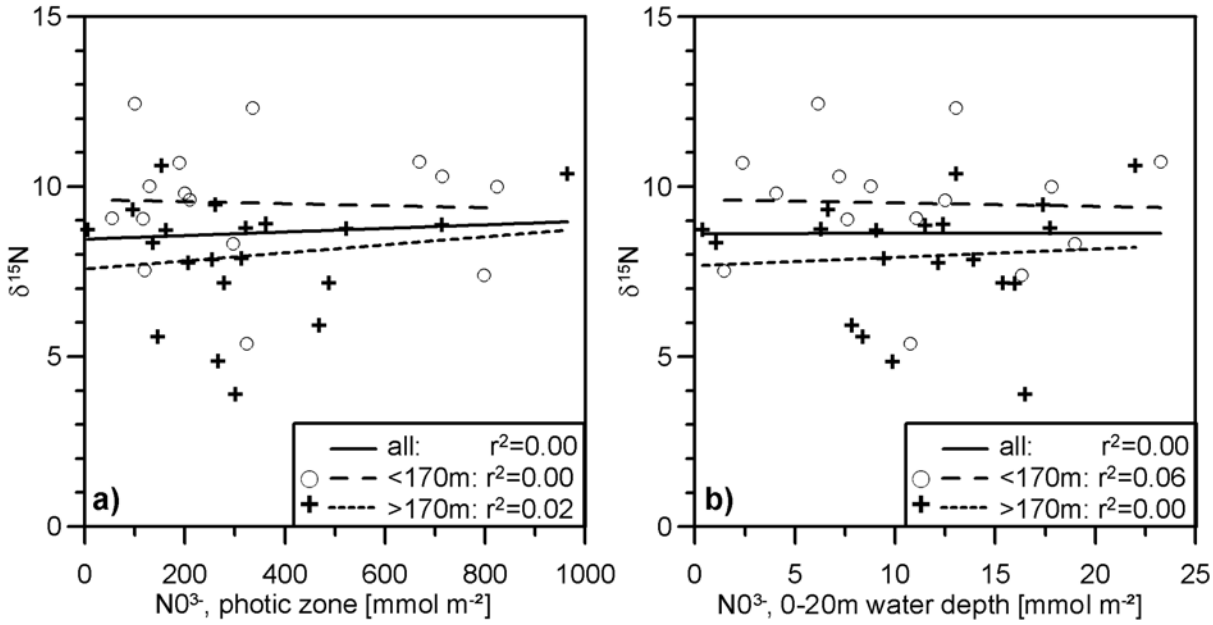

Fig. 6.4. Total available nitrate in (a) the photic zone and (b) the uppermost 20m of the water column (cf. Table 6.2). Samples from stations below 170m water depth (open circle, slashed line) are differentiated from samples below that depth (crosses, dotted line). The linear regression line (solid line) for all samples is indicated as well.

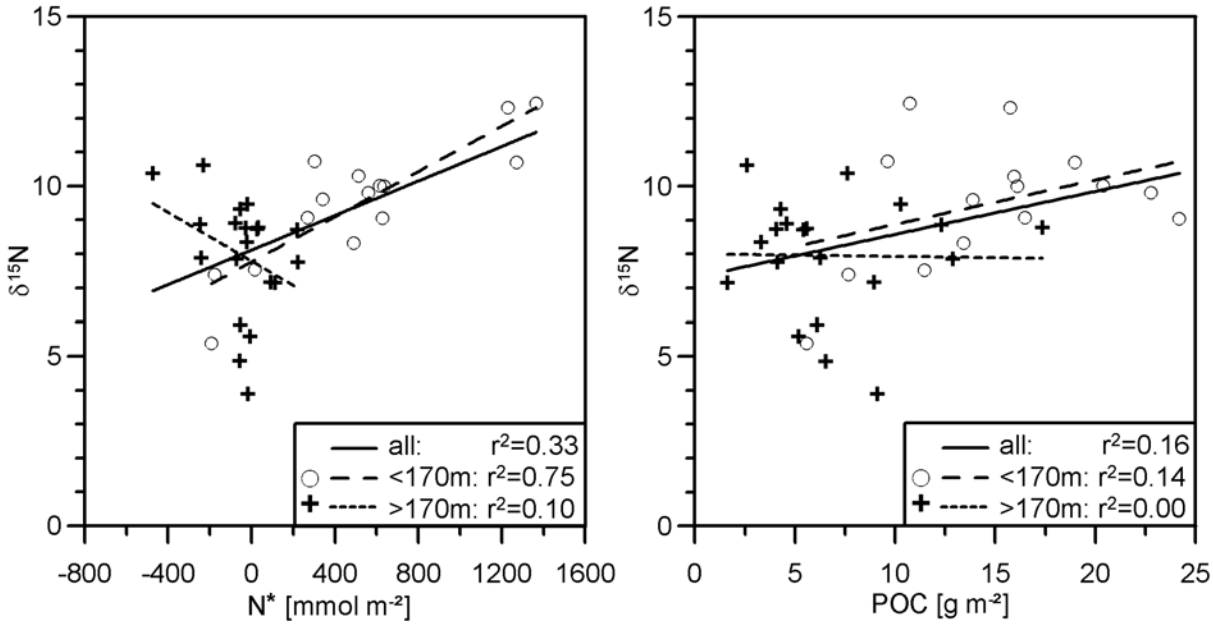

Fig. 6.5. (a) Fixed inorganic nitrogen deficit and (b) particulate organic carbon concent in the photic zone (cf. Table 6.2). Samples from stations below 170m water depth (open circle, slashed line) are differentiated from samples below that depth (crosses, dotted line). The linear regression line (solid line) for all samples is indicated as well.

6.7. Discussion

Above the shelf, especially the inner shelf, there is a strong correlation between rising $\delta^{15}N$ of the PON with increasing N* (Fig. 6.5 a). The particle load, expressed as POC (Fig. 6.5b), shows a similar trend, corresponding to highest $\delta^{15}N$ values above the shelf. This supports suggestions from earlier studies (i.e. Chapman and Shannon, 1985; Tyrrell and Lucas, 2002) that enhanced particle load due to high primary production is the driving force in the creation of suboxa and consequently the removal of fixed inorganic nitrogen (N*). A recent study by Kuypers et al (2005) provides evidence for the removal of fixed organic nitrogen in the water column of the Benguela upwelling system by anammox bacteria, but found no indications for heterotrophic denitrification. Accordingly, we will consider anammox and not denitrification as the process responsible for the N*. Figure 6.2 shows concurrent occurrence of highest N^*-values and lowest oxygen concentrations close to the coast. The increasing influence of nitrogen removal towards the coast is reflected in the $\delta^{15}N$ of the PON, with values of 9-12.4‰ (avg. 10.4‰) for the water column closest to the coast (less than 106m water depth) compared to 7-8.7‰ (avg. 7.9‰) on the outer shelf (200-400m water depth). There are only few sedimentary $\delta^{15}N$ values available close to the coast (Table 6.1 and Fig. 6.3). However, a comparison of the numbers in Tables 6.1 and 6.2 reveals a trend with 2-3% heavier $\delta^{15}N$ in suspended particle and sediment samples close to the coast compared to samples from the outer shelf. One exception is the southernmost part of the study area (26-27°S) where the $\delta^{15}N$ in the PON as well as the surface sediments do not increase towards the coastline (Fig. 6.3). A general increase in the anammox activity in the water column from south to north is also seen in the data from Kuypers et al (2005). The $\delta^{15}N$ of the PON is on average 2‰ higher/heavier than the underlying sediments. This discrepancy can be explained by a more extensive oxygen minimum zone during our cruise in January 2004 compared to the average conditions. Nevertheless, our data demonstrate the major effect of the removal of fixed inorganic nitrogen, probably due to anammox activity, on the $\delta^{15}N$ composition of the sediments, implicating that fixed nitrogen loss by anammox activity in a suboxic water column prevailed at least seasonally during the last decades. We can not find any evidence for the postulated (Holmes et al., 1999; Holmes et al., 2002; Holmes et al., 2003) relation between increasing $\delta^{15}N$ of the PON and increasing nitrate utilization, which should correspond to decreasing availability of nitrate in the water column. Our data result from a cruise with 3 weeks duration and the conditions prevailing during the above mentioned studies might have been different to what we encountered. We would, however, expect to find a correlation between the $\delta^{15}N$ of the PON and the nitrate availability outside the inner shelf (dominated by N*), if nitrate availability were important for $\delta^{15}N$ of the organic matter. Nor is there a relevant correlation between $\delta^{15}N$ of the PON and the depth of the photic zone (chlorophyll distribution) or distance to the coast. This somewhat contradicts the findings of a sediment trap study by Holmes et al. (2002), where $\delta^{15}N$ in the sinking matter was as low as 3‰ corresponding to the coldest calculated sea surface temperatures, indicating maximum upwelling intensity. The strength of this sediment trap study (Holmes et al., 2002) is the continuous sampling at one site for almost three annual cycles with the lowest $\delta^{15}N$ isotope values (3-6‰) during austral winter to spring. On the other hand, its

expressiveness is limited due to missing nutrient measurements as well as the lack of control on the origin of the material caught with a sediment trap at 1600m. In contrast, our dataset has high areal extent, and the $\delta^{15}N$ composition of the PON can be directly linked to specific nutrient conditions. Seasonal differences and/or regional differences may provide explanations to these contradicting results.

Reconstruction of past nutrient utilization, as it was repeatedly done, using the $\delta^{15}N$ of sedimentary organic matter as a proxy (Altabet and Francois, 1994; Altabet et al., 1995; Altabet et al., 1999a; Farrell et al., 1995; Francois et al., 1992; Ganeshram et al., 1995; Holmes et al., 1999; Holmes et al., 2003; Lavik, 2001; Pichevin et al., 2005; Pride et al., 1999) requires an efficient transfer of the surface-water $\delta^{15}N$-signal towards the sediments by approximately vertically settling particles as well as proper preservation of the signal in the sediment. A variety of diagenetic processes can alter the original signal in both the water column (Nakatsuka et al., 1997), and at the sediment-water interface (Altabet and McCarthy, 1985; Francois et al., 1992; Freudenthal et al., 2001; Saino and Hattori, 1980). Nevertheless, several studies indicate persistent transfer of the surface water $\delta^{15}N$ signal to the sediment (Altabet et al., 1999b; Francois et al., 1992; Gaye-Haake et al., 2005). These authors reported a consistent 4±2‰ $\delta^{15}N$-enrichment in the sediments compared to sinking matter in different regions. However, Altabet et al. (1999b) demonstrated that this difference is less than 1‰ in high production areas and ascribed this to better nitrogen preservation due to higher sedimentation rates in a coastal upwelling zone. In the study of Holmes et al. (2002) an offset <1‰ between sinking matter and surface sediments is reported from a sediment trap (1600m deep) at 2200m water depth. Further south, a sediment trap study by Romero et al. (2002) at 3000m water depth revealed comparable flux rates and similar average $\delta^{15}N$ values of the sinking particulate matter (both ~6‰), but the underlying sediments were about ~4‰ heavier than the sinking matter (Holmes et al., 2003). Variations in the discrepancy between $\delta^{15}N$ in sinking matter and the sedimentary $\delta^{15}N$ are reported from other upwelling regions (Altabet et al., 1999b; Brummer et al., 2002; Freudenthal et al., 2001; Gaye-Haake et al., 2005). This has been attributed to diagenetic effects, varying with the intensity of bacterial degradation (Dauwe et al., 1999; Gaye-Haake et al., 2005) and oxygen conditions during sedimentation (Freudenthal et al., 2001). Accordingly, we can expect good preservation of the PON and isotope signals in the organic carbon rich sediments on the shelf. On the contrary, the increasing $\delta^{15}N$ in the sediment with increasing water depth, increasing distance to the coast, and lower organic matter content can be explained by diagenetic effects up to 4‰ related to the degradation index (Dauwe et al., 1999; Gaye-Haake et al., 2005). Consequently, no relation between relative nitrate availability and $\delta^{15}N$ of the PON is required to explain the increasing $\delta^{15}N$ of the sediments with increasing distance to the coast (Table 6.1).

Another mechanism with influence on the sedimentary $\delta^{15}N$ values is lateral particle displacement in intermediate and bottom nepheloid layers offshore Namibia (Giraudeau et al., 2000; Inthorn et al., subm.-b; chapter 2). Offshore transport seaward of the inner shelf break would transfer particles with presumably high $\delta^{15}N$ values from the mid-shelf towards

the outer shelf and the upper slope. Accordingly, the proposed landward bottom transport on the inner shelf can transport PON that is barely influenced by fixed nitrogen loss towards the coast and smoothen the sedimentary isotope signal.

6.8. Summary and conclusions

The massive loss of fixed inorganic nitrogen from the water column attributed to anammox activity is governing the $\delta^{15}N$ values of the PON in the water column, and this isotope signal is transferred to the sediments. The higher $\delta^{15}N$ values in the PON compared to the sediment on the inner shelf might be caused by comparatively strong oxygen depletion of the low water column and, accordingly, high fixed nitrogen loss during our three week cruise. Additionally, the sedimentary $\delta^{15}N$ signal can be smoothened by onshore particle transport in the bottom waters, transferring PON with lighter isotope signal towards the coast. Increasing $\delta^{15}N$ values with increasing POC concentrations in the photic zone states that the organic load is an important factor driving the extend of the OMZ on the Namibian shelf, leading to increasing $\delta^{15}N$ values in the sediment with increasing primary production on the shelf. The previously postulated increase in $\delta^{15}N$ due to enhanced nitrate utilization, and decreasing nitrate availability in the photic zone with increasing distance to the coast was not found. Based on the results from sediment trap deployments in the Benguela upwelling system (and other regions) the increasing sedimentary $\delta^{15}N$ values with increasing water depth / distance to the coast is explainable by the diagenetic isotope effects related to the degradation index.

Theoretically, the nitrogen isotopes in sediments on the continental slope can still be used as a paleoproxy for upwelling intensity. However, in contrast to what has been proposed by earlier studies (Lavik, 2001; Pichevin et al., 2005) a negative correlation between $\delta^{15}N$ and TOC would relate to the degradation index, and not the relative nitrate utilization. These findings might also have major implications for the use of $\delta^{15}N$ as a paleoproxy in other regions.

Acknowledgements

We thank the officers and crew aboard R/V *A.v.Humboldt* and RV *Meteor* for their help during core recovery and sampling, and Monika Segl and Wolfgang Bevern for the assistance with the mass spectrometry analyses, Gabi Klockgehter for nutrient analyses, Siegfried Krüger and Ulrich Lass for CTD-rosette data and samples, as well as Marlene Bausch and Marcel Kuypers for assistance onboard.

7. Conclusions and perspectives

This thesis represents the first comprehensive, integrated approach to localize the pathways of the transport, to quantify the fluxes, and to estimate the influence of lateral transport on the quality and preservation of organic matter (OM) in the Benguela upwelling system (BUS). To achieve this, a broad range of different methods have been used. The BUS was chosen as the area of study due to its extraordinary high primary production of marine OM in the nutrient-rich surface waters close to the coast, and the resulting importance of this ocean margin environment for the global marine biogeochemical cycles. In spite of its importance, the particle and associated OM flux within the water column of the BUS had not been thoroughly investigated yet, and very little data were published. Accordingly, most of the processes of marine production of OM, nutrient recycling, transport and final burial of OM in the BUS shelf and slope sediments were poorly understood. The BUS is exceptionally suitable for investigations on later particle transport and its influence on the fate of the marine bioproduction due to little terrigenous input into the system that would otherwise dilute many of the primary signals (e.g. C/N-ratio, ^{14}C age).

The snapshot view of the particle distribution in the water column, made possible by the combined optical sensor and sampling approach, testifies the existence of strong nepheloid layers in intermediate and bottom waters of the BUS. It provides first insights into particle size and composition. Additionally, the general oceanographic settings in the BUS and their influence on particle transport are outlined. All results stress the special situation at 24.5 to 26°S, leading to intensive nepheloid layers. These provide an explanation for the existence of the slope depth OM depocenter in this area. The optical sensor study should be extended to a periodical, regular survey, supported by moored instruments at selected depths and positions, to approach seasonal changes in the nepheloid layer distribution. A well-aimed sampling of particles from intermediate nepheloid layers would provide important information on the origin of these particles and the influence of this transport mechanism on the composition of the underlying sediments. The role of internal tides and waves as a likely cause of particle resuspension and intermediate nepheloid layers should be investigated. In general, the knowledge concerning flow direction and velocity of all subsurface water masses, especially the bottom currents, is very limited in the area, but nevertheless crucial for the understanding of particle redistribution processes.

The ^{234}Th approach combines optical sensor data with information provided by this radioactive particle tracer. Despite the limited amount of sampled stations on the slope off Namibia, the calculated residence times of particles in the BNL, the resuspension flux, and mass accumulation in the sediment are important quantities to understand the sedimentary system of the slope depocenter. Several of these parameters indicate a predominant role of lateral particle transport compared to the vertical input of contemporary, fresh particles to the Namibian slope. However, future studies will have to extend the existing set of samples considerably to verify the quantities, to localize sources and sinks, and to quantify the fluxes on larger scales in time and space. Additionally, sediment trap deployments in combination

with appropriate calibration by radionuclide measurements should accompany such a survey.

The ^{234}Th-results indicate the dominant role of lateral particle transport in the deep water column. They are supported by the high ^{14}C-age and C/N-ratio, and the results of the Rock-Eval pyrolysis. To the best of our knowledge, the parallel approach using surface sediment samples and suspended particles in the BNL was carried out for the first time. The results enabled us to develop a conceptual particle transport model for the Namibian continental margin. The key features of this model may be applicable to other high-productive continental margin settings and will also improve the understanding of comparable systems in the geological record. Such OM depocenters below the shelf-break have a good preservation potential in the sedimentary system, unaffected even by sea level changes. Thus, they might represent a modern analogue to petroleum source rocks. Enhanced sedimentation rate due to intensive lateral transport in nepheloid layers is suggested to cause the high accumulation and preservation of OM in the slope depocenter offshore Namibia. This is contrary to the common interpretation of enhanced preservation of OM in such depocenters, proposing either oxygen content of the bottom waters or vertical input of freshly produced OM from the surface waters as the most important factors. ^{14}C-age determination on specific types of organisms and component classes of OM (Hwang et al., 2005; Mollenhauer et al., 2003) provides a powerful tool to specify our results, and to characterize the significance of lateral particle transport in the paleoceanographic record. Other methods of organic geochemistry (e.g. gas-chromatography) are necessary to identify, which OM components generate the "labile" hydrocarbon signal we detected with Rock-Eval pyrolysis. These approaches may provide new proxies suitable for tracing laterally transported OM in the sedimentary record.

With the bottom water sampler BeaWiS, a sampling and monitoring tool was developed that fills a gap in common ship-borne sampling techniques. It enabled us to gather the special sample and data sets from the lowermost meter of the water column, necessary to achieve many of the results described in this thesis. Additionally, BeaWiS proved to be useful to obtain water samples that reflect the steep geochemical gradients in bottom waters, often occurring directly above the seafloor. On the other hand, our results show limitations of the recently widely applied sampling technique using horizontally fixated, Niskin-type water bottles to gain undisturbed particle samples from the lowermost water column. To avoid the consequence of a self-induced resuspension event, a modified method should be developed, keeping the bottles closed prior to sampling, until the self-resuspended particles have drifted away or resettled. Although the boundary layer, induced by the walls of the bottles, might still have some effect on the results, this technique is likely to become the new work horse in BBL-sampling.

The intensive recoupling of processes in the deep water column to the surface waters is reflected in the study on nitrogen isotope composition of particulate matter in the BUS. Upwelling of nitrogen depleted waters from the oxygen deficient subsurface water column

above the Namibian shelf controls $\delta^{15}N$-values of suspended and sedimented particles. No influence of nitrate limitation in the surface waters on $\delta^{15}N$-signal could be detected. This has broader impact on the interpretation of $\delta^{15}N$ of OM in the sedimentary record that is commonly used as a proxy to reconstruct changes in past upwelling intensity, nutrient availability, and primary production. The influence of the fixed nitrogen deficit on $\delta^{15}N$ should be explored in other high productive upwelling areas with oxygen minimum zones.

In conclusion, a conceptual model of the continental margin offshore Namibia at 25.5°S is shown in Fig. 7.1. Upwelling of nutrient rich, already oxygen-depleted central waters from up to 200 m water depth takes place along the coast in the Lüderitz upwelling cell, and induces high primary production (mainly diatomea) above the shelf area. Remnants of the organisms are remineralized during their settling through the water column and enhance the oxygen depletion of the bottom waters so that anaerobic oxidation of ammonium sets in. However, burial efficiency is high along the inner shelf due to shallow water depth, high particle fluxes, and anoxia in the lowermost water column and in the sediment porewater. This causes the extremely high organic carbon (OC) content of the sediments of the diatomaceaous mudbelt. The equatorward flow of the Benguela coastal current and the upwelling process itself probably induce onshore directed flow in the benthic boundary layer. Downwelling was proposed to take place along the inner and outer shelf break due to the comparatively high density of the cold, upwelled water. In combination of these flows, a semi-enclosed recirculation cell would develop above the inner shelf. This situation limits export of particulate matter from the inner shelf towards deeper parts of the continental margin. In contrast, the poleward directed undercurrent causes offshore directed flow of the bottom waters at the outer shelf. Thus, the offshore transport in the very particle-rich BNL prohibits particle deposition at the sea floor, although considerable OM production takes place in the surface waters. Instead, the particles are transported in the form of comparatively fine-grained, deep-water aggregates across the shelf break, depleted in OC with respect to SNL particles, but nevertheless richer in OC compared to the sediments at the outer shelf. The strong BNL together with the intensive shelf break depth INL induce effective lateral transfer of these pre-aged particles towards the upper slope depocenter. Another explanation for the high OM content of the depocenter is that at about 25.5°S poleward directed currents from the north presumably meet equatorward directed currents from the south in the subsurface. Such a collision would be accompanied by a decrease in current velocity, and, therewith, in particle transport capacity, leading to enhanced deposition at the seafloor. Primary production vertically above the slope-depth depocenter is restricted to the temporary occurring high-productive filaments. However, remineralization of the particles during settling through the water column is much more intensive due to the higher water depth. Thus, comparatively few particles reach the sediment.

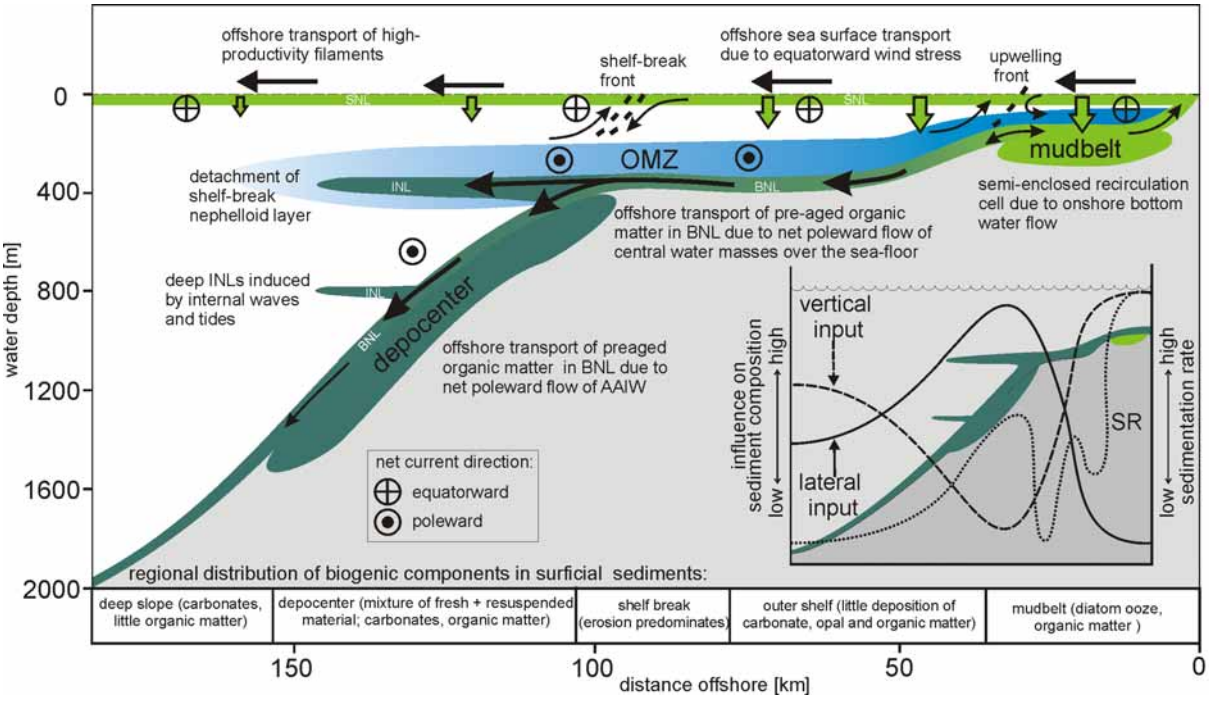

Fig. 7.1: Conceptual model of the continental margin offshore Namibia at 25.5°S with OC enrichments in the sediment (mudbelt and depocenter) and the oxygen minimum zone (OMZ, blue area) above shelf and slope. The general flow field (encircled dots and crosses, black arrows), the nepheloid layer distribution (green areas), the strength of the primary production (green arrows), and the composition of the surficial sediments are displayed. Different shades of green indicate OM age/preservation (the brighter the younger/better preserved). The inlay visualizes the relative importance of vertical (dashed line) and lateral (solid line) organic matter input to the sediments, as well as rate of the sedimentation (dotted line). BNL: bottom nepheloid layer, INL: intermediate nepheloid layer, AAIW: Antarctic Intermediate Water, SR: sedimentation rate,

Long-term moorings of sediment traps just above the BNL would be necessary to determine, if algae blooms in the surface waters above the slope are occasionally sufficiently strong to produce marine snow events that settle fast enough to reach the seafloor in considerable amounts. Below the depocenter, particle density and thickness of the BNL is obviously reduced. Therefore, the relative influence of the lateral input and the overall sedimentation rate decrease. However, the cause of the high ^{14}C-age of the suspended particles in the BNL above the slope remains ambiguous. The particles might stay in continuous resuspension loops with repeated back and force motions due to tidal currents and little net transport for long time periods. Additionally, exchange with the surface sediments and the influence of bioturbative mixing, or admixture of old particles eroded at a distant source would increase the average particle age. However, the high content of the fraction of "labile" OM in the sediments of the shelf and slope depocenters suggests the local shelf as the most reasonable source. The good preservation of OM surely benefits from the low oxygen exposure of the particles on their journey from the anoxic inner shelf environment along the suboxic BNL and INL towards the slope. There, high sedimentation rates provide high burial efficiency. Although the Lüderitz cell is proposed to be the most

stable and perennial of all upwelling cells in the BUS, a more dynamic upwelling system than reflected in this model must be considered, e.g. due to seasonal changes in the wind field and the current system.

The results of this thesis reveal the huge potential of advective processes to displace areas of enhanced OC burial effectively from the maximum production cells above the shelf towards the slope and possibly the deep-sea. For the BUS, this implies limited applicability of frequently used, state-of-the-art vertical particle flux models to approach OC flux to the sediment. This work focuses on the BUS, but comparison with results from the literature suggests that it can also be seen as a case study, transferable to other highly productive continental margins. The results of this thesis will help to evaluate and calibrate existing particle flux models and to develop new models, considering the high influence of lateral transport on particle and OM/OC fluxes. Therewith, the author of this thesis hopes to contribute to an improvement of the predictability of the impact of environmental change on the oceanic system.

8. References

Alldredge, A.L. and Gotschalk, C., 1988. In situ settling behaviour of marine snow. Limnology and Oceanography, 33: 339-351.

Aller, R.C. and DeMaster, D.J., 1984. Estimates of particle flux and reworking at the deep-sea floor using $^{234}Th/^{238}U$ disequilibrium. Earth and Planetary Science Letters, 67: 308-318.

Alperin, M.J., Suayah, I.B., Benninger, L.K. and Martens, C.S., 2002. Modern organic carbon burial fluxes, recent sedimentation rates, and particle mixing rates from the upper continental slope near Cape Hatteras, North Carolina (USA). Deep-Sea Research II, 49(20): 4645-4665.

Altabet, M.A., Deuser, W.G., Honjo, S. and Stienen, C., 1991. Seasonal and depth-related changes in the source of sinking particles in the North Atlantic. Nature, 354: 136-139.

Altabet, M.A. and Francois, R., 1994. Sedimentary nitrogen isotopic ratio as a recorder for surface ocean nitrate utilization. Global Biogeochemical Cycles, 8: 103-116.

Altabet, M.A., Francois, R., Murray, D.W. and Prell, W.L., 1995. Climate-related variations in denitrification in the Arabian Sea from sediment 15N/14N ratios. Nature, 373: 506-509.

Altabet, M.A. and McCarthy, J.J., 1985. Temporal and spatial variations in the natural abundance of 15N in PON from a warm-core ring. Deep Sea Research Part A, 32(7): 755-772.

Altabet, M.A., Murray, D.W. and Prell, W.L., 1999a. Climatically linked oscillations in Arabian Sea denitrification over the past 1 m.y.: Implications for the marine N cycle. Paleoceanography, 14: 732-743.

Altabet, M.A. et al., 1999b. The nitrogen isotope biogeochemistry of sinking particles from the margin of the Eastern North Pacific. Deep-Sea Research I, 46: 655-679.

Anderson, R.F., Rowe, G.T., Kemp, P.F., Trumbore, S. and Biscaye, P.E., 1994. Carbon budget for the mid-slope depocenter of the Middle Atlantic Bight. Deep-Sea Research II, 41(2/3): 669-703.

Antia, A.N. et al., 2001. Basin-wide particulate carbon flux in the Atlantic Ocean: Regional export patterns and potential for atmospheric CO2 sequestration. Global Biogeochemical Cycles, 15: 845– 862.

Antoine, D., André, J.-M. and Morel, A., 1996. Oceanic primary production: 2. Estimation at global scale from satellite (coastal zone color scanner) chlorophyll. Global Biogeochemical Cycles, 10(1): 57-69.

Armstrong, R.A., Lee, C., Hedges, J.I., Honjo, S. and Wakeham, S.G., 2002. A new, mechanistic model for organic carbon fluxes in the ocean based on the quantitative association of POC with ballast minerals. Deep-Sea Research II, 49(1-3): 219-236.

Arthur, M.A., Dean, W.E. and Laarkamp, K., 1998. Organic carbon accumulation and preservation in surface sediments on the Peru margin. Chemical Geology, 152(3-4): 273-286, doi: 10.1016/S0009-2541(98)00120-X.

Aspetsberger, F., Ferdelman, T., Witte, U. and Zabel, M., subm.-a. Organic matter reactivity driving diffusive benthic fluxes in the Benguela Upwelling System.

Aspetsberger, F. et al., subm.-b. Instantaneous benthic response to varying organic matter quality: In situ experiments in the Benguela Upwelling System.

Azetsu-Scott, K. and Johnson, B.D., 1994. Time series of the vertical distribution of particles during and after a spring phytoplankton bloom in a coastal basin. Continental Shelf Research, 14(6): 687-705.

Azetsu-Scott, K., Johnson, B.D. and Petrie, B., 1995. An intermittent, intermediate nepheloid layer in Emerald Basin, Scotian Shelf. Continental Shelf Research, 15(2-3): 281-293.

Bacon, M.P. and Rutgers van der Loeff, M.M., 1989. Removal of thorium-234 by scavenging in the bottom nepheloid layer of the ocean. Earth and Planetary Science Letters, 92: 157-164.

Bailey, G.W., 1991. Organic carbon flux and development of oxygen deficiency on the modern Benguela continental shelf south of 22°S: spatial and temporal variability. In: R. Tyson and T.H. Pearson (Editors), Modern and Ancient Continental Shelf Anoxia. Geological Society, London, Special Publication, pp. 171-183.

Barange, M. and Pillar, S.C., 1992. Cross-shelf circulation, zonation and maintenance mechanisms of Nyctiphanes capensis and Euphausia hanseni (Euphausiacea) in the northern Benguela upwelling system. Continental Shelf Research, 12(9): 1027-1042.

Barford, C.C., Montoya, J.P., Altabet, M.A. and Mitchell, R., 1999. Steady-state nitrogen isotope effects of N2 and N2O production in Paracoccus denitrificans. Applied Environmental Microbiology, 65: 989-994.

Barnett, P.R.O., Watson, J. and Connelly, D., 1984. A multiple corer for taking virtually undisturbed samples from shelf, bathyal and abyssal sediments. Oceanologica Acta, 7(4): 399-408.

Bauer, J.E. and Druffel, E.R.M., 1998. Ocean margins as a significant source of organic matter to the deep open ocean. Nature, 392: 482-485.

Behrenfeld, M.J. and Falkowski, P.G., 1997. Photosynthetic rates derived from satellite-based chlorophyll concentration. Limnology and Oceanography, 42(1): 1-20.

Berger, W.H., Smetacek, V.S. and Wefer, G., 1989. Ocean productivity and paleoproductivity - an overview. Productivity of the ocean: present and past. John Wiley & Sons Lim., 1-34 pp.

Berger, W.H. and Wefer, G., 2002. On the reconstruction of upwelling history: Namibia upwelling in context. Marine Geology, 180(1-4): 3-28.

Birch, G.F., 1975. Sediments on the continental margin off the west coast of South West Africa. PhD Thesis, University of Cape Town, Cape Town, 210 pp.

Biscaye, P.E. and Anderson, R.F., 1994. Fluxes of particulate matter on the slope of the southern Middle Atlantic Bight: SEEP-II. Deep-Sea Research II, 41(2/3): 459-509.

Biscaye, P.E., Flagg, C.N. and Falkowski, P.G., 1994. The shelf edge exchange processes experiment, SEEP-II: an introduction to hypotheses, results and conclusions. Deep-Sea Research II, 41(2/3): 231-252.

Bishop, J.K.B., 1986. The correction and suspended particulate matter calibration of Sea Tech transmissometer data. Deep-Sea Research, 33: 121-134.

Bishop, J.K.B., 1999. Transmissometer measurement of POC. Deep-Sea Research I, 46(2 SU): 353-369.

Bishop, J.K.B., Ketten, D.R. and Edmond, J.M., 1978. The chemistry, biology and vertical flux of particulate matter from the upper 400 m of the Cape Basin in the southeast Atlantic Ocean. Deep Sea Research, 25(12): 1121-1154.

Boetius, A., Ferdelman, T. and Lochte, K., 2000a. Bacterial activity in sediments of the deep Arabian Sea in relation to vertical flux. Deep-Sea Research II, 47: 2835-2875.

Boetius, A., Springer, B. and Petry, C., 2000b. Microbial activity and particulate matter in the benthic nepheloid layer (BNL) of the deep Arabian Sea. Deep-Sea Research II, 47: 2687-2706.

Bremner, J.M., 1981. Sediments on the continental margin off South West Africa between latitudes 17° and 25° S. PhD Thesis, University of Cape Town, Cape Town, 300 pp.

Bremner, J.M. and Willis, P.C., 1993. Mineralogy and geochemistry of the clay fraction of sediments from the Namibian continental margin and the adjacent hinterland. Marine Geology, 115: 85-116.

Brongersma-Sanders, M., 1948. The importance of upwelling water to vertebrate paleontology and oil geology. Verh. Kon. Ned. Akad. Wetensch., Afd. Natuurk. Sect. 2, Pt. 45: 1-112.

Brüchert, V. et al., 2003. Regulation of bacterial sulfate reduction and hydrogen sulfide fluxes in the central namibian coastal upwelling zone. Geochimica et Cosmochimica Acta, 67(23): 4505-4518.

Brummer, G.J.A., H.T., K. and W., H., 2002. Monsoon-driven export fluxes and early diagenesis of particulate nitrogen and its d15N across the Somalia margin. In: P.D. Clift, D. Kroon, C. Gaedicke and J. Craig (Editors), The tectonic and climatic Evolution of the Arabian Sea Region. Special Publications. Geological Society, London, pp. 353-370.

Cacchione, D.A. and Drake, D.E., 1986. Nepheloid layers and internal waves over continental shelves and slopes. Geo-Marine Letters, 16: 147-152.

Cacchione, D.A., Wiberg, P.L., Lynch, J., Irish, J. and Traykovski, P., 1999. Estimates of suspended-sediment flux and bedform activity on the inner portion of the Eel continental shelf. Marine Geology, 154(1-4): 83-97.

Cacchione, D.A. and Wunsch, C., 1974. Experimental study of internal waves over a slope. Journal of Fluid Mechanics, 66(2): 223-239.

Calvert, S.E., Bustin, R.M. and Pedersen, T.F., 1992. Lack of evidence for enhanced preservation of sedimentary organic matter in the oxygen minimum of the Gulf of California. Geology, 20: 757-760.

Calvert, S.E. and Pedersen, T.F., 1992. Organic carbon accumulation and preservation in marine sediments: how important is anoxia? In: J.K. Whelan and J.W. Farrington (Editors), Organic Matter: Productivity, Accumulation, and Preservation in Recent and Ancient Sediments. Columbia University Press, New York, pp. 231-263.

Calvert, S.E., Pedersen, T.F., Naidu, P.D. and Stackelberg, U.v., 1995. On the organic carbon maximum on the continental slope of the eastern Arabian Sea. Journal of Marine Research, 53: 269-296, doi: 10.1357/0022240953213232.

Calvert, S.E. and Price, N.B., 1970. Minor metal contents of recent organic-rich sediments off South West Africa. Nature, 227: 593-595.

Calvert, S.E. and Price, N.B., 1983. Geochemistry of Namibian shelf sediments. In: J. Thiede and E. Suess (Editors), Coastal upwelling: It s sedimentary record. Plenum Press, New York, pp. 337-375.

Campillo-Campbell, C. and Gordoa, A., 2004. Physical and biological variability in the Namibian upwelling system: October 1997-October 2001. Deep-Sea Research II, 51(1-3): 147-158.

Canfield, D.E., 1994. Factors influencing organic carbon preservation in marine sediments. Chemical Geology, 114: 315-329.

Carr, M.E., 2001. Estimation of potential productivity in Eastern Boundary Currents using remote sensing. Deep-Sea Research II, 49(1-3): 59-80, doi: 10.1016/S0967-0645(01)00094-7.

Chapalain, G. and Thais, L., 2004. A sampler-based technique for the study of near-bed sediment dynamics: application in the eastern English Channel. Geo-Marine Letters, 24(2): 125-132.

Chapman, P. and Shannon, L.V., 1985. The Benguela Ecosystem Part II. Chemistry and related Processes. Oceanogr. Mar. Biol. Annu. Rev., 23: 183-251.

Chen, J.H., Edwards, R.L. and Wasserburg, G.J., 1986. ^{238}U, ^{234}U and ^{232}Th in seawater. Earth and Planetary Science Letters, 80: 241-251.

Cline, J.D. and Kaplan, I.R., 1975. Isotopic fractionation of dissolved nitrate during denitrification in the eastern tropical north pacific ocean. Marine Chemistry, 3(4): 271-299.

Coale, K.H. and Bruland, K.W., 1985. $^{234}Th/^{238}U$ disequilibria within the California current. Limnology and Oceanography, 30(1): 22–33.

Codispoti, L.A. et al., 2001. The oceanic fixed nitrogen and nitrous oxide budgets: Moving targets as we enter the anthropocene? Scientia Marina, 65: 85-105.

Dauwe, B., Middelburg, J.J., Hershey, A.E. and Heip, C.H.R., 1999. Linking diagenetic alteration of amino acids and bulk organic matter reactivity. Limnology and Oceanography, 44(7): 1809-1814.

Dean, W.E. and Gardner, J.V., 1998. Pleistocene to Holocene contrasts in organic matter production and preservation on the California continental margin. Geological Society of America Bulletin, 110(7): 888-899.

Dean, W.E., Gardner, J.V. and Anderson, R.Y., 1994. Geochemical evidence for enhanced perservation of organic matter in the oxygen minimum zone of the continental margin of northern California during the late Pleistocene. Paleoceanography, 9(1): 47-61, doi: 10.1029/93PA02829.

DeMaster, D.J., Brewster, D.C., McKee, B.A. and Nittrouer, C.A., 1991. Rates of particle scavenging, sediment reworking and longitudinal ripple formation at the HEBBLE site based on measurements of ^{234}Th and ^{210}Pb. Marine Geology, 99: 423-444.

Dickens, A.F., G?linas, Y., Masiello, C.A., Wakeham, S. and Hedges, J.I., 2004. Reburial of fossil organic carbon in marine sediments. Nature, 427: 336-339.

Diekmann, B. and Kuhn, G., 2002. Sedimentary record of the mid-Pleistocene climate transition in the southeastern South Atlantic (ODP Site 1090). Palaeogeography, Palaeoclimatology, Palaeoecology, 182(3-4): 241-258.

Engel, A., 2004. Distribution of transparent exopolymer particles (TEP) in the northeast Atlantic Ocean and their potential significance for aggregation processes. Deep-Sea Research I, 51(1): 83-92.

Farrell, J.W., Pedersen, T.F., Calvert, S.E. and Nielsen, B., 1995. Glacial-interglacial changes in nutrient utilization in the equatorial Pacific Ocean. Nature, 377: 514-517.

Ferdelman, T.G., Fossing, H. and Neumann, K., 1999. Sulfate reduction in surface sediments of the southeast Atlantic continental margin between 15°38′ S and 27°57′S (Angola and Namibia). Limnology and Oceanography, 44(3): 650-661.

Fischer, G., Müller, P.J. and Wefer, G., 1998. Latitudinal d13Corg variations in sinking matter and sediments from the South Atlantic: effects of anthropogenic CO2 and implications for palaeo-PCO2 reconstructions. Journal of Marine Systems, 17: 471-495.

Fohrmann, H. et al., 2001. Modern Ocean Current-Controlled Sediment Transport in the Greenland-Iceland-Norwegian (GIN) Seas. In: P. Schäfer, W. Ritzrau, M. Schlüter and J. Thiede (Editors), The Northern North Atlantic: A Changing Environment. Springer, Berlin, pp. 135-154.

Francois, R., Altabet, M.A. and Burckle, L.H., 1992. Glacial to interglacial changes in surface nitrate utilization in the Indian sector of the Southern Ocean as recorded by sediment d15N. Paleoceanography, 7: 589-606.

Freudenthal, T. et al., 2002. Upwelling intensity and filament activity off Morocco during the last 250,000 years. Deep-Sea Research II, 49(17): 3655-3674.

Freudenthal, T., Wagner, T., Wenzhofer2, F., Zabel, M. and Wefer, G., 2001. Early diagenesis of organic matter from sediments of the eastern subtropical Atlantic: evidence from stable nitrogen and carbon isotopes. Geochimica et Cosmochimica Acta, 65(11): 1795-1808.

Ganeshram, R.S., Calvert, S.E., Pedersen, T.F. and Cowie, G.L., 1999. Factors controlling the burial of organic carbon in laminated and bioturbated sediments off NW Mexico: implications for hydrocarbon preservation. Geochimica et Cosmochimica Acta, 63(11-12): 1723-1734, doi: 10.1016/S0016-7037(99)00073-3.

Ganeshram, R.S., Pedersen, T.P., Calvert, S.E. and Murray, J.W., 1995. Large changes in oceanic nutrient inventories from glacial to interglacial periods. Nature, Vol.376: 755-757.

Gardner, W.D., Richardson, M.J., Carlson, C.A., Hansell, D. and Mishonov, A.V., 2003. Determining true particulate organic carbon: bottles, pumps and methodologies. Deep-Sea Research II, 50(3-4): 655-674.

Gardner, W.D., Walsh, I.D. and Richardson, M.J., 1993. Biophysical forcing of particle production and distribution during a spring bloom in the North Atlantic. Deep-Sea Research II, 40(1/2): 171-195.

Gaye-Haake, B. et al., 2005. Stable nitrogen isotopic ratios of sinking particles and sediments from the northern Indian Ocean. Marine Chemistry, 96(3-4): 243-255, doi: 10.1016/j.marchem.2005.02.001.

Gelinas, Y., Baldock, J.A. and Hedges, J.I., 2001. Organic Carbon Composition of Marine Sediments: Effect of Oxygen Exposure on Oil Generation Potential. Science, 294(5540): 145-148.

Giraudeau, J., Bailey, G.W. and Pujol, C., 2000. A high-resolution time-series analyses of particle fluxes in the Northern Benguela coastal upwelling system: carbonate record of changes in biogenic production and particle transfer processes. Deep-Sea Research II, 47(9-11): 1999-2028.

Glud, R.N., Gundersen, J.K., Jörgensen, B.B., Revsbech, N.P. and Schulz, H.D., 1994. Diffusive and total oxygen uptake of deep-sea sediments in the eastern South Atlantic Ocean: in situ and laboratory measurements. Deep Sea Research, 41(11/12): 1767-1788.

Gordon, A.L., Bosley, K.T. and Aikman, I., Frank, 1995. Tropical atlantic water within the Benguela upwelling system at 27°S. Deep-Sea Research I, 42(1): 1-12.

Graf, G., 1989. Benthic-pelagic coupling in a deep-sea benthic community. Nature, 341: 437-439.

Graf, G. and Rosenberg, R., 1997. Bioresuspension and biodeposition: a review. Journal of Marine Systems, 11(3-4): 269-278.

Gruber, N. and Sarmiento, J.L., 1997. Global patterns of marine nitrogen fixation and denitrification. Global Biogeochemical Cycles, 11(2): 235-266.

Gundersen, J.S., Gardner, W.D., Richardson, M.J. and Walsh, I.D., 1998. Effects of monsoons on the seasonal and spatial distributions of POC and chlorophyll in the Arabian Sea. Deep-Sea Research II, 45(10-11): 2103-2132.

Hall, I.R. and McCave, I.N., 1998. Glacial-interglacial variation in organic carbon burial on the slope of the N.W. European Continental Margin (48°-50°N). Progress In Oceanography, 42(1-4): 37-60.

Hall, I.R., Schmidt, S., McCave, I.N. and Reyss, J.L., 2000. Particulate matter distribution and $^{234}Th/^{238}U$ disequilibrium along the Northern Iberian Margin: implications for particulate organic carbon export. Deep-Sea Research I, 47: 557-582.

Hart, T.J. and Currie, R.I., 1960. The Benguela Current, Discovery Report, pp. 123-298.

Hartnett, H.E., Keil, R.G., Hedges, J.I. and Devol, A.H., 1998. Influence of oxygen exposure time on organic carbon preservation in continental margin sediments. Nature, 391: 572-574.

Hedges, J.I. et al., 2001. Evidence for non-selective preservation of organic matter in sinking marine particles. Nature, 409: 801-804.

Hensen, C., Zabel, M. and Schulz, H.D., 2000. A comparison of benthic nutrient fluxes from deep-sea sediments off Namibia and Argentine. Deep-Sea Research II, 47: 2029-2050.

Holmes, M.E., Eichner, C., Struck, U. and Wefer, G., 1999. Reconstruction of Surface Ocean Nitrate Utilization Using Stable Nitrogen Isotopes in Sinking Particles and Sediments. In: G. Fischer and G. Wefer (Editors), Use of Proxies in Paleoceanography. Springer, Berlin, pp. 447-468.

Holmes, M.E. et al., 2002. Seasonal variability of d15N in sinking particles in the Benguela upwelling region. Deep-Sea Research I, 49: 377-394.

Holmes, M.E., Lavik, G., Fischer, G. and Wefer, G., 2003. Nitrogen isotopes in sinking particles and surface sediments in the Central and Southern Atlantic. In: G. Wefer, S. Mulitza and V. Rathmeyer (Editors), The South Atlantic in the Late Quaternary:

Reconstruction of Material Budgets and Current Systems. Springer, Berlin, pp. 143-165.

Holmes, M.E., Schneider, R., Müller, P.J., Segl, M. and Wefer, G., 1997. Reconstruction of past nutrient utilization in the eastern Angola Basin based on sedimentary 15N/14N ratios. Paleoceanography, 12: 604-614.

Holtvoeth, J., Wagner, T., Horsfield, B., Schubert, C.J. and Wand, U., 2001. Late-Quaternary supply of terrigenous organic matter to the Congo deep-sea fan (ODP site 1075): implications for equatorial African paleoclimate. Geo-Marine Letters, 21: 23-33, doi: 10.1007/s003670100060.

Hwang, J., Druffel, E.R.M. and Komada, T., 2005. Transport of organic carbon from the California coast to the slope region: A study of d14C and d13C signatures of organic compound classes. Global Biogeochemical Cycles, 19, doi: 10.1029/2004GB002422.

Inthorn, M., Mohrholz, V. and Zabel, M., subm.-a. Nepheloid layer distribution in the Benguela upwelling area offshore Namibia. Deep-Sea Research I.

Inthorn, M., Rutgers van der Loeff, M.M. and Zabel, M., subm.-b. Approaching particle exchange processes at the sediment water interface in the Benguela upwelling area based on $^{234}Th/^{238}U$ disequilibrium. Deep-Sea Research I.

Inthorn, M., Wagner, T., Scheeder, G. and Zabel, M., in press. Lateral transport controls distribution, quality and burial of organic matter along continental slopes in high-productivity areas. Geology.

Jahnke, R.A., 1996. The global ocean flux of particulate organic carbon: areal distribution and magnitude. Global Biogeochemical Cycles, 10(1): 71-88.

Jahnke, R.A., Reimers, C.E. and Craven, D.B., 1990. Intensification of recycling of organic matter at the sea floor near ocean margins. Nature, 348: 50-54 , doi: 10.1038/348050a0.

Keil, R.G., Dickens, A.F., Arnarson, T., Nunn, B.L. and Devol, A.H., 2004. What is the oxygen exposure time of laterally transported organic matter along the Washington margin? Marine Chemistry, 92(1-4): 157-165.

Klaas, C. and Archer, D.E., 2002. Association of sinking organic matter with various types of mineral ballast in the deep sea: Implications for the rain ratio. Global Biogeochemical Cycles, 16(4), doi: 10.1029/2001GB001765.

Kuypers, M.M.M., G., L. and B., T., in Press. Anammox in the marine environment. In: L. Neretin (Editor), Past and present water column anoxia. NATO Book Series. Kluwer academic publishers.

Kuypers, M.M.M. et al., 2005. Massive nitrogen loss from the Benguela upwelling system through anaerobic ammonium oxidation. PNAS, 102(18): 0502088102.

Kuypers, M.M.M. et al., 2003. Anaerobic ammonium oxidation by anammox bacteria in the Black Sea. Nature, 422: 608-611.

Lampitt, R.S., Raine, R.C.T., Billet, D.S.M. and Rise, A.L., 1995. Material supply to the European continental slope: A budget based on benthic oxygen demand and organic supply. Deep-Sea Research I, 42(11/12): 1865-1880.

Langford, F.F. and Blanc-Valleron, M.M., 1990. Interpreting Rock-Eval pyrolysis data using graphs of pyrolizable hydrocarbons vs. total organic carbon. The American Association of Petroleum Geologists Bulletin, 74(6): 799-804.

Lavik, G., 2001. Nitrogen isotopes of sinking matter and sediments in the South Atlantic. Berichte aus dem FB Geowissenschaften der Universität Bremen. Uni Bremen, Fachbereich 5, Bremen, 140 pp.

Levitan, M.A., Ditrikh, P.G. and Gorbunova, Z.N., 1990. Bottom sediments in transocean section (Southern part of the Atlantic Ocean) (in Russian), Transactions of IOAN. Biological and geological research of bottom of southern part of the Atlantic Ocean, pp. 172-184.

Lisitzin, A.P. et al., 1975. Distribution of bottom sediments in th Atlantic Ocean. In: A.P. Lisitzin (Editor), Sedimentation in the Atlantic Ocean (in Russian). Kalinigradskaya Pravda, Kaliningrad, pp. 323.

Liu, Z. et al., 2005. Why do POC concentrations measured using Niskin bottle collections sometimes differ from those using in-situ pumps? Deep Sea Research Part I: Oceanographic Research Papers, 52(7): 1324-1344.

Lutjeharms, J.R.E., Shillington , F.A. and Duncombe Rae, C.M., 1991. Observing of extreme upwelling filaments in the Southeast Atlantic ocean. Science, 253: 774-776.

Mau, S. et al., subm. Methane flux estimates of mud extrusions along the erosive convergent margin of Costa Rica. Marine Geology.

McCave, I.N., 1986. Local and global aspects of the bottom nepheloid layers in the world ocean. Netherlands Journal of Sea Research, 20(2/3): 167-181.

McCave, I.N., 2003. Sedimentary Settings on Continental Margins - an Overview. In: G. Wefer et al. (Editors), Ocean Margin Systems. Springer, Berlin Heidelberg, pp. 1-14.

McCave, I.N. and Hall, I.R., 2002. Turbidity of waters over the Northwest Iberian continental margin. Progress In Oceanography, 52(2-4): 299-313.

McCave, I.N. et al., 2001. Distribution,composition and flux of particulate material over the European margin at 47°50′ N. Deep-Sea Research II, 48: 3107-3139.

McClain, C.R., Feldman, G.C. and Hooker, S.B., 2004. An overview of the SeaWiFS project and strategies for producing a climate research quality global ocean bio-optical time series. Deep-Sea Research II, 51(1-3): 5-42.

McPhee-Shaw, E.E. and Kunze, E., 2002. Boundary layer intrusions from a sloping bottom: A mechanism for generating intermediate nepheloid layers. Journal of Geophysical Research, 107(C6), doi: 10.1029/2001JC000801.

McPhee-Shaw, E.E., Sternberg, R.W., Mullenbach, B. and Ogston, A.S., 2004. Observations of intermediate nepheloid layers on the northern California continental margin. Continental Shelf Research, 24(6): 693-720.

Mienert, J. et al., 1998. European North Atlantic Margin (ENAM I): sediment pathways, processes, and fluxes - an introduction. Marine Geology, 152: 3–6.

Milligan, T.G., Belliveau, D., Muschenheim, D.K. and Morton, G.R., 1998. New equipment for benthic habitat studies. Sea Technology, 39(9): 56–61.

Mishonov, A.V., Gardner, W.D. and Jo Richardson, M., 2003. Remote sensing and surface POC concentration in the South Atlantic. Deep-Sea Research II, 50: 2997-3015.

Mohrholz, V., Schmidt, M. and Lutjeharms, J.R.E., 2001. The hydrography and dynamics of the Angola-Benguela Frontal Zone and environment in April 1999. South African Journal of Science, 97(5-6): 199-208.

Mollenhauer, G. et al., 2003. Asynchronous alkenone and foraminifera records from the Benguela Upwelling System. Geochimica et Cosmochimica Acta, 67(12): 2157-2171, doi: 10.1016/S0016-7037(03)00168-6.

Mollenhauer, G., Schneider, R.R., Müller, P.J., Spieß, V. and Wefer, G., 2002. Glacial/interglacial variability in the Benguela upwelling system: Spatial distribution and budgets of organic carbon accumulation. Global Biogeochemical Cycles, 16(4), doi: 10.1029/2001GB001488.

Montoya, J.P., 1994. Nitrogen isotope fractionation in the modern ocean: implications for the sedimentary record. In: R. Zahn, M.A. Kaminski, L. Labeyrie and T.F. Pederson (Editors), Carbon Cycling in the Glacial Ocean: Constraints on the Ocean's Role in Global Change. NATO ASI Series. Springer, pp. 260-279.

Moran, S.B., Charette, M.A., Pike, S.M. and Wicklund, C.A., 1999. Differences in seawater particulate organic carbon concentration in samples collected using small- and large-volume methods: the importance of DOC adsorption to the filter blank. Marine Chemistry, 67: 33–42.

Müller, P.J. and Suess, E., 1979. Productivity, sedimentation rate, and sedimentary organic matter in the oceans - I. Organic carbon preservation. Deep-Sea Res., 26: 1347-1362.

Nakatsuka, T., Handa, N., Harada, N., Sugimoto, T. and Imaizumi, S., 1997. Origin and decomposition of sinking particulate organic matter in the deep water column inferred from the vertical distributions of its [delta]15N, [delta]13 and [delta]14. Deep-Sea Research I, 44(12): 1957-1979.

Nelson, G. and Hutchings, L., 1983. The Benguela upwelling area. Progress in Oceanography, 12: 333-356.

Nittrouer, C.A., 1999. STRATAFORM: overview of its design and synthesis of its results. Marine Geology, 154: 3-12.

Oliveira, A. et al., 2002. Nepheloid layer dynamics in the northern Portuguese shelf. Progress in Oceanography, 52(2-4): 195-213.

Pak, H., Codispoti, L.A. and Zaneveld, J.R.V., 1980. On the intermediate particle maxima associated with oxygen-poor water off western South America. Deep Sea Research Part A, 27(10): 783-797.

Passow, U. et al., 2001. The origin of transparent exopolymer particles (TEP) and their role in the sedimentation of particulate matter. Continental Shelf Research, 21(4): 327-346.

Pedersen, T.F., Shimmield, G.B. and Price, N.B., 1992. Lack of enhanced preservation of organic matter in sediments under the oxygen minimum on the Oman Margin. Geochemica et Cosmochemica Acta, 56: 545-551.

Peterson, R.G. and Stramma, L., 1991. Upper-level circulation in the South Atlantic Ocean. Progress In Oceanography, 26(1): 1-73.

Pichevin, L., Bertrand, P., Boussafir, M. and Disnar, J.-R., 2004. Organic matter accumulation and preservation controls in a deep sea modern environment: an example from Namibian slope sediments. Organic Geochemistry, 35(5): 543-559, doi: 10.1016/j.orggeochem.2004.01.018.

Pichevin, L. et al., 2005. Nitrogen cycling on the Namibian shelf and slope over the last two climatic cycles: Local and global forcings. Paleoceanography, 20.

Premuzic, E.T., Benkovitz, C.M., Gaffney, J.S. and Walsh, J.J., 1982. The nature and distribution of organic matter in the surface sediments of world oceans and seas. Organic Geochemistry, 4: 63-77.

Pride, C. et al., 1999. Nitrogen isotopic variations in the Gulf of California since the last deglaciation: Response to global climate change. Paleoceanography, 14: 397-408.

Puig, P. and Palanques, A., 1998. Nepheloid structure and hydrographic control on the Barcelona continental margin, northwestern Mediterranean. Marine Geology, 149(1-4): 39-54.

Ransom, B., Shea, K.F., Burkett, P.J., Bennett, R.H. and Baerwald, R., 1998. Comparison of pelagic and nepheloid layer marine snow: implications for carbon cycling. Marine Geology, 150(1-4): 39-50.

Redfield, A.C., Ketchum, B.H. and Richards, F.A., 1963. The influence of organisms on the composition of seawater. In: M.N. Hill (Editor), The Sea. Interscience, New York, pp. 26–77.

Reed, A., Carmichael, A. and De Angelis, M.A., 1997. An inexpensive bottom water sampler. Continental Shelf Research, 17(6): 717-721.

Reimers, C.E., Jahnke, R.H. and McCorkle, D.C., 1992. Carbon fluxes and burial rates over the continental slope and rise off central California with implications for the global carbon cycle. Global Biogeochemical Cycles, 6: 199-224.

Richardson, M.J., 1987. Particle size, light scattering and composition of suspended particulate matter in the North Atlantic. Deep Sea Research Part A, 34(8): 1301-1329.

Ritzrau, W., 1996. Microbial activity in the benthic boundary layer: small-scale distribution and its relationship with the hydrodynamic regime. Netherlands Journal of Sea Research, 36(3/4): 171-180.

Rogers, J., 1977. Sediments on the continental margin off the Orange River and the Namib Desert. PhD Thesis, University of Cape Town, Cape Town, 212 pp.

Rogers, J., 1979. Dispersal of sediment from the Orange River along the Namib Desert coast. South African Journal of Science, 75: 567.

Rogers, J. and Bremner, J.M., 1991. The Benguela Ecosystem. Part VII. Marine-Geological Aspects. Oceanogr. Mar. Biol. Annu. Rev., 29: 1-85.

Romankevich, E.A., 1994. Biogeochemistry of the boundary zones in the Atlantic Ocean. Nauka, Moskow, 400 pp.

Romero, O. et al., 2002. Seasonal productivity dynamics in the pelagic central Benguela System inferred from the flux of carbonate and silicate organisms. Journail of Marine Systems, 37(4): 259-278.

Rumohr, J. et al., 2001. Records and Processes of Near-Bottom Sediment Transport along the Norwegian-Greenland Sea Margins during Holocene and Late Weichselian (Termination I) Times. In: P. Schäfer, W. Ritzrau, M. Schlüter and J. Thiede (Editors), The Northern North Atlantic: A Changing Environment. Springer, Berlin, pp. 155-178.

Rutgers van der Loeff, M.M. and Boudreau, B.P., 1997. The effect of resuspension on chemical exchanges at the sediment-water interface in the deep sea -- A modelling and natural radiotracer approach. Journal of Marine Systems, 11(3-4): 305-342.

Rutgers van der Loeff, M.M., Meyer, R., Rudels, B. and Rachor, E., 2002. Resuspension and particle transport in the Benthic Nepheloid Layer in and near Fram Strait in relation to faunal abundances and 234 Th depletion. Deep-Sea Research I, 49: 1941-1958.

Rutgers van der Loeff, M.M. and Moore, W.S., 1999. Determination of natural radioactive tracers. In: K. Grasshoff, M. Ehrhardt and K. Kremling (Editors), Methods of Seawater Analysis. Verlag Chemie, Weinheim, pp. 365–397.

Saino, T. and Hattori, A., 1980. 15N natural abundance in oceanic suspended particulate matter. Nature, 283: 752-754.

Santschi, P.H., Guo, L., Walsh, I.D., Quigley, M.S. and Baskaran, M., 1999. Boundary exchange and scavenging of radionuclides in continental margin waters of the Middle Atlantic Bight: implications for organic carbon fluxes. Continental Shelf Research, 19(5): 609-636.

Sauter, E.J., Schluter, M., Wegner, J. and Labahn, E., 2005. A routine device for high resolution bottom water sampling. Journal of Sea Research, 54(3): 204-210, doi: 10.1016/j.seares.2005.04.005.

Savoye, N., Buesseler, K.O., Cardinal, D. and Dehairs, F., 2004. ^{234}Th deficit and excess in the Southern Ocean during spring 2001: Particle export and remineralization. Geophysical Research Letters, 31(12), doi:10.1029/2004GL019744.

Schink, D.R., Fanning, K.A. and Piety, J., 1966. A sea-bottom sampler that collects both water and sediment simultaneously. Journal of Marine Research, 24: 365-373.

Schmiedl, G., Mackensen, A. and Muller, P.J., 1997. Recent benthic foraminifera from the eastern South Atlantic Ocean: Dependence on food supply and water masses. Marine Micropaleontology, 32(3-4): 249-287.

Schulz, H.N. et al., 1999. Dense populations of a giant sulfur bacterium in Namibian shelf sediments. Science, 284: 493-495.

Schulz, H.N. and Schulz, H.D., 2005. Large Sulfur Bacteria and the Formation of Phosphorite. Science, 307: 416-418.

Seiter, K., 2004. Regionalisierung und Quantifizierung benthischer Mineralisationsprozesse. Berichte, Fachbereich Geowissenschaften, Universität Bremen. Universität Bremen, Bremen, 136 pp.

Seiter, K., Hensen, C., Schroter, J. and Zabel, M., 2004. Organic carbon content in surface sediments--defining regional provinces. Deep-Sea Research I, 51(12): 2001-2026.

Seiter, K., Hensen, C. and Zabel, M., 2005. Benthic carbon mineralization on a global scale. Global Biogeochemical Cycles, 19, doi: 10.1029/2004GB002225.

Shannon, L.V. and Nelson, G., 1996. The Benguela: Large Scale Features and Processes and System Variability. In: G. Wefer, W. Berger, G. Siedler and D. Webb (Editors), The South Atlantic: Present and Past Circulation. Springer, NewYork, pp. 163-210.

Smith, R.L., 1995. The Physical Processes of Coastal Ocean Upwelling Systems. In: B. Zeitzschel (Editor), Dahlem Workshop on Upwelling in the Ocean: Modern Processes and Ancient Records (1994: Berlin, Germany). Dahlem Workshop Reports. Wiley, Chichester, pp. 39-64.

Sternberg, R.W., Johnson, R.V., Cacchione, D.A. and Drake, D.E., 1986. An instrument system for monitoring and sampling suspended sediment in the benthic boundary layer. Marine Geology, 71(3-4): 187-199.

Suess, E., 1980. Particulate organic carbon flux in the oceans - surface productivity and oxygen utilization. Nature, 288: 260-263.

Summerhayes, C.P., Emeis, K.-C., Angel, M.V., Smith, R.L. and Zeitzschel, B., 1995a. Upwelling in the Ocean: Modern Processes and Ancient Records. In: C.P. Summerhayes, K.-C. Emeis, M.V. Angel, R.L. Smith and B. Zeitzschel (Editors), Dahlem Workshop on Upwelling in the Ocean: Modern Processes and Ancient Records (1994: Berlin, Germany). Dahlem Workshop Reports. Wiley, Chichester, pp. 1-38.

Summerhayes, C.P. et al., 1995b. Variability in the Benguela Current upwelling system over the past 70,000 years. Progress in Oceanography, 35(3): 207-251, doi: 10.1016/0079-6611(95)00008-5.

Thomsen, L., 1999. Processes in the benthic boundary layer at continental margins and their implication for the benthic carbon cycle. Journal of Sea Research, 41: 73-86.

Thomsen, L., 2003. The Benthic Boundary Layer. In: G. Wefer et al. (Editors), Ocean Margin Systems. Springer, Berlin, pp. 143-155.

Thomsen, L., Graf, G., Martens, V. and Steen, E., 1994. An instrument for sampling water from the benthic boundary layer. Continental Shelf Research, 14(7-8): 871-882.

Thomsen, L. and McCave, I.N., 2000. Aggregation processes in the benthic boundary layer at the Celtic Sea continental margin. Deep-Sea Research I, 47(8): 1389-1404.

Thomsen, L. and van Weering, T.C.E., 1998. Spatial and temporal variability of particulate matter in the benthic boundary layer at the N.W. European Continental Margin (Goban Spur). Progress in Oceanography, 42: 61-76.

Thorpe, S.A. and White, M., 1988. A deep intermediate nepheloid layer. Deep Sea Research Part A, 35(9): 1665-1671.

Turnewitsch, R. and Springer, B., 2001. Do bottom mixed layers influence ^{234}Th dynamics in the abyssal near-bottom water column? Deep-Sea Research II, 48: 1279-1307.

Tyrrell, T. and Lucas, M.I., 2002. Geochemical evidence of denitrification in the Benguela upwelling system. Continental Shelf Research, 22(17): 2497-2511.

Tyson, R.V., 1995. Sedimentary Organic Matter: Organic Facies and Palynofacies. Chapman & Hall, London, 615 pp.

Usbeck, R., Schlitzer, R., Fischer, G. and Wefer, G., 2003. Particle fluxes in the ocean: comparison of sediment trap data with results from inverse modeling. Journal of Marine Systems, 39(3-4): 167-183.

van Weering, T.C.E., H.C. deStigter, W. Boer and deHaas, H., 2002. Recent sediment transport and accumulation on the NW Iberian margin. Progress in Oceanography, 52(2-4): 349-371.

van Weering, T.C.E. and McCave, I.N., 2002. Benthic processes and dynamics at the NW Iberian margin: an introduction. Progress in Oceanography, 52(2-4): 123-128.

van Weering, T.C.E., McCave, I.N. and Hall, I.R., 1998. Ocean Margin Exchange (Omex I) benthic processes study. Progress in Oceanography, 42: 1-4.

Voss, M., Altabet, M.A. and Bodungen, B.v., 1996. d15N in sedimenting particles as indicator of euphotic-zone processes. Deep-Sea Research I, 43(1): 33-47.

Wada, E., 1980. Nitrogen isotope fractionation and is significance in biogeochemical processes occurring in marine environments. In: E.D. Goldberg, Y. Horibe and K. Saruhashi (Editors), Isotope Marine Chemistry. Uchida Rokakuho, Tokyo, pp. 375-398.

Wada, E. and Hattori, A., 1978. Nitrogen isotope effects in the assimilation of inorganic nitrogenous compounds by marine diatoms. Geomicrobiology Journal, 1: 85-100.

Wagner, T. and Dupont, L.M., 1999. Terrestrial Organic Matter in Marine Sediments: Analytical Approaches and Eolian-Marine Records in the Central Equatorial Atlantic. In: G. Fischer and G. Wefer (Editors), Use of Proxies in Paleoceanography. Springer, Berlin, pp. 547-574.

Wagner, T., Zabel, M., Dupont, L., Holtvoeth, J. and Schubert, C.J., 2004. Terrigenous Signals in Sediments of the Low Latitude Atlantic - Implications for Environmental Variations during the Late Quarternary: Part I: Organic Carbon. In: G. Wefer, Mulitza, S., Ratmeyer, V. (Editor), The South Atlantic in the Late Quarternary: Reconstrucion of Material Budgets and Current Systems. Springer Verlag, Berlin.

Walsh, J.J., 1991. Importance of continental margins in the marine biochemical cycling of carbon and nitrogen. Nature, 350: 53-55.

Walsh, J.J., Biscaye, P.E. and Csanady, G.T., 1988. The 1983-1984 Shelf Edge Exchange Processes (SEEP)-1 experiment: hypotheses and highlights. Continental Shelf Research, 8: 435–457.

Weeks, S.J., 2001. Massive emissions of toxic gas in the Atlantic. Nature, 415: 493-494.

Wefer, G. and Fischer, G., 1993. Seasonal Patterns of vertical Particle Flux in equatorial and coastal Upwelling Areas of the Eastern Atlantic. Deep-Sea Research, 40: 1613-1645.

Wenzhöfer, F. and Glud, R.N., 2002. Benthic carbon mineralization in the Atlantic: a synthesis based on in situ data from the last decade. Deep-Sea Research I, 49(7): 1255-1279.

Wollast, R., 1998. Evaluation and comparison of the global carbon cycle in the coastal zone and in the open ocean. In: K.H. Brink and A.R. Robinson (Editors), The Sea. University of Brussels, pp. 213–252.

Zabel, M. and Hensen, C., 2003. The importance of Mineralization Processes in Surface Sediments at Continental Margins. In: G. Wefer et al. (Editors), Ocean Margin Systems. Springer, Berlin Heidelberg, pp. 253-267.

Appendix 1: Methane in sediments of the deep Marmara Sea and its relation to local tectonic structures

Peter Halbach[1], Ismail Kuşçu[2], Maik Inthorn[1], Thomas Kuhn[3], Asaf Pekdeğer[1], Richard Seifert[4]

[1]*Free University of Berlin, Dept. for Economic and Environmental Geology, 12249 Berlin,Germany. *e-mail: hbrumgeo@zedat.fu-berlin.de*

[2]*General Directorate of Mineral Research and Exploration (MTA), Ankara, Turkey*

[3]*Technical University of Freiberg, Inst. for Mineralogy, 09596 Freiberg, Germany*

[4]*University of Hamburg, Dept. for Biogeochemistry and Marine Chemistry, Bundesstr. 55, 20146 Hamburg, Germany*

in Görür, N., Papadopoulos, G.A., and Okay, N., eds.
Integration of Earth Science Research on the Turkish and Greek 1999 Earthquakes
NATO Science Series IV: Earth and Environmental Sciences
2002, v. 9, p. 71-85.

Abstract

The central and western part of the Sea of Marmara consists of two deep pull-apart-basins and an intermediate push-up structure. The bathymetric high between the Tekirdağ and the Central Marmara Basin is cut by a deep E-W-trending furrow, which is the eastern branch of the Ganos Fault, which in turn is part of the active North Anatolian Fracture Zone. This area was mapped during the Meteor cruise M44/1 in February 1999. During the cruise, seafloor observations and sediment coring within this prominent furrow structure have shown that methane is emanating at several sites into the water column and that the sediments are also methane-enriched in their deeper parts. Within the porewater regime of hemipelagic clay sediments, the typical process of bacterially mediated anoxic methane oxidation is taking place. The resulting geochemical profiles indicate a reaction-zone in a depth of several meters, where methane is oxidized to H_2 and CO_2; the H_2 reduces the sulfate that finally is converted to H_2S. This H_2S forms iron-sulfide precipitates in the presence of reduced iron. However, our geochemical concentration profiles are not typical for steady-state conditions, but are rather characterized by a very steep drop in sulfate-concentrations just above the reaction zone. We suggest that this specific gradient is caused by a situation that is superimposed by an advective upward-migragtion of a methane-enriched fluid. This advective fluid flow is controlled by the tectonic strain of the Ganos Fault system.

Appendix 2: Marine tephra from the Cape Riva eruption (22 ka) of Santorini in the Sea of Marmara

Sabine Wulf[1] , Michael Kraml[2], Thomas Kuhn[3], Michael Schwarz[2], Maik Inthorn[4], Jörg Keller[2], Ismail Kuşçu[5], Peter Halbach[4]

[1] *GeoForschungsZentrum Potsdam, PB 3.3 - Sedimentation and Basin Analysis, Telegrafenberg, D-14473 Potsdam, Germany*

[2] *Institute of Mineralogy, Petrology and Geochemistry, Albert-Ludwigs-University Freiburg, Albertstrasse 23b, D-79104 Freiburg i.Br., Germany*

[3] *Freiberg University of Mining and Technology, Department of Economic Geology and Leibniz-Laboratory for Applied Marine Research, Brennhausgasse 14, D-09596 Freiberg, Germany*

[4] *Institute of Geology, Free University of Berlin, Malteserstr. 74-100, D-12249 Berlin, Germany*

[5] *Marine Geology and Geophysics, MTA, 06520 Ankara, Turkey*

Marine Geology, 2002, v. 183, p. 131-141.

Abstract

A discrete tephra layer has been discovered in three marine sediment cores from the Sea of Marmara, eastern Mediterranean. The rhyodacitic glass chemistry and the stratigraphical position suggest a Santorini provenance and, in particular, a correlation with the marine Y-2 tephra that is known from the southern Aegean Sea and eastern Levantine Basin. This tephra represents the distal facies of the Cape Riva eruption of Santorini, which has been dated by ^{14}C on land at 21 950 cal. yr BP. Hitherto, the Y-2 tephra has been detected only in marine sediment cores recovered south to southeast of its volcanic source. The new occurrence in the Sea of Marmara approximately 530 km NNE of the Santorini eruptive centre suggests a more north-easterly dispersal of fallout products of the Cape Riva eruption than previously supposed.

Appendix 3: Water column particle data

Table. A3.1. Suspended particulate matter (SPM), particulate organic carbon (POC) and C/N-ratio of particle samples, received during cruise M57/2 with RV *Meteor* in February/March 2003. Methods are according to chapter 4.4. n/d: no data.

station	latitude [°S]	longitude [°E]	water depth [m]	sample depth [m]	SPM [mg l^{-1}]	POC [µg l^{-1}]	C/N
GeoB 8418	24.36	13.14	980	5	1.31	224	9.9
				25	0.63	95	7.2
				50	0.40	61	7.4
				75	0.60	28	8.0
				100	0.32	21	9.2
				298	0.78	25	9.6
				497	0.54	14	8.3
				794	0.40	23	8.8
				922	0.54	18	9.7
				961	1.48	21	8.8
				974	0.48	61	10.1
				978	1.00	33	12.5
GeoB 8419	24.35	13.22	817	5	0.90	332	11.1
				25	0.36	86	8.0
				798	0.51	36	11.7
				811	0.52	40	14.4
				816	0.39	45	15.2
GeoB 8421	24.39	13.06	1187	10	0.52	134	8.7
				30	0.49	160	9.7
				60	0.21	32	8.2
				100	0.43	25	8.9
				149	0.16	23	10.9
				199	0.34	43	8.6
				298	0.65	15	9.6
				397	0.19	21	10.3
				596	0.12	23	11.1
				794	0.19	20	11.4
				1179	0.21	34	11.7
GeoB 8422	24.46	12.72	1959	10	0.91	73	9.0
				30	0.96	123	7.7
				60	0.84	91	10.5
				100	0.30	46	8.4
				199	0.17	35	8.4
				398	0.16	28	9.8
				794	0.21	21	11.0
				1189	0.20	28	9.7
				1584	0.17	14	10.4
				1934	0.33	23	10.9
				1947	0.30	30	12.5
				1957	0.37	23	10.6
GeoB 8424	24.42	12.92	1500	10	1.82	281	10.6
				30	1.42	331	9.4
				60	0.28	64	7.2
				100	0.22	46	8.8
				199	0.21	27	9.6
				397	0.25	32	8.3

station	latitude [°S]	longitude [°E]	water depth [m]	sample depth [m]	SPM [mg l^{-1}]	POC [µg l^{-1}]	C/N
GeoB 8424	24.42	12.92	1500	596	0.23	42	7.6
				794	0.23	32	7.9
				1189	0.50	61	7.9
				1478	0.53	70	8.5
				1491	0.47	59	8.7
GeoB 8440	23.00	13.31	355	5	0.75	94	6.7
				10	0.66	101	6.9
				30	0.92	87	5.6
				50	0.46	51	6.1
				70	0.37	46	5.6
				100	0.29	22	6.8
				149	0.35	24	6.1
				199	0.37	25	5.8
				249	0.23	19	6.1
				298	0.36	40	6.1
				356	1.31	83	7.5
GeoB 8442	23.00	12.95	590	10	0.86	118	5.9
				30	1.20	133	5.7
				50	0.47	62	6.1
				70	0.32	28	5.5
				100	0.32	27	5.8
				149	0.34	34	6.9
				199	0.25	23	6.8
GeoB 8419	24.35	13.22	817	50	n/d	28	8.9
				100	n/d	18	9.2
				298	0.19	29	10.2
				397	0.19	15	10.7
				596	0.18	23	11.8
GeoB 8442	23.00	12.95	590	298	0.33	29	5.4
				398	0.32	32	5.4
				497	0.50	25	5.3
				589	0.55	35	6.8
GeoB 8443	23.00	12.78	940	10	0.55	77	6.3
				30	0.67	79	5.7
				50	0.89	112	6.0
				70	0.46	39	5.2
				100	0.38	35	5.5
				149	0.43	25	6.7
				199	0.53	27	5.7
				298	0.26	26	5.4
				397	0.39	33	6.2
				596	0.34	25	5.8
				794	0.28	32	4.7
				935	0.48	36	5.1
GeoB 8444	23.00	12.58	1420	10	0.60	89	6.3
				30	0.33	54	6.2
				60	0.38	38	6.9
				100	0.39	35	6.5
				149	0.30	40	6.4
				199	0.26	27	6.3
				298	0.31	32	5.9
				398	0.30	27	6.8
				596	0.39	20	7.0
				794	0.29	12	7.8

station	latitude [°S]	longitude [°E]	water depth [m]	sample depth [m]	SPM [mg l^{-1}]	POC [µg l^{-1}]	C/N
GeoB 8444	23.00	12.58	1420	993	0.28	23	6.5
GeoB 8445	23.00	12.33	2080	10	0.45	66	7.5
				30	0.81	120	5.9
				70	0.22	17	8.2
				120	0.30	27	7.7
				199	0.39	20	8.4
				298	0.58	26	9.2
				398	0.45	17	8.5
				596	0.51	21	9.2
				794	0.46	17	9.9
				1189	0.43	13	10.1
				1584	0.41	20	9.8
				2067	0.77	16	10.4
GeoB 8446	23.00	12.00	2715	10	0.62	68	7.2
				30	0.40	66	6.4
				70	0.28	26	8.7
				120	0.35	19	8.7
				199	0.35	17	8.6
				298	0.31	17	10.8
				397	0.27	11	11.4
				794	0.26	13	9.3
				1189	0.31	15	10.4
				1584	0.33	14	9.5
				1978	0.36	11	11.8
				2693	0.69	18	11.7
GeoB 8448	25.47	13.45	795	10	0.56	105	7.3
				50	0.30	45	7.7
				70	0.37	34	6.8
				100	0.30	34	7.4
				179	0.34	47	7.2
				298	0.43	23	9.1
				397	0.38	20	7.7
				596	n/d	23	9.0
				773	0.51	40	10.7
				787	0.47	39	10.2
				791	0.57	45	9.2
GeoB 8456	25.48	13.54	620	10	2.43	791	8.6
				30	1.08	223	7.5
				50	0.81	130	6.8
				70	0.39	68	6.9
				100	0.33	45	7.1
				199	0.45	97	8.3
				298	0.41	63	7.1
				397	n/d	59	8.1
				497	0.71	33	8.6
				601	0.51	53	8.1
				615	0.55	43	6.2
				619	0.58	79	8.0
GeoB 8457	25.43	13.69	383	10	1.94	233	6.5
				30	1.02	188	6.7
				50	0.47	95	6.8
				70	0.30	57	7.3
				100	0.31	57	7.8
				149	0.29	53	7.7

station	latitude [°S]	longitude [°E]	water depth [m]	sample depth [m]	SPM [mg l^{-1}]	POC [µg l^{-1}]	C/N
GeoB 8457	25.43	13.69	383	199		55	6.7
				249	0.42	67	7.3
				231	0.41	62	8.8
				298	0.58	78	8.6
				384	0.49	64	7.5
				376	0.51	89	8.3
GeoB 8458	25.48	13.61	493	10	0.82	206	7.6
				30	0.87	185	6.2
				50	0.55	123	6.3
				70	0.64	165	6.3
				100	0.46	98	6.5
				149	0.57	68	8.1
				199	0.38	59	6.8
				298	0.58	144	7.6
				397	0.37	63	6.5
				475	0.58	113	6.9
				490	0.62	102	6.7
				494	0.74	152	7.8
GeoB 8462	25.53	12.94	2261	10	0.84	157	9.4
				30	0.97	238	6.8
				70	0.36	40	8.5
				120	0.45	68	8.4
				199	0.33	57	7.5
				397	0.37	72	8.7
				794	0.26	39	9.1
				1189	0.34	63	7.6
				1584	0.38	64	8.3
				2243	0.57	41	10.7
				2255	0.55	62	13.7
				2258	0.49	64	6.8
GeoB 8464	26.34	13.70	425	10	2.55	87	12.0
				30	1.35	54	7.7
				50	n/d	51	6.9
				70	1.04	40	6.9
				100	1.15	44	7.0
				149	1.11	42	7.3
				199	1.19	44	7.6
				248	0.27	48	6.7
				298	0.22	63	8.1
				403	0.48	77	9.6
				419	0.64	83	10.1
				422	1.17	129	7.8
GeoB 8465	26.75	13.43	1329	30	0.41	47	9.1
				60	0.60	49	12.0
				100	0.28	44	7.5
				149	0.17	15	9.1
				199	0.27	19	10.4
				298	0.21	23	9.3
				397	0.25	26	10.0
				595	0.18	14	10.8
				794	0.17	13	15.0
				991	0.25	22	14.7
				1333	0.22		
				13	0.26	24	9.3

station	latitude [°S]	longitude [°E]	water depth [m]	sample depth [m]	SPM [mg l^{-1}]	POC [µg l^{-1}]	C/N
GeoB 8466	26.73	13.57	935	10	0.80	118	7.9
				30	0.73	80	8.8
				60	0.79	60	13.8
				100	0.32	46	10.0
				149	0.23	36	9.0
				199	0.44	58	8.1
				298	0.48	82	8.2
				397	0.38	37	11.2
				794	0.38	49	8.7
				905	0.67	79	17.4
				923	0.73	113	9.2
GeoB 8489	25.51	13.18	1484	10	1.31	446	11.9
				30	1.09	369	8.9
				60	0.32	79	6.9
				100	n/d	44	7.2
				149	n/d	50	7.2
				199	0.31	60	7.2
				397	0.25	41	8.8
				596	0.24	45	8.6
				794	0.31	45	12.3
				1090	0.26	46	8.4
				1492	0.54	n/d	n/d
GeoB 8490	25.48	13.36	1011	10	1.11	291	8.2
				30	1.25	255	7.8
				60	0.87	183	6.9
				100	0.55	157	10.0
				199	0.36	63	7.7
				298	0.34	61	8.4
				397	0.49	98	9.6
				596	0.41	65	9.0
				794	0.50	147	19.1
				991	0.41	66	8.9
				1005	0.55	104	7.4
				1009	0.75	142	9.5
GeoB 8491	25.47	13.55	591	10	0.79	135	6.9
				30	0.78	158	6.7
				50	0.61	131	6.2
				70	0.59	67	7.1
				100	0.40	119	10.3
				149	0.40	93	8.4
				199	0.37	60	8.7
				298	0.50	95	8.0
				397	0.45	105	12.7
				576	0.63	91	9.3
				589	0.91	128	8.4
				594	0.99	120	8.6

Table. A3.2. Suspended particulate matter (SPM), particulate organic carbon (POC) and C/N-ratio of particle samples, received during cruise AHAB1 with RV *A. v. Humboldt* in January 2004. Methods are according to chapter 4.4. n/d: no data.

station	latitude [°S]	longitude [°E]	water depth [m]	sample depth [m]	SPM [mg l^{-1}]	POC [µg l^{-1}]	C/N
WW23020-1	22.97	14.05	130	2	2.44	482	6.7
				10	2.24	448	6.9
				20	2.00	271	7.7
				30	1.13	183	7.7
				40	0.88	83	8.1
				60	0.51	63	7.9
				70	0.60	107	7.1
				80	0.42	55	8.3
				90	0.54	75	10.9
				100	0.46	68	8.5
				110	1.22	70	7.9
				120	0.56	101	8.4
				125	1.24	113	6.8
WW23100	23.00	12.58	1423	4	0.39	87	7.6
				9	0.38	91	7.4
				19	0.56	63	7.5
				29	0.59	72	7.6
				49	1.06	135	7.1
				75	0.69	63	10.4
				399	0.24	33	9.1
				800	n/d	17	7.2
				1299	0.42	40	8.5
				1380	0.34	29	11.6
				1419	0.41	18	10.7
WW23090-1	23.00	12.78	938	6	0.55	63	7.4
				10	0.52	78	8.6
				18	0.66	79	7.3
				30	0.72	85	9.0
				50	0.83	73	8.3
				99	0.23	39	8.3
				149	n/d	42	7.7
				198	0.21	50	9.2
				298	1.42	48	9.9
				398	0.24	75	9.9
				600	0.18	16	8.0
				837	0.45	34	9.4
				918	0.94	113	11.1
				935	0.42	27	10.3
WW23080-1	23.00	12.95	596	4	0.61	104	6.4
				10	0.77	109	7.3
				19	0.87	120	7.1
				29	0.81	121	6.8
				50	0.77	39	7.4
				74	0.13	65	10.4
				98	0.35	17	7.6
				149	0.01	30	9.6
				199	0.22	48	10.0
				299	0.22	35	9.4

station	latitude [°S]	longitude [°E]	water depth [m]	sample depth [m]	SPM [mg l^{-1}]	POC [µg l^{-1}]	C/N
WW23080-1	23.00	12.95	596	400	0.30	25	7.9
				495	0.74	42	8.6
				570	0.30	37	12.4
				597	0.35	26	9.2
WW23005-1	23.00	14.32	74	10	1.30	224	7.7
				39	2.00	351	6.8
				70	0.72	92	7.6
WW24030-1	23.99	13.90	231	9	1.84	279	6.9
				40	0.37	87	7.0
				99	0.18	52	8.0
				150	0.33	33	10.0
				210	0.30	46	10.5
				228	0.41	41	8.9
WW24040-1	24.00	13.72	256	10	1.31	287	7.5
				49	0.21	48	8.0
				99	0.28	42	8.2
				149	0.26	33	10.1
				200	0.21	26	10.5
				253	0.40	42	8.8
WW24080	24.00	13.00	1031	10	1.37	230	6.1
				50	0.46	58	9.0
				99	0.48	30	7.2
				198	0.23	22	10.9
				398	0.25	21	11.3
				600	0.20	22	10.3
				898	0.40	32	7.3
				1000	0.09	24	11.8
				1028	0.16	21	10.3
WW24070	23.99	13.17	589	5	1.27	144	7.2
				99	0.25	26	8.3
				299	0.44	27	8.0
				399	0.17	13	11.5
				500	0.17	20	12.2
				548	0.50	31	10.2
				582	0.41	23	9.4
WW25080	25.00	13.38	966	9	0.94	160	7.5
				48	0.43	91	6.5
				100	0.42	52	6.8
				200	0.16	24	9.8
				299	0.21	25	9.3
				400	-0.24	26	9.7
				598	0.43	19	9.7
				699	0.19	16	15.7
				850	0.31	24	10.6
				940	0.27	25	13.0
				974	0.44	44	9.5
WW25060	25.00	13.74	305	9	0.91	148	7.1
				50	0.57	70	7.3
				99	0.40	50	7.4
				149	0.34	36	8.4
				199	0.30	50	8.4
				279	0.41	65	6.5
				307	1.09	143	7.7
WW25050	25.00	13.92	184	178	2.56	256	8.1

station	latitude [°S]	longitude [°E]	water depth [m]	sample depth [m]	SPM [mg l^{-1}]	POC [µg l^{-1}]	C/N
WW25050	25.00	13.92	184	149	1.06	160	7.6
				100	0.43	55	7.1
				50	0.34	47	6.4
				10	0.66	150	7.4
WW25040	25.00	14.10	174	10	2.82	574	7.3
				40	1.08	192	6.9
				100	0.92	93	7.2
				160	0.74	103	7.0
				171	0.73	102	7.0
WW25020	25.00	14.47	119	10	2.76	447	5.6
				50	2.04	415	5.8
				70	1.15	177	6.8
				99	1.01	129	5.8
				112	0.91	137	5.9
WW25005	25.00	14.73	55	10	5.61	1207	7.2
				50	1.58	253	6.7
				51	1.60	251	7.0
WW25002	25.00	14.80	29	10	2.60	453	9.6
				28	1.84	225	7.0
RCOM 2506	25.47	13.53	646	10	0.66	93	7.2
				49	0.34	66	7.0
				100	0.19	23	6.6
				150	0.23	27	8.6
				199	0.25	36	8.3
				250	0.30	38	7.5
				298	0.21	22	7.8
				400	0.21	23	10.3
				499	0.27	26	8.9
				620	0.28	30	10.1
				645	0.43	50	8.6
RCOM 2503	25.62	13.27	1363	10	0.76	104	6.9
				50	0.43	56	6.9
				99	0.31	36	7.0
				150	0.24	21	9.5
				249	0.22	21	9.1
				500	0.36	13	7.5
				798	0.16	9	15.5
				1259	0.24	18	10.3
				1340	0.31	33	11.7
				1358	0.28	23	9.5
WW26080	26.00	13.48	847	9	0.54	130	6.4
				50	0.31	33	7.0
				99	0.29	33	8.1
				149	0.23	27	8.5
				200	0.20	28	8.6
				299	0.22	15	7.8
				499	0.27	21	8.0
				750	0.20	21	9.1
				824	0.37	36	10.7
				849	0.57	53	9.4
WW26070	26.00	13.67	505	10	0.92	155	6.3
				49	0.41	72	6.9
				99	0.25	21	7.7
				149	0.27	46	7.1

station	latitude [°S]	longitude [°E]	water depth [m]	sample depth [m]	SPM [mg l^{-1}]	POC [µg l^{-1}]	C/N
WW26070	26.00	13.67	505	199	0.24	22	8.4
				299	0.12	15	6.6
				399	0.15	21	8.6
				479	0.44	72	8.1
				502	0.47	56	9.0
WW26060	26.00	13.85	374	10	1.32	239	6.5
				50	0.44	69	6.7
				99	0.29	36	7.1
				149	0.32	42	7.8
				200	0.32	29	8.0
				298	0.30	31	7.9
				350	0.78	85	9.5
				374	0.90	113	10.5
WW26040	26.00	14.22	259	9	1.46	278	6.0
				50	0.84	142	5.8
				149	0.35	29	6.5
				200	0.47	71	6.4
				257	0.87	138	8.6
WW26030	26.00	14.40	199	10	1.81	349	6.1
				59	0.51	76	6.7
				100	0.39	45	7.0
				140	0.42	47	7.5
				159	0.52	44	6.9
				180	0.46	52	7.6
				196	0.81	74	7.8
WW26010	26.00	14.77	118	10	3.28	722	5.8
				59	0.88	126	7.7
				90	0.58	75	6.3
				100	0.59	55	6.5
				110	0.71	56	6.6
				115	0.62	53	6.9
WW27005	26.99	15.10	120	10	0.92	121	5.8
				40	1.04	155	5.7
				100	0.56	80	6.2
				110	1.07	121	6.1
				118	1.21	154	6.0
WW27010	27.00	15.00	146	10	1.28	156	5.6
				40	0.45	75	6.1
				100	0.44	53	6.2
				120	1.31	189	6.6
				144	2.20	248	7.4
WW27020	27.00	14.81	208	10	0.81	142	5.6
				60	0.20	16	7.0
				100	0.23	15	7.9
				160	0.27	20	6.5
				180	0.29	30	7.2
				205	0.99	102	7.9
WW27030	26.98	14.60	283	10	0.69	137	6.0
				49	0.24	24	6.8
				100	0.23	22	8.0
				149	0.23	15	9.0
				199	0.24	14	6.9
				250	0.24	21	9.4
				279	1.02	107	9.8

station	latitude [°S]	longitude [°E]	water depth [m]	sample depth [m]	SPM [mg l^{-1}]	POC [µg l^{-1}]	C/N
WW27040	27.00	14.45	338	10	0.52	75	6.2
				49	0.24	18	7.8
				100	0.35	52	6.4
				199	0.23	27	7.5
				250	0.25	10	7.1
				314	0.36	39	8.9
				335	0.46	50	8.6
WW27050	26.99	14.26	382	10	0.63	62	6.4
				50	0.27	47	8.5
				99	0.55	13	5.0
				149	0.18	8	4.0
				200	0.26	11	5.1
				249	0.19	14	5.8
				298	0.35	17	6.6
				359	0.32	31	8.4
				380	0.65	69	10.2
WW24005-1	24.00	14.35	85	10	2.53	452	6.2
				40	0.47	79	6.6
				69	0.55	75	6.6
				80	0.39	95	6.6
				83	0.78	124	6.7
WW24010	24.00	14.25	118	9	3.30	666	6.5
				48	0.31	126	6.9
				88	0.40	74	6.4
				99	0.52	87	6.2
				115	0.86	161	6.9
WW24020-1	24.00	14.06	183	10	1.48	344	6.7
				50	0.59	70	8.1
				100	0.30	43	7.7
				159	0.27	31	6.9
				170	0.39	75	9.3
				178	0.46	54	6.6
WW24030-2	24.00	13.90	232	9	0.71	139	5.6
				49	0.44	75	5.8
				98	0.70	30	7.5
				198	0.38	33	7.2
				209	0.35	91	5.8
				226	0.56	56	7.3
				200	0.27	30	7.8
				10	0.71	142	6.2
				50	0.36	72	8.2
				99	0.31	37	7.4
				149	1.68	29	6.9
				252	0.30	32	7.9
AH0007	23.67	14.30	104	10	1.80	791	6.5
				49	1.08	195	7.8
				80	0.70	90	6.7
				89	0.71	103	6.6
				100	2.37	207	6.9
AH0008	23.33	14.28	99	10	3.26	659	6.3
				50	0.45	98	7.4
				79	0.47	50	6.4
				90	0.40	60	7.2
				95	0.60	133	7.0

station	latitude [°S]	longitude [°E]	water depth [m]	sample depth [m]	SPM [mg l^{-1}]	POC [µg l^{-1}]	C/N
WW23010	23.00	14.22	110	9	3.58	720	7.0
				49	0.76	75	6.8
				90	0.37	54	6.8
				99	0.52	58	6.8
				106	0.50	72	7.0
WW23002	23.00	14.37	43	10	2.73	427	7.1
				41	3.15	322	7.6
WW23005-2	23.00	14.32	73	9	2.30	398	6.2
				39	0.73	91	6.5
				58	0.92	111	6.7
				70	1.72	238	7.1
WW23020-2	23.00	14.05	131	9	2.41	457	6.1
				59	0.47	49	6.9
				98	0.51	23	6.5
				119	0.15	32	7.9
				127	0.35	38	6.2
WW23030-1	23.00	13.87	146	10	0.92	224	7.0
				40	0.40	51	7.4
				130	0.26	49	7.9
				140	0.27	38	7.9
				143	2.76	70	6.5
AH0009	22.67	14.17	102	10	1.93	555	7.2
				50	0.27	41	7.7
				80	0.34	52	7.2
				90	0.33	49	7.3
				98	1.08	310	7.2
WW24060	24.00	13.34	309	10	0.59	65	6.2
				49	0.35	36	7.2
				100	0.28	22	7.2
				150	0.35	19	7.0
				250	0.27	29	7.5
				280	0.37	45	9.8
				306	0.58	93	13.2
RCOM 2403	24.36	13.13	1003	10	0.66	75	6.0
				50	0.13	28	6.5
				99	0.31	29	6.9
				150	0.16	21	7.5
				198	0.30	21	6.4
				299	0.27	20	7.7
				399	0.27	17	6.6
				599	0.17	9	7.7
				800	0.33	18	6.9
				979	0.30	25	8.3
				1009	0.31	21	8.3
RCOM 2507	25.57	13.01	2103	10	0.60	72	6.1
				49	0.57	84	6.3
				100	0.42	40	6.9
				149	0.27	40	8.3
				100	0.42	40	6.9
				149	0.27	40	8.3
				100	0.42	40	6.9
				149	0.27	40	8.3
				200	0.31	29	7.0
				399	0.25	25	7.7

station	latitude [°S]	longitude [°E]	water depth [m]	sample depth [m]	SPM [mg l^{-1}]	POC [µg l^{-1}]	C/N
RCOM 2507	25.57	13.01	2103	579	0.23	15	7.9
				999	0.19	20	8.3
				1998	0.24	17	7.2
				2080	0.45	21	8.5
				2127	0.70	89	6.1
RCOM 2402	24.41	12.92	1585	9	0.66	158	6.5
				50	0.39	39	6.5
				100	0.25	24	7.2
				150	0.22	12	7.2
				199	0.28	9	7.8
				399	0.31	27	7.4
				600	0.25	37	8.7
				799	0.19	11	9.9
				1099	0.28	21	8.7
				1535	0.31	15	7.6
WW23090-2	23.00	12.78	935	10	0.67	88	6.7
				50	0.38	62	7.0
				100	0.24	24	7.4
				149	0.24	40	7.4
				199	0.24	21	7.1
				299	0.16	23	7.4
				400	0.36	34	5.8
				599	0.23	35	6.7
				799	0.18	35	6.5
				858	0.23	24	8.0
				899	0.35	50	6.7
WW23080-2	23.00	12.95	585	10	0.82	132	6.8
				50	0.32	44	7.0
				100	0.27	40	6.8
				149	6.45	32	7.2
				199	0.24	38	7.4
				299	0.27	24	7.1
				499	0.22	24	7.4
				573	0.28	18	8.3
				581	0.39	35	7.6
WW23070	23.00	13.15	316	10	0.94	186	6.2
				50	0.26	41	7.4
				100	0.26	34	7.4
				150	0.26	28	7.3
				199	0.26	38	7.4
				289	0.47	34	7.5
				314	0.78	62	8.0
WW23060	23.00	13.32	360	10	0.85	189	6.6
				49	0.28	38	7.8
				100	0.26	33	7.2
				149	0.26	28	7.1
				200	0.32	44	7.3
				299	0.19	29	7.0
				340	0.35	46	7.0
				355	1.03	113	9.2
				254	0.34	40	8.1
WW24002	24.00	14.41	60	10	2.63	425	6.2
				55	1.00	134	7.0
WW24005-2	24.00	14.36	84	10	4.01	1029	7.1

station	latitude [°S]	longitude [°E]	water depth [m]	sample depth [m]	SPM [mg l^{-1}]	POC [µg l^{-1}]	C/N
WW24005-2	24.00	14.36	84	50	0.62	66	6.3
				70	0.83	112	6.3
				81	1.03	115	6.3
WW24020-2	23.99	14.07	181	10	0.89	284	6.7
				40	0.47	98	6.7
				60	0.51	96	7.2
				90	0.33	63	9.2
				141	0.47	156	13.2
				177	0.33	50	8.0
WW24050	23.99	13.53	280	10	0.75	76	6.1
				50	0.40	64	5.9
				100	0.30	25	8.0
				150	0.24	25	7.2
				201	0.33	33	10.6
				250	0.36	45	8.4
				260	0.41	34	8.3
				278	0.66	55	8.3
WW23050	23.00	13.50	238	10	1.58	441	6.4
				50	0.40	70	6.7
				110	0.36	108	16.1
				160	0.24	32	9.1
				235	0.32	38	7.9
WW23040	22.99	13.68	152	11	1.46	453	6.6
				50	0.33	69	7.8
				100	0.38	93	12.1
				150	0.38	55	7.7
WW23030-2	23.00	13.87	145	10	1.84	370	6.6
				50	0.33	52	7.2
				143	0.31	57	7.8
WW23020-3	23.00	14.05	133	10	1.57	493	6.8
				60	0.64	93	7.1
				110	0.32	46	8.0
				130	0.60	137	6.4

Danksagung

Für die Vergabe und Betreuung meiner Arbeit, die vielen aufmunternden Worte sowie die Unterstützung in langen Schiffsnächten und bei verknoteten Leinen danke ich PD Dr. Matthias Zabel herzlich.

Prof. Dr. Gerhard Bohrmann danke ich für die spontane Bereitschaft das Zweitgutachten für meine Arbeit zu erstellen und sein Interesse auch an weit entfernten Themen.

Professor Dr. Horst D. Schulz und allen Mitgliedern der Arbeitsgruppe Geochemie bin ich für die angeregten Diskussionen in der Dienstagsrunde und um sie herum sowie für die Bereitstellung der diversen Büro- und Laborarbeitsplätze dankbar.

Das Max Planck Institut Bremen, das Alfred-Wegener-Institut Bremerhaven und das Bundesamt für Geowissenschaften und Rohstoffe ermöglichten mir freundlicherweise die Nutzung verschiedener Laborgeräte, und die Deutsche Forschungsgemeinschaft gewährte die Finanzierung, ohne die diese Arbeit unmöglich gewesen wäre.

Tom Wagner, Michiel Rutgers van der Loeff, Tim Ferdelman, Gesine Mollenhauer, Volker Mohrholz, Toralf Heene, Georg Scheeder, Katherina Seiter, Christian Hensen, Ursula Witte und Gaute Lavik danke ich für die wissenschaftliche Zusammenarbeit und Unterstützung.

Für ihre große Hilfsbereitschaft in den Laboren bin ich Silvana Hessler, Ingrid Voege, Gabi Klockgether, Monica Segl, Nicole Zatloukal, Karsten Enneking, und Susanne Siemer sehr dankbar.

Wie lange hätte diese Doktorarbeit wohl ohne die Hilfe meiner studentischen Hilfskräfte Marlene Bausch, Anna Kathrin Guthmann, Simone Pannike und Bianca Rajes gedauert?

BeaWiS wäre ohne die Hilfe und Hinweise von Jens Langreder, Axel Nordhausen, Christoph Waldmann, Volker Rathmeyer, Stefan Forster, Holger Pielenz, Gregor Rehder, Klaus Dehning sowie den Mitarbeitern der Firma KUM weder entstanden noch zu bändigen gewesen.

Den Kaptitänen und der Besatzung der Forschungsschiffe Meteor, Alexander von Humboldt und Philia gilt mein Dank für die Unterstützung bei der Probenahme auf hoher See.

Amalia Zacher trainierte meine English grammar Kenntnisse – hoffentlich erfolgreich.

Natascha Riedinger und Alexander Mock korrigierten mehr als Tippfehler.

Die Donnerstagsrunde mit Fanni, Natascha, Volker, Tanja, Katherina, Henrik, Urte und Kerstin ermöglichte mir eine weiche Landung im Bremer Sozialleben und war mir zudem ein unersetzlicher Frustableiter und Freudenbereiter. In ähnlichen Funktionen agierten Steffi, Joachim, Lars, Martina, Karen, Solveig, Anna, André, Jutta, Uwe, Astrid, meine Fußballer, Taucher und mein Maiskolben.

Den Nachbarn danke ich für den mehr als vollwertigen Ersatz einer WG und ihre Freundschaft.

Meine Eltern, mein Bruder (!), meine Oma und der Rest meiner Familie waren mir immer der stärkste Rückhalt und Antrieb.

Mein ganz besonderer Dank gilt Kathrin – für ihr Verständnis, Strahlen, Hüpfen und für alles andere.

Publications of this series:

No. 1 **Wefer, G., E. Suess and cruise participants**
Bericht über die POLARSTERN-Fahrt ANT IV/2, Rio de Janeiro - Punta Arenas, 6.11. - 1.12.1985.
60 pages, Bremen, 1986.

No. 2 **Hoffmann, G.**
Holozänstratigraphie und Küstenlinienverlagerung an der andalusischen Mittelmeerküste.
173 pages, Bremen, 1988. (out of print)

No. 3 **Wefer, G. and cruise participants**
Bericht über die METEOR-Fahrt M 6/6, Libreville - Las Palmas, 18.2. - 23.3.1988.
97 pages, Bremen, 1988.

No. 4 **Wefer, G., G.F. Lutze, T.J. Müller, O. Pfannkuche, W. Schenke, G. Siedler, W. Zenk**
Kurzbericht über die METEOR-Expedition No. 6, Hamburg - Hamburg, 28.10.1987 - 19.5.1988.
29 pages, Bremen, 1988. (out of print)

No. 5 **Fischer, G.**
Stabile Kohlenstoff-Isotope in partikulärer organischer Substanz aus dem Südpolarmeer (Atlantischer Sektor). 161 pages, Bremen, 1989.

No. 6 **Berger, W.H. and G. Wefer**
Partikelfluß und Kohlenstoffkreislauf im Ozean.
Bericht und Kurzfassungen über den Workshop vom 3.-4. Juli 1989 in Bremen.
57 pages, Bremen, 1989.

No. 7 **Wefer, G. and cruise participants**
Bericht über die METEOR - Fahrt M 9/4, Dakar - Santa Cruz, 19.2. - 16.3.1989.
103 pages, Bremen, 1989.

No. 8 **Kölling, M.**
Modellierung geochemischer Prozesse im Sickerwasser und Grundwasser.
135 pages, Bremen, 1990.

No. 9 **Heinze, P.-M.**
Das Auftriebsgeschehen vor Peru im Spätquartär. 204 pages, Bremen, 1990. (out of print)

No. 10 **Willems, H., G. Wefer, M. Rinski, B. Donner, H.-J. Bellmann, L. Eißmann, A. Müller, B.W. Flemming, H.-C. Höfle, J. Merkt, H. Streif, G. Hertweck, H. Kuntze, J. Schwaar, W. Schäfer, M.-G. Schulz, F. Grube, B. Menke**
Beiträge zur Geologie und Paläontologie Norddeutschlands: Exkursionsführer.
202 pages, Bremen, 1990.

No. 11 **Wefer, G. and cruise participants**
Bericht über die METEOR-Fahrt M 12/1, Kapstadt - Funchal, 13.3.1990 - 14.4.1990.
66 pages, Bremen, 1990.

No. 12 **Dahmke, A., H.D. Schulz, A. Kölling, F. Kracht, A. Lücke**
Schwermetallspuren und geochemische Gleichgewichte zwischen Porenlösung und Sediment im Wesermündungsgebiet. BMFT-Projekt MFU 0562, Abschlußbericht. 121 pages, Bremen, 1991.

No. 13 **Rostek, F.**
Physikalische Strukturen von Tiefseesedimenten des Südatlantiks und ihre Erfassung in Echolotregistrierungen. 209 pages, Bremen, 1991.

No. 14 **Baumann, M.**
Die Ablagerung von Tschernobyl-Radiocäsium in der Norwegischen See und in der Nordsee.
133 pages, Bremen, 1991. (out of print)

No. 15 **Kölling, A.**
Frühdiagenetische Prozesse und Stoff-Flüsse in marinen und ästuarinen Sedimenten.
140 pages, Bremen, 1991.

No. 16 **SFB 261 (ed.)**
1. Kolloquium des Sonderforschungsbereichs 261 der Universität Bremen (14.Juni 1991):
Der Südatlantik im Spätquartär: Rekonstruktion von Stoffhaushalt und Stromsystemen.
Kurzfassungen der Vorträge und Poster. 66 pages, Bremen, 1991.

No. 17 **Pätzold, J. and cruise participants**
Bericht und erste Ergebnisse über die METEOR-Fahrt M 15/2, Rio de Janeiro - Vitoria,
18.1. - 7.2.1991. 46 pages, Bremen, 1993.

No. 18 **Wefer, G. and cruise participants**
Bericht und erste Ergebnisse über die METEOR-Fahrt M 16/1, Pointe Noire - Recife,
27.3. - 25.4.1991. 120 pages, Bremen, 1991.

No. 19 **Schulz, H.D. and cruise participants**
Bericht und erste Ergebnisse über die METEOR-Fahrt M 16/2, Recife - Belem, 28.4. - 20.5.1991.
149 pages, Bremen, 1991.

No. 20 **Berner, H.**
Mechanismen der Sedimentbildung in der Fram-Straße, im Arktischen Ozean und in der Norwegischen See. 167 pages, Bremen, 1991.

No. 21 **Schneider, R.**
Spätquartäre Produktivitätsänderungen im östlichen Angola-Becken: Reaktion auf Variationen im Passat-Monsun-Windsystem und in der Advektion des Benguela-Küstenstroms.
198 pages, Bremen, 1991. (out of print)

No. 22 **Hebbeln, D.**
Spätquartäre Stratigraphie und Paläozeanographie in der Fram-Straße. 174 pages, Bremen, 1991.

No. 23 **Lücke, A.**
Umsetzungsprozesse organischer Substanz während der Frühdiagenese in ästuarinen Sedimenten.
137 pages, Bremen, 1991.

No. 24 **Wefer, G. and cruise participants**
Bericht und erste Ergebnisse der METEOR-Fahrt M 20/1, Bremen - Abidjan, 18.11.- 22.12.1991.
74 pages, Bremen, 1992.

No. 25 **Schulz, H.D. and cruise participants**
Bericht und erste Ergebnisse der METEOR-Fahrt M 20/2, Abidjan - Dakar, 27.12.1991 - 3.2.1992.
173 pages, Bremen, 1992.

No. 26 **Gingele, F.**
Zur klimaabhängigen Bildung biogener und terrigener Sedimente und ihrer Veränderung durch die Frühdiagenese im zentralen und östlichen Südatlantik. 202 pages, Bremen, 1992.

No. 27 **Bickert, T.**
Rekonstruktion der spätquartären Bodenwasserzirkulation im östlichen Südatlantik über stabile Isotope benthischer Foraminiferen. 205 pages, Bremen, 1992. (out of print)

No. 28 **Schmidt, H.**
Der Benguela-Strom im Bereich des Walfisch-Rückens im Spätquartär. 172 pages, Bremen, 1992.

No. 29 **Meinecke, G.**
Spätquartäre Oberflächenwassertemperaturen im östlichen äquatorialen Atlantik.
181 pages, Bremen, 1992.

No. 30 **Bathmann, U., U. Bleil, A. Dahmke, P. Müller, A. Nehrkorn, E.-M. Nöthig, M. Olesch, J. Pätzold, H.D. Schulz, V. Smetacek, V. Spieß, G. Wefer, H. Willems**
Bericht des Graduierten Kollegs. Stoff-Flüsse in marinen Geosystemen.
Berichtszeitraum Oktober 1990 - Dezember 1992. 396 pages, Bremen, 1992.

No. 31 **Damm, E.**
Frühdiagenetische Verteilung von Schwermetallen in Schlicksedimenten der westlichen Ostsee.
115 pages, Bremen, 1992.

No. 32 **Antia, E.E.**
Sedimentology, Morphodynamics and Facies Association of a mesotidal Barrier Island Shoreface (Spiekeroog, Southern North Sea). 370 pages, Bremen, 1993.

No. 33 **Duinker, J. and G. Wefer (ed.)**
Bericht über den 1. JGOFS-Workshop. 1./2. Dezember 1992 in Bremen. 83 pages, Bremen, 1993.

No. 34 **Kasten, S.**
Die Verteilung von Schwermetallen in den Sedimenten eines stadtbremischen Hafenbeckens.
103 pages, Bremen, 1993.

No. 35 **Spieß, V.**
Digitale Sedimentographie. Neue Wege zu einer hochauflösenden Akustostratigraphie.
199 pages, Bremen, 1993.

No. 36 **Schinzel, U.**
Laborversuche zu frühdiagenetischen Reaktionen von Eisen (III) - Oxidhydraten in marinen Sedimenten.189 pages, Bremen, 1993.

No. 37 **Sieger, R.**
CoTAM - ein Modell zur Modellierung des Schwermetalltransports in Grundwasserleitern.
56 pages, Bremen, 1993. (out of print)

No. 38 **Willems, H. (ed.)**
Geoscientific Investigations in the Tethyan Himalayas. 183 pages, Bremen, 1993.

No. 39 **Hamer, K.**
Entwicklung von Laborversuchen als Grundlage für die Modellierung des Transportverhaltens von Arsenat, Blei, Cadmium und Kupfer in wassergesättigten Säulen. 147 pages, Bremen, 1993.

No. 40 **Sieger, R.**
Modellierung des Stofftransports in porösen Medien unter Ankopplung kinetisch gesteuerter Sorptions- und Redoxprozesse sowie thermischer Gleichgewichte. 158 pages, Bremen, 1993.

No. 41 **Thießen, W.**
Magnetische Eigenschaften von Sedimenten des östlichen Südatlantiks und ihre paläozeanographische Relevanz. 170 pages, Bremen, 1993.

No. 42 **Spieß, V. and cruise participants**
Report and preliminary results of METEOR-Cruise M 23/1, Kapstadt - Rio de Janeiro, 4.-25.2.1993. 139 pages, Bremen, 1994.

No. 43 **Bleil, U. and cruise participants**
Report and preliminary results of METEOR-Cruise M 23/2, Rio de Janeiro - Recife, 27.2.-19.3.1993 133 pages, Bremen, 1994.

No. 44 **Wefer, G. and cruise participants**
Report and preliminary results of METEOR-Cruise M 23/3, Recife - Las Palmas, 21.3. - 12.4.1993 71 pages, Bremen, 1994.

No. 45 **Giese, M. and G. Wefer (ed.)**
Bericht über den 2. JGOFS-Workshop. 18../19. November 1993 in Bremen. 93 pages, Bremen, 1994.

No. 46 **Balzer, W. and cruise participants**
Report and preliminary results of METEOR-Cruise M 22/1, Hamburg - Recife, 22.9. - 21.10.1992. 24 pages, Bremen, 1994.

No. 47 **Stax, R.**
Zyklische Sedimentation von organischem Kohlenstoff in der Japan See: Anzeiger für Änderungen von Paläoozeanographie und Paläoklima im Spätkänozoikum. 150 pages, Bremen, 1994.

No. 48 **Skowronek, F.**
Frühdiagenetische Stoff-Flüsse gelöster Schwermetalle an der Oberfläche von Sedimenten des Weser Ästuares. 107 pages, Bremen, 1994.

No. 49 **Dersch-Hansmann, M.**
Zur Klimaentwicklung in Ostasien während der letzten 5 Millionen Jahre: Terrigener Sedimenteintrag in die Japan See (ODP Ausfahrt 128). 149 pages, Bremen, 1994.

No. 50 **Zabel, M.**
Frühdiagenetische Stoff-Flüsse in Oberflächen-Sedimenten des äquatorialen und östlichen Südatlantik. 129 pages, Bremen, 1994.

No. 51 **Bleil, U. and cruise participants**
Report and preliminary results of SONNE-Cruise SO 86, Buenos Aires - Capetown, 22.4. - 31.5.93 116 pages, Bremen, 1994.

No. 52 **Symposium: The South Atlantic: Present and Past Circulation.**
Bremen, Germany, 15 - 19 August 1994. Abstracts. 167 pages, Bremen, 1994.

No. 53 **Kretzmann, U.B.**
^{57}Fe-Mössbauer-Spektroskopie an Sedimenten - Möglichkeiten und Grenzen. 183 pages, Bremen, 1994.

No. 54 **Bachmann, M.**
Die Karbonatrampe von Organyà im oberen Oberapt und unteren Unteralb (NE-Spanien, Prov. Lerida): Fazies, Zyklo- und Sequenzstratigraphie. 147 pages, Bremen, 1994. (out of print)

No. 55 **Kemle-von Mücke, S.**
Oberflächenwasserstruktur und -zirkulation des Südostatlantiks im Spätquartär. 151 pages, Bremen, 1994.

No. 56 **Petermann, H.**
Magnetotaktische Bakterien und ihre Magnetosome in Oberflächensedimenten des Südatlantiks. 134 pages, Bremen, 1994.

No. 57 **Mulitza, S.**
Spätquartäre Variationen der oberflächennahen Hydrographie im westlichen äquatorialen Atlantik. 97 pages, Bremen, 1994.

No. 58 **Segl, M. and cruise participants**
Report and preliminary results of METEOR-Cruise M 29/1, Buenos-Aires - Montevideo, 17.6. - 13.7.1994
94 pages, Bremen, 1994.

No. 59 **Bleil, U. and cruise participants**
Report and preliminary results of METEOR-Cruise M 29/2, Montevideo - Rio de Janiero 15.7. - 8.8.1994. 153 pages, Bremen, 1994.

No. 60 **Henrich, R. and cruise participants**
Report and preliminary results of METEOR-Cruise M 29/3, Rio de Janeiro - Las Palmas 11.8. - 5.9.1994. Bremen, 1994. (out of print)

No. 61 **Sagemann, J.**
Saisonale Variationen von Porenwasserprofilen, Nährstoff-Flüssen und Reaktionen in intertidalen Sedimenten des Weser-Ästuars. 110 pages, Bremen, 1994. (out of print)

No. 62 **Giese, M. and G. Wefer**
Bericht über den 3. JGOFS-Workshop. 5./6. Dezember 1994 in Bremen.
84 pages, Bremen, 1995.

No. 63 **Mann, U.**
Genese kretazischer Schwarzschiefer in Kolumbien: Globale vs. regionale/lokale Prozesse.
153 pages, Bremen, 1995. (out of print)

No. 64 **Willems, H., Wan X., Yin J., Dongdui L., Liu G., S. Dürr, K.-U. Gräfe**
The Mesozoic development of the N-Indian passive margin and of the Xigaze Forearc Basin in southern Tibet, China. – Excursion Guide to IGCP 362 Working-Group Meeting "Integrated Stratigraphy". 113 pages, Bremen, 1995. (out of print)

No. 65 **Hünken, U.**
Liefergebiets - Charakterisierung proterozoischer Goldseifen in Ghana anhand von Fluideinschluß - Untersuchungen. 270 pages, Bremen, 1995.

No. 66 **Nyandwi, N.**
The Nature of the Sediment Distribution Patterns in ther Spiekeroog Backbarrier Area, the East Frisian Islands. 162 pages, Bremen, 1995.

No. 67 **Isenbeck-Schröter, M.**
Transportverhalten von Schwermetallkationen und Oxoanionen in wassergesättigten Sanden. - Laborversuche in Säulen und ihre Modellierung -. 182 pages, Bremen, 1995.

No. 68 **Hebbeln, D. and cruise participants**
Report and preliminary results of SONNE-Cruise SO 102, Valparaiso - Valparaiso, 95.
134 pages, Bremen, 1995.

No. 69 **Willems, H. (Sprecher), U.Bathmann, U. Bleil, T. v. Dobeneck, K. Herterich, B.B. Jorgensen, E.-M. Nöthig, M. Olesch, J. Pätzold, H.D. Schulz, V. Smetacek, V. Speiß. G. Wefer**
Bericht des Graduierten-Kollegs Stoff-Flüsse in marine Geosystemen.
Berichtszeitraum Januar 1993 - Dezember 1995.
45 & 468 pages, Bremen, 1995.

No. 70 **Giese, M. and G. Wefer**
Bericht über den 4. JGOFS-Workshop. 20./21. November 1995 in Bremen. 60 pages, Bremen, 1996. (out of print)

No. 71 **Meggers, H.**
Pliozän-quartäre Karbonatsedimentation und Paläozeanographie des Nordatlantiks und des Europäischen Nordmeeres - Hinweise aus planktischen Foraminiferengemeinschaften.
143 pages, Bremen, 1996. (out of print)

No. 72 **Teske, A.**
Phylogenetische und ökologische Untersuchungen an Bakterien des oxidativen und reduktiven marinen Schwefelkreislaufs mittels ribosomaler RNA. 220 pages, Bremen, 1996. (out of print)

No. 73 **Andersen, N.**
Biogeochemische Charakterisierung von Sinkstoffen und Sedimenten aus ostatlantischen Produktions-Systemen mit Hilfe von Biomarkern. 215 pages, Bremen, 1996.

No. 74 **Treppke, U.**
Saisonalität im Diatomeen- und Silikoflagellatenfluß im östlichen tropischen und subtropischen Atlantik. 200 pages, Bremen, 1996.

No. 75 **Schüring, J.**
Die Verwendung von Steinkohlebergematerialien im Deponiebau im Hinblick auf die Pyritverwitterung und die Eignung als geochemische Barriere. 110 pages, Bremen, 1996.

No. 76 **Pätzold, J. and cruise participants**
Report and preliminary results of VICTOR HENSEN cruise JOPS II, Leg 6, Fortaleza - Recife, 10.3. - 26.3. 1995 and Leg 8, Vítoria - Vítoria, 10.4. - 23.4.1995.
87 pages, Bremen, 1996.

No. 77 **Bleil, U. and cruise participants**
Report and preliminary results of METEOR-Cruise M 34/1, Cape Town - Walvis Bay, 3.-26.1.1996.
129 pages, Bremen, 1996.

No. 78 **Schulz, H.D. and cruise participants**
Report and preliminary results of METEOR-Cruise M 34/2, Walvis Bay - Walvis Bay, 29.1.-18.2.96
133 pages, Bremen, 1996.

No. 79 **Wefer, G. and cruise participants**
Report and preliminary results of METEOR-Cruise M 34/3, Walvis Bay - Recife, 21.2.-17.3.1996.
168 pages, Bremen, 1996.

No. 80 **Fischer, G. and cruise participants**
Report and preliminary results of METEOR-Cruise M 34/4, Recife - Bridgetown, 19.3.-15.4.1996. 105 pages, Bremen, 1996.

No. 81 **Kulbrok, F.**
Biostratigraphie, Fazies und Sequenzstratigraphie einer Karbonatrampe in den Schichten der Oberkreide und des Alttertiärs Nordost-Ägyptens (Eastern Desert, N'Golf von Suez, Sinai). 153 pages, Bremen, 1996.

No. 82 **Kasten, S.**
Early Diagenetic Metal Enrichments in Marine Sediments as Documents of Nonsteady-State Depositional Conditions. Bremen, 1996.

No. 83 **Holmes, M.E.**
Reconstruction of Surface Ocean Nitrate Utilization in the Southeast Atlantic Ocean Based on Stable Nitrogen Isotopes. 113 pages, Bremen, 1996.

No. 84 **Rühlemann, C.**
Akkumulation von Carbonat und organischem Kohlenstoff im tropischen Atlantik: Spätquartäre Produktivitäts-Variationen und ihre Steuerungsmechanismen. 139 pages, Bremen, 1996.

No. 85 **Ratmeyer, V.**
Untersuchungen zum Eintrag und Transport lithogener und organischer partikulärer Substanz im östlichen subtropischen Nordatlantik. 154 pages, Bremen, 1996.

No. 86 **Cepek, M.**
Zeitliche und räumliche Variationen von Coccolithophoriden-Gemeinschaften im subtropischen Ost-Atlantik: Untersuchungen an Plankton, Sinkstoffen und Sedimenten. 156 pages, Bremen, 1996.

No. 87 **Otto, S.**
Die Bedeutung von gelöstem organischen Kohlenstoff (DOC) für den Kohlenstoffffluß im Ozean. 150 pages, Bremen, 1996.

No. 88 **Hensen, C.**
Frühdiagenetische Prozesse und Quantifizierung benthischer Stoff-Flüsse in Oberflächensedimenten des Südatlantiks. 132 pages, Bremen, 1996.

No. 89 **Giese, M. and G. Wefer**
Bericht über den 5. JGOFS-Workshop. 27./28. November 1996 in Bremen. 73 pages, Bremen, 1997.

No. 90 **Wefer, G. and cruise participants**
Report and preliminary results of METEOR-Cruise M 37/1, Lisbon - Las Palmas, 4.-23.12.1996. 79 pages, Bremen, 1997.

No. 91 **Isenbeck-Schröter, M., E. Bedbur, M. Kofod, B. König, T. Schramm & G. Mattheß**
Occurrence of Pesticide Residues in Water - Assessment of the Current Situation in Selected EU Countries. 65 pages, Bremen 1997.

No. 92 **Kühn, M.**
Geochemische Folgereaktionen bei der hydrogeothermalen Energiegewinnung. 129 pages, Bremen 1997.

No. 93 **Determann, S. & K. Herterich**
JGOFS-A6 "Daten und Modelle": Sammlung JGOFS-relevanter Modelle in Deutschland. 26 pages, Bremen, 1997.

No. 94 **Fischer, G. and cruise participants**
Report and preliminary results of METEOR-Cruise M 38/1, Las Palmas - Recife, 25.1.-1.3.1997, with Appendix: Core Descriptions from METEOR Cruise M 37/1. Bremen, 1997.

No. 95 **Bleil, U. and cruise participants**
Report and preliminary results of METEOR-Cruise M 38/2, Recife - Las Palmas, 4.3.-14.4.1997. 126 pages, Bremen, 1997.

No. 96 **Neuer, S. and cruise participants**
Report and preliminary results of VICTOR HENSEN-Cruise 96/1. Bremen, 1997.

No. 97 **Villinger, H. and cruise participants**
Fahrtbericht SO 111, 20.8. - 16.9.1996. 115 pages, Bremen, 1997.

No. 98 **Lüning, S.**
Late Cretaceous - Early Tertiary sequence stratigraphy, paleoecology and geodynamics of Eastern Sinai, Egypt. 218 pages, Bremen, 1997.

No. 99 **Haese, R.R.**
Beschreibung und Quantifizierung frühdiagenetischer Reaktionen des Eisens in Sedimenten des Südatlantiks. 118 pages, Bremen, 1997.

No. 100 **Lührte, R. von**
Verwertung von Bremer Baggergut als Material zur Oberflächenabdichtung von Deponien - Geochemisches Langzeitverhalten und Schwermetall-Mobilität (Cd, Cu, Ni, Pb, Zn). Bremen, 1997.

No. 101 **Ebert, M.**
Der Einfluß des Redoxmilieus auf die Mobilität von Chrom im durchströmten Aquifer. 135 pages, Bremen, 1997.

No. 102 **Krögel, F.**
Einfluß von Viskosität und Dichte des Seewassers auf Transport und Ablagerung von Wattsedimenten (Langeooger Rückseitenwatt, südliche Nordsee). 168 pages, Bremen, 1997.

No. 103 **Kerntopf, B.**
Dinoflagellate Distribution Patterns and Preservation in the Equatorial Atlantic and Offshore North-West Africa. 137 pages, Bremen, 1997.

No. 104 **Breitzke, M.**
Elastische Wellenausbreitung in marinen Sedimenten - Neue Entwicklungen der Ultraschall Sedimentphysik und Sedimentechographie. 298 pages, Bremen, 1997.

No. 105 **Marchant, M.**
Rezente und spätquartäre Sedimentation planktischer Foraminiferen im Peru-Chile Strom. 115 pages, Bremen, 1997.

No. 106 **Habicht, K.S.**
Sulfur isotope fractionation in marine sediments and bacterial cultures. 125 pages, Bremen, 1997.

No. 107 **Hamer, K., R.v. Lührte, G. Becker, T. Felis, S. Keffel, B. Strotmann, C. Waschkowitz, M. Kölling, M. Isenbeck-Schröter, H.D. Schulz**
Endbericht zum Forschungsvorhaben 060 des Landes Bremen: Baggergut der Hafengruppe Bremen-Stadt: Modelluntersuchungen zur Schwermetallmobilität und Möglichkeiten der Verwertung von Hafenschlick aus Bremischen Häfen. 98 pages, Bremen, 1997.

No. 108 **Greeff, O.W.**
Entwicklung und Erprobung eines benthischen Landersystemes zur *in situ*-Bestimmung von Sulfatreduktionsraten mariner Sedimente. 121 pages, Bremen, 1997.

No. 109 **Pätzold, M. und G. Wefer**
Bericht über den 6. JGOFS-Workshop am 4./5.12.1997 in Bremen. Im Anhang: Publikationen zum deutschen Beitrag zur Joint Global Ocean Flux Study (JGOFS), Stand 1/1998. 122 pages, Bremen, 1998.

No. 110 **Landenberger, H.**
CoTReM, ein Multi-Komponenten Transport- und Reaktions-Modell. 142 pages, Bremen, 1998.

No. 111 **Villinger, H. und Fahrtteilnehmer**
Fahrtbericht SO 124, 4.10. - 16.10.199. 90 pages, Bremen, 1997.

No. 112 **Gietl, R.**
Biostratigraphie und Sedimentationsmuster einer nordostägyptischen Karbonatrampe unter Berücksichtigung der Alveolinen-Faunen. 142 pages, Bremen, 1998.

No. 113 **Ziebis, W.**
The Impact of the Thalassinidean Shrimp *Callianassa truncata* on the Geochemistry of permeable, coastal Sediments. 158 pages, Bremen 1998.

No. 114 **Schulz, H.D. and cruise participants**
Report and preliminary results of METEOR-Cruise M 41/1, Málaga - Libreville, 13.2.-15.3.1998. Bremen, 1998.

No. 115 **Völker, D.J.**
Untersuchungen an strömungsbeeinflußten Sedimentationsmustern im Südozean. Interpretation sedimentechographischer Daten und numerische Modellierung. 152 pages, Bremen, 1998.

No. 116 **Schlünz, B.**
Riverine Organic Carbon Input into the Ocean in Relation to Late Quaternary Climate Change. 136 pages, Bremen, 1998.

No. 117 **Kuhnert, H.**
Aufzeichnug des Klimas vor Westaustralien in stabilen Isotopen in Korallenskeletten. 109 pages, Bremen, 1998.

No. 118 **Kirst, G.**
Rekonstruktion von Oberflächenwassertemperaturen im östlichen Südatlantik anhand von Alkenonen. 130 pages, Bremen, 1998.

No. 119 **Dürkoop, A.**
Der Brasil-Strom im Spätquartär: Rekonstruktion der oberflächennahen Hydrographie während der letzten 400 000 Jahre. 121 pages, Bremen, 1998.

No. 120 **Lamy, F.**
Spätquartäre Variationen des terrigenen Sedimenteintrags entlang des chilenischen Kontinentalhangs als Abbild von Klimavariabilität im Milankovi¿- und Sub-Milankovi¿-Zeitbereich. 141 pages, Bremen, 1998.

No. 121 **Neuer, S. and cruise participants**
Report and preliminary results of POSEIDON-Cruise Pos 237/2, Vigo – Las Palmas, 18.3.-31.3.1998. 39 pages, Bremen, 1998

No. 122 **Romero, O.E.**
Marine planktonic diatoms from the tropical and equatorial Atlantic: temporal flux patterns and the sediment record. 205 pages, Bremen, 1998.

No. 123 **Spiess, V. und Fahrtteilnehmer**
Report and preliminary results of RV SONNE Cruise 125, Cochin – Chittagong, 17.10.-17.11.1997. 128 pages, Bremen, 1998.

No. 124 **Arz, H.W.**
Dokumentation von kurzfristigen Klimaschwankungen des Spätquartärs in Sedimenten des westlichen äquatorialen Atlantiks. 96 pages, Bremen, 1998.

No. 125 **Wolff, T.**
Mixed layer characteristics in the equatorial Atlantic during the late Quaternary as deduced from planktonic foraminifera. 132 pages, Bremen, 1998.

No. 126 **Dittert, N.**
Late Quaternary Planktic Foraminifera Assemblages in the South Atlantic Ocean: Quantitative Determination and Preservational Aspects. 165 pages, Bremen, 1998.

No. 127 **Höll, C.**
Kalkige und organisch-wandige Dinoflagellaten-Zysten in Spätquartären Sedimenten des tropischen Atlantiks und ihre palökologische Auswertbarkeit. 121 pages, Bremen, 1998.

No. 128 **Hencke, J.**
Redoxreaktionen im Grundwasser: Etablierung und Verlagerung von Reaktionsfronten und ihre Bedeutung für die Spurenelement-Mobilität. 122 pages, Bremen 1998.

No. 129 **Pätzold, J. and cruise participants**
Report and preliminary results of METEOR-Cruise M 41/3, Vítoria, Brasil – Salvador de Bahia, Brasil, 18.4. - 15.5.1998. Bremen, 1999.

No. 130 **Fischer, G. and cruise participants**
Report and preliminary results of METEOR-Cruise M 41/4, Salvador de Bahia, Brasil – Las Palmas, Spain, 18.5. – 13.6.1998. Bremen, 1999.

No. 131 **Schlünz, B. und G. Wefer**
Bericht über den 7. JGOFS-Workshop am 3. und 4.12.1998 in Bremen. Im Anhang: Publikationen zum deutschen Beitrag zur Joint Global Ocean Flux Study (JGOFS), Stand 1/ 1999. 100 pages, Bremen, 1999.

No. 132 **Wefer, G. and cruise participants**
Report and preliminary results of METEOR-Cruise M 42/4, Las Palmas - Las Palmas - Viena do Castelo; 26.09.1998 - 26.10.1998. 104 pages, Bremen, 1999.

No. 133 **Felis, T.**
Climate and ocean variability reconstructed from stable isotope records of modern subtropical corals (Northern Red Sea). 111 pages, Bremen, 1999.

No. 134 **Draschba , S.**
North Atlantic climate variability recorded in reef corals from Bermuda. 108 pages, Bremen, 1999.

No. 135 **Schmieder, F.**
Magnetic Cyclostratigraphy of South Atlantic Sediments. 82 pages, Bremen, 1999.

No. 136 **Rieß, W.**
In situ measurements of respiration and mineralisation processes – Interaction between fauna and geochemical fluxes at active interfaces. 68 pages, Bremen, 1999.

No. 137 **Devey, C.W. and cruise participants**
Report and shipboard results from METEOR-cruise M 41/2, Libreville – Vitoria, 18.3. – 15.4.98. 59 pages, Bremen, 1999.

No. 138 **Wenzhöfer, F.**
Biogeochemical processes at the sediment water interface and quantification of metabolically driven calcite dissolution in deep sea sediments. 103 pages, Bremen, 1999.

No. 139 **Klump, J.**
Biogenic barite as a proxy of paleoproductivity variations in the Southern Peru-Chile Current. 107 pages, Bremen, 1999.

No. 140 **Huber, R.**
Carbonate sedimentation in the northern Northatlantic since the late pliocene. 103 pages, Bremen, 1999.

No. 141 **Schulz, H.**
Nitrate-storing sulfur bacteria in sediments of coastal upwelling. 94 pages, Bremen, 1999.

No. 142 **Mai, S.**
Die Sedimentverteilung im Wattenmeer: ein Simulationsmodell. 114 pages, Bremen, 1999.

No. 143 **Neuer, S. and cruise participants**
Report and preliminary results of Poseidon Cruise 248, Las Palmas - Las Palmas, 15.2.-26.2.1999.
45 pages, Bremen, 1999.

No. 144 **Weber, A.**
Schwefelkreislauf in marinen Sedimenten und Messung von *in situ* Sulfatreduktionsraten.
122 pages, Bremen, 1999.

No. 145 **Hadeler, A.**
Sorptionsreaktionen im Grundwasser: Unterschiedliche Aspekte bei der Modellierung des Transportverhaltens von Zink. 122 pages, 1999.

No. 146 **Dierßen, H.**
Zum Kreislauf ausgewählter Spurenmetalle im Südatlantik: Vertikaltransport und Wechselwirkung zwischen Partikeln und Lösung. 167 pages, Bremen, 1999.

No. 147 **Zühlsdorff, L.**
High resolution multi-frequency seismic surveys at the Eastern Juan de Fuca Ridge Flank and the Cascadia Margin – Evidence for thermally and tectonically driven fluid upflow in marine sediments. 118 pages, Bremen 1999.

No. 148 **Kinkel, H.**
Living and late Quaternary Coccolithophores in the equatorial Atlantic Ocean: response of distribution and productivity patterns to changing surface water circulation. 183 pages, Bremen, 2000.

No. 149 **Pätzold, J. and cruise participants**
Report and preliminary results of METEOR Cruise M 44/3, Aqaba (Jordan) - Safaga (Egypt) – Dubá (Saudi Arabia) – Suez (Egypt) - Haifa (Israel), 12.3.-26.3.-2.4.-4.4.1999. 135 pages, Bremen, 2000.

No. 150 **Schlünz, B. and G. Wefer**
Bericht über den 8. JGOFS-Workshop am 2. und 3.12.1999 in Bremen. Im Anhang:
Publikationen zum deutschen Beitrag zur Joint Global Ocean Flux Study (JGOFS), Stand 1/ 2000.
95 pages, Bremen, 2000.

No. 151 **Schnack, K.**
Biostratigraphie und fazielle Entwicklung in der Oberkreide und im Alttertiär im Bereich der Kharga Schwelle, Westliche Wüste, SW-Ägypten. 142 pages, Bremen, 2000.

No. 152 **Karwath, B.**
Ecological studies on living and fossil calcareous dinoflagellates of the equatorial and tropical Atlantic Ocean. 175 pages, Bremen, 2000.

No. 153 **Moustafa, Y.**
Paleoclimatic reconstructions of the Northern Red Sea during the Holocene inferred from stable isotope records of modern and fossil corals and molluscs. 102 pages, Bremen, 2000.

No. 154 **Villinger, H. and cruise participants**
Report and preliminary results of SONNE-cruise 145-1 Balboa – Talcahuana, 21.12.1999 – 28.01.2000.
147 pages, Bremen, 2000.

No. 155 **Rusch, A.**
Dynamik der Feinfraktion im Oberflächenhorizont permeabler Schelfsedimente. 102 pages, Bremen, 2000.

No. 156 **Moos, C.**
Reconstruction of upwelling intensity and paleo-nutrient gradients in the northwest Arabian Sea derived from stable carbon and oxygen isotopes of planktic foraminifera. 103 pages, Bremen, 2000.

No. 157 **Xu, W.**
Mass physical sediment properties and trends in a Wadden Sea tidal basin. 127 pages, Bremen, 2000.

No. 158 **Meinecke, G. and cruise participants**
Report and preliminary results of METEOR Cruise M 45/1, Malaga (Spain) - Lissabon (Portugal),
19.05. - 08.06.1999. 39 pages, Bremen, 2000.

No. 159 **Vink, A.**
Reconstruction of recent and late Quaternary surface water masses of the western subtropical Atlantic Ocean based on calcareous and organic-walled dinoflagellate cysts. 160 pages, Bremen, 2000.

No. 160 **Willems, H. (Sprecher), U. Bleil, R. Henrich, K. Herterich, B.B. Jørgensen, H.-J. Kuß, M. Olesch, H.D. Schulz,V. Spieß, G. Wefer**
Abschlußbericht des Graduierten-Kollegs Stoff-Flüsse in marine Geosystemen.
Zusammenfassung und Berichtszeitraum Januar 1996 - Dezember 2000. 340 pages, Bremen, 2000.

No. 161 **Sprengel, C.**
Untersuchungen zur Sedimentation und Ökologie von Coccolithophoriden im Bereich der Kanarischen Inseln: Saisonale Flussmuster und Karbonatexport. 165 pages, Bremen, 2000.

No. 162 **Donner, B. and G. Wefer**
Bericht über den JGOFS-Workshop am 18.-21.9.2000 in Bremen:
Biogeochemical Cycles: German Contributions to the International Joint Global Ocean Flux Study.
87 pages, Bremen, 2000.

No. 163 **Neuer, S. and cruise participants**
Report and preliminary results of Meteor Cruise M 45/5, Bremen – Las Palmas, October 1 – November 3, 1999. 93 pages, Bremen, 2000.

No. 164 **Devey, C. and cruise participants**
Report and preliminary results of Sonne Cruise SO 145/2, Talcahuano (Chile) - Arica (Chile), February 4 – February 29, 2000. 63 pages, Bremen, 2000.

No. 165 **Freudenthal, T.**
Reconstruction of productivity gradients in the Canary Islands region off Morocco by means of sinking particles and sediments. 147 pages, Bremen, 2000.

No. 166 **Adler, M.**
Modeling of one-dimensional transport in porous media with respect to simultaneous geochemical reactions in CoTReM. 147 pages, Bremen, 2000.

No. 167 **Santamarina Cuneo, P.**
Fluxes of suspended particulate matter through a tidal inlet of the East Frisian Wadden Sea (southern North Sea). 91 pages, Bremen, 2000.

No. 168 **Benthien, A.**
Effects of CO_2 and nutrient concentration on the stable carbon isotope composition of C37:2 alkenones in sediments of the South Atlantic Ocean. 104 pages, Bremen, 2001.

No. 169 **Lavik, G.**
Nitrogen isotopes of sinking matter and sediments in the South Atlantic. 140 pages, Bremen, 2001.

No. 170 **Budziak, D.**
Late Quaternary monsoonal climate and related variations in paleoproductivity and alkenone-derived sea-surface temperatures in the western Arabian Sea. 114 pages, Bremen, 2001.

No. 171 **Gerhardt, S.**
Late Quaternary water mass variability derived from the pteropod preservation state in sediments of the western South Atlantic Ocean and the Caribbean Sea. 109 pages, Bremen, 2001.

No. 172 **Bleil, U. and cruise participants**
Report and preliminary results of Meteor Cruise M 46/3, Montevideo (Uruguay) – Mar del Plata (Argentina), January 4 – February 7, 2000. Bremen, 2001.

No. 173 **Wefer, G. and cruise participants**
Report and preliminary results of Meteor Cruise M 46/4, Mar del Plata (Argentina) – Salvador da Bahia (Brazil), February 10 – March 13, 2000. With partial results of METEOR cruise M 46/2. 136 pages, Bremen, 2001.

No. 174 **Schulz, H.D. and cruise participants**
Report and preliminary results of Meteor Cruise M 46/2, Recife (Brazil) – Montevideo (Uruguay), December 2 – December 29, 1999. 107 pages, Bremen, 2001.

No. 175 **Schmidt, A.**
Magnetic mineral fluxes in the Quaternary South Atlantic: Implications for the paleoenvironment.
97 pages, Bremen, 2001.

No. 176 **Bruhns, P.**
Crystal chemical characterization of heavy metal incorporation in brick burning processes.
93 pages, Bremen, 2001.

No. 177 **Karius, V.**
Baggergut der Hafengruppe Bremen-Stadt in der Ziegelherstellung. 131 pages, Bremen, 2001.

No. 178 **Adegbie, A. T.**
Reconstruction of paleoenvironmental conditions in Equatorial Atlantic and the Gulf of Guinea Basins for the last 245,000 years. 113 pages, Bremen, 2001.

No. 179 **Spieß, V. and cruise participants**
Report and preliminary results of R/V Sonne Cruise SO 149, Victoria - Victoria, 16.8. - 16.9.2000.
100 pages, Bremen, 2001.

No. 180 **Kim, J.-H.**
Reconstruction of past sea-surface temperatures in the eastern South Atlantic and the eastern South Pacific across Termination I based on the Alkenone Method. 114 pages, Bremen, 2001.

No. 181 **von Lom-Keil, H.**
Sedimentary waves on the Namibian continental margin and in the Argentine Basin – Bottom flow reconstructions based on high resolution echosounder data. 126 pages, Bremen, 2001.

No. 182 **Hebbeln, D. and cruise participants**
PUCK: Report and preliminary results of R/V Sonne Cruise SO 156, Valparaiso (Chile) - Talcahuano (Chile), March 29 - May 14, 2001. 195 pages, Bremen, 2001.

No. 183 **Wendler, J.**
Reconstruction of astronomically-forced cyclic and abrupt paleoecological changes in the Upper Cretaceous Boreal Realm based on calcareous dinoflagellate cysts. 149 pages, Bremen, 2001.

No. 184 **Volbers, A.**
Planktic foraminifera as paleoceanographic indicators: production, preservation, and reconstruction of upwelling intensity. Implications from late Quaternary South Atlantic sediments. 122 pages, Bremen, 2001.

No. 185 **Bleil, U. and cruise participants**
Report and preliminary results of R/V METEOR Cruise M 49/3, Montevideo (Uruguay) - Salvador (Brasil), March 9 - April 1, 2001. 99 pages, Bremen, 2001.

No. 186 **Scheibner, C.**
Architecture of a carbonate platform-to-basin transition on a structural high (Campanian-early Eocene, Eastern Desert, Egypt) – classical and modelling approaches combined. 173 pages, Bremen, 2001.

No. 187 **Schneider, S.**
Quartäre Schwankungen in Strömungsintensität und Produktivität als Abbild der Wassermassen-Variabilität im äquatorialen Atlantik (ODP Sites 959 und 663): Ergebnisse aus Siltkorn-Analysen. 134 pages, Bremen, 2001.

No. 188 **Uliana, E.**
Late Quaternary biogenic opal sedimentation in diatom assemblages in Kongo Fan sediments. 96 pages, Bremen, 2002.

No. 189 **Esper, O.**
Reconstruction of Recent and Late Quaternary oceanographic conditions in the eastern South Atlantic Ocean based on calcareous- and organic-walled dinoflagellate cysts. 130 pages, Bremen, 2001.

No. 190 **Wendler, I.**
Production and preservation of calcareous dinoflagellate cysts in the modern Arabian Sea. 117 pages, Bremen, 2002.

No. 191 **Bauer, J.**
Late Cenomanian – Santonian carbonate platform evolution of Sinai (Egypt): stratigraphy, facies, and sequence architecture. 178 pages, Bremen, 2002.

No. 192 **Hildebrand-Habel, T.**
Die Entwicklung kalkiger Dinoflagellaten im Südatlantik seit der höheren Oberkreide. 152 pages, Bremen, 2002.

No. 193 **Hecht, H.**
Sauerstoff-Optopoden zur Quantifizierung von Pyritverwitterungsprozessen im Labor- und Langzeit-in-situ-Einsatz. Entwicklung - Anwendung – Modellierung. 130 pages, Bremen, 2002.

No. 194 **Fischer, G. and cruise participants**
Report and Preliminary Results of RV METEOR-Cruise M49/4, Salvador da Bahia – Halifax, 4.4.-5.5.2001. 84 pages, Bremen, 2002.

No. 195 **Gröger, M.**
Deep-water circulation in the western equatorial Atlantic: inferences from carbonate preservation studies and silt grain-size analysis. 95 pages, Bremen, 2002.

No. 196 **Meinecke,G. and cruise participants**
Report of RV POSEIDON Cruise POS 271, Las Palmas - Las Palmas, 19.3.-29.3.2001. 19 pages, Bremen, 2002.

No. 197 **Meggers, H. and cruise participants**
Report of RV POSEIDON Cruise POS 272, Las Palmas - Las Palmas, 1.4.-14.4.2001. 19 pages, Bremen, 2002.

No. 198 **Gräfe, K.-U.**
Stratigraphische Korrelation und Steuerungsfaktoren Sedimentärer Zyklen in ausgewählten Borealen und Tethyalen Becken des Cenoman/Turon (Oberkreide) Europas und Nordwestafrikas. 197 pages, Bremen, 2002.

No. 199 **Jahn, B.**
Mid to Late Pleistocene Variations of Marine Productivity in and Terrigenous Input to the Southeast Atlantic. 97 pages, Bremen, 2002.

No. 200 **Al-Rousan, S.**
Ocean and climate history recorded in stable isotopes of coral and foraminifers from the northern Gulf of Aqaba. 116 pages, Bremen, 2002.

No. 201 **Azouzi, B.**
Regionalisierung hydraulischer und hydrogeochemischer Daten mit geostatistischen Methoden.
108 pages, Bremen, 2002.

No. 202 **Spieß, V. and cruise participants**
Report and preliminary results of METEOR Cruise M 47/3, Libreville (Gabun) - Walvis Bay (Namibia), 01.06 - 03.07.2000. 70 pages, Bremen 2002.

No. 203 **Spieß, V. and cruise participants**
Report and preliminary results of METEOR Cruise M 49/2, Montevideo (Uruguay) - Montevideo, 13.02 - 07.03.2001. 84 pages, Bremen 2002.

No. 204 **Mollenhauer, G.**
Organic carbon accumulation in the South Atlantic Ocean: Sedimentary processes and glacial/interglacial Budgets. 139 pages, Bremen 2002.

No. 205 **Spieß, V. and cruise participants**
Report and preliminary results of METEOR Cruise M49/1, Cape Town (South Africa) - Montevideo (Uruguay), 04.01.2000 - 10.02.2000. 57 pages, Bremen, 2003.

No. 206 **Meier, K.J.S.**
Calcareous dinoflagellates from the Mediterranean Sea: taxonomy, ecology and palaeoenvironmental application. 126 pages, Bremen, 2003.

No. 207 **Rakic, S.**
Untersuchungen zur Polymorphie und Kristallchemie von Silikaten der Zusammensetzung $Me_2Si_2O_5$ (Me:Na, K). 139 pages, Bremen, 2003.

No. 208 **Pfeifer, K.**
Auswirkungen frühdiagenetischer Prozesse auf Calcit- und Barytgehalte in marinen Oberflächen-sedimenten. 110 pages, Bremen, 2003.

No. 209 **Heuer, V.**
Spurenelemente in Sedimenten des Südatlantik. Primärer Eintrag und frühdiagenetische Überprägung. 136 pages, Bremen, 2003.

No. 210 **Streng, M.**
Phylogenetic Aspects and Taxonomy of Calcareous Dinoflagellates. 157 pages, Bremen 2003.

No. 211 **Boeckel, B.**
Present and past coccolith assemblages in the South Atlantic: implications for species ecology, carbonate contribution and palaeoceanographic applicability. 157 pages, Bremen, 2003.

No. 212 **Precht, E.**
Advective interfacial exchange in permeable sediments driven by surface gravity waves and its ecological consequences. 131 pages, Bremen, 2003.

No. 213 **Frenz, M.**
Grain-size composition of Quaternary South Atlantic sediments and its paleoceanographic significance. 123 pages, Bremen, 2003.

No. 214 **Meggers, H. and cruise participants**
Report and preliminary results of METEOR Cruise M 53/1, Limassol - Las Palmas – Mindelo, 30.03.2002 - 03.05.2002. 81 pages, Bremen, 2003.

No. 215 **Schulz, H.D. and cruise participants**
Report and preliminary results of METEOR Cruise M 58/1, Dakar – Las Palmas, 15.04..2003 - 12.05.2003. Bremen, 2003.

No. 216 **Schneider, R. and cruise participants**
Report and preliminary results of METEOR Cruise M 57/1, Cape Town – Walvis Bay, 20.01. – 08.02.2003. 123 pages, Bremen, 2003.

No. 217 **Kallmeyer, J.**
Sulfate reduction in the deep Biosphere. 157 pages, Bremen, 2003.

No. 218 **Røy, H.**
Dynamic Structure and Function of the Diffusive Boundary Layer at the Seafloor. 149 pages, Bremen, 2003.

No. 219 **Pätzold, J., C. Hübscher and cruise participants**
Report and preliminary results of METEOR Cruise M 52/2&3, Istanbul – Limassol – Limassol, 04.02. – 27.03.2002. Bremen, 2003.

No. 220 **Zabel, M. and cruise participants**
Report and preliminary results of METEOR Cruise M 57/2, Walvis Bay – Walvis Bay, 11.02. – 12.03.2003. 136 pages, Bremen 2003.

No. 221 **Salem, M.**
Geophysical investigations of submarine prolongations of alluvial fans on the western side of the Gulf of Aqaba-Red Sea. 100 pages, Bremen, 2003.

No. 222 **Tilch, E.**
Oszillation von Wattflächen und deren fossiles Erhaltungspotential (Spiekerooger Rückseitenwatt, südliche Nordsee). 137 pages, Bremen, 2003.

No. 223 **Frisch, U. and F. Kockel**
Der Bremen-Knoten im Strukturnetz Nordwest-Deutschlands. Stratigraphie, Paläogeographie, Strukturgeologie. 379 pages, Bremen, 2004.

No. 224 **Kolonic, S.**
Mechanisms and biogeochemical implications of Cenomanian/Turonian black shale formation in North Africa: An integrated geochemical, millennial-scale study from the Tarfaya-LaAyoune Basin in SW Morocco. 174 pages, Bremen, 2004. Report online available only.

No. 225 **Panteleit, B.**
Geochemische Prozesse in der Salz- Süßwasser Übergangszone. 106 pages, Bremen, 2004.

No. 226 **Seiter, K.**
Regionalisierung und Quantifizierung benthischer Mineralisationsprozesse. 135 pages, Bremen, 2004.

No. 227 **Bleil, U. and cruise participants**
Report and preliminary results of METEOR Cruise M 58/2, Las Palmas – Las Palmas (Canary Islands, Spain), 15.05. – 08.06.2003. 123 pages, Bremen, 2004.

No. 228 **Kopf, A. and cruise participants**
Report and preliminary results of SONNE Cruise SO175, Miami - Bremerhaven, 12.11 - 30.12.2003. 218 pages, Bremen, 2004.

No. 229 **Fabian, M.**
Near Surface Tilt and Pore Pressure Changes Induced by Pumping in Multi-Layered Poroelastic Half-Spaces. 121 pages, Bremen, 2004.

No. 230 **Segl, M. , and cruise participants**
Report and preliminary results of POSEIDON cruise 304 Galway – Lisbon, 5. – 22. Oct. 2004, 27 pages, Bremen 2004

No. 231 **Meinecke, G. and cruise participants**
Report and preliminary results of POSEIDON Cruise 296, 42 pages, Bremen 2005.

No. 232 **Meinecke, G. and cruise participants**
Report and preliminary results of POSEIDON Cruise 310, 49 pages, Bremen 2005.

No. 233 **Meinecke, G. and cruise participants**
Report and preliminary results of METEOR Cruise 58/3, Bremen 2005.

No. 234 **Feseker, T.**
Numerical Studies on Groundwater Flow in Coastal Aquifers. 219 pages. Bremen 2004.

No. 235 **Sahling, H. and cruise participants**
Report and preliminary results of R/V POSEIDON Cruise P317/4, Istanbul-Istanbul , 16 October - 4 November 2004. 92 pages, Bremen 2004.

No. 236 **Meinecke, G. und Fahrtteilnehmer**
Report and preliminary results of POSEIDON Cruise 305, Las Palmas (Spain) - Lisbon (Portugal), October 28th – November 6th, 2003. 43 pages, Bremen 2005.

No. 237 **Ruhland, G. and cruise participants**
Report and preliminary results of POSEIDON Cruise 319, Las Palmas (Spain) - Las Palmas (Spain), December 6th – December 17th, 2004. 50 pages, Bremen 2005.

No. 238 **Chang, T.S.**
Dynamics of fine-grained sediments and stratigraphic evolution of a back-barrier tidal basin of the German Wadden Sea (southern North Sea). 102 pages, Bremen 2005.

No. 239 **Lager, T.**
Predicting the source strength of recycling materials within the scope of a seepage water prognosis by means of standardized laboratory methods. 141 pages, Bremen 2005.

No. 240 **Meinecke, G.**
DOLAN - Operationelle Datenübertragung im Ozean und Laterales Akustisches Netzwerk in der Tiefsee. Abschlußbericht. 42 pages, Bremen 2005.

No. 241 **Guasti, E.**
Early Paleogene environmental turnover in the southern Tethys as recorded by foraminiferal and organic-walled dinoflagellate cysts assemblages. 203 pages, Bremen 2005.

No. 242 **Riedinger, N.**
Preservation and diagenetic overprint of geochemical and geophysical signals in ocean margin sediments related to depositional dynamics. 91 pages, Bremen 2005.

No. 243 **Ruhland, G. and cruise participants**
Report and preliminary results of POSEIDON cruise 320, Las Palmas (Spain) - Las Palmas (Spain), March 08th - March 18th, 2005. 57 pages, Bremen 2005.

No. 244 **Inthorn, M.**
Lateral particle transport in nepheloid layers – a key factor for organic matter distribution and quality in the Benguela high-productivity area. 124 pages, Bremen, 2006.